StARR Research Meeting
Thursday, December 11, 2025
Research Complex 2, 3109

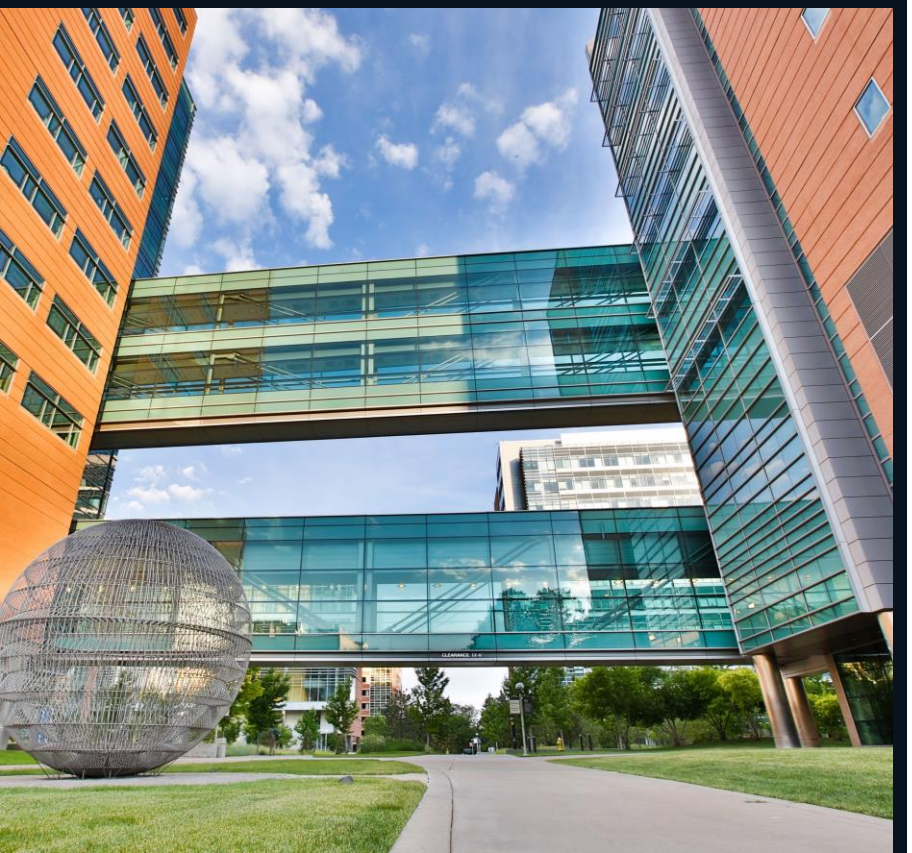

Attendees:

PI's:
David Schwartz, MD, Distinguished Professor of Medicine and Immunology; Associate Dean for Translational Sciences; Director, Program to Advance Physician Scientists and Translational Research
Peter Buttrick, MD, S. Gilbert Blount Endowed Professor
Steve Abman, MD, Director, Pediatric Heart-Lung Center; Founder and Co-Director, Pediatric Pulmonary Hypertension Program; Professor of Pediatrics

Residency Directors:
Mark Nehler, MD, Professor, Vice Chair of Education for Surgery; Director, General Surgery Residency Program
Julia Limes, MD, Associate Professor, Medicine-Hospital Medicine; Director, Internal Medicine Residency Program
Jason Espinoza, MD, Assistant Professor, Pediatrics-Critical Care Medicine; Director, Pediatrics Residency Program

Mentors:
Maria Amaya, MD, PhD, Assistant Professor, Medicine-Hematology (mentee-Kellen Gil, MD)
Sarkis (Chris) Derderian, MD, Assistant Professor, Surgery-Pediatric Surgery (mentee-Caitlin Eason, MD)
Sarah Taylor, MD, Associate Professor, Pediatrics-Gastroenterology, Hepatology, and Nutrition (mentees-Ioannis Ziogas, MD, and Lauren Maloney, MD)
T. Brett Reece, MD, Professor, Surgery-Cardiothoracic Surgery; Director, Thoracic Aortic Program (mentee-Brian Wu, MD)
Ken Tyler, MD, Professor, Louise Baum Endowed Chair of Neurology

Scholars:
Kellen Gil, MD, Department of Medicine
Caitlin Eason, MD, Department of Surgery
Lauren Maloney, MD, Department of Pediatrics
Ioannis Ziogas, MD, Department of Surgery
Sadie Meller, MD, Department of Pediatrics
Brian Wu, MD, Department of Surgery

Scholar Presentations:

- ***4:20-4:40 pm:*** *Kellen Gil, MD, Department of Medicine: The STAT3-VDAC1 Axis Modulates Mitochondrial Function and Plays a Critical Role in the Survival of Acute Myeloid Leukemia Cells*

- ***4:40-5 pm:*** *Caitlin Eason, MD, Department of Surgery: An In Vitro Model of Fetal Growth Restriction Inhibits Angiogenesis via Extracellular Vesicle Release of microRNA 141-3p.*

- ***5-5:20 pm:*** *Lauren Maloney, MD, Department of Pediatrics: Concurrent changes in macrophage and T cell subsets over time in murine obstructive cholestasis suggest interplay between macrophage and T cell function in promotion of hepatic injury*

- ***5:40-6 pm:*** *Ioannis Ziogas, MD: Cellular Senescence in Obstructive Cholangiopathies*

- ***5:20-5:40 pm****: Sadie Meller, MD, Department of Pediatrics: Microglial phagocytic response to EV-D68 infection in the spinal cord during early postnatal development*

- ***6-6:20 pm:*** *Brian Wu, MD, Department of Surgery: Exploring Mitochondrial Transplantation as a Novel Therapy for Embolic Stroke*

The STAT3-VDAC1 Axis Modulates Mitochondrial Function and Plays a Critical Role in the Survival of Leukemic Stem Cells

Kellen Gil
(PI: Maria Amaya)

Acute Myeloid Leukemia

- AML is an aggressive leukemia
- The average age of diagnosis is 69
- Estimated 20,380 new cases of AML in 2023
- About 11,310 deaths from AML yearly

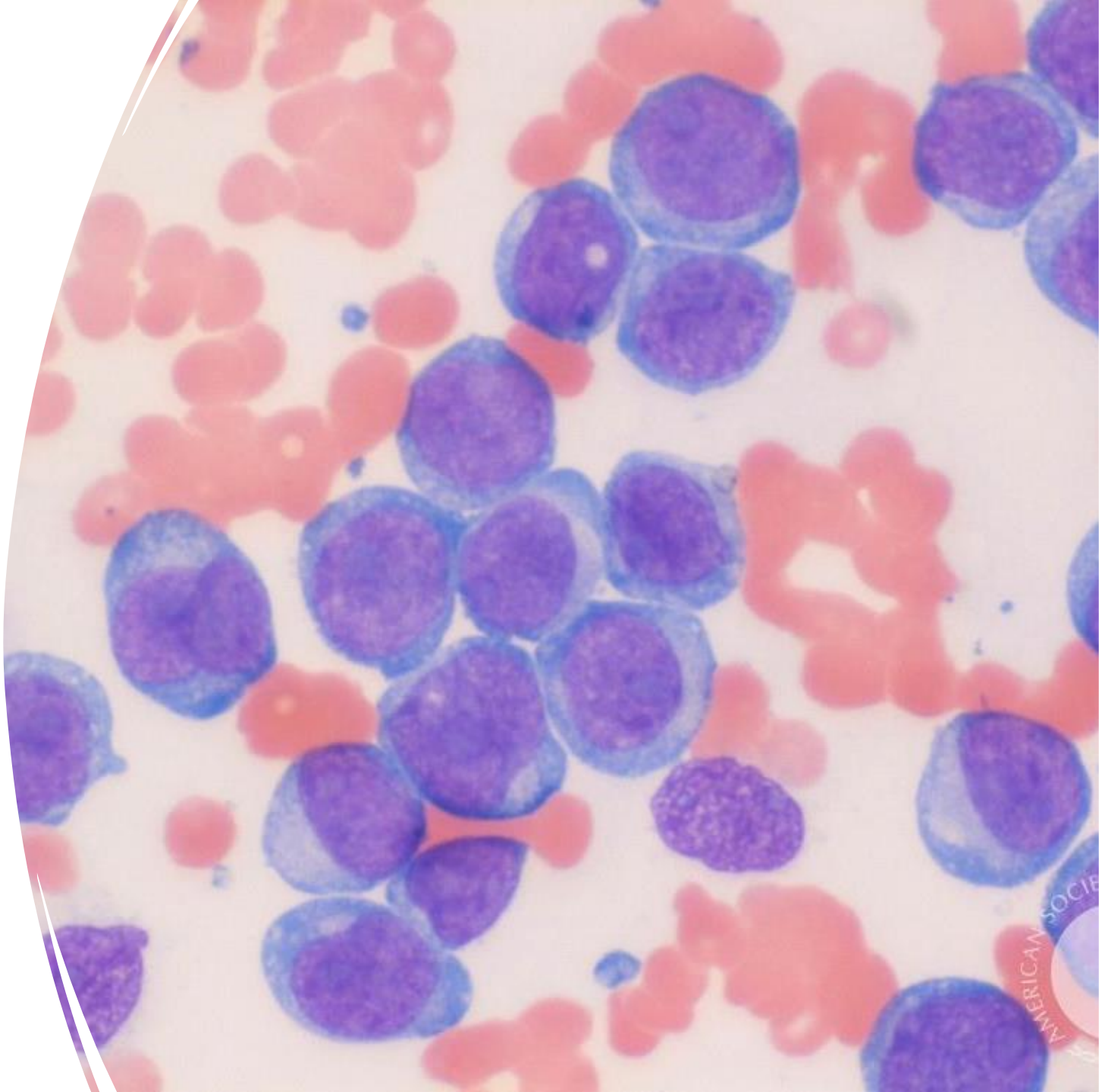

Incidence and Prognosis of Acute Myeloid Leukemia

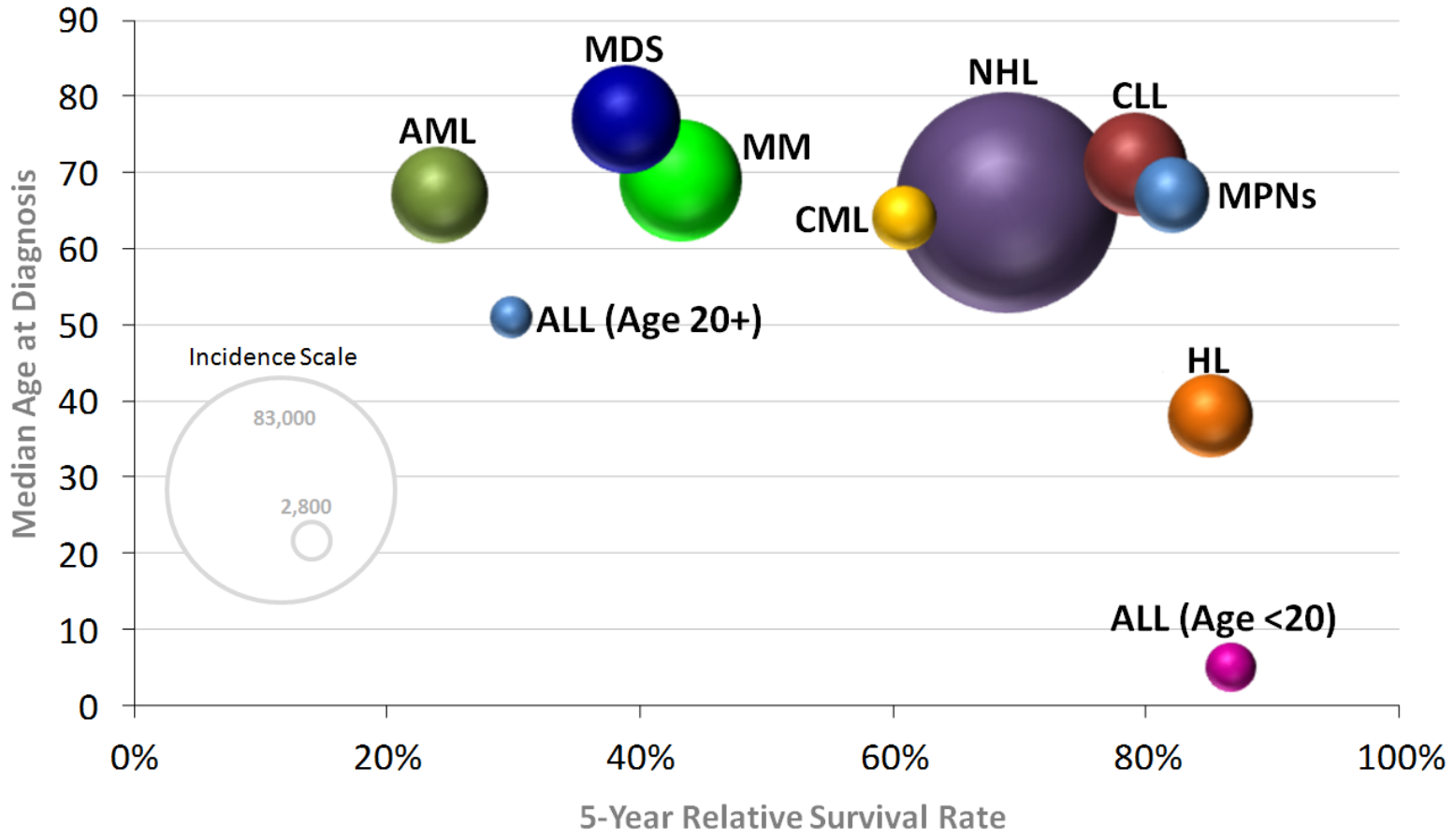

Source: SEER 18 areas (San Francisco, Connecticut, Detroit, Hawaii, Iowa, New Mexico, Seattle, Utah, Atlanta, San Jose-Monterey, Los Angeles, Alaska Native Registry, Rural Georgia, California excluding SF/SJM/LA, Kentucky, Louisiana, New Jersey and Georgia excluding ATL/RG). Median age and incidence counts include cases diagnosed in 2006-2010. Relative survival rates include cases diagnosed in 2003-2009.

Management of Acute Myeloid Leukemia

Remission

Cherry, E et al. Blood Advances 5(24):5565-5573, 2021

Management of Acute Myeloid Leukemia

Cherry, E et al. Blood Advances 5(24):5565-5573, 2021

Remission

Transplant

Cure

Management of Acute Myeloid Leukemia

Cherry, E et al. Blood Advances 5(24):5565-5573, 2021

Remission

Transplant

Relapse/Refractory

Cure

Role of STAT3 in AML

- STAT3 = transcription factor
- Known to regulate glutamine uptake via MYC-SLC1A5
- Regulates Oxidative Phosphorylation
- Also known to transport to the mitochondria directly, signaled by pSTAT3 S727

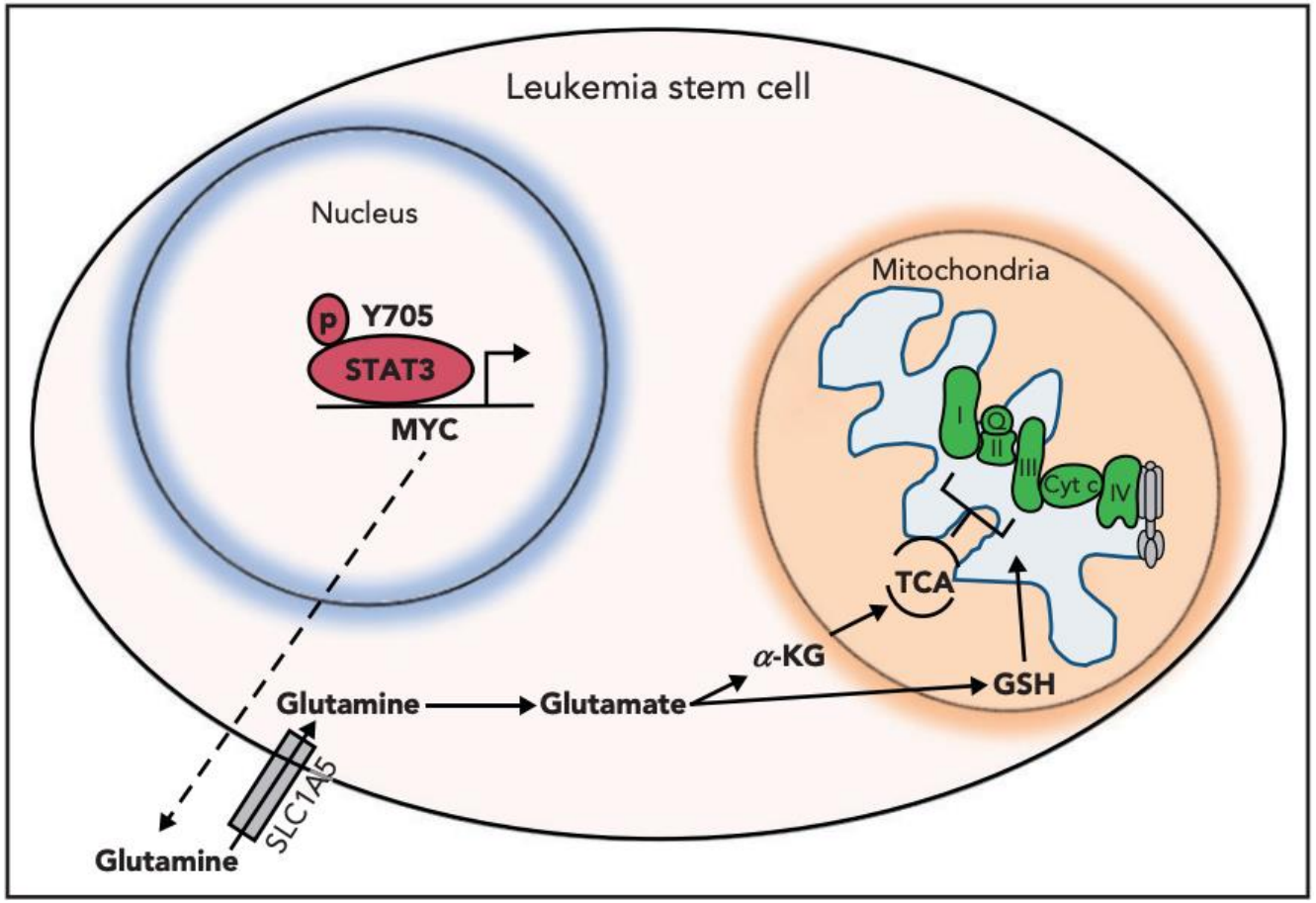

Amaya M.L., et al, *Blood* 2022; 139 (4): 584–596.

Current Work

AIMs

- Determine how mitochondrial STAT3 modulates mitochondrial metabolism in AML
- Determine STAT3's interaction with mitochondrial proteins
- Determine the therapeutic potential of targeting STAT3 in AML

Results

STAT3 expression and inhibition

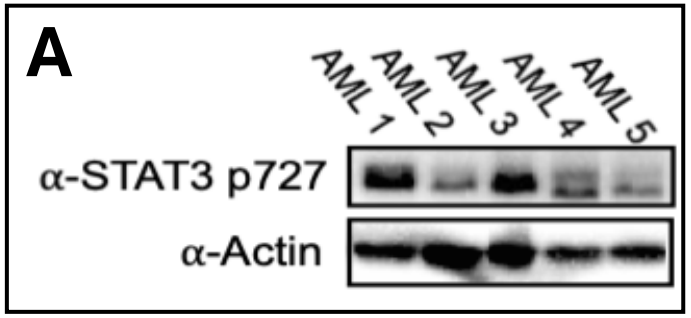

STAT3 is prominently expressed in AML patient samples and Molm13 cells.

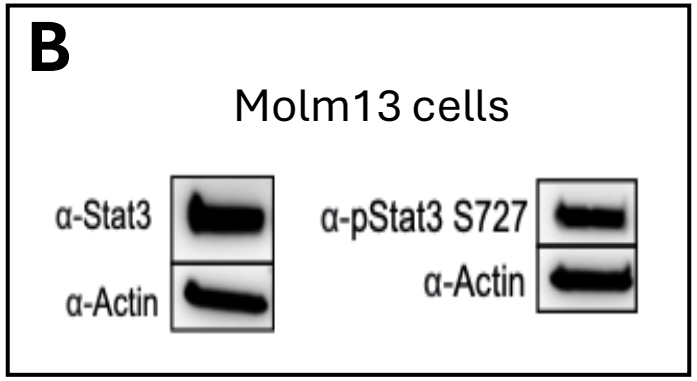

Phosphorylated STAT3 (pSTAT3) translocates to the mitochondria

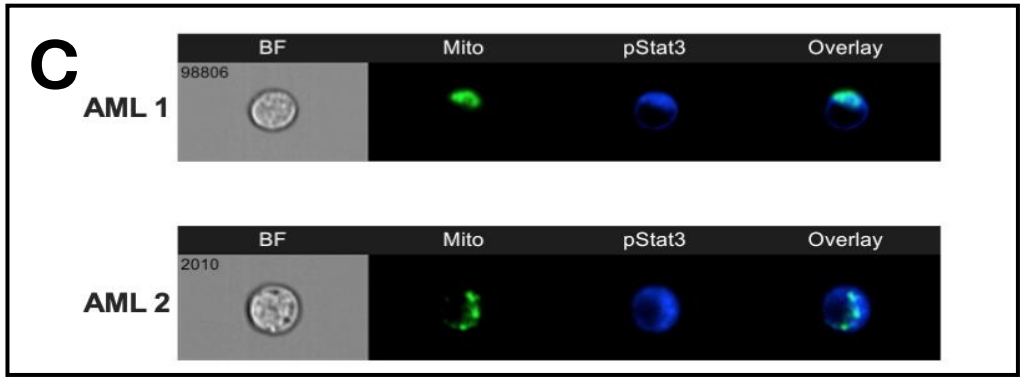

STAT3 inhibition decreases pSTAT3 in the whole cell (left) and in the mitochondria (right)

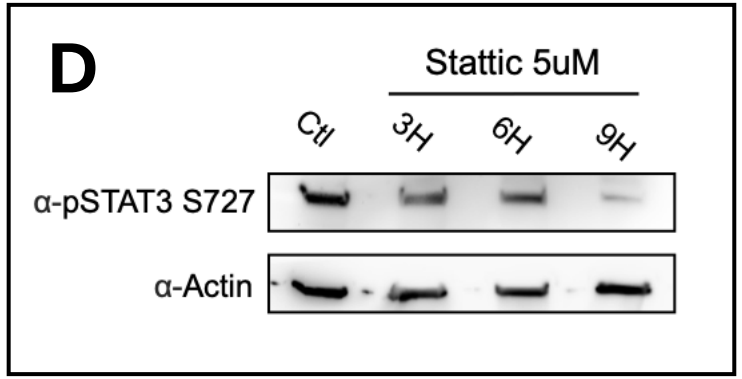

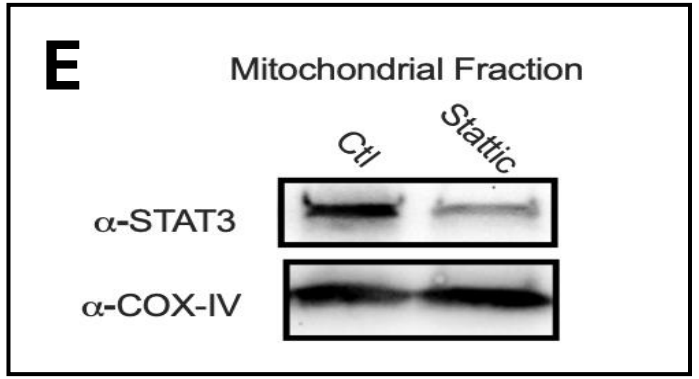

Results

Mitochondrial STAT3 interacts with Voltage Dependent Anion Channel-1 (VDAC1)

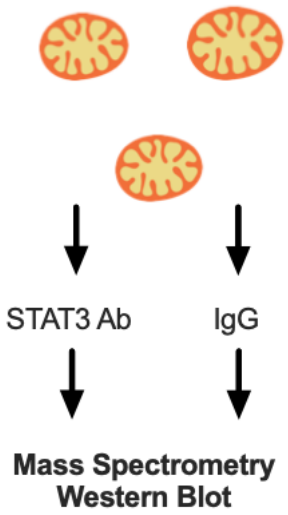

Co-IP Assay

Results

Mitochondrial STAT3 interacts with Voltage Dependent Anion Channel-1 (VDAC1)

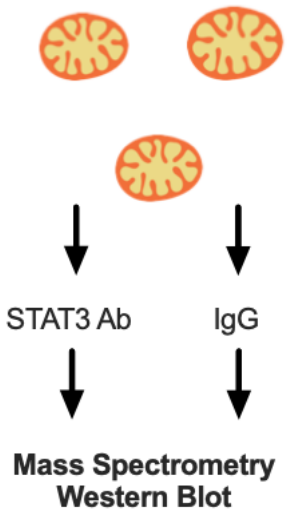

STAT3 Binding Proteins	
ATP5PO –	Complex V
FABP5 –	Fatty Acid Binding Protein
IDH3 –	TCA cycle
MRPS5 –	Mitochondrial Ribosomal Protein
SLC25A5/ ANT2-	- ADP/ATP Transport
VDAC1-	Anion Channel (including Ca+)

Co-IP Assay

Proteomic Analysis

Results

Mitochondrial STAT3 interacts with Voltage Dependent Anion Channel-1 (VDAC1)

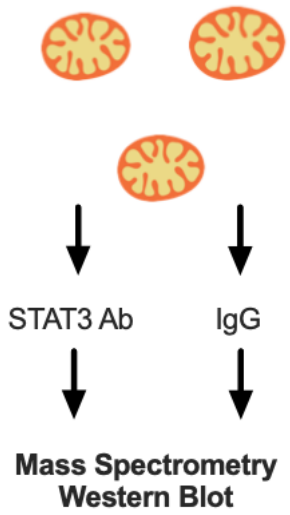

STAT3 Binding Proteins	
ATP5PO –	Complex V
FABP5 –	Fatty Acid Binding Protein
IDH3 –	TCA cycle
MRPS5 –	Mitochondrial Ribosomal Protein
SLC25A5/ ANT2-	- ADP/ATP Transport
VDAC1-	Anion Channel (including Ca+)

Co-IP Assay

Proteomic Analysis

Results

Mitochondrial STAT3 interacts with Voltage Dependent Anion Channel-1 (VDAC1)

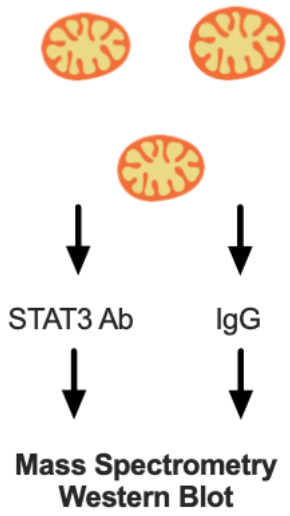

Co-IP Assay

STAT3 Binding Proteins	
ATP5PO –	Complex V
FABP5 –	Fatty Acid Binding Protein
IDH3 –	TCA cycle
MRPS5 –	Mitochondrial Ribosomal Protein
SLC25A5/ ANT2-	- ADP/ATP Transport
VDAC1-	Anion Channel (including Ca+)

Proteomic Analysis

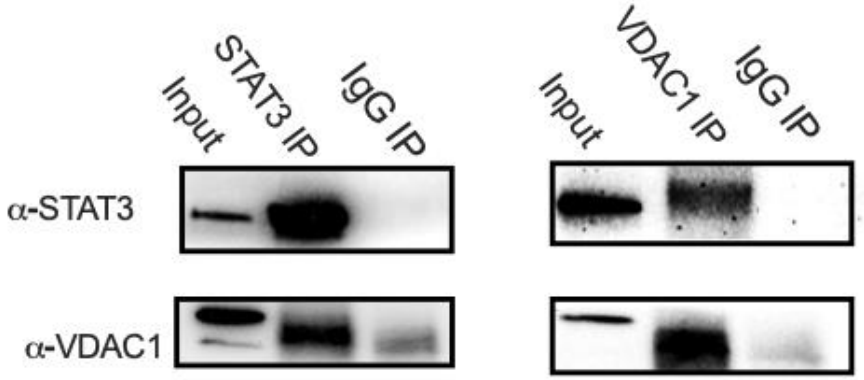

Western Blot

Results

Mitochondrial STAT3 interacts with Voltage Dependent Anion Channel-1 (VDAC1)

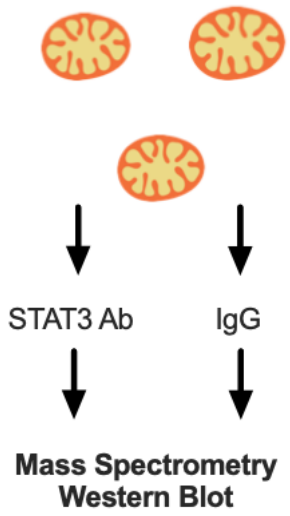

Co-IP Assay

STAT3 Binding Proteins	
ATP5PO –	Complex V
FABP5 –	Fatty Acid Binding Protein
IDH3 –	TCA cycle
MRPS5 –	Mitochondrial Ribosomal Protein
SLC25A5/ ANT2-	- ADP/ATP Transport
VDAC1-	Anion Channel (including Ca+)

Proteomic Analysis

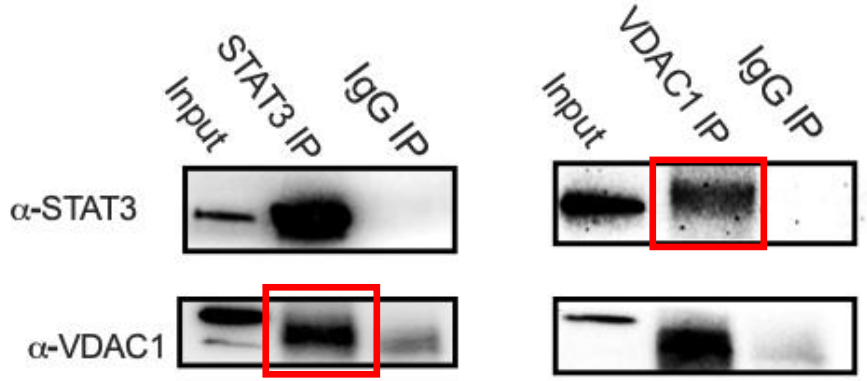

Western Blot

Physiologic roles of VDAC1

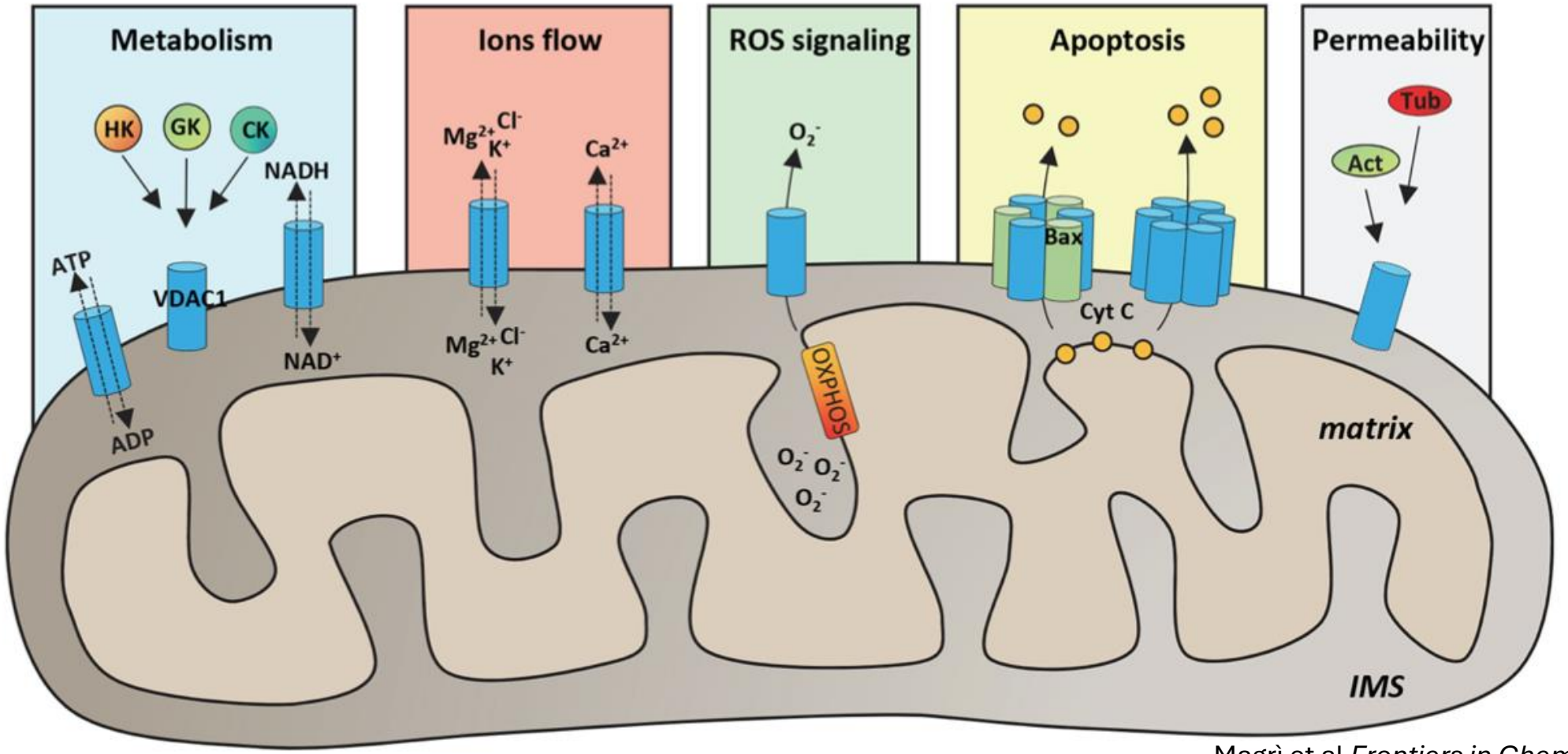

Magrì et al *Frontiers in Chemistry*, 2018

Physiologic roles of VDAC1

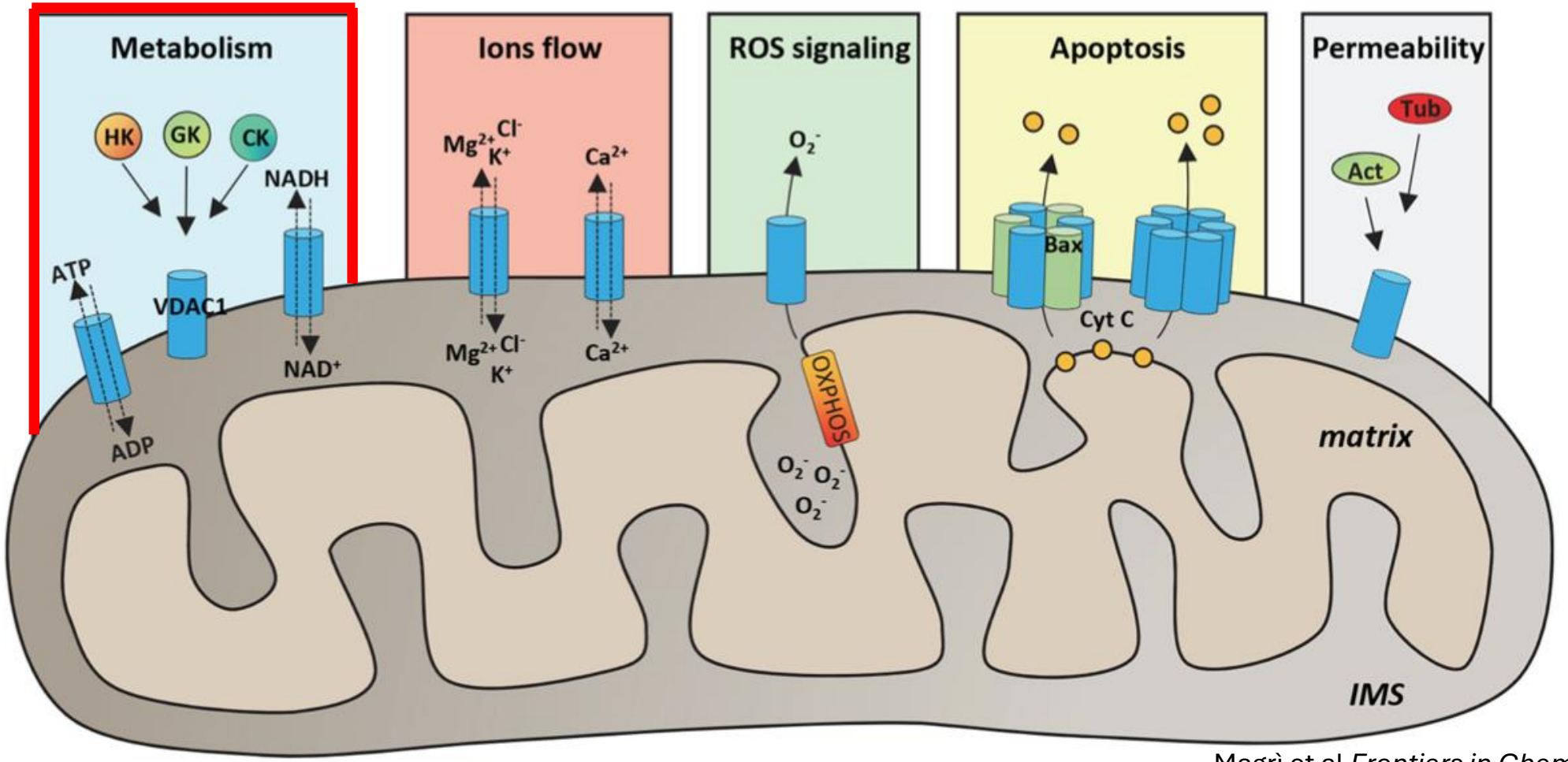

Magrì et al *Frontiers in Chemistry*, 2018

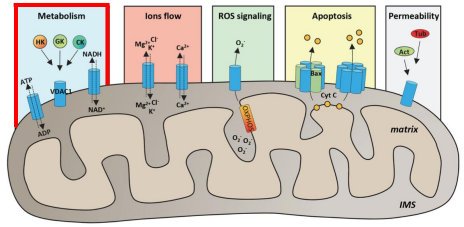

Results

STAT3 and VDAC1 affect energy metabolism in leukemic cells

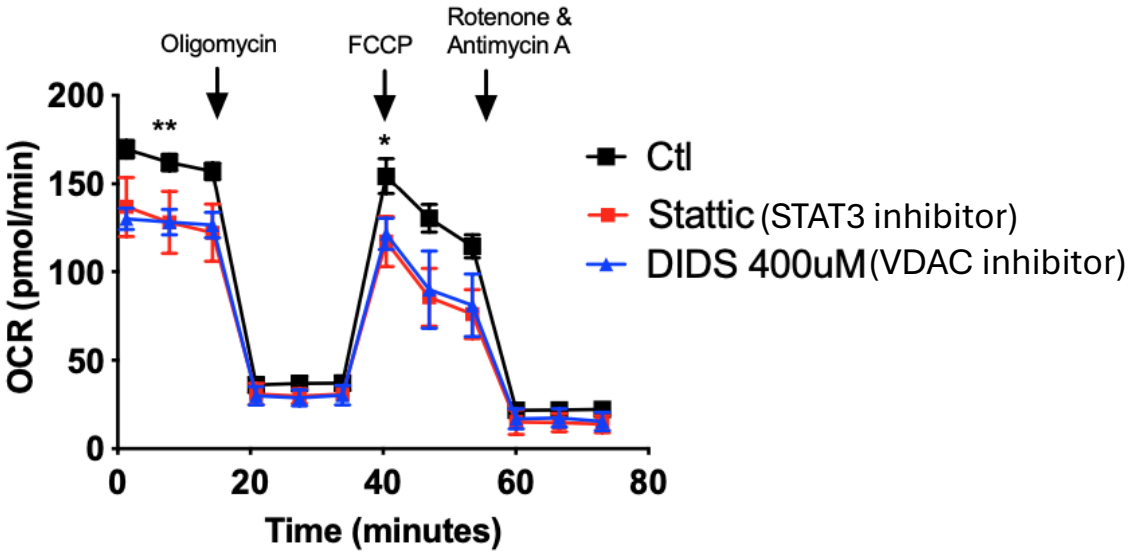

Seahorse Mito Stress Testing

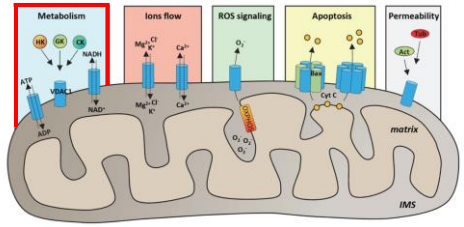

Results

STAT3 and VDAC1 affect energy metabolism in leukemic cells

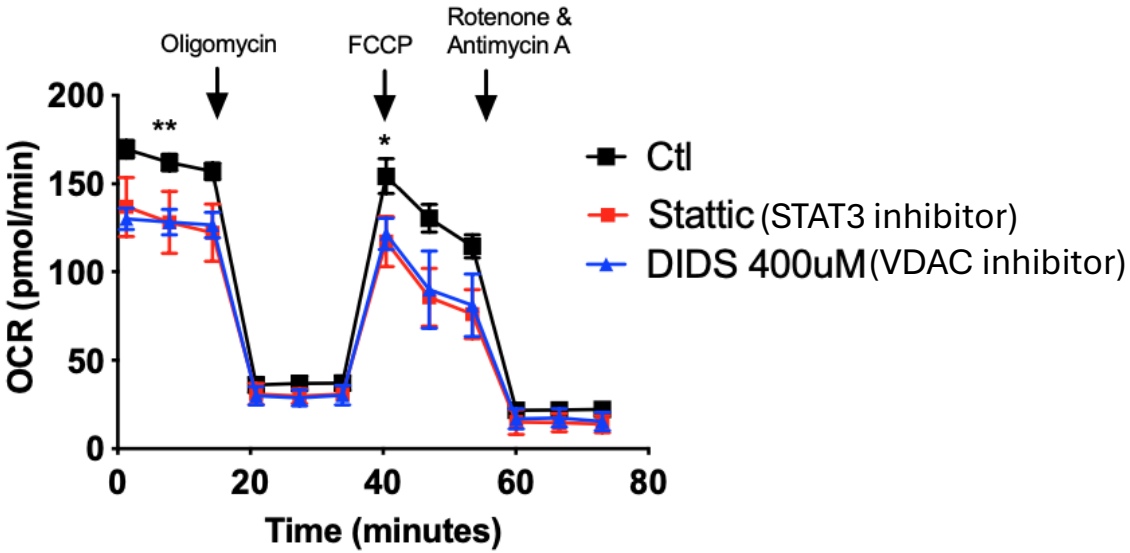

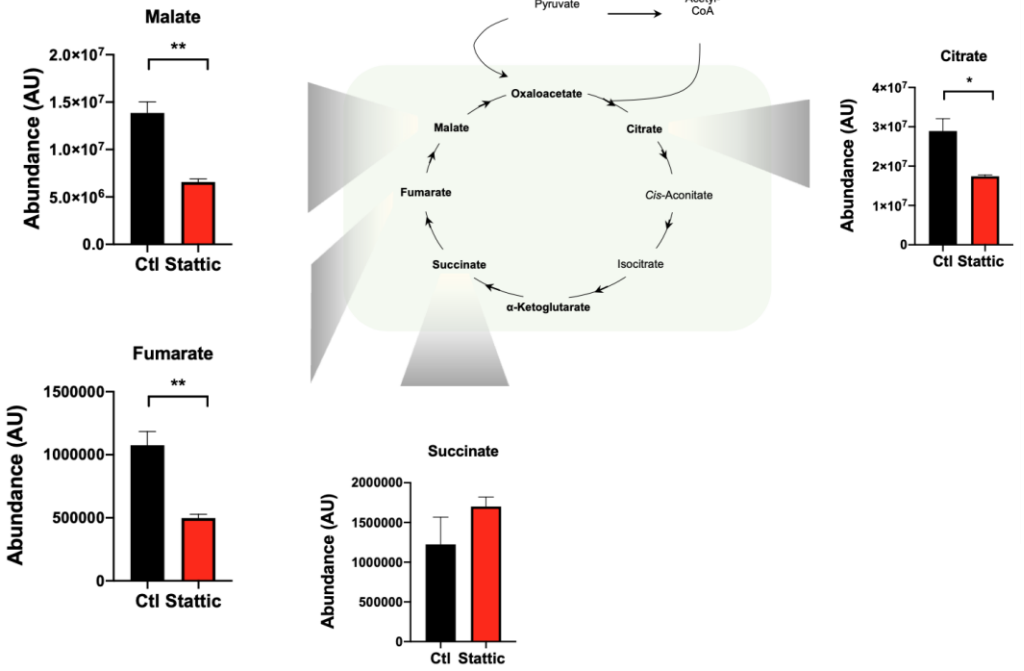

Seahorse Mito Stress Testing

Metabolomics Assay

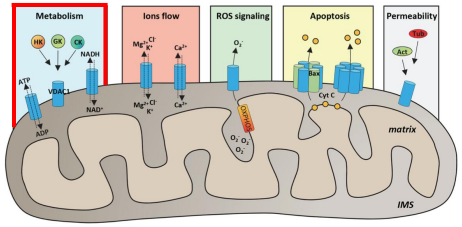

Results

STAT3 and VDAC1 affect energy metabolism in leukemic cells

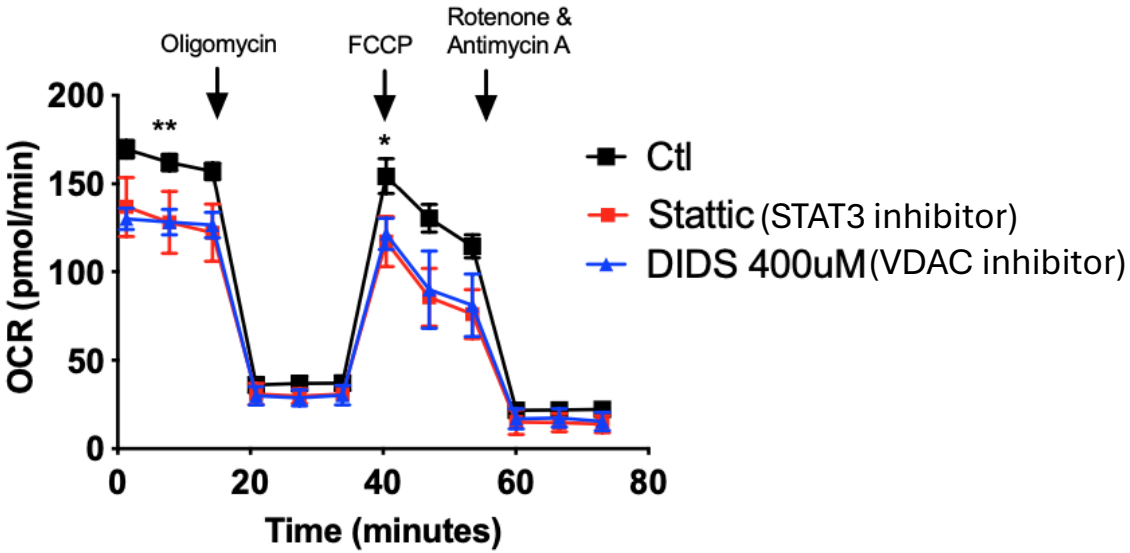

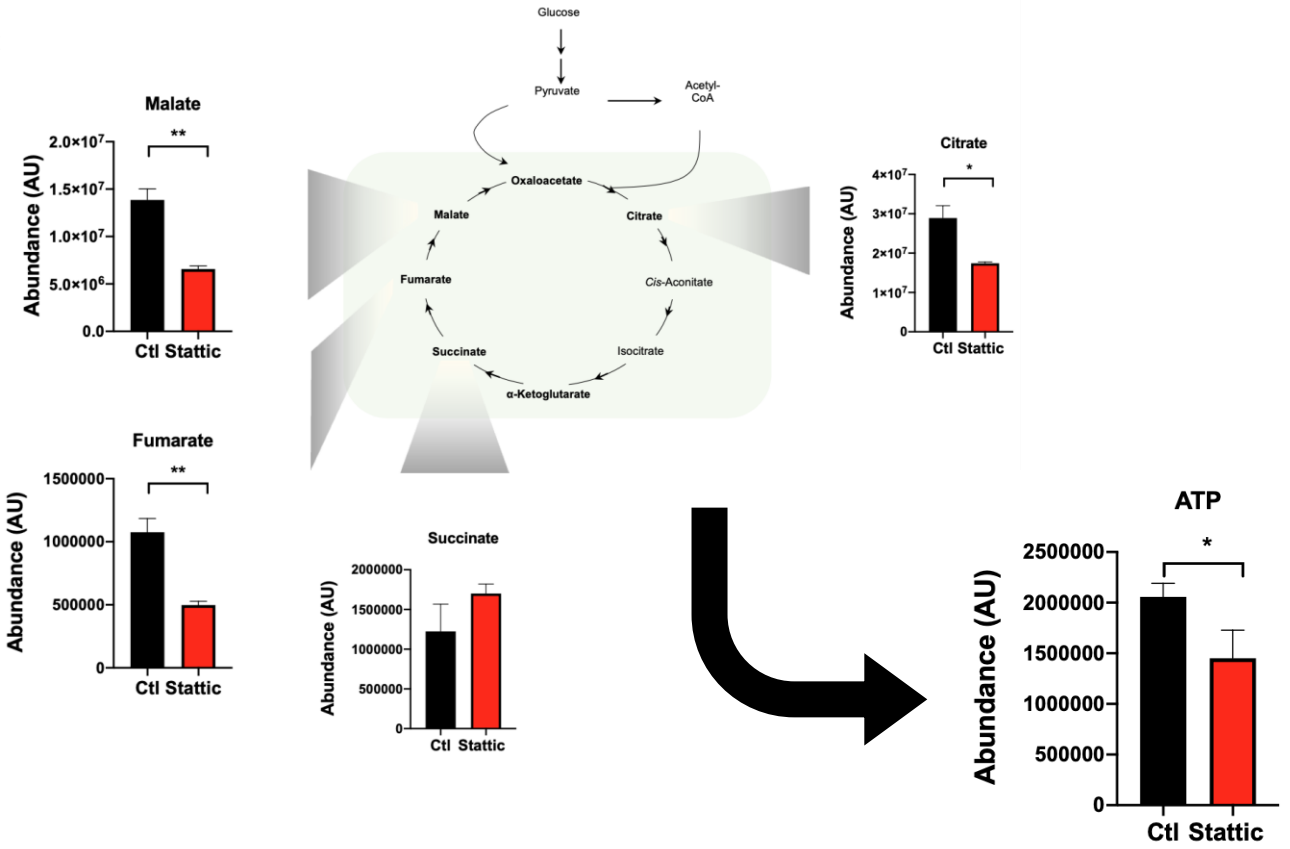

Seahorse Mito Stress Testing

Metabolomics Assay

Physiologic roles of VDAC1

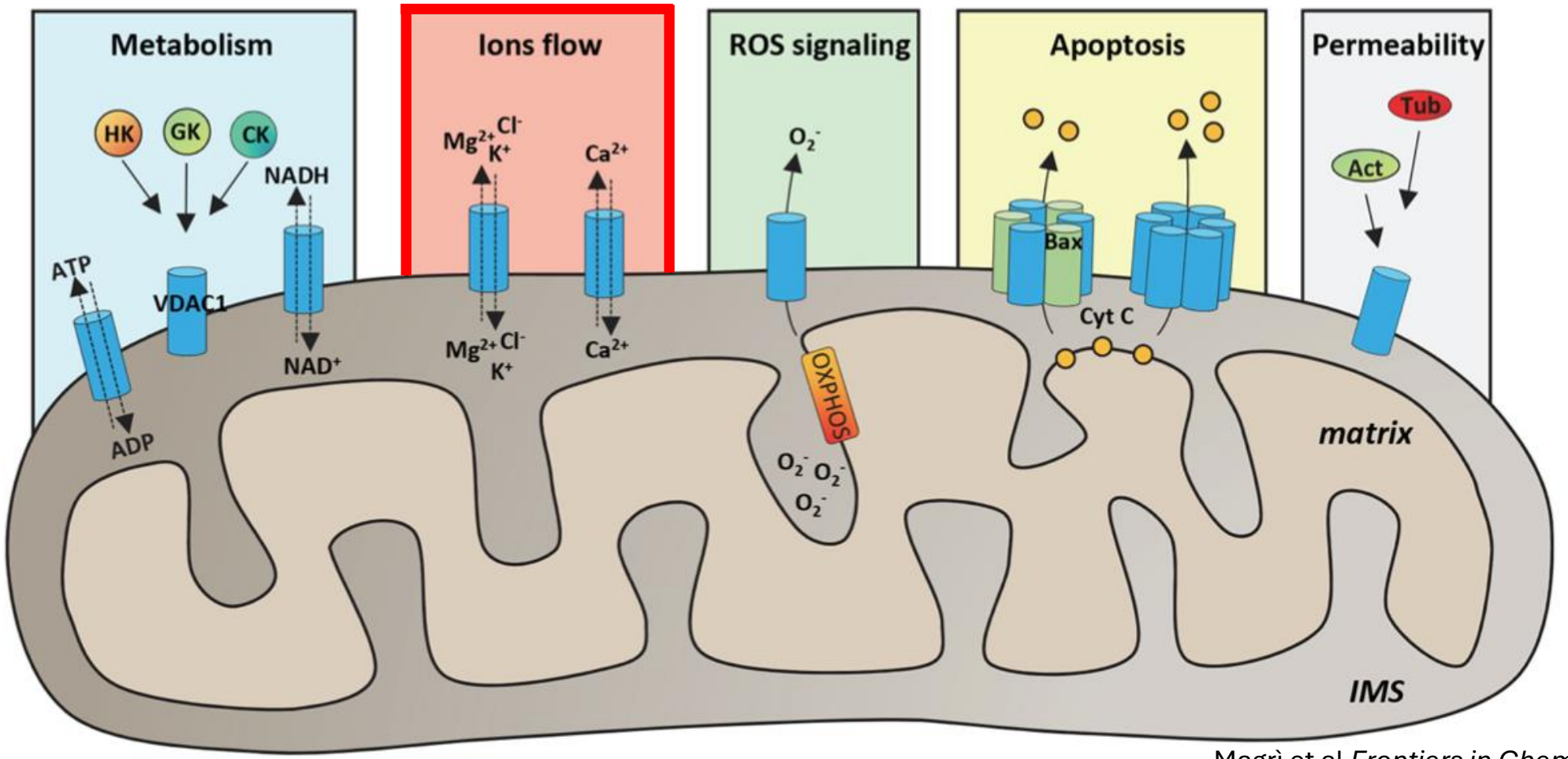

Magrì et al *Frontiers in Chemistry*, 2018

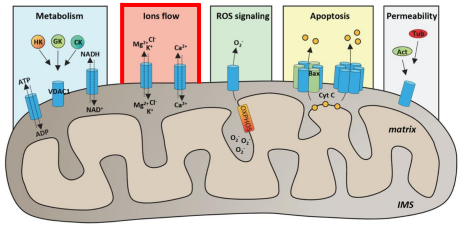

Results

STAT3 and VDAC1 inhibition decreases mitochondrial Ca^{2+}

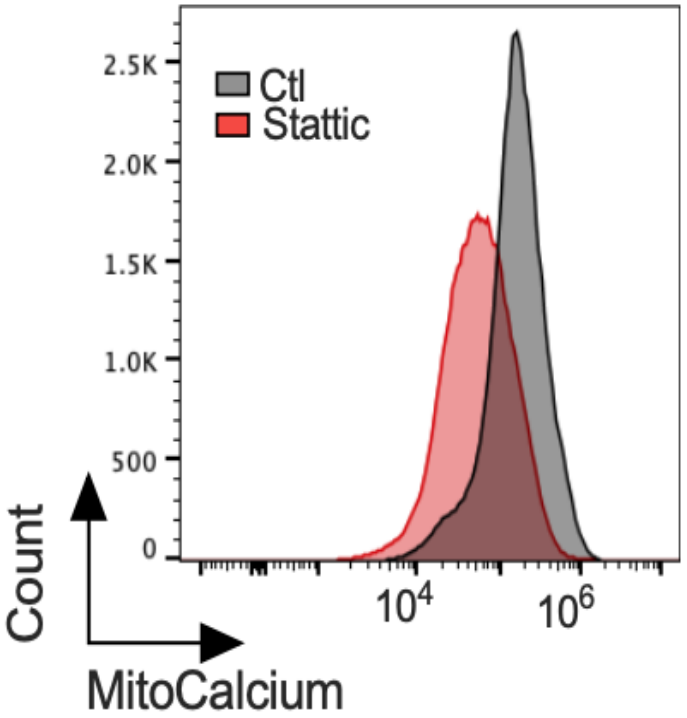

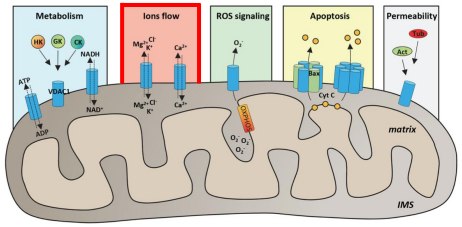

Results

STAT3 and VDAC1 inhibition decreases mitochondrial Ca^{2+}

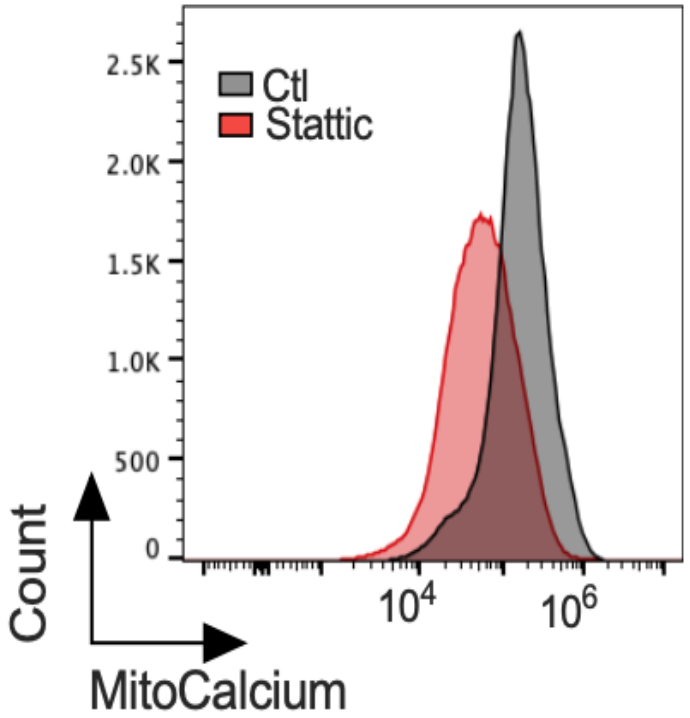

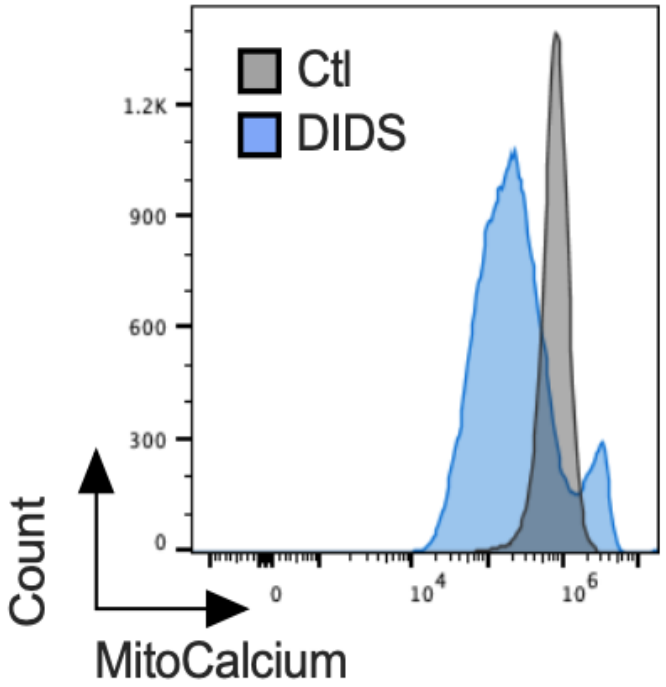

Results

STAT3 and VDAC1 inhibition decreases mitochondrial Ca^{2+}

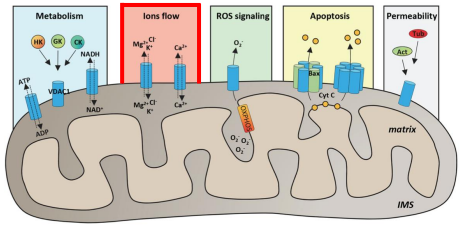

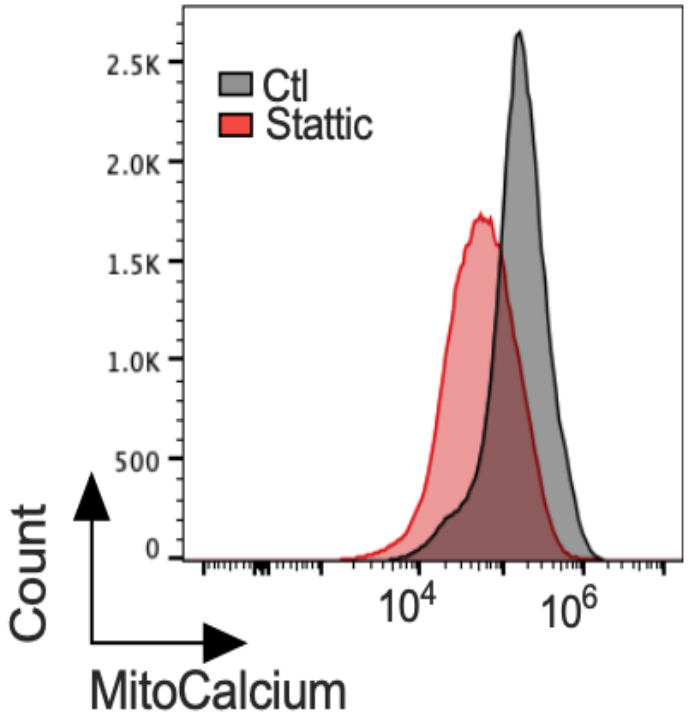

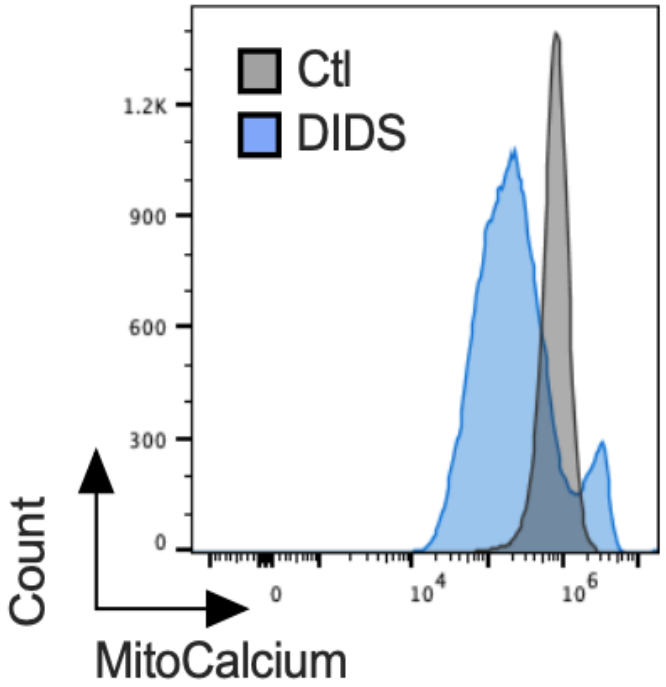

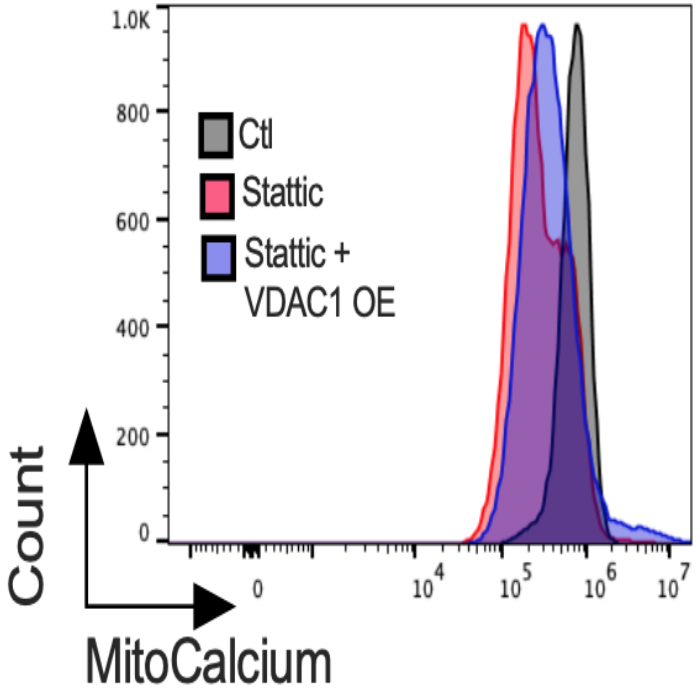

Physiologic roles of VDAC1

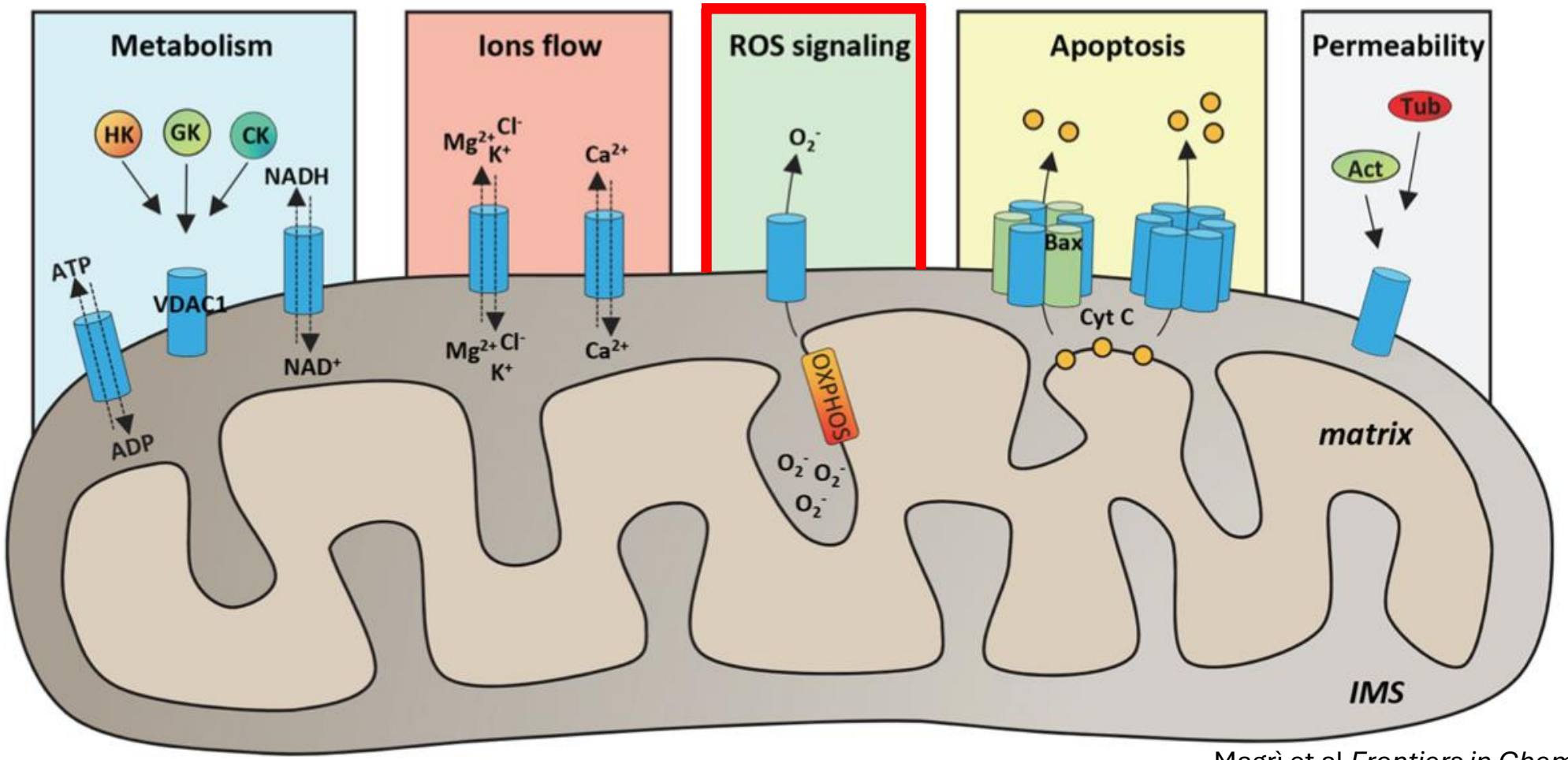

Magrì et al *Frontiers in Chemistry*, 2018

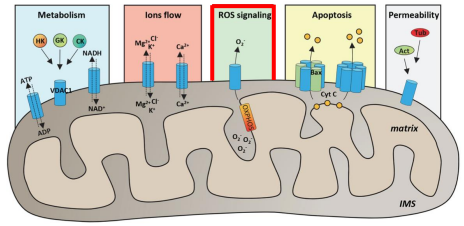

Results

STAT3 inhibition increases mitochondrial ROS

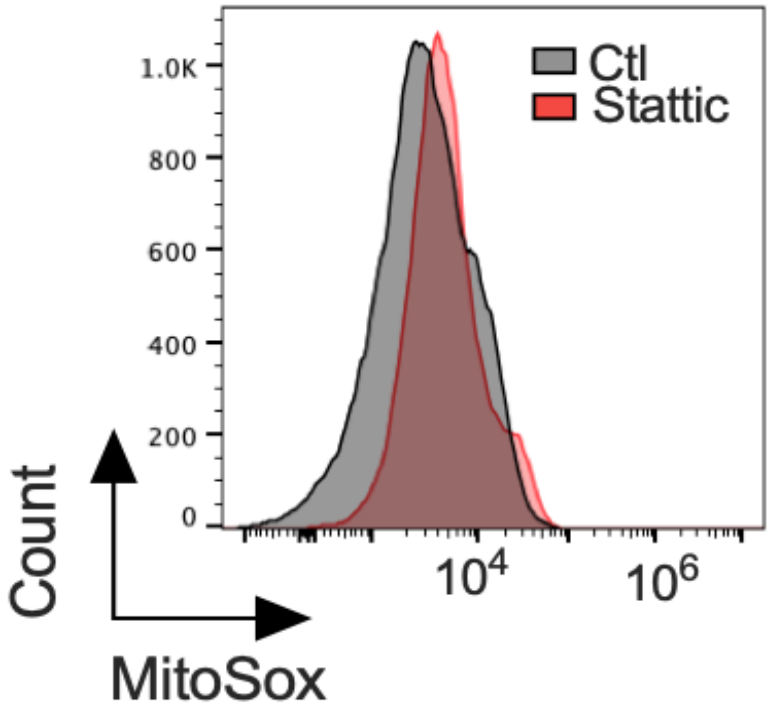

STAT3 inhibition *increases* ROS…

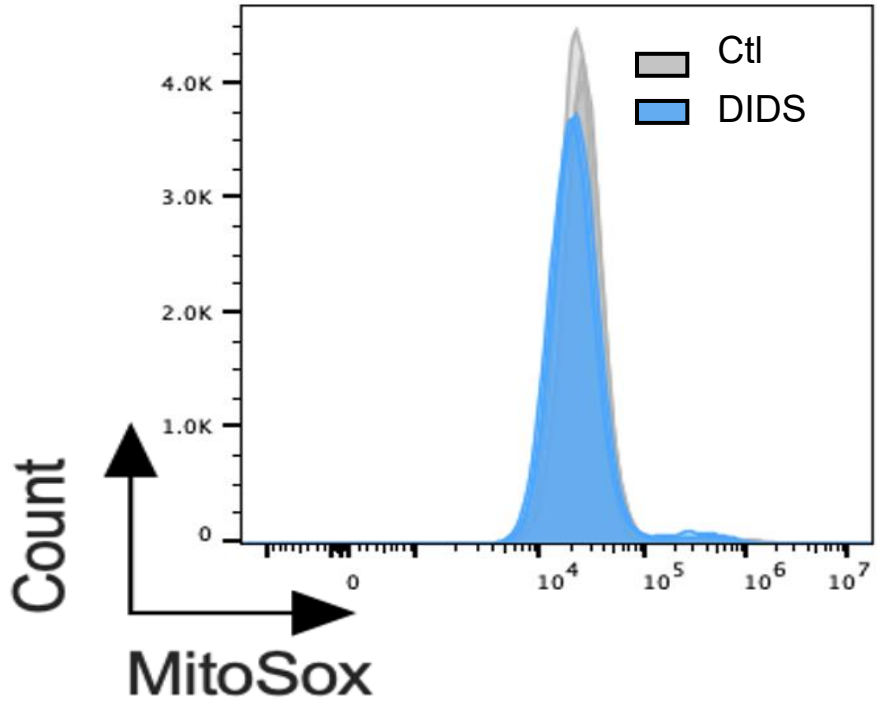

VDAC1 inhibition *does not change* ROS

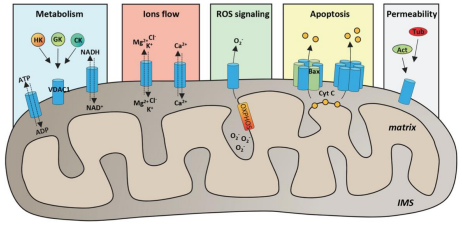

Results

Mitochondrial changes with STAT3 and VDAC1 inhibition

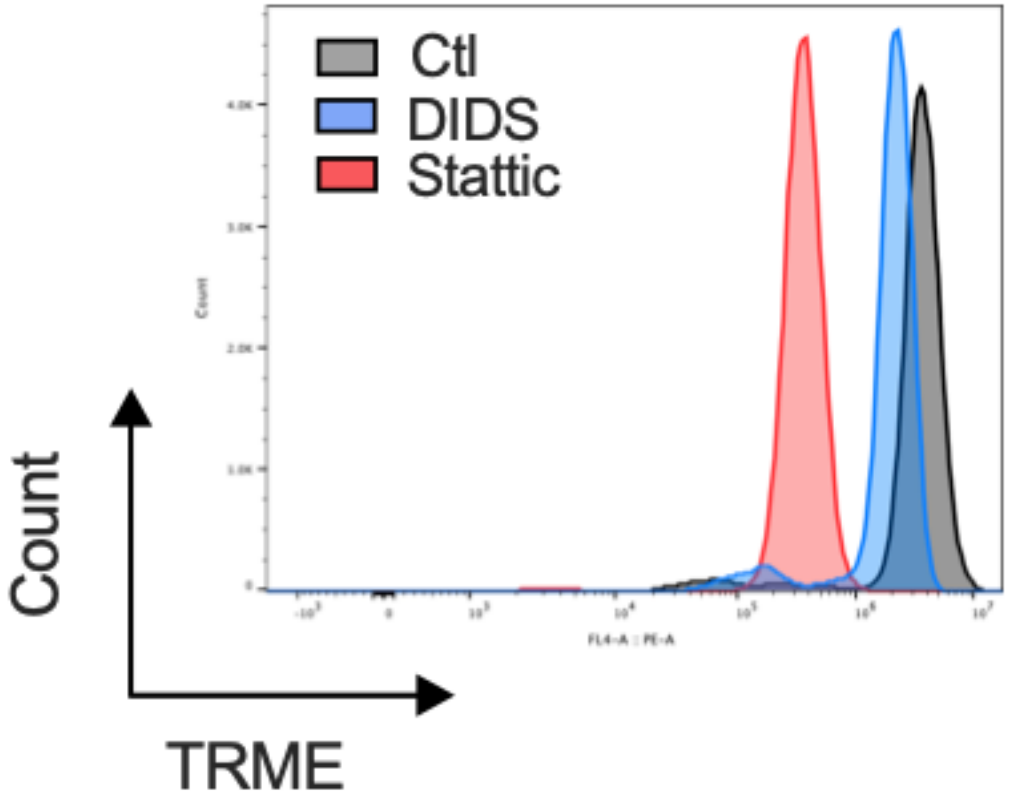

Both STAT3 and VDAC1 inhibition result in *decreased* mitochondrial membrane potential

Results

STAT3 and VDAC1 inhibition disrupt mitochondrial dynamics

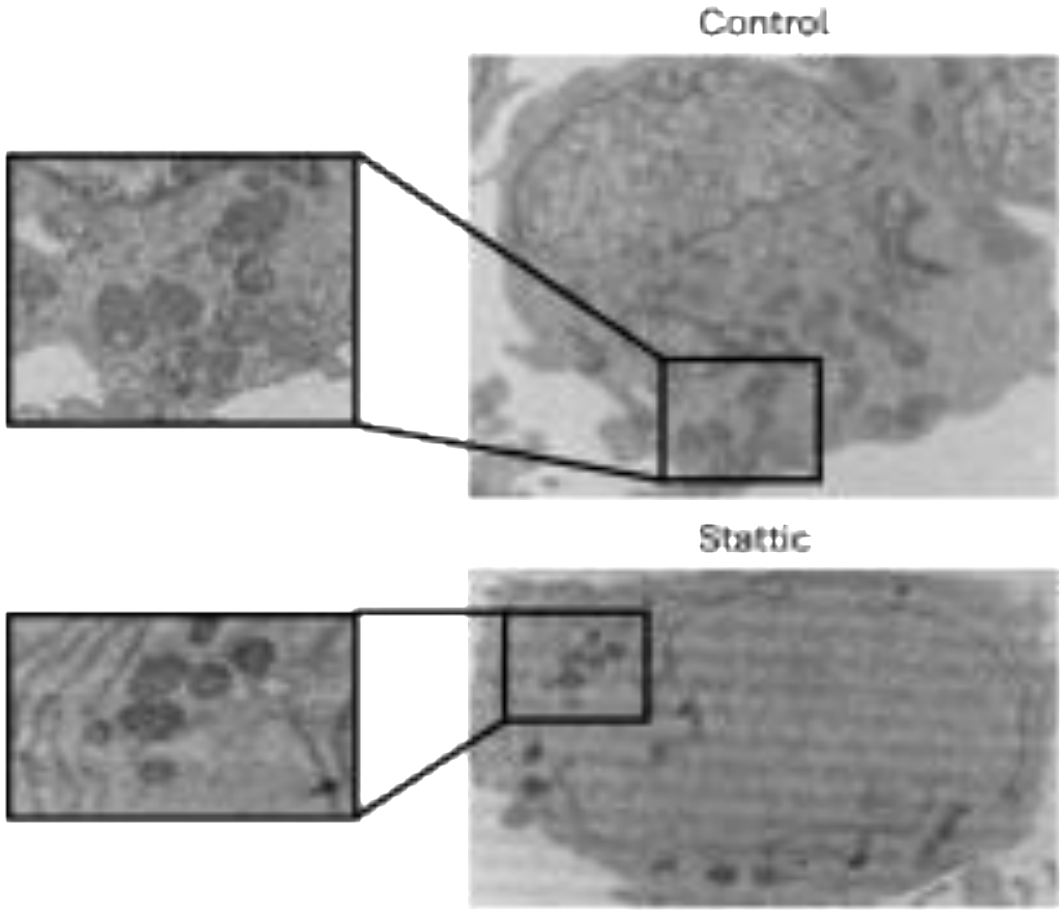

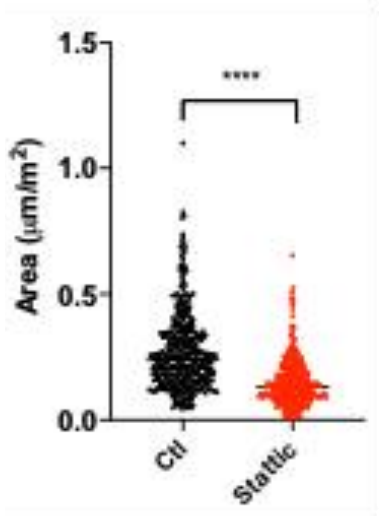

Decreases size of mitochondria…

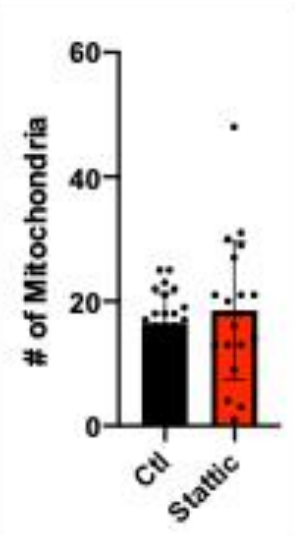

But no significant change in number

Results

Mitochondrial changes with STAT3 and VDAC1 inhibition

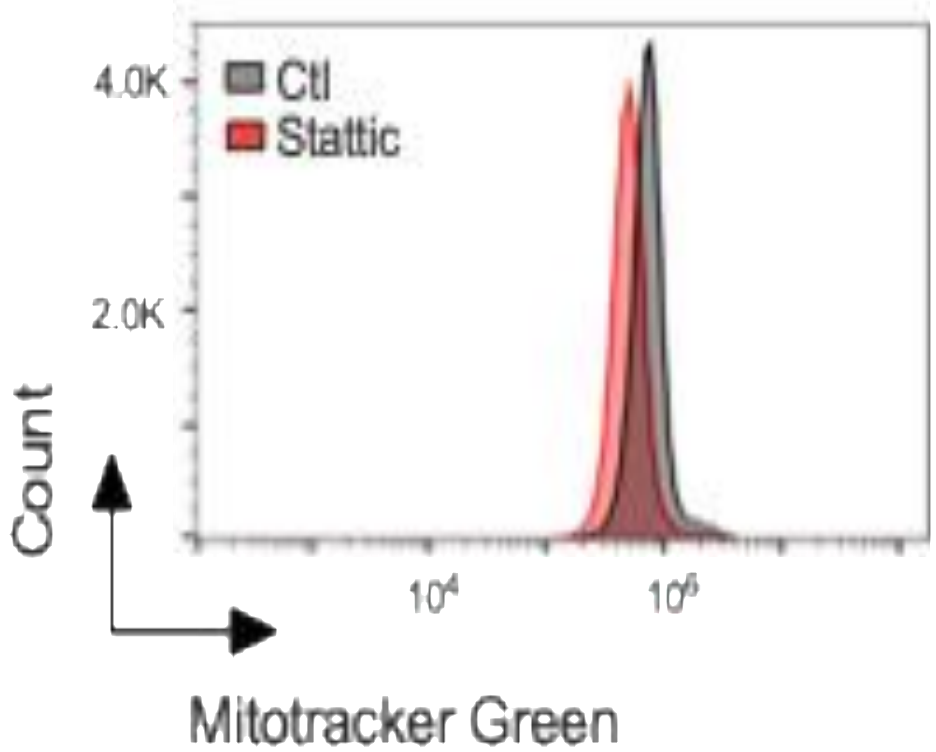

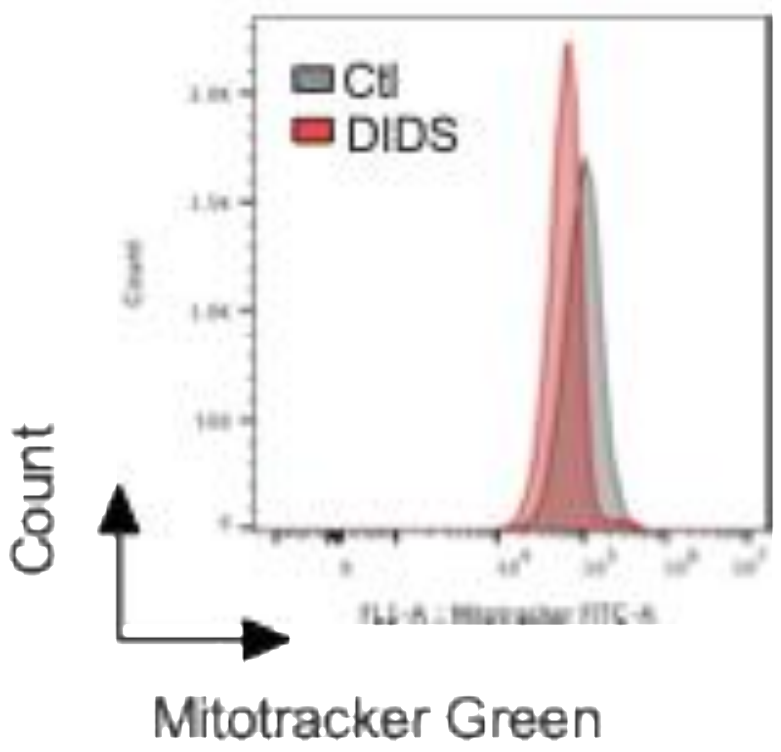

Results

STAT3 and VDAC1 inhibition decrease viability and impair engraftment potential

In vitro treatments

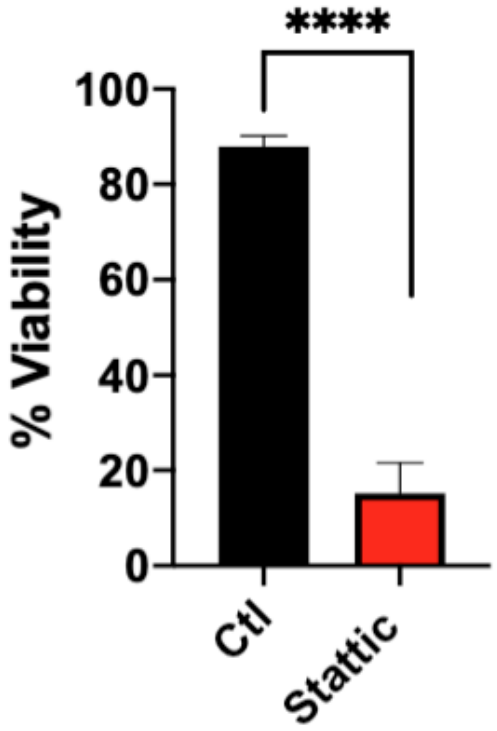

Molm13 cells

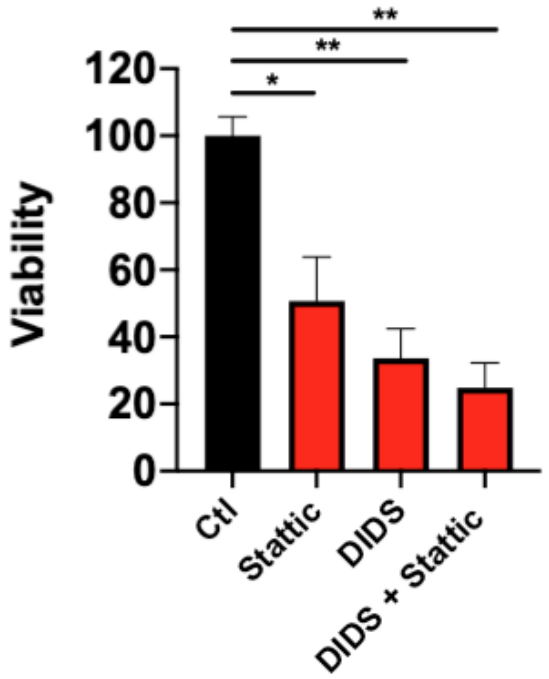

Primary AML Samples

Results

STAT3 and VDAC1 inhibition decrease viability and impair engraftment potential

Ex vivo PDX mouse models

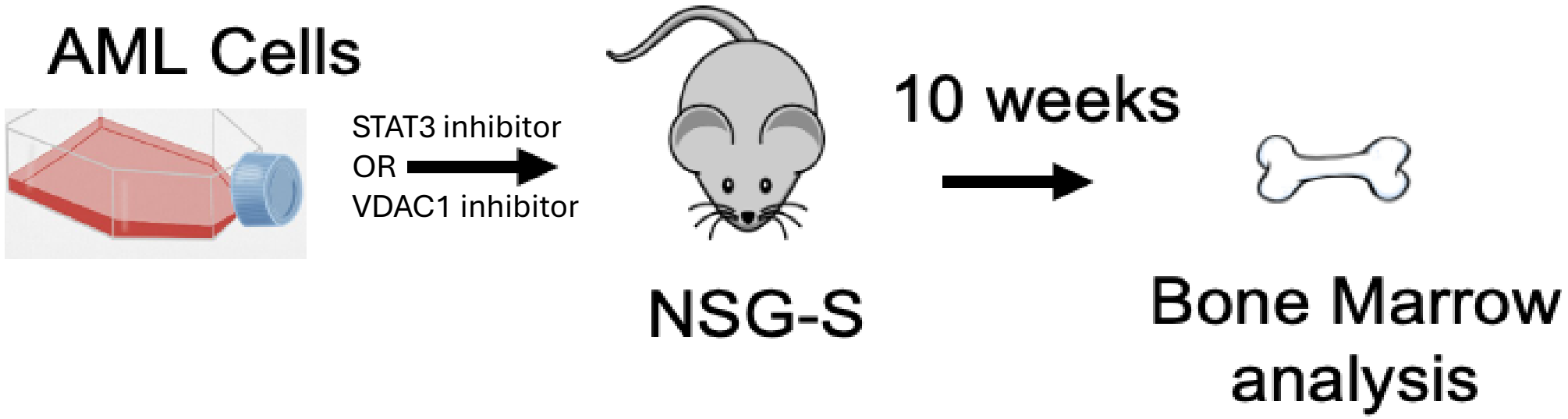

Results

STAT3 and VDAC1 inhibition decrease viability and impair engraftment potential

Ex vivo PDX mouse models

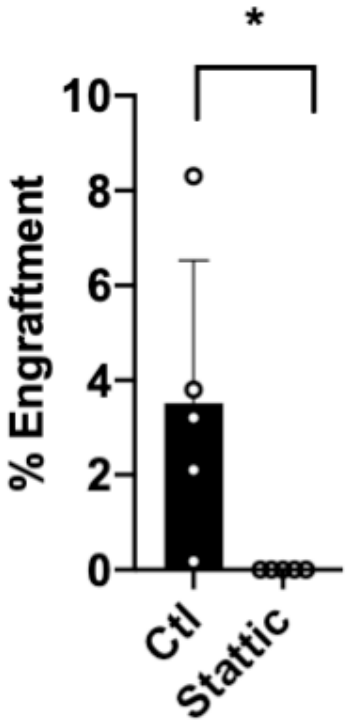

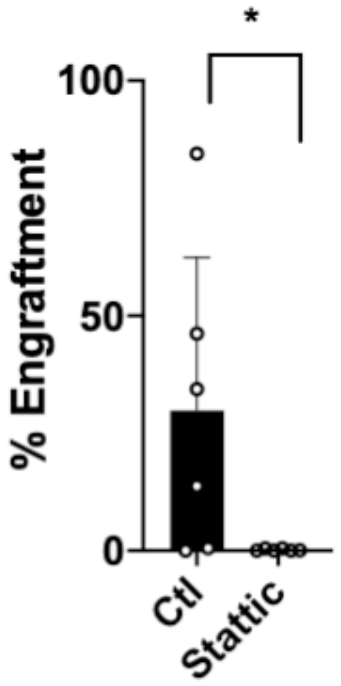

Inhibition of STAT3

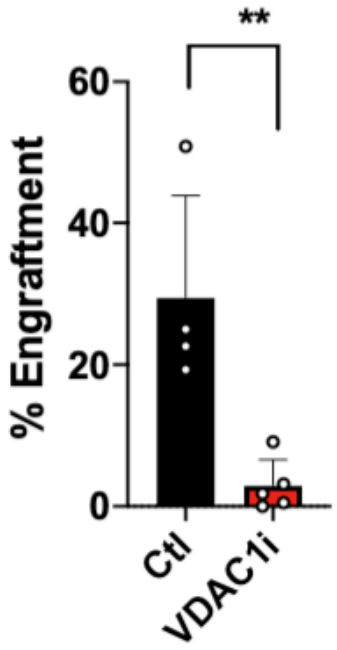

Inhibition of VDAC1

Results

STAT3 and VDAC1 inhibition decrease viability and impair engraftment potential

Ex vivo PDX mouse models

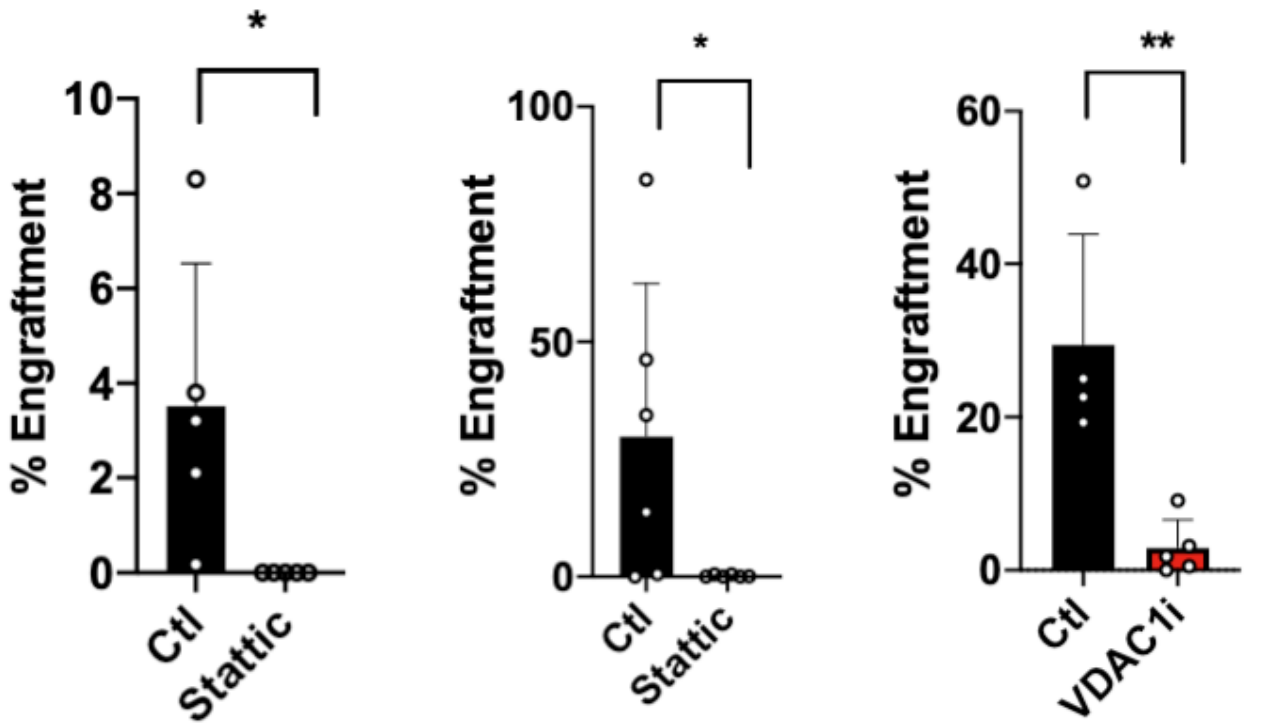

Inhibition of STAT3

Inhibition of VDAC1

HSC Colony Forming Assays

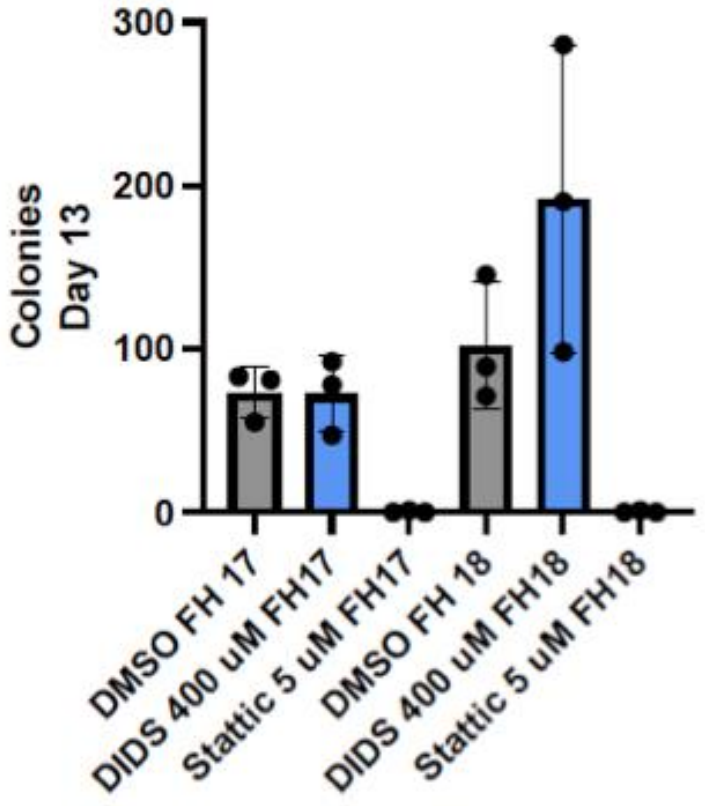

Results

STAT3 and VDAC1 inhibition decrease viability and impair engraftment potential

Ex vivo PDX mouse models

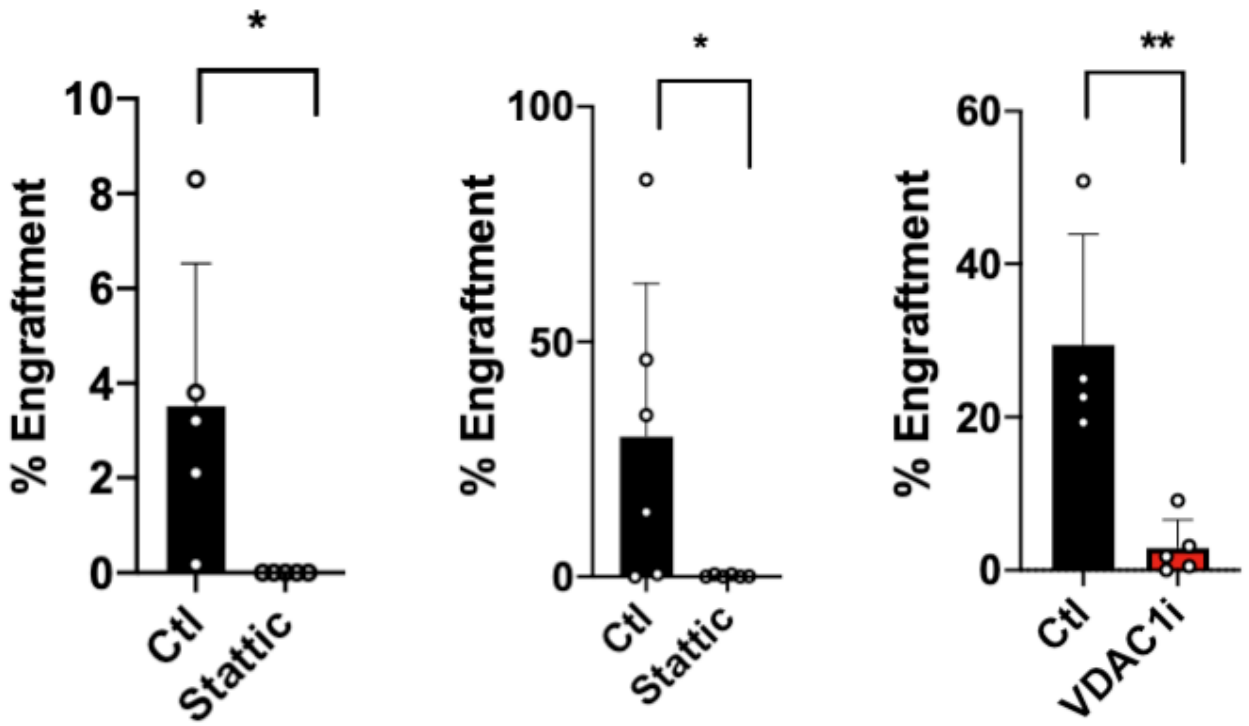

Inhibition of STAT3

Inhibition of VDAC1

HSC Colony Forming Assays

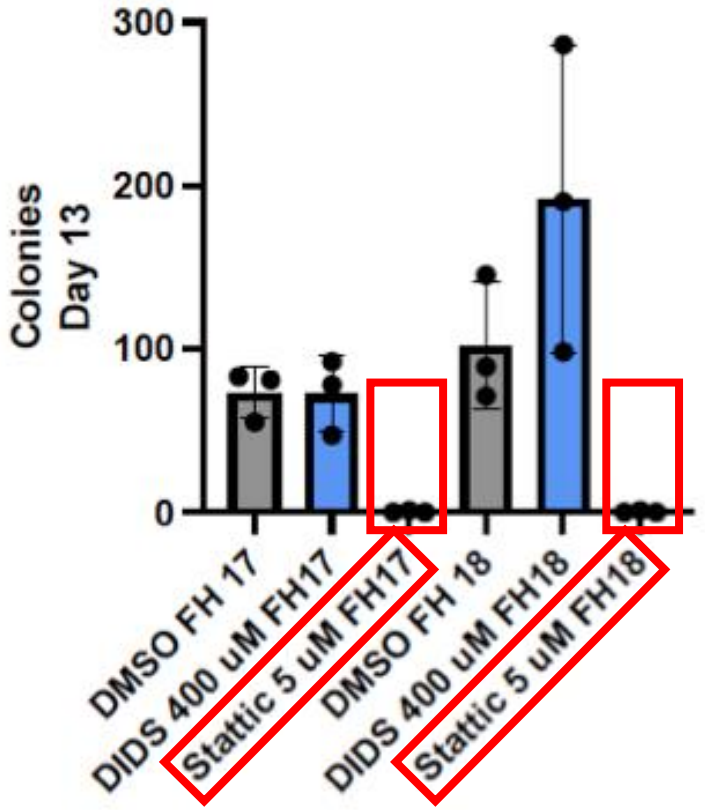

Conclusions

- STAT3 is prominently expression in AML and phosphorylation triggers mitochondrial localization
- STAT3 interacts with VDAC1 in the mitochondria, a novel protein-protein interaction
- Inhibition of STAT3 and VDAC1 results in:
  - Impaired OXPHOS
  - Decreased mitochondrial calcium
  - Decreased Mito Membrane Potential
  - Decreased AML cell viability
  - Impairs AML engraftment potential
  - Altered ROS

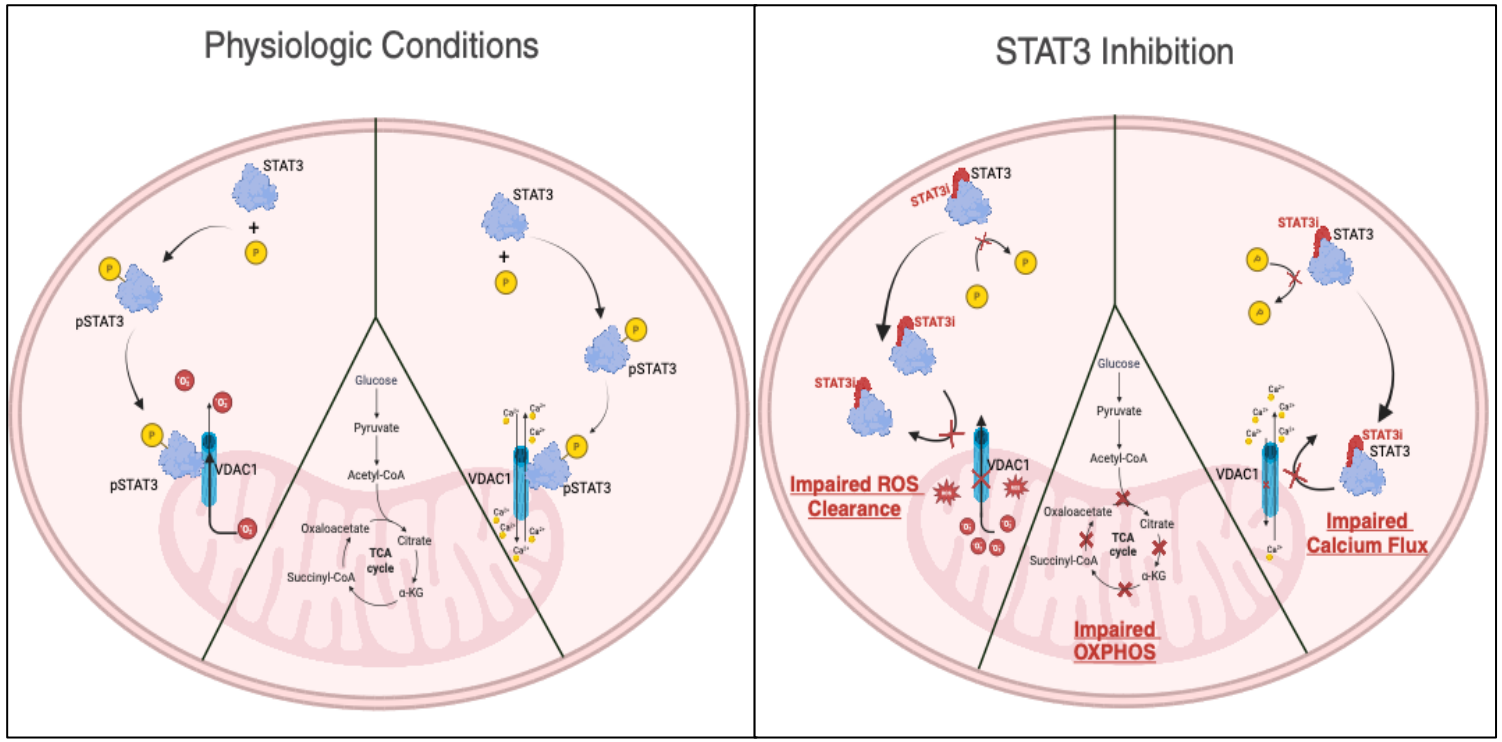

haematologica
Journal of the Ferrata Storti Foundation

The STAT3-VDAC1 axis modulates mitochondrial function and plays a critical role in the survival of acute myeloid leukemia cells

by Kellen B. Gil, Jamie Borg, Rosana Moreira Pereira, Anagha Inguva-Sheth, Geovana Araujo, Jeremy Rahkola, William Showers, Abby Grier, Angelo D'Alessandro, Clayton Smith, Christine McMahon, Daniel A. Pollyea, Austin E. Gillen and Maria L. Amaya

Received: January 10, 2025.
Accepted: June 6, 2025.

Citation: Kellen B. Gil, Jamie Borg, Rosana Moreira Pereira, Anagha Inguva-Sheth, Geovana Araujo, Jeremy Rahkola, William Showers, Abby Grier, Angelo D'Alessandro, Clayton Smith, Christine McMahon, Daniel A. Pollyea, Austin E. Gillen and Maria L. Amaya. The STAT3-VDAC1 axis modulates mitochondrial function and plays a critical role in the survival of acute myeloid leukemia cells.
Haematologica. 2025 June 19. doi: 10.3324/haematol.2025.287352 [Epub ahead of print]

Future Directions

- STAT3 KI mouse experiments
- Recapitulation with CRISPR'd pSTAT3 S727 cell lines
- Investigation of other STAT3 associated proteins
  - ANT2
  - Cyclophilin D
- Studying role in mitochondrial Permeability Transition Pore (MPTP)

Acknowledgements

Amaya Lab
- Maria Amaya (PI)
- Jamie Borg
- Rosana Pereira
- Makenna May

Jordan Lab
- Anagha Inguva-Sheth
- Geovana Araujo
- Sweta Patel

Core Services & Bioinformatics
- Jeremy Rahkola
- Bill Showers
- Abby Grier
- Angelo D'Alessandro
- Austin Gillen

Clinical Collaborators
- Daniel Pollyea
- Clayton Smith
- Christine McMahon
- Aditi Shastri

An *In Vitro* Model of Fetal Growth Restriction Inhibits Angiogenesis via Extracellular Vesicle Release of microRNA 141-3p

Caitlin (Cait) Eason, MD, MPH

Derderian Lab

University of Colorado School of Medicine

December 11, 2025

Children's Hospital Colorado
Here, it's different.™

Affiliated with
University of Colorado
Anschutz Medical Campus

Background: Fetal Growth Restriction

- Fetal weight below the 10th percentile
- Affects 3-10% of pregnancies and accounts for nearly 50% of stillbirths
- High rate of perinatal morbidity/mortality
- Associated with cognitive and developmental delays
- Annual US healthcare cost > $15 billion

Background

- Placental pathology demonstrates reduced feto-placental angiogenesis in FGR
- microRNAs (miRNAs) within the fetal growth restricted placenta have altered levels of expression

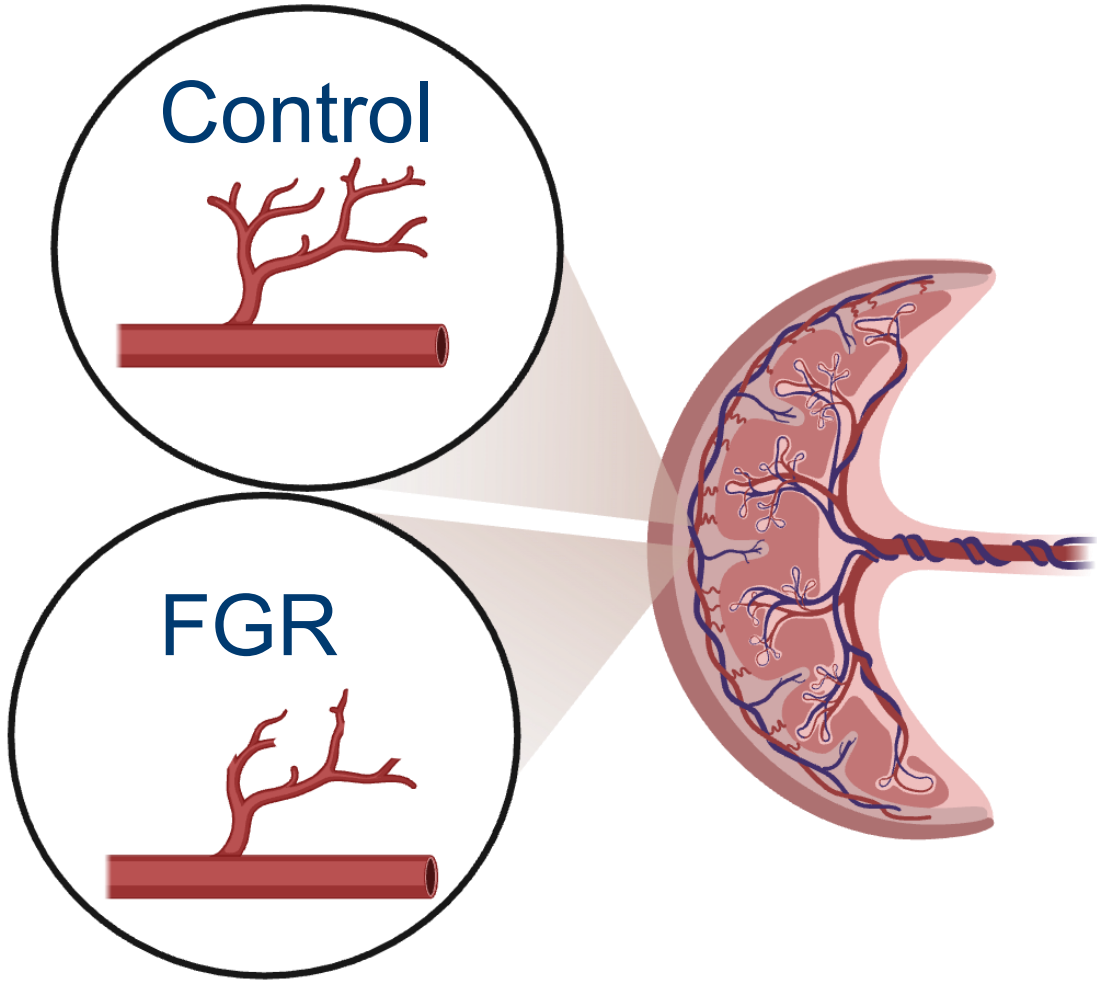

Background

- microRNA

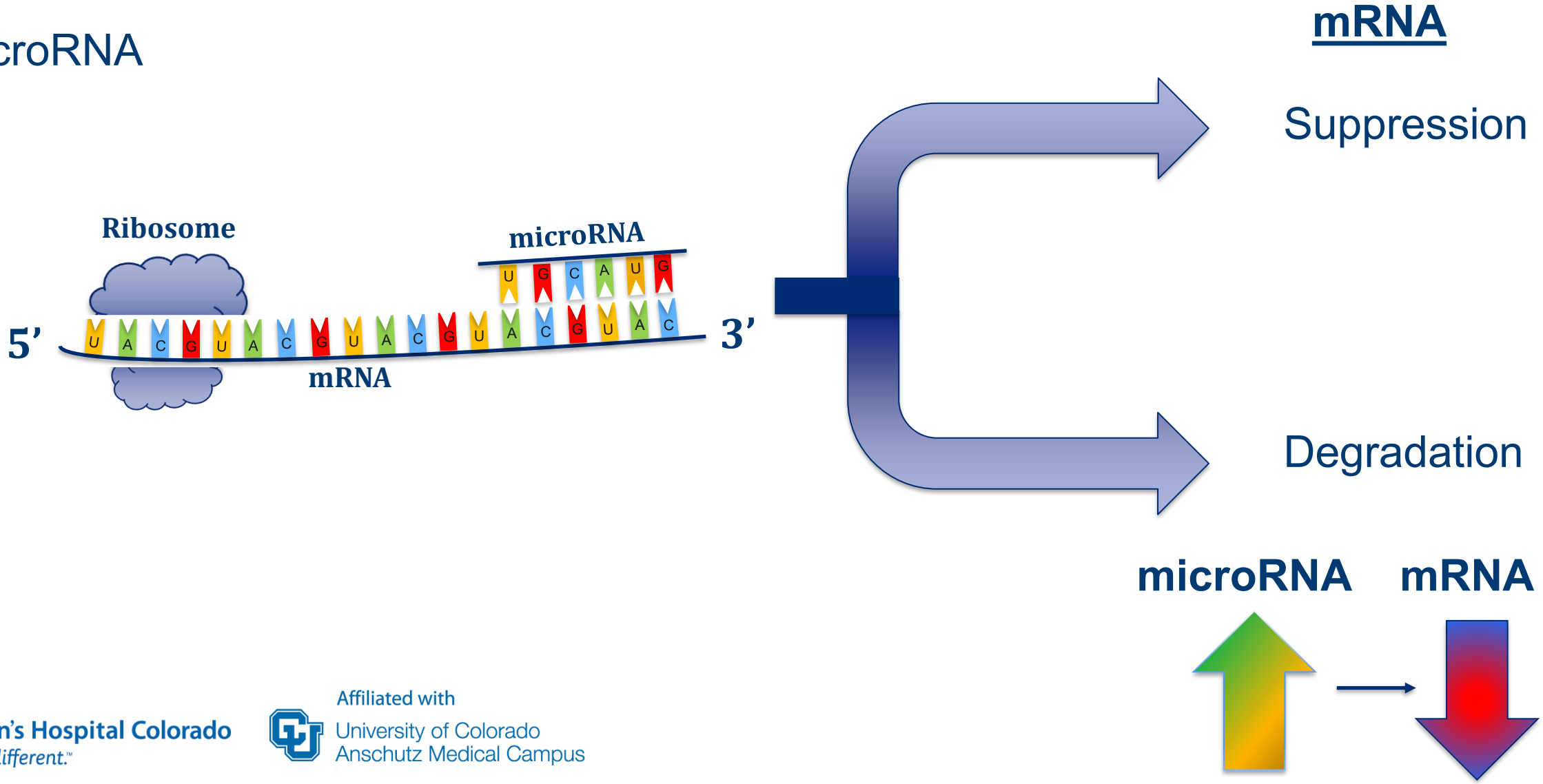

Background

Intracellular Effects

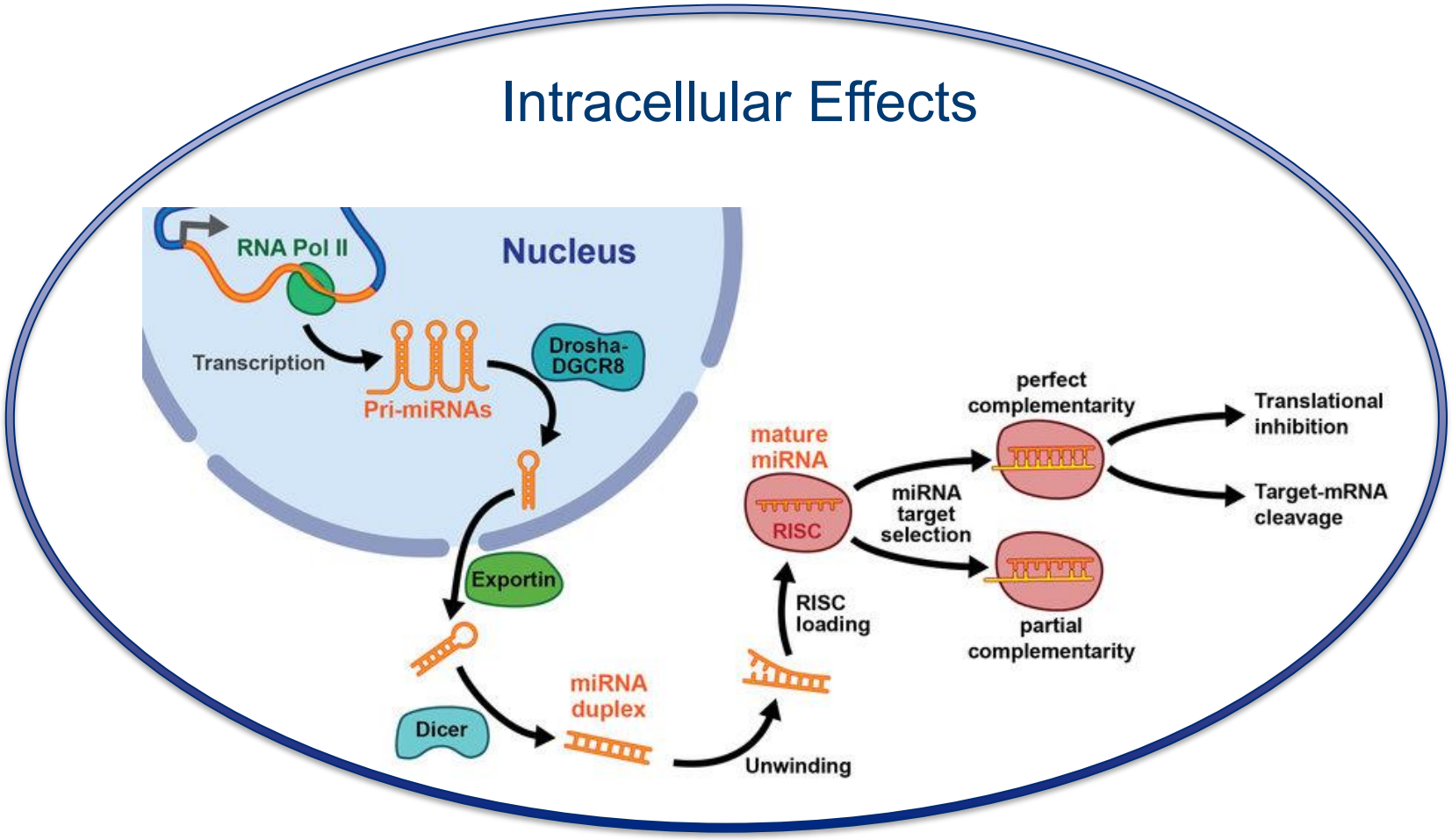

Extracellular Vesicles

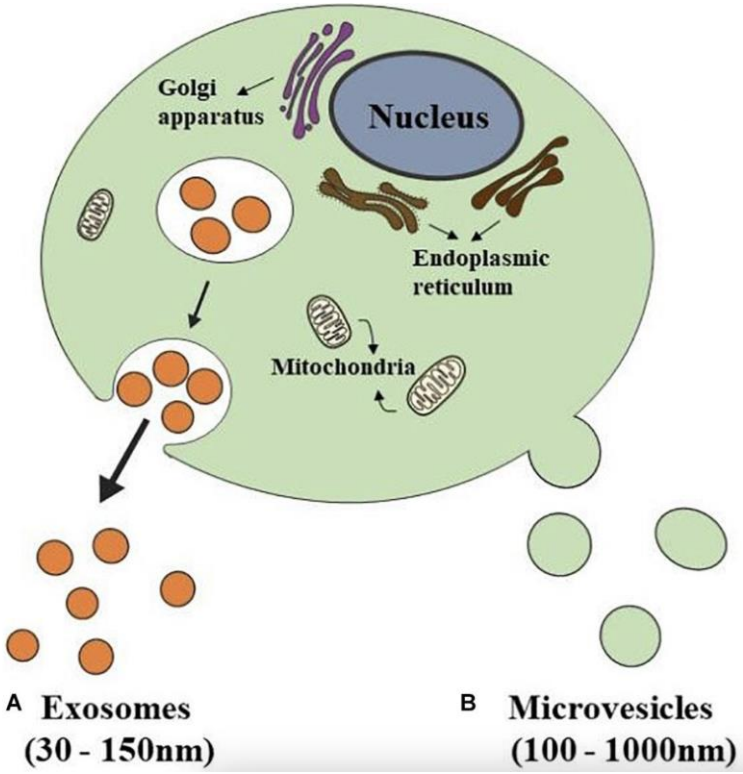

Background

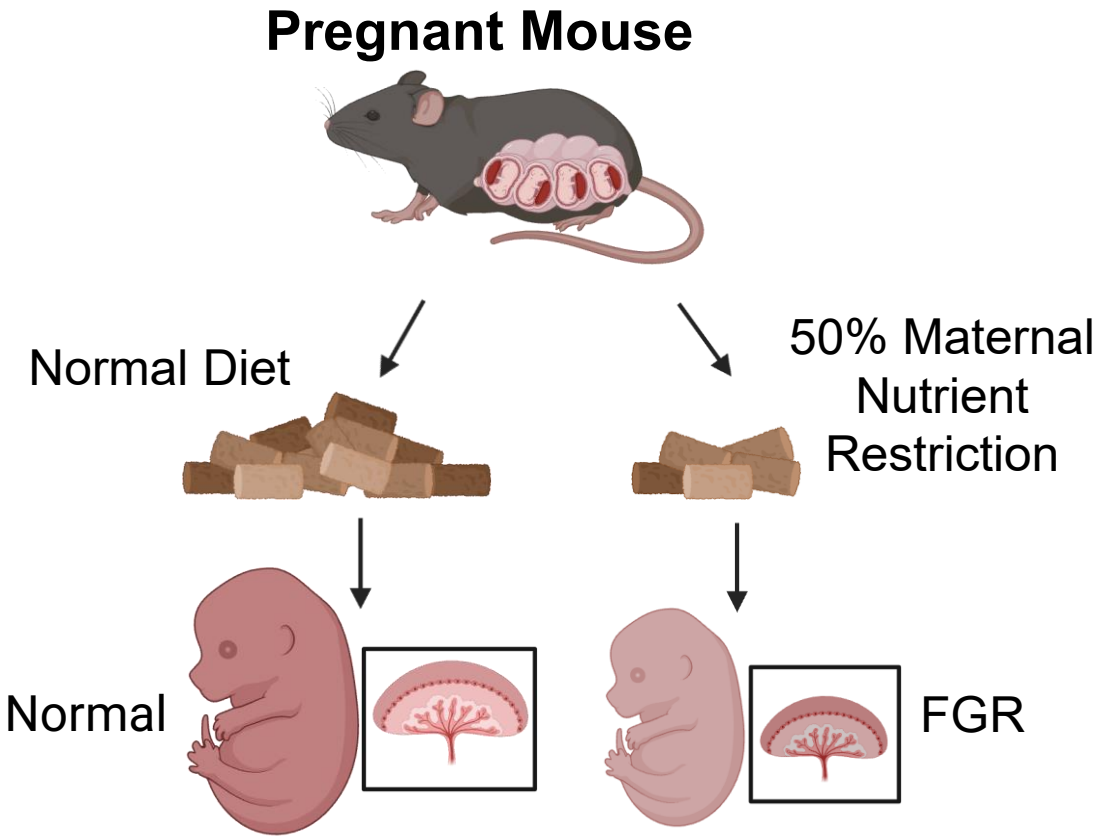
Pregnant Mouse
Normal Diet
50% Maternal Nutrient Restriction
Normal
FGR

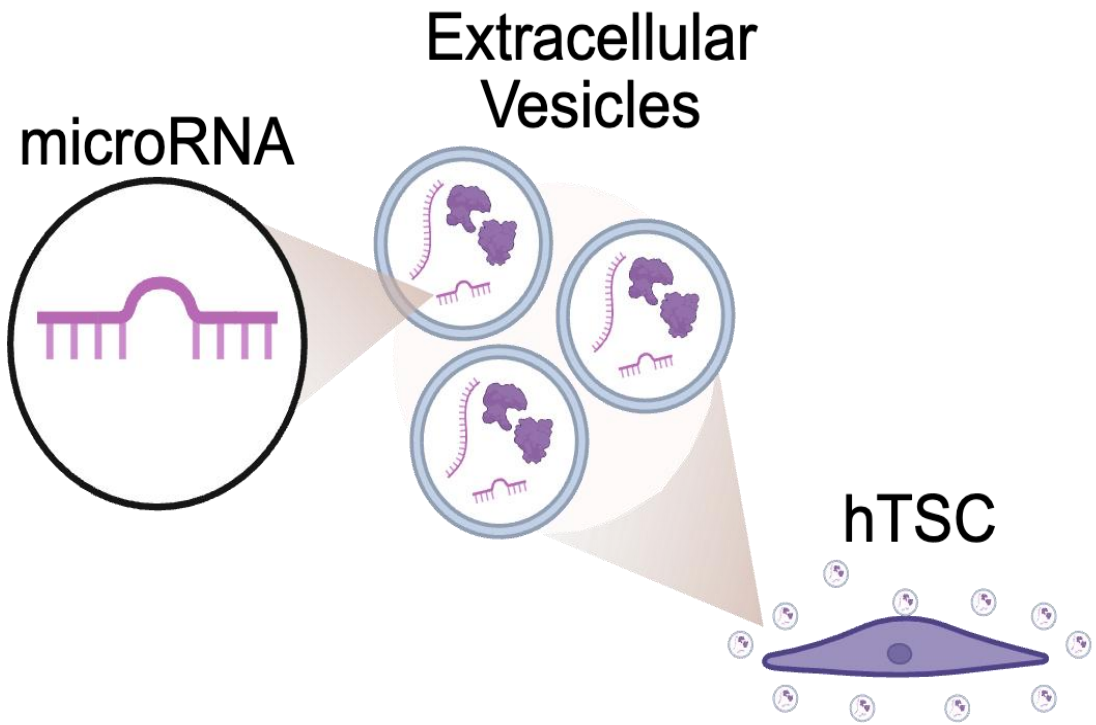
microRNA
Extracellular Vesicles
hTSC

Hypothesis

We hypothesize that nutrient restriction in trophoblasts (hTSCs) simulate the release of EV-miRNAs that communicate with placental endothelial cells to suppress angiogenesis

Methods

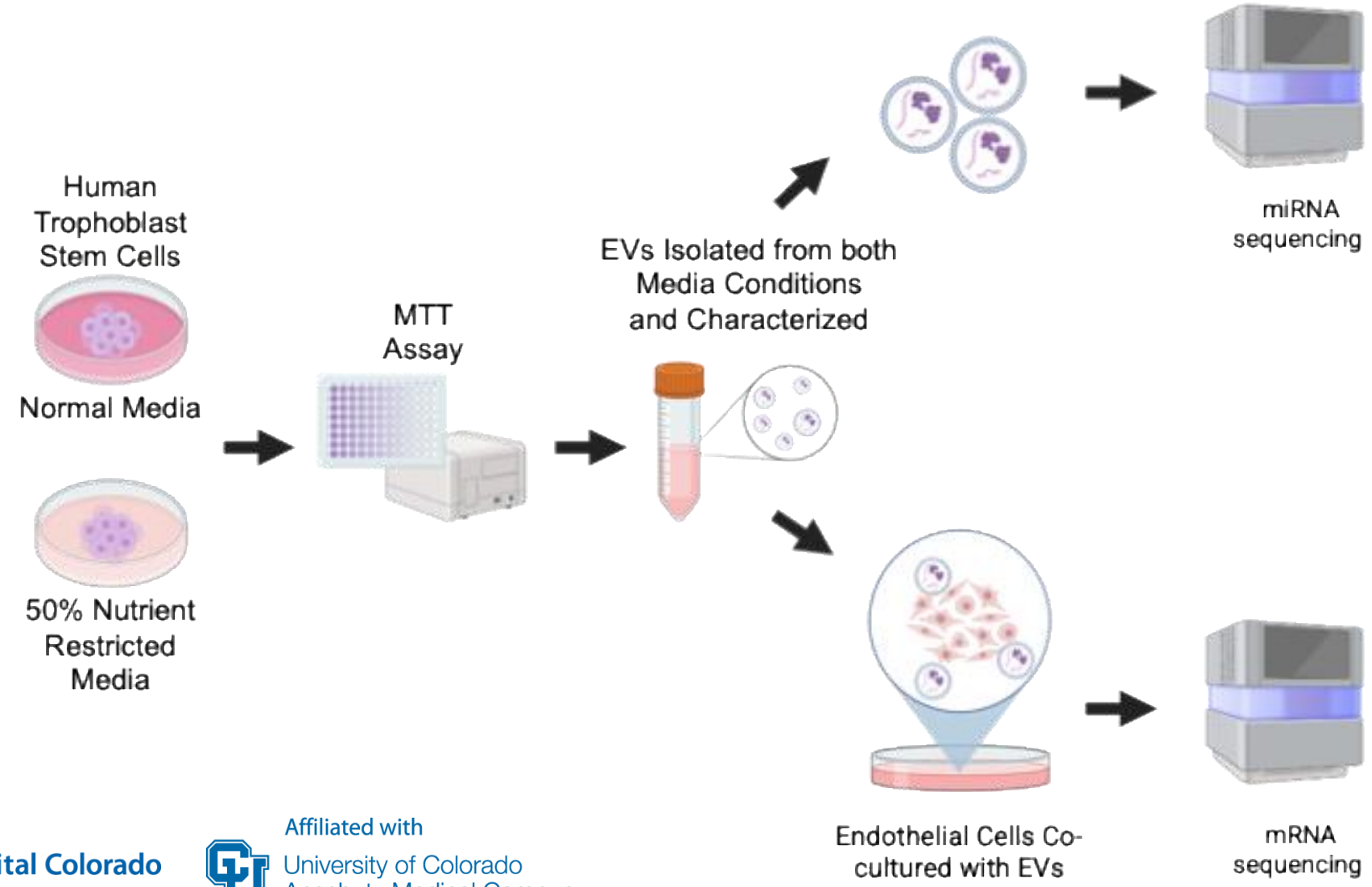
Human Trophoblast Stem Cells
Normal Media
50% Nutrient Restricted Media
MTT Assay
EVs Isolated from both Media Conditions and Characterized
miRNA sequencing
Endothelial Cells Co-cultured with EVs
mRNA sequencing

Methods

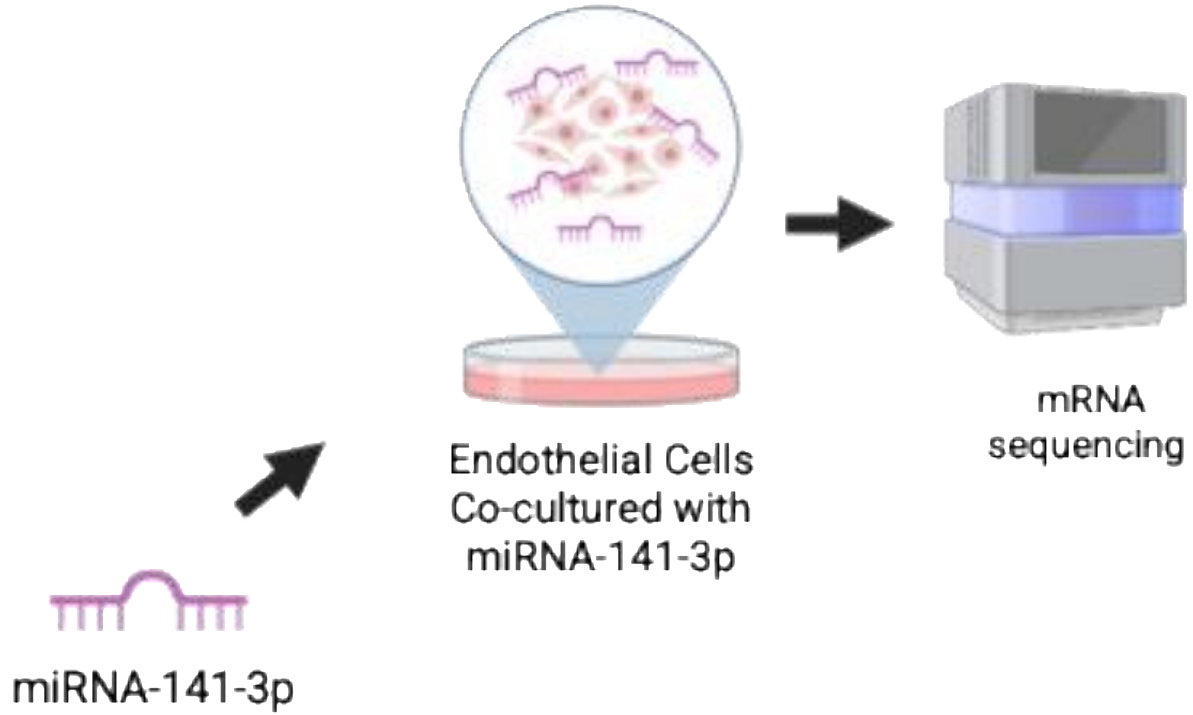
Endothelial Cells
Co-cultured with
miRNA-141-3p
mRNA
sequencing
miRNA-141-3p
Mechanistic & Targeted
Gene Studies
- Tube Formation Assay
- Dual Luciferase Assay

Results

In 8 “Simple” Steps…

Step 1: Confirm Nutrient Restriction Model

A

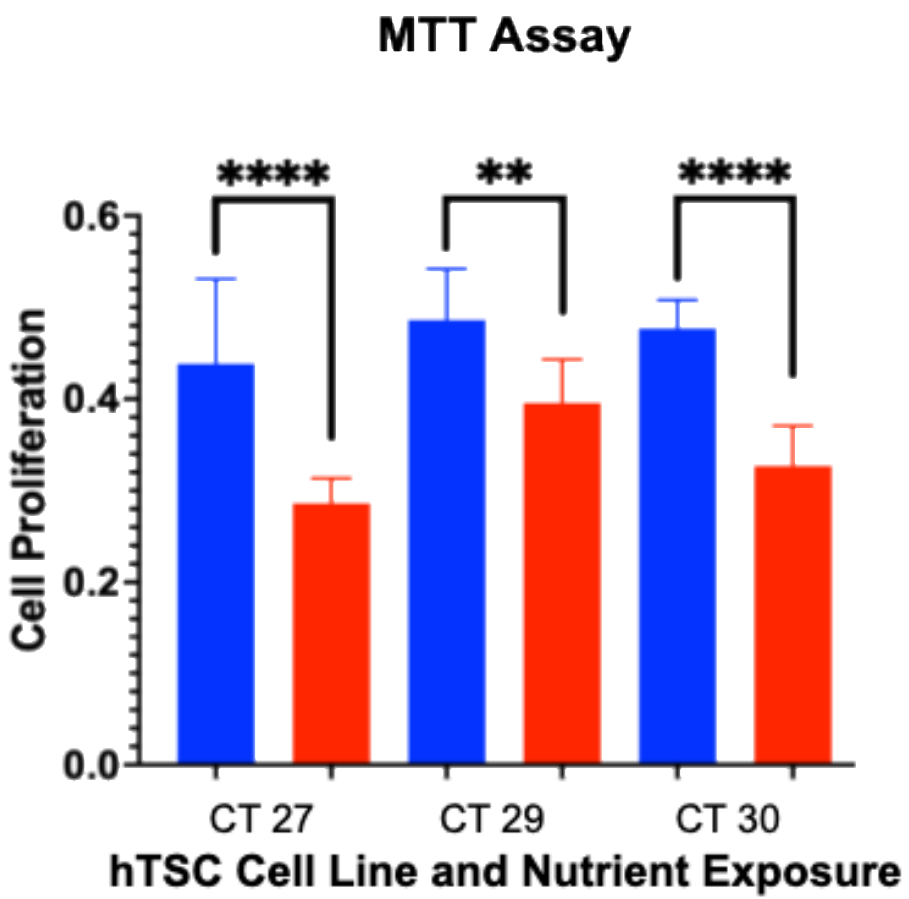

B

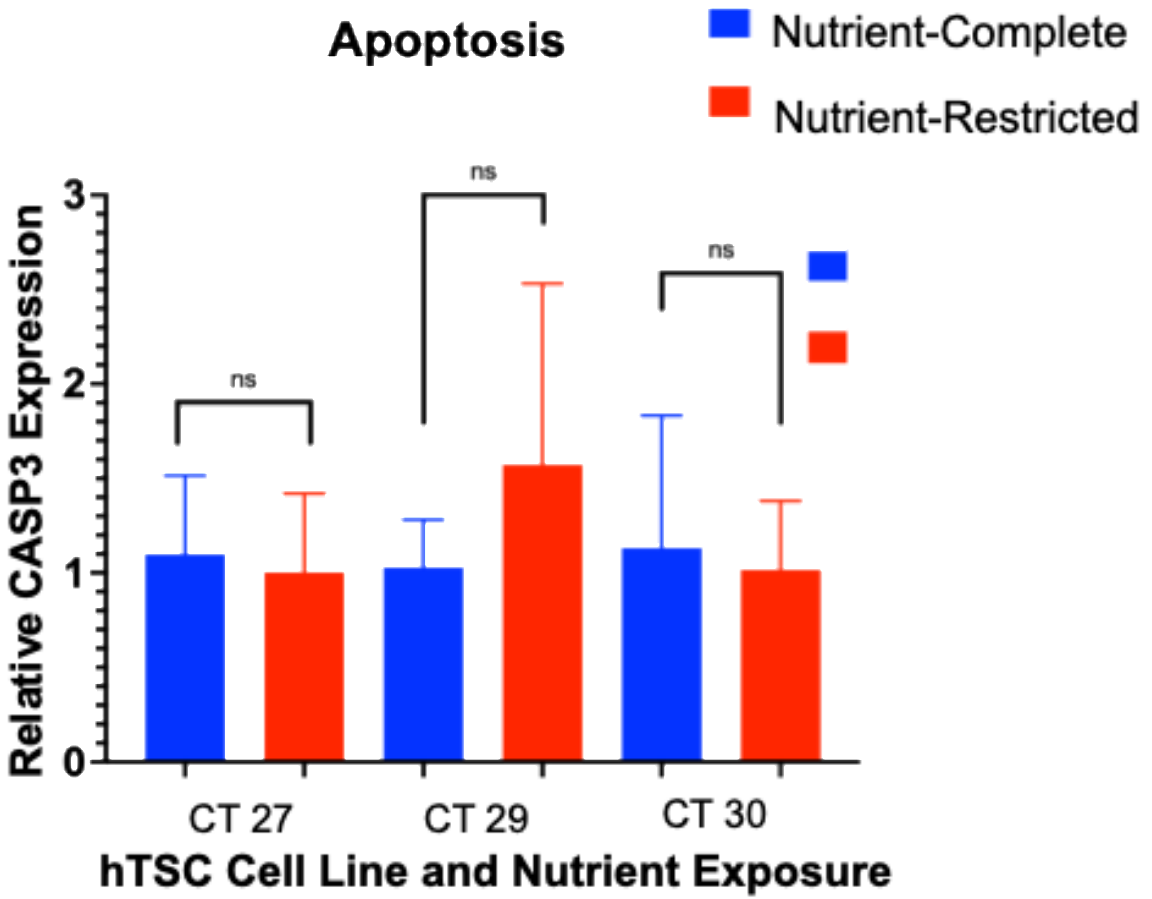

Step 2: Characterization of Extracellular Vesicles

A

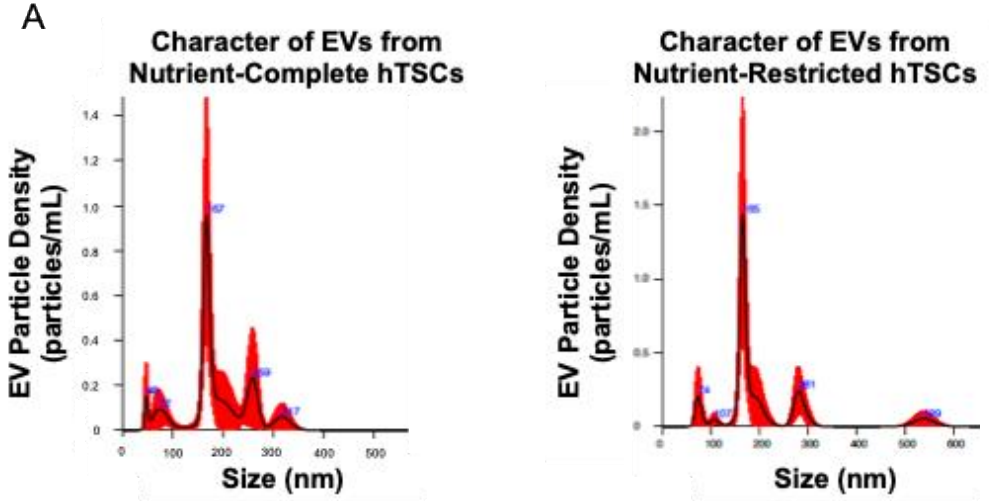

B

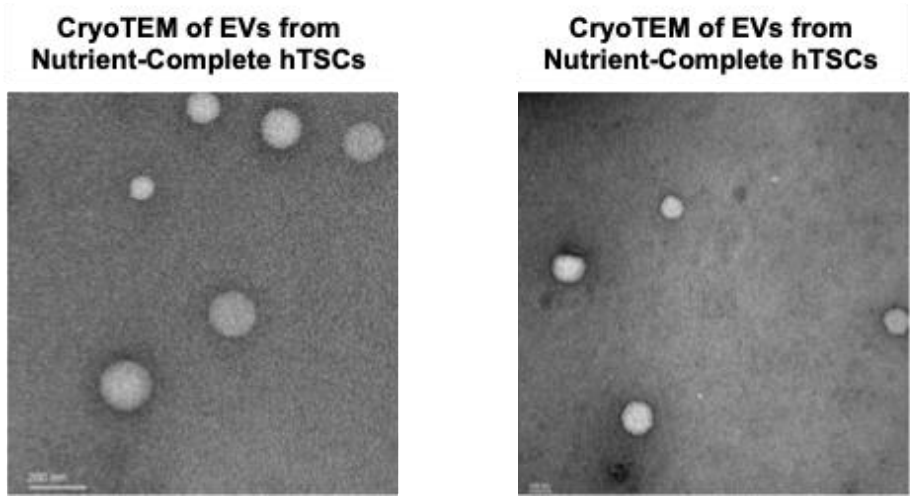

C

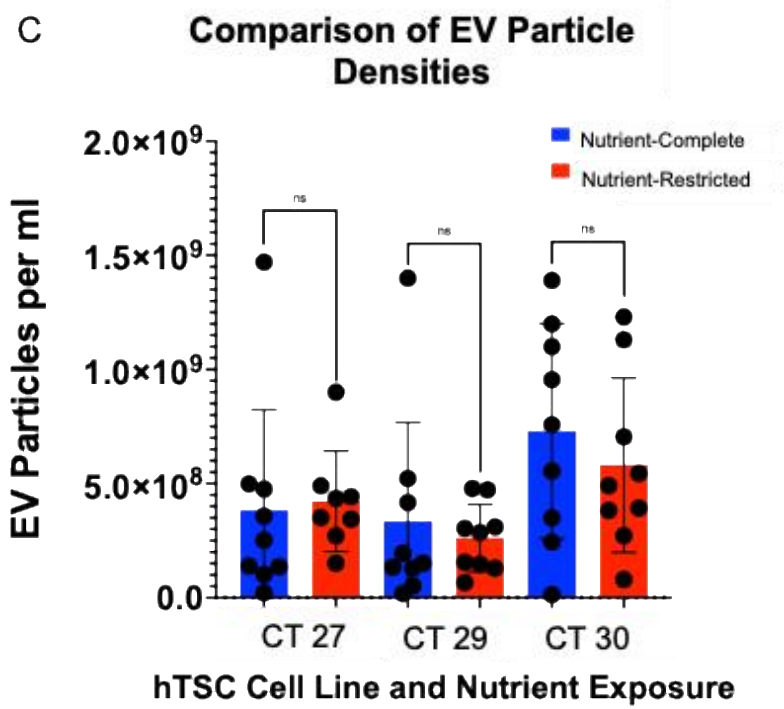

Children's Hospital Colorado
Here, it's different.™

Affiliated with
University of Colorado
Anschutz Medical Campus

Step 3: mRNA seq of HUVECs + EVs

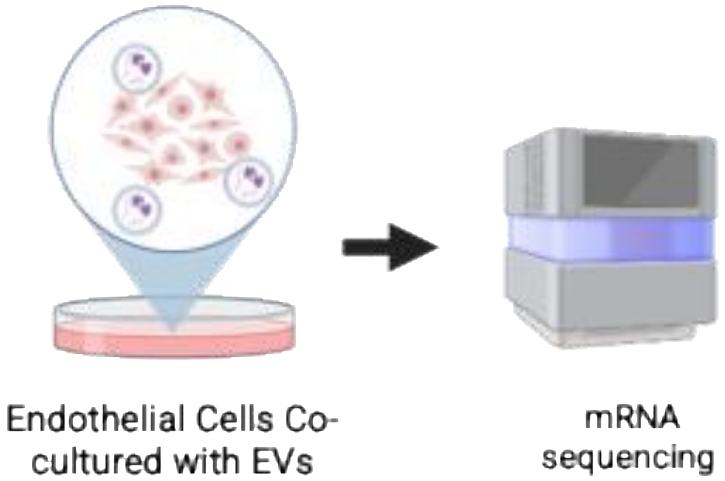

mRNA Expression of HUVECs Exposed to hTSC EVs

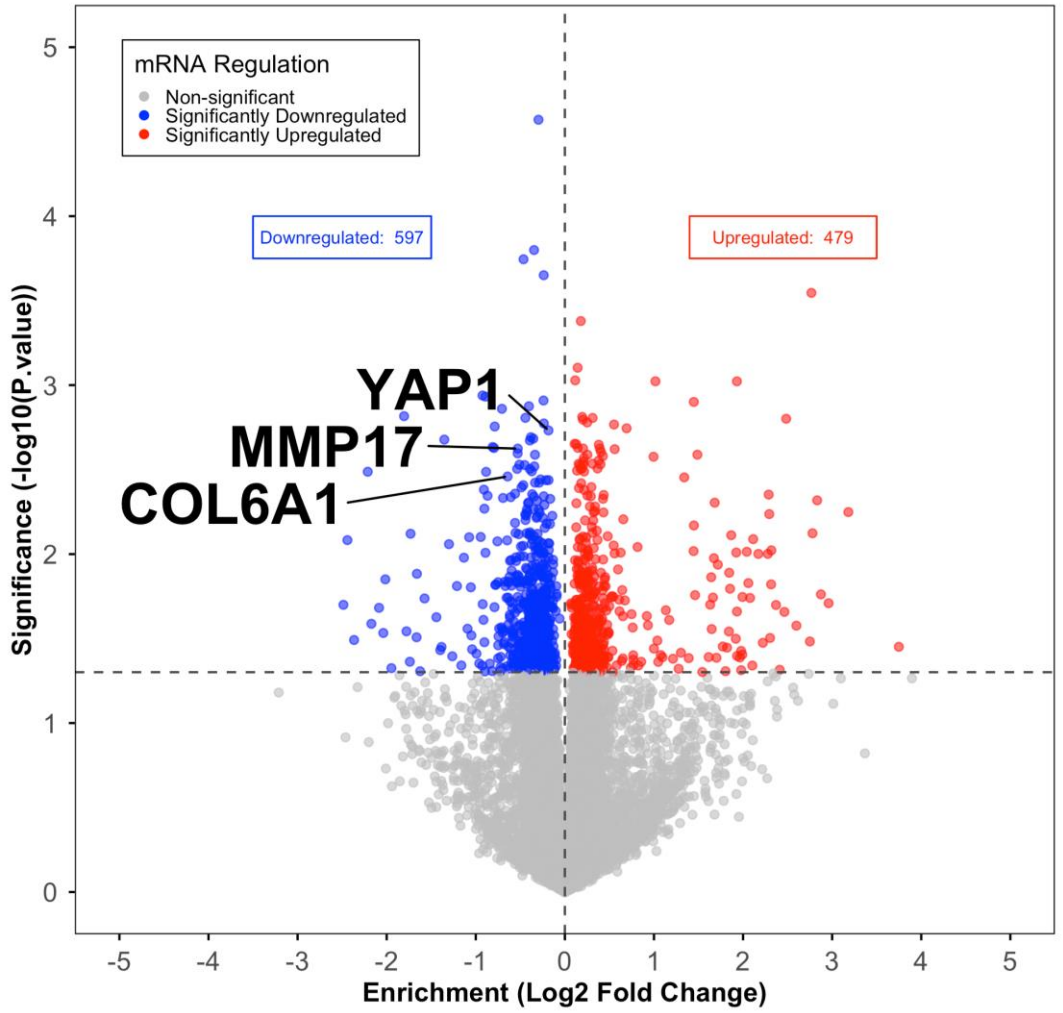

Children's Hospital Colorado
Here, it's different.™

Affiliated with
University of Colorado
Anschutz Medical Campus

Step 3: mRNA seq of HUVECs + EVs

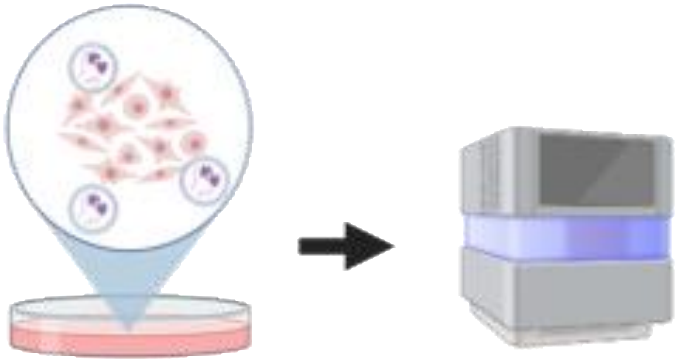

Endothelial Cells Co-cultured with EVs

mRNA sequencing

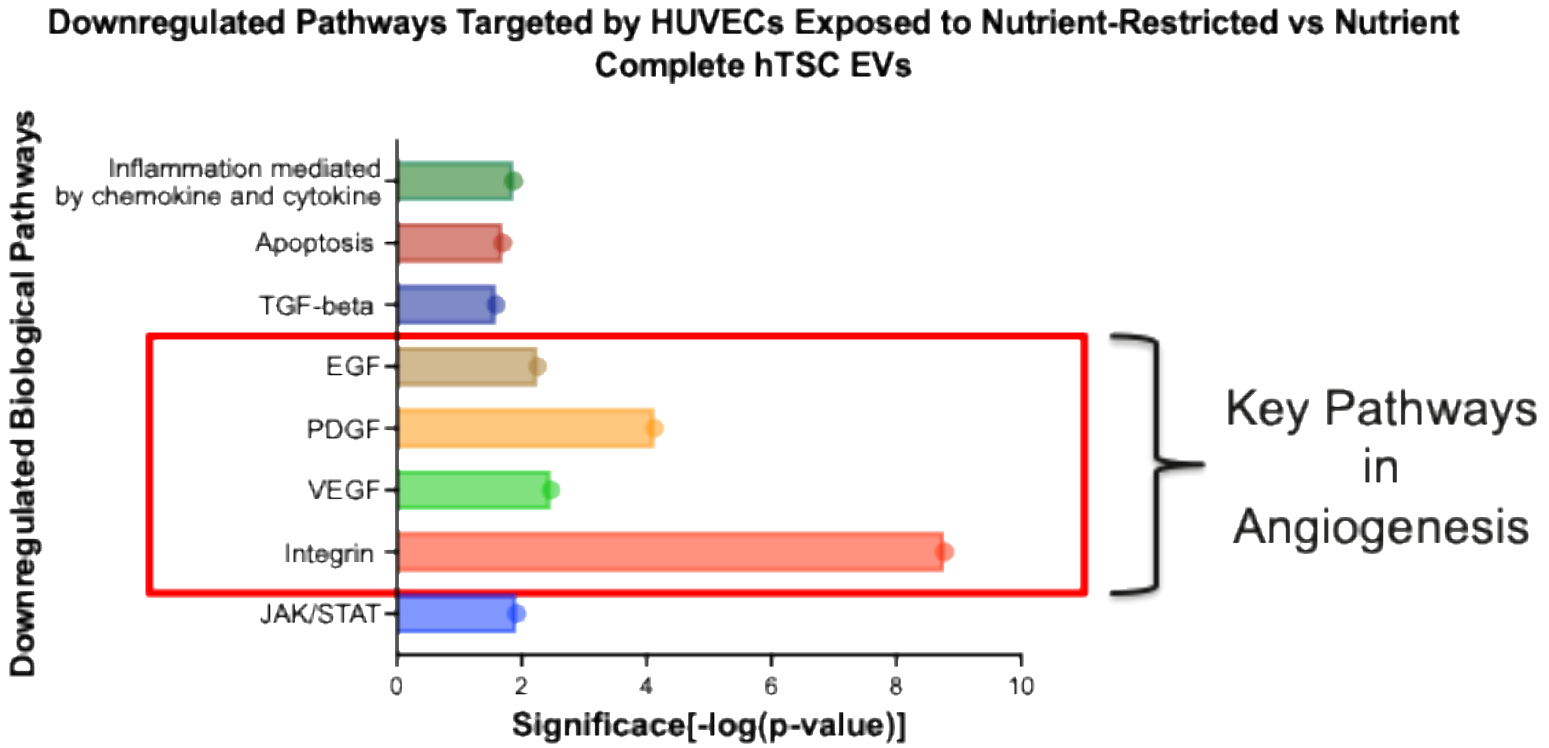

Step 4: miRNA seq of EVs

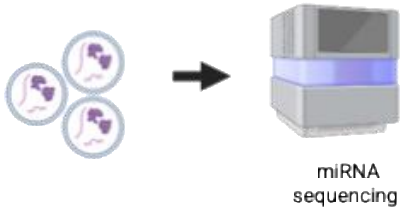

A

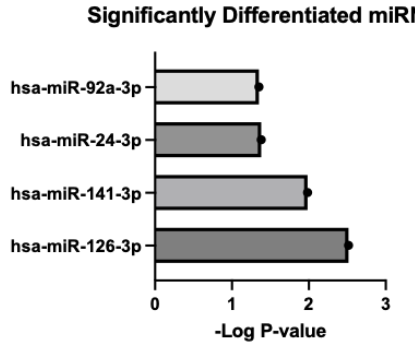

B

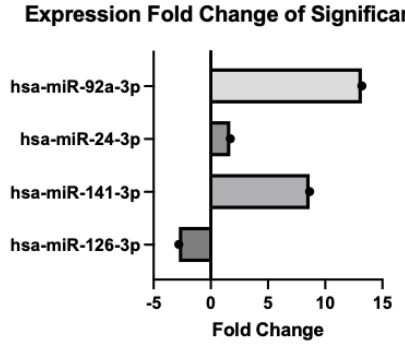

D

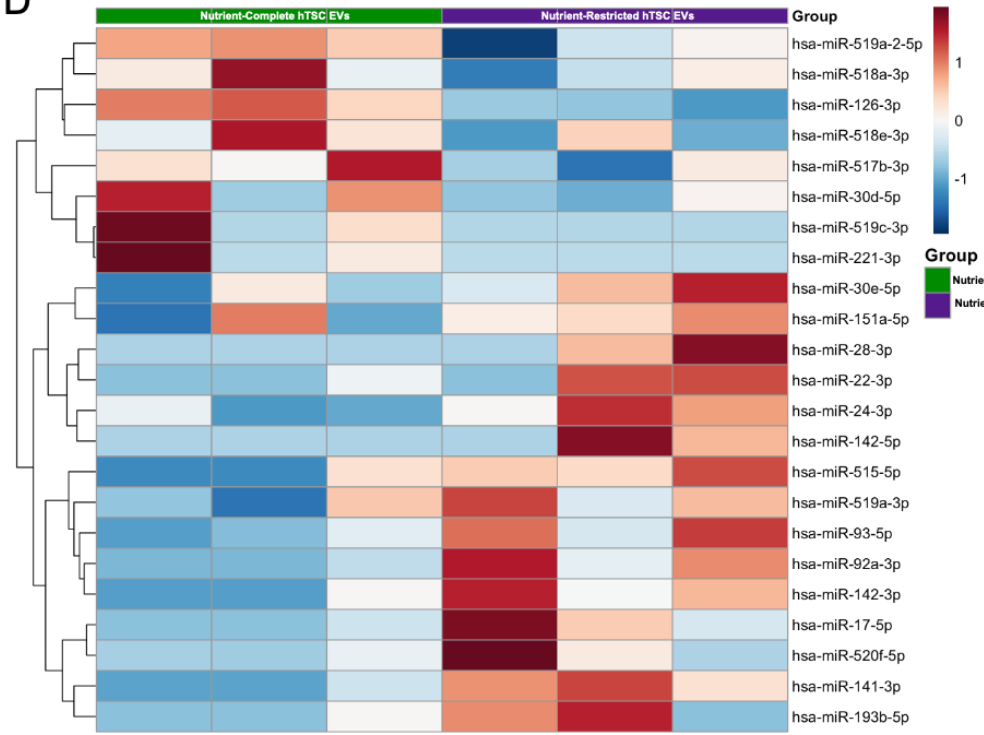

C

miRNA Expression of hTSC EVs

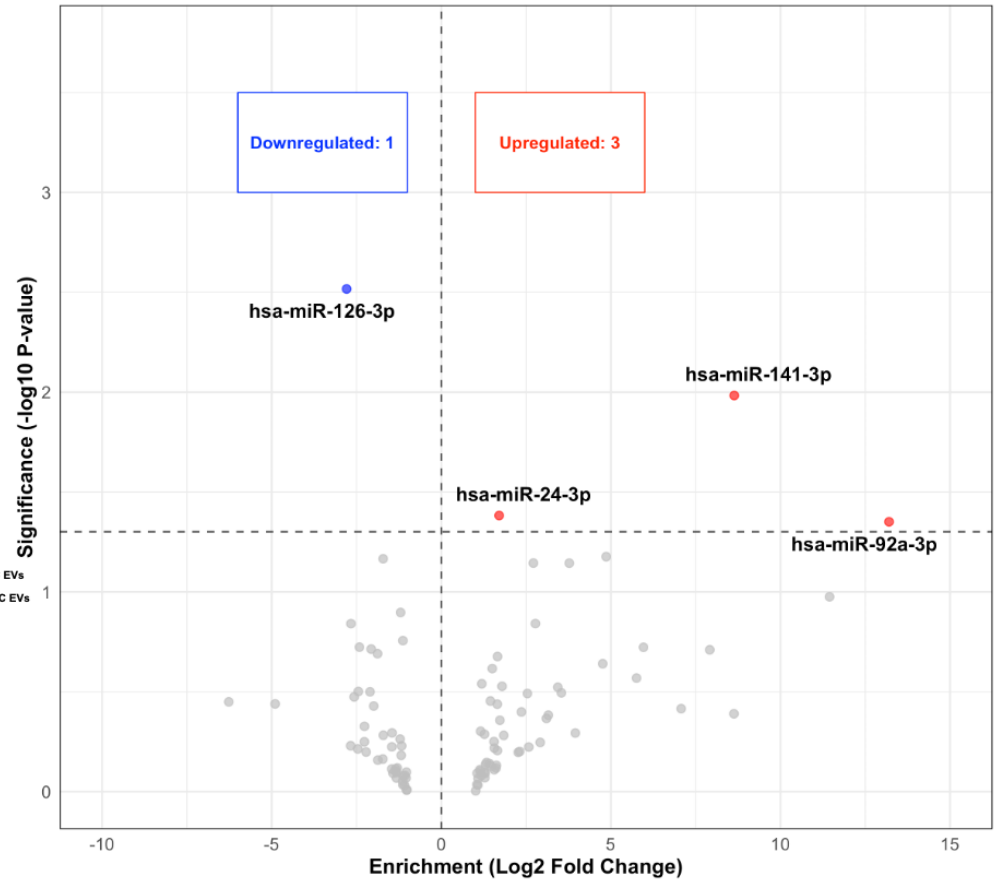

Step 5: mRNA seq of HUVECs + miR-141-3p

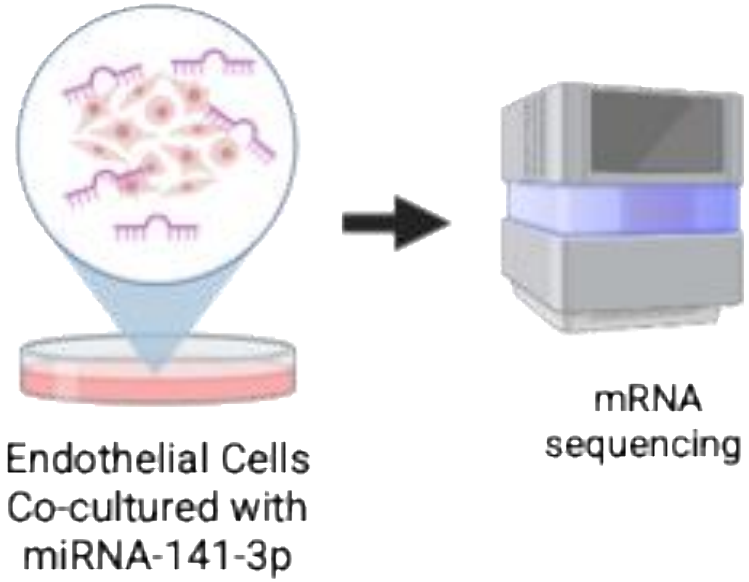

mRNA Expression of HUVECs Exposed to miR-141-3p

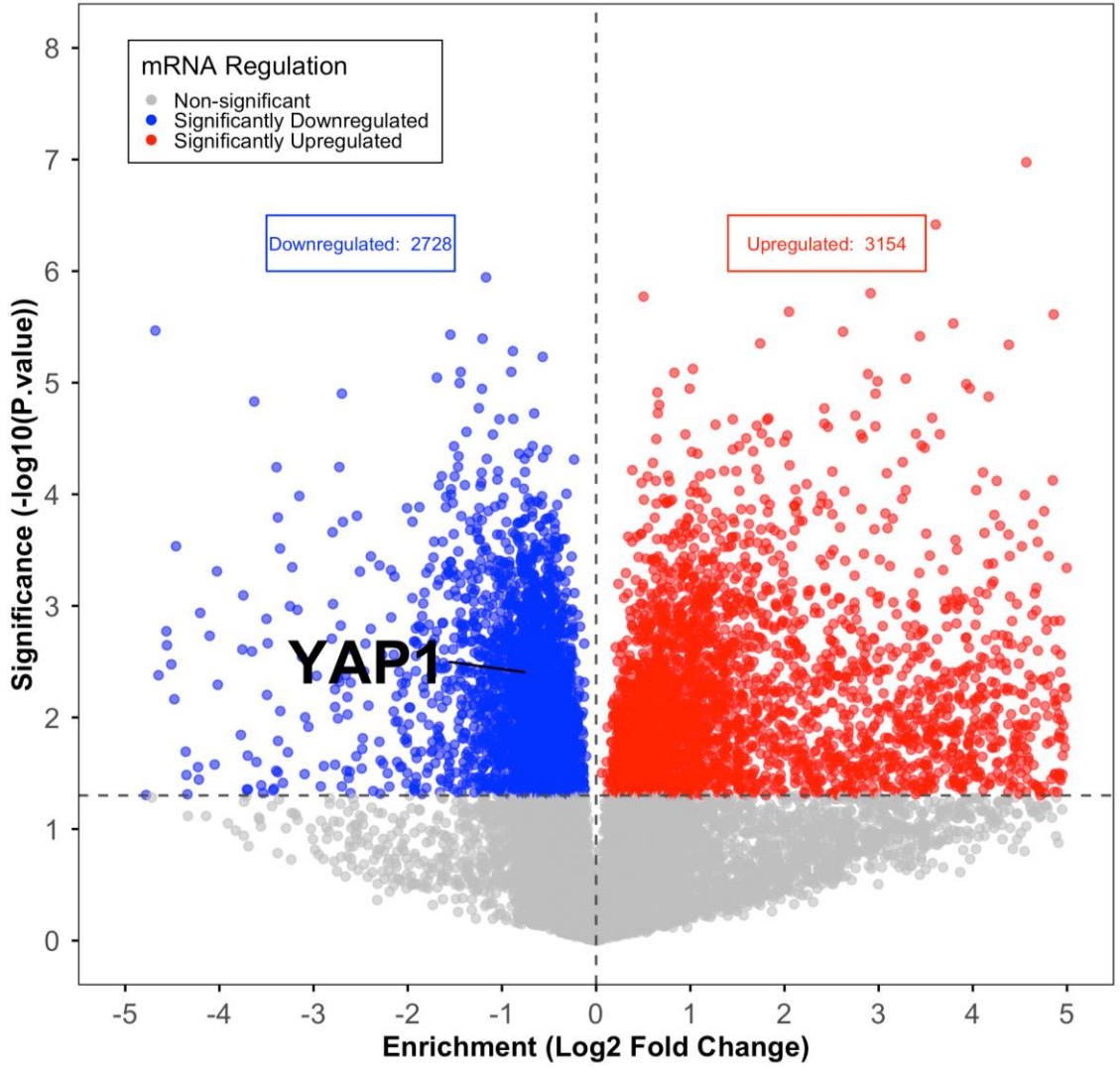

Children's Hospital Colorado
Here, it's different.™

Affiliated with
University of Colorado
Anschutz Medical Campus

Step 5: mRNA seq of HUVECs + miR-141-3p

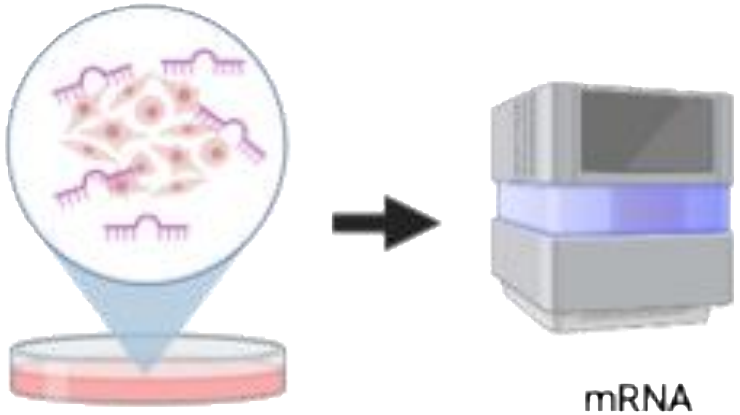

Endothelial Cells Co-cultured with miRNA-141-3p

mRNA sequencing

Downregulated Pathways Targeted by HUVECs Exposed to miRNA 141-3p

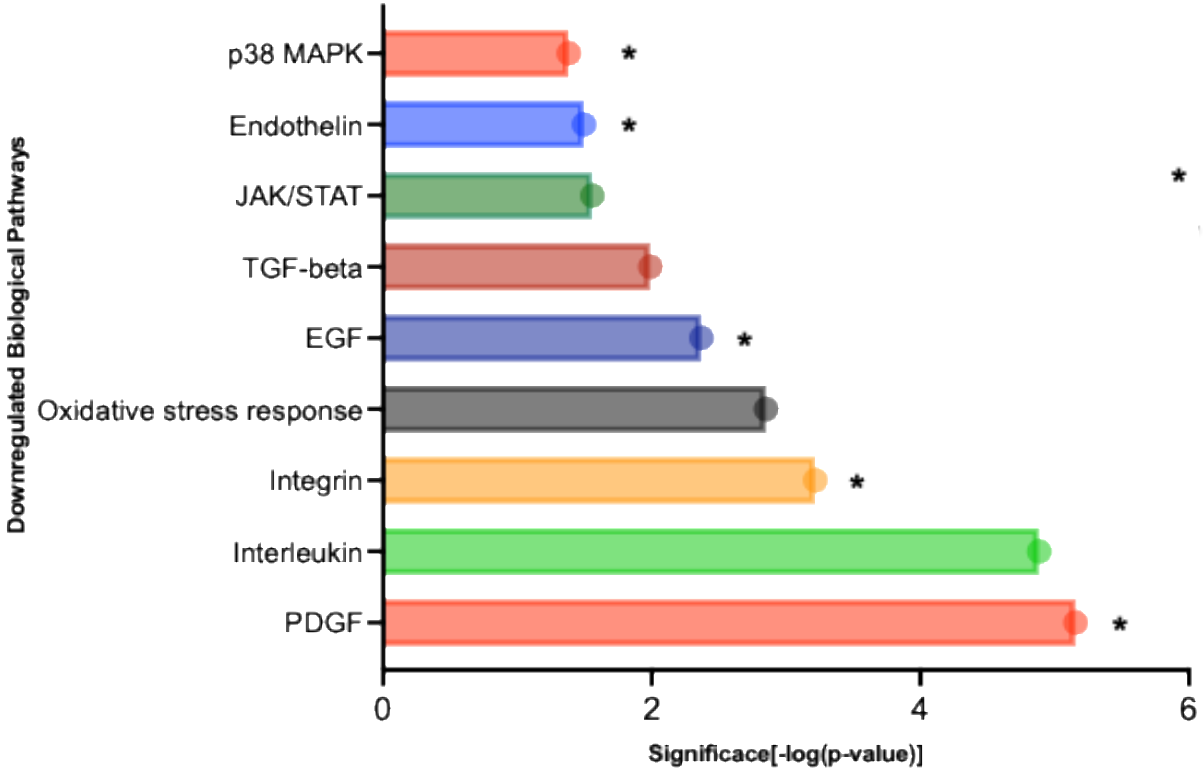

* Key Pathways in Angiogenesis

Step 6: Mechanistic Study- Tube Formation Assay

miRNA-141-3p

Mechanistic & Targeted Gene Studies

- Tube Formation Assay
- Dual Luciferase Assay

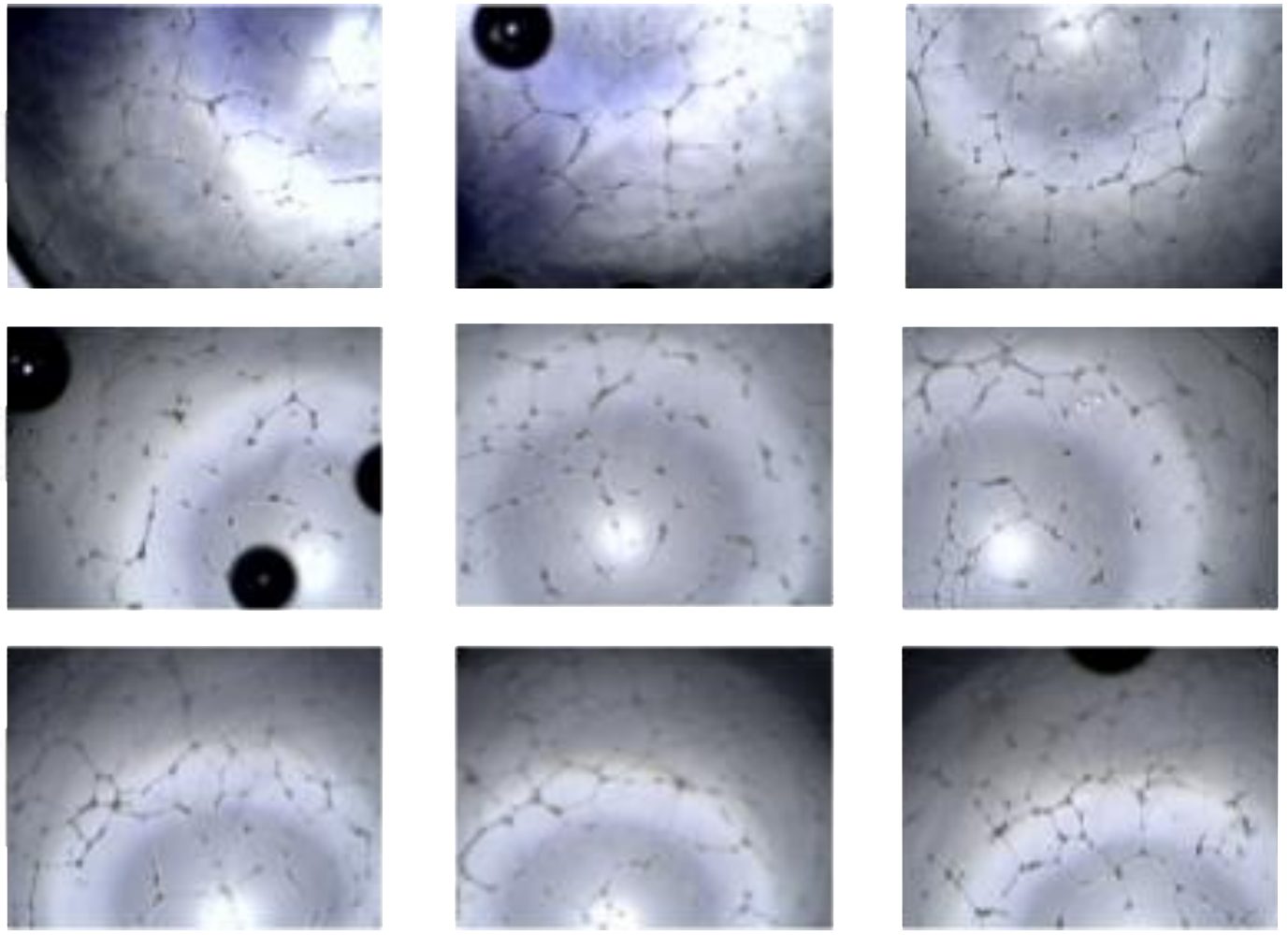

Step 6: Mechanistic Study- Tube Formation Assay

miRNA-141-3p

Mechanistic & Targeted Gene Studies

- Tube Formation Assay
- Dual Luciferase Assay

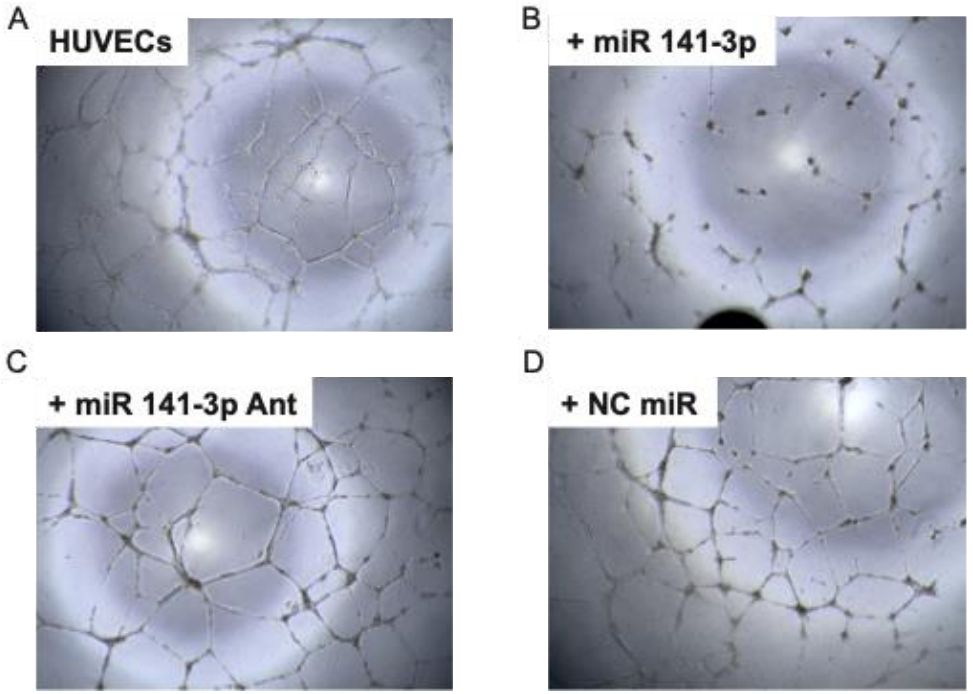

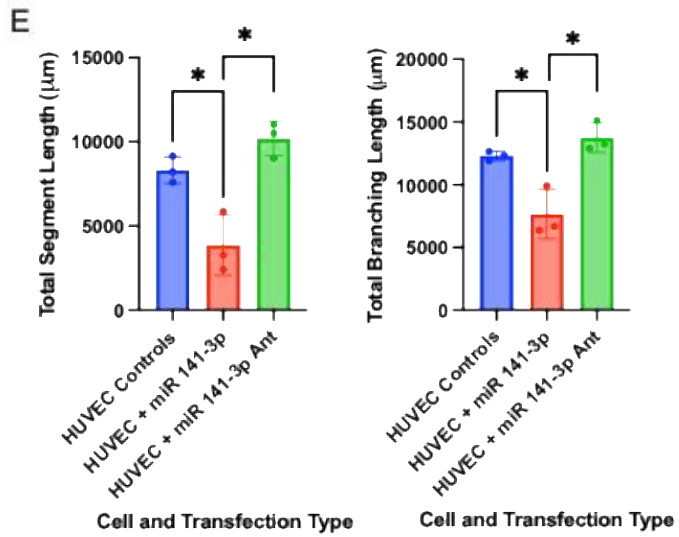

Step 7: Targeted Gene Study- Dual Luciferase Assay

miRNA-141-3p

Mechanistic & Targeted Gene Studies

- Tube Formation Assay
- Dual Luciferase Assay

Wild Type YAP-1 UTR (x2 miR-141-3p Binding Sites)

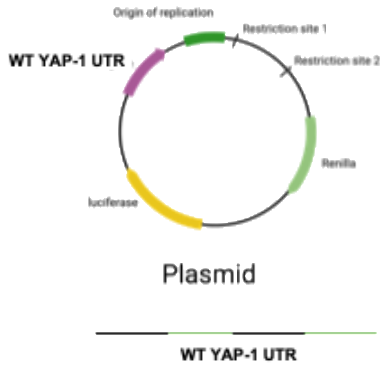

NO2: 2nd Binding site Mutated on YAP-1 UTR

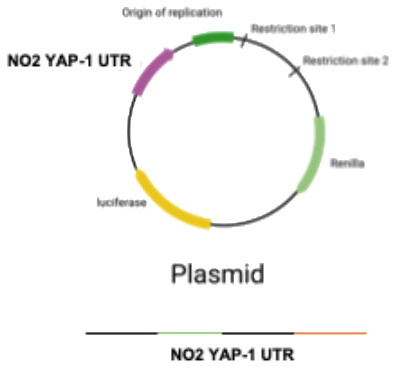

NO1: 1 Binding site Mutated on YAP-1 UTR

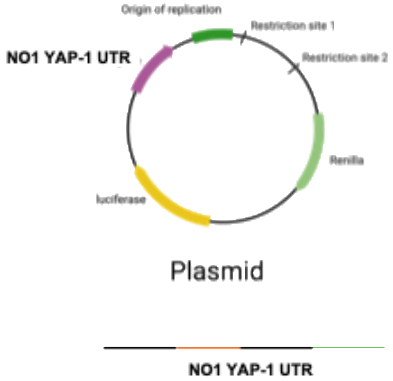

NO-NO: BOTH Binding site Mutated on YAP-1 UTR

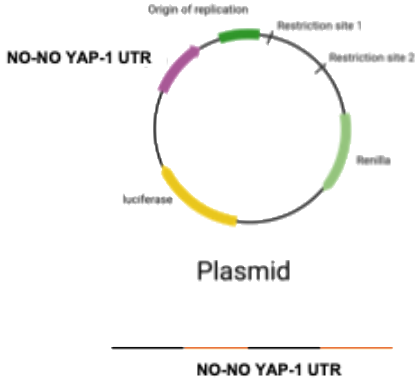

Anticipated Results IF miR-141-3p Targets YAP-1

- **WT YAP-1 UTR:** reduced luc activity when +miR 141-3p, return to baseline with +miR 141-3p Ant
- **NO1:** +miR 141 slightly reduced luc activity but less than WT
- **NO2:** +miR 141 slightly reduced luc activity but less than WT
- **NO-NO:** +miR 141 remains the same at WT without miR added, no change with +miR 141 Ant

Step 7: Targeted Gene Study- Dual Luciferase Assay

miRNA-141-3p

Mechanistic & Targeted Gene Studies

- Tube Formation Assay
- Dual Luciferase Assay

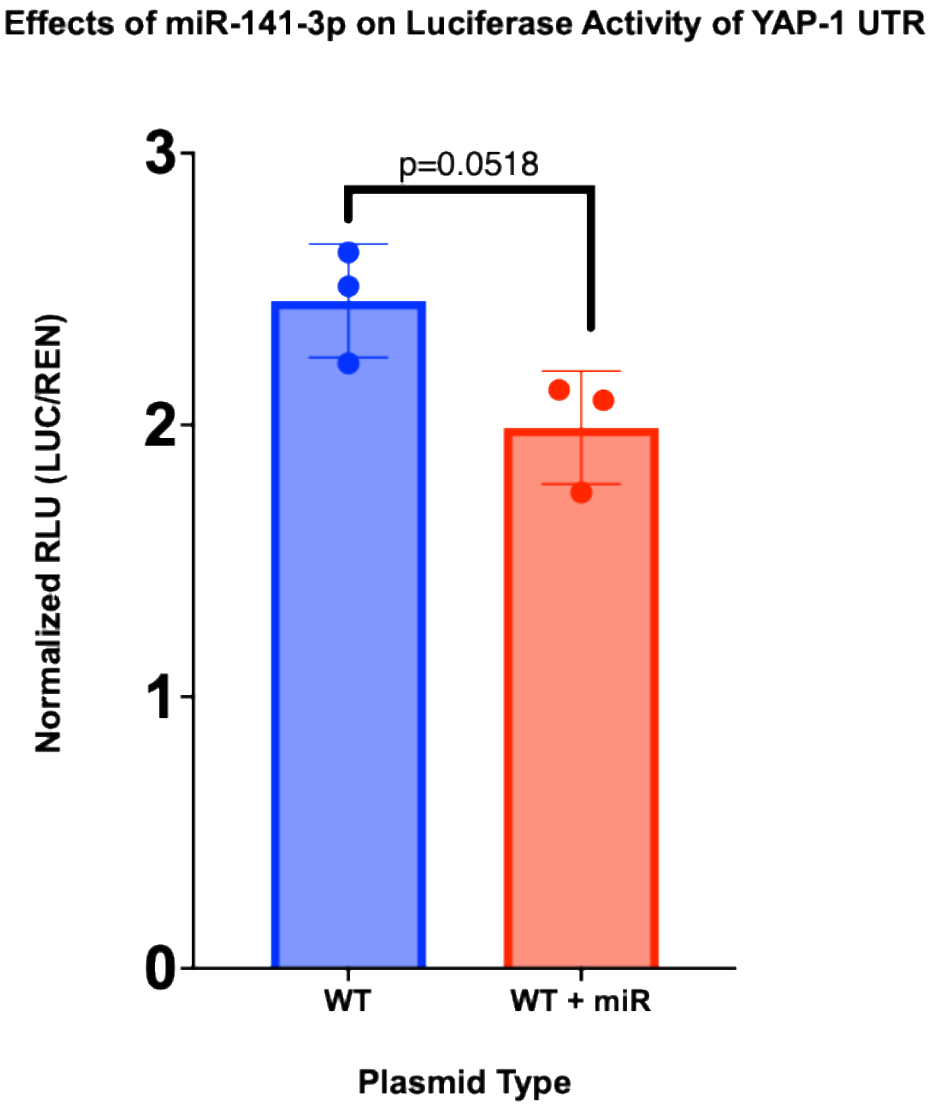

Children's Hospital Colorado
Here, it's different.

Affiliated with
University of Colorado
Anschutz Medical Campus

Step 8: Targeted Gene Study- YAP-1 ELISA & Western

miRNA-141-3p

Mechanistic & Targeted Gene Studies

- Tube Formation Assay
- Dual Luciferase Assay

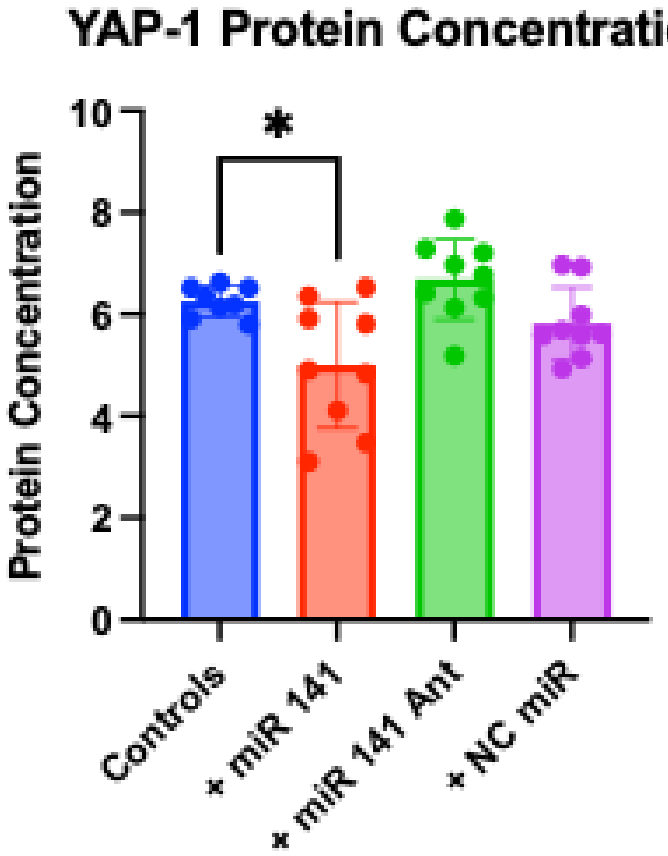

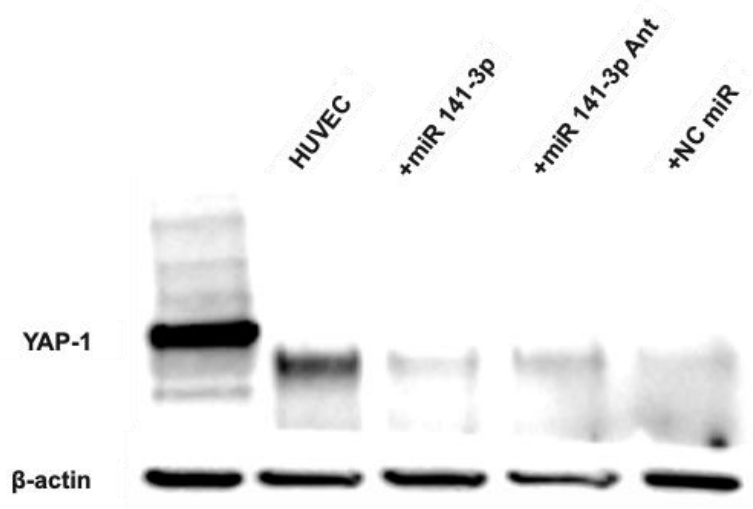

Conclusions

- Nutrient-restriction in hTSCs stimulates the release of EVs with upregulated miR-141-3p
- Endothelial cell exposure to nutrient-restricted hTSC EVs and miR-141-3p
  - Downregulate pathways essential to angiogenesis
  - Reductions in *YAP-1* gene expression, a potential mechanism
- miR-141-3p decreases *in vitro* tube formation of endothelial cells
- Endothelial cell exposure to miR-141-3p demonstrates diminished YAP-1 protein expression
  - Additional studies needed to confirm specific targeting

Future Directions

- Mouse blastocyst with upregulated miR-141-3p
- Nutrient restriction in early placental organoids

Thank you

Questions?

PI: S Chris Derderian, MD

Lab Members:

- James Bardill, PhD
- Courtney Breckenfelder, BS
- Madison Crew, MS

Collaborators:

- Anis Karimpour-Fard, PhD
- Clyde Wright, MD
- Theresa Powell, PhD
- Kika Sucharov, PhD

Colorado Fetal Care Center
Children's Hospital Colorado

APSA
American Pediatric Surgical Association
Saving Lifetimes™

Grant funding NIH R38 StARR
(Stimulating Access to Research in Residency)

AMNION FOUNDATION

Children's Hospital Colorado
Here, it's different.™

Affiliated with
University of Colorado Anschutz Medical Campus

Children's Hospital Colorado

Anschutz SURGERY

Concurrent changes in macrophage and T cell subsets over time in murine obstructive cholestasis suggest interplay between macrophage and T cell function in promotion of hepatic injury

Lauren (Lo) Maloney, MD
Mentor: Dr. Sarah Taylor

Background: Biliary Atresia (BA)

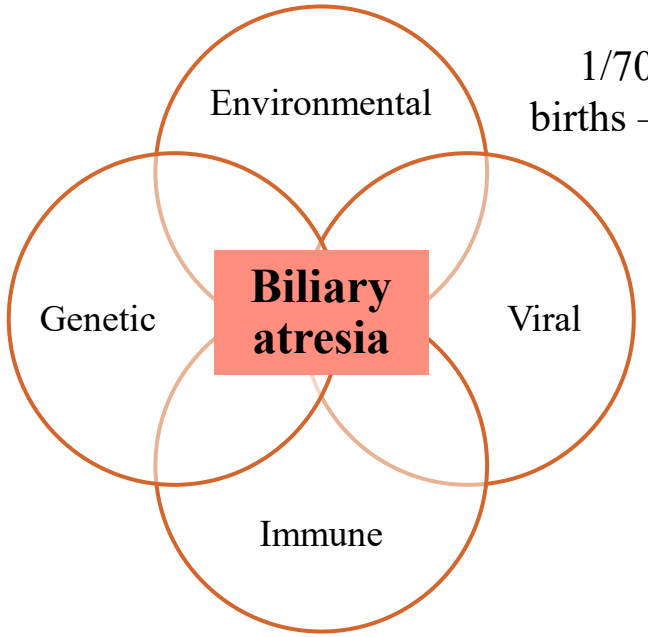

1/7000 live births – 1/15,000

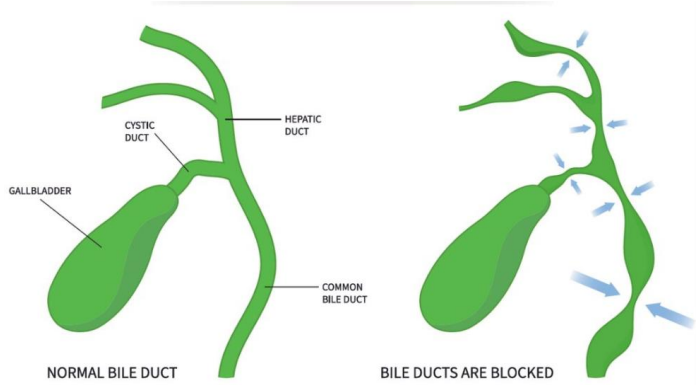

Transplant

Leading indication in children worldwide

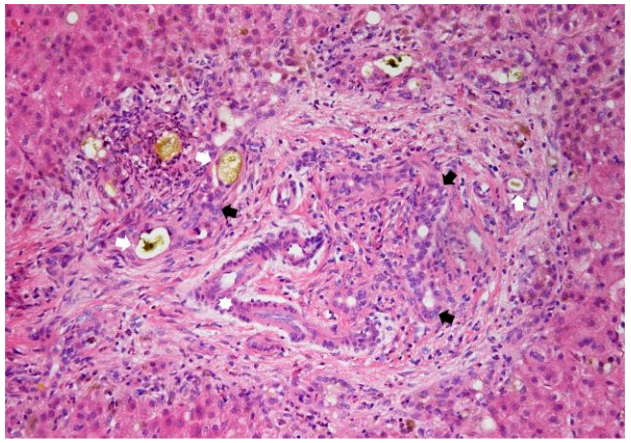

Liver biopsy from an infant with BA at diagnosis that underwent liver transplant before 2 years of age. Histologic findings include expansion of the portal tract with stromal edema, prominent fibrosis, bile duct proliferation (black arrows), and bile plugs (white arrows).

Background: immunology

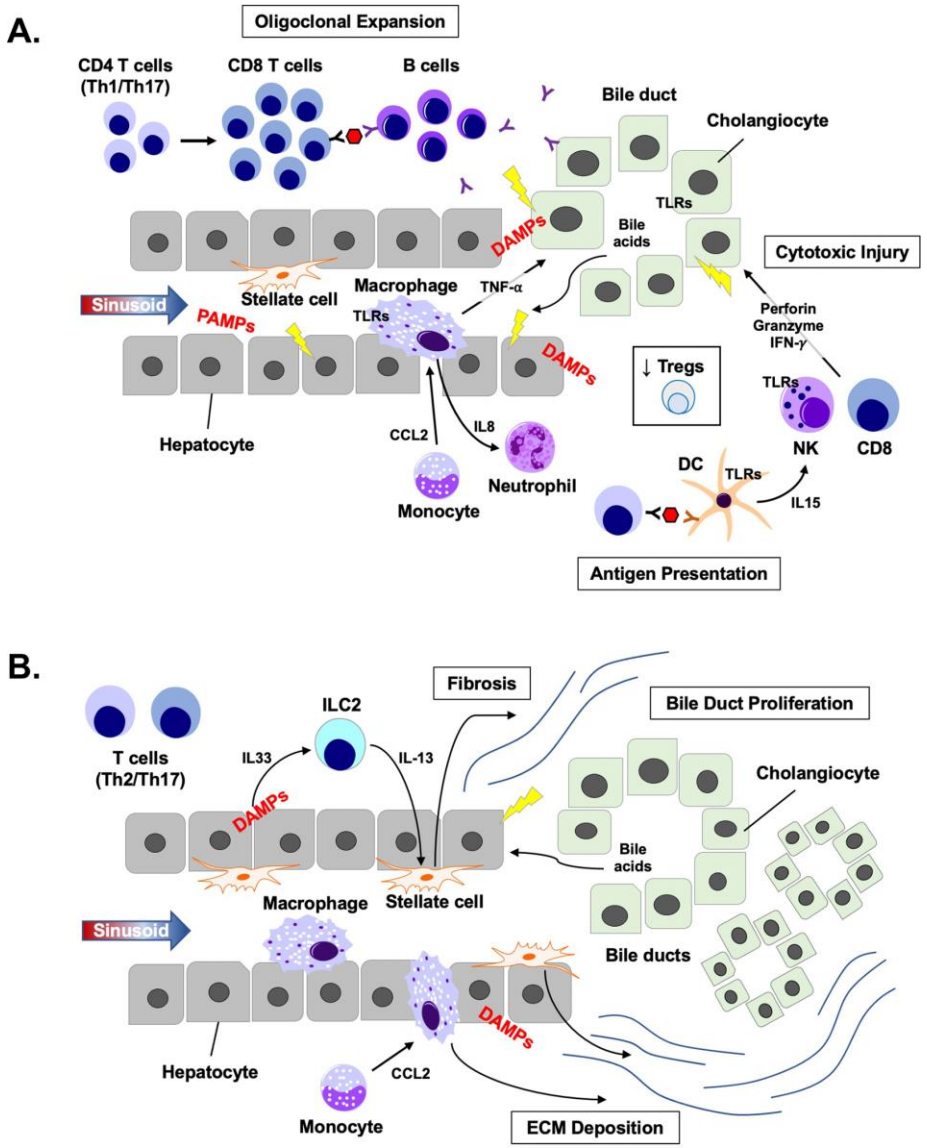

- **Unique tolerogenic microenvironment** of the liver → impaired in disease.
- **Oligoclonal expansion of T & B cells in cholestatic injury = supports presence of antigen-driven immune stimulation to autoantigens.**
- **Impaired function of Tregs & Th1 dominant immune response** in most infants early in disease have been shown in BA.
- Recent work from Taylor lab → **macrophage heterogeneity in neonatal murine models of obstructive cholestasis; reduction in immune regulatory function of hepatic macrophages in cholestatic models compared to non-diseased mice.**

Background: BA model

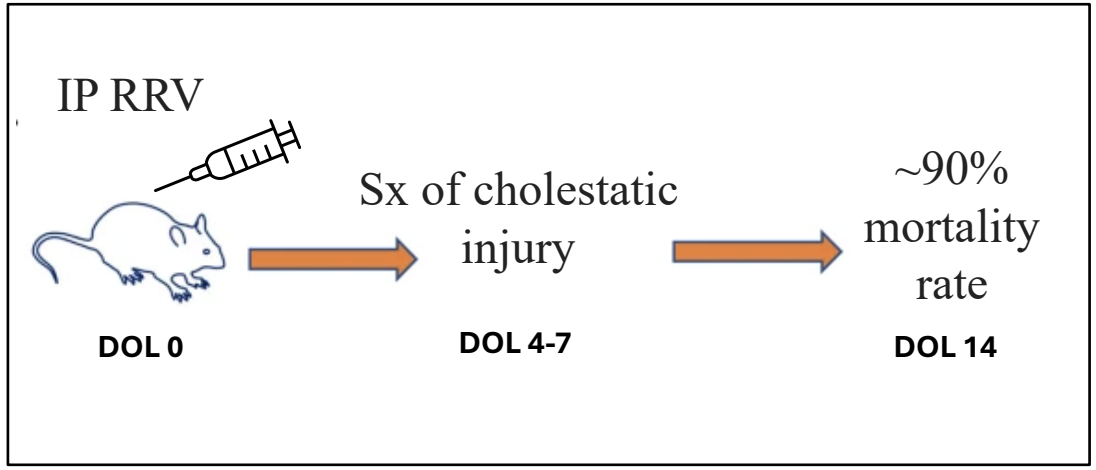

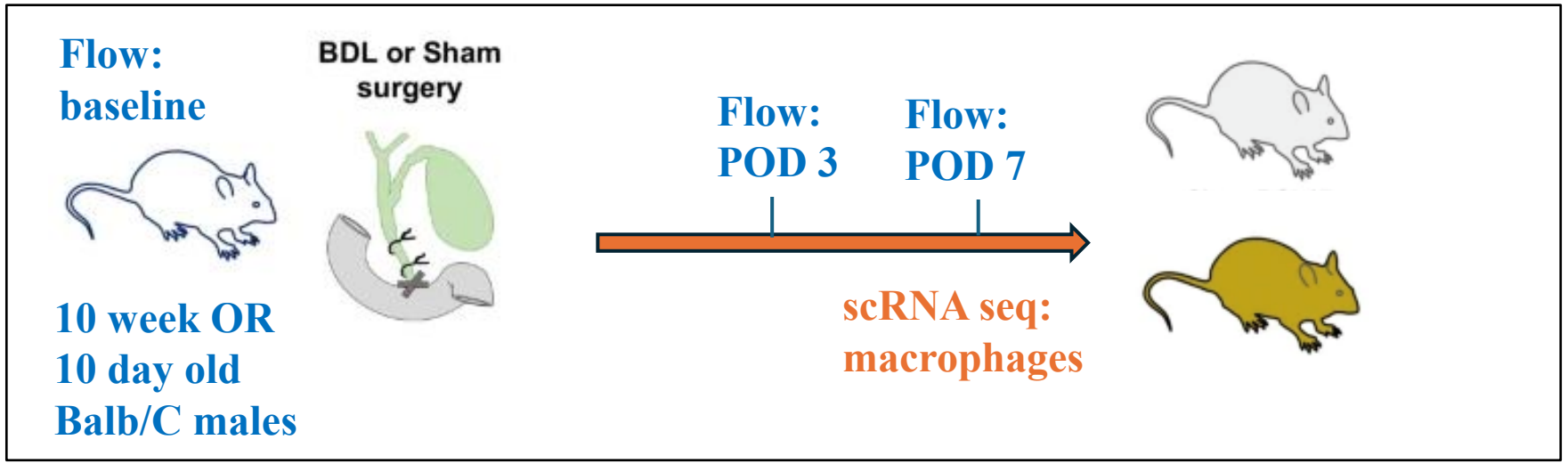

CD8 T cells

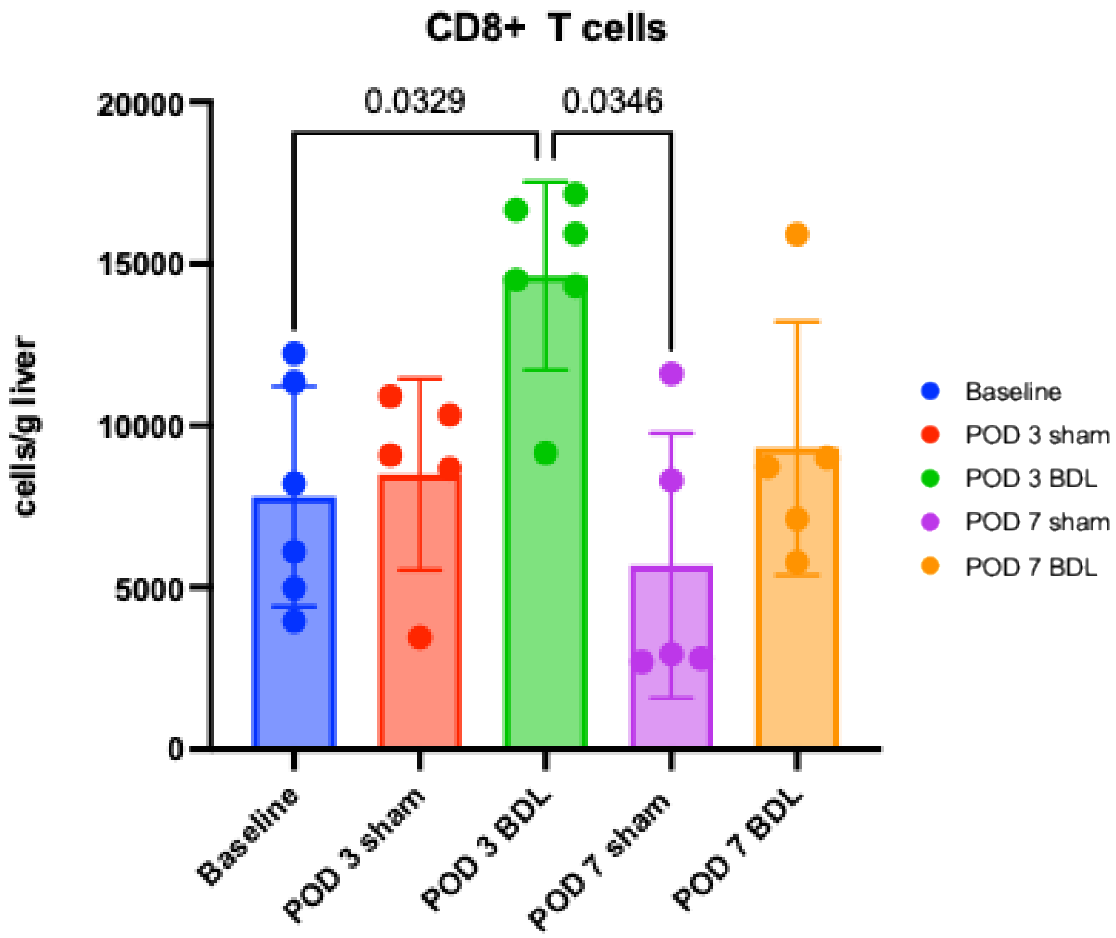
CD8+ T cells
0.0329
0.0346
20000
15000
10000
5000
0
cells/g liver
Baseline
POD 3 sham
POD 3 BDL
POD 7 sham
POD 7 BDL
Baseline
POD 3 sham
POD 3 BDL
POD 7 sham
POD 7 BDL

CD4 T cells

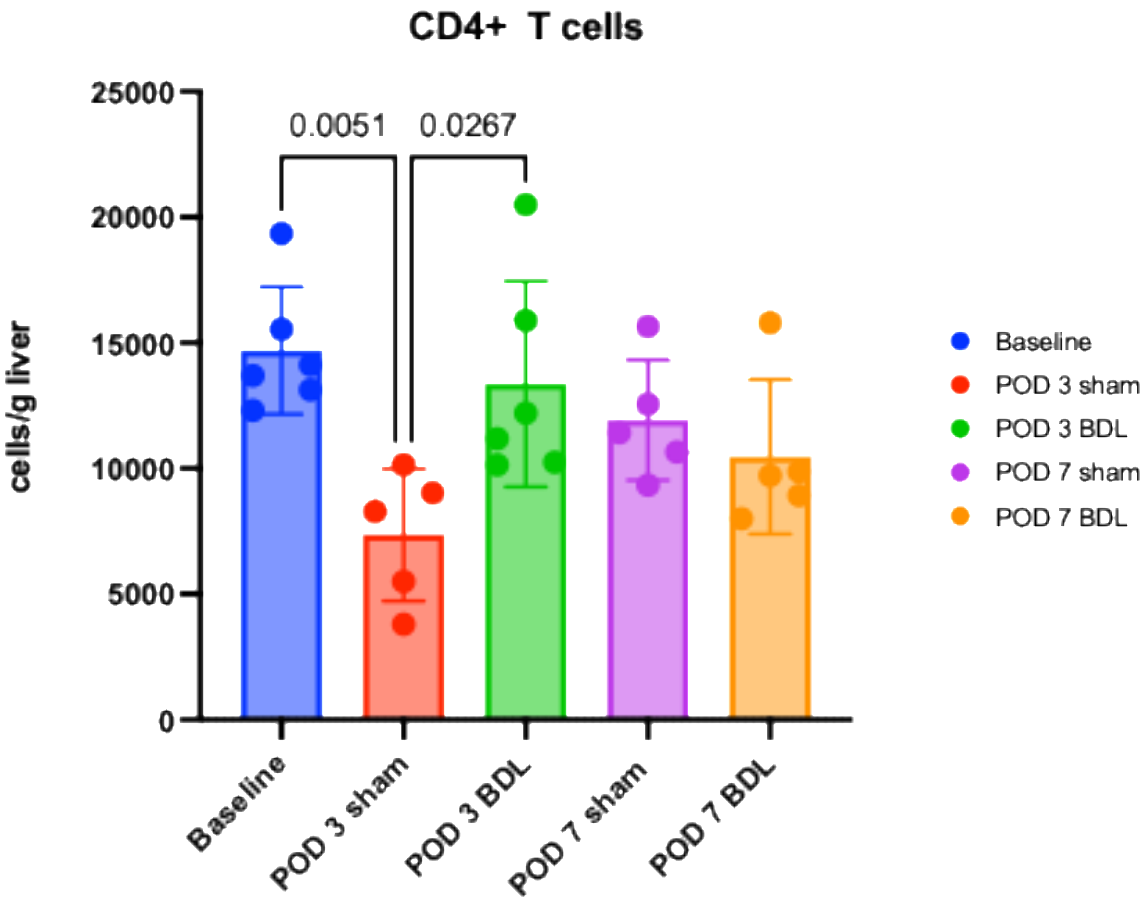
CD4+ T cells
cells/g liver
25000
20000
15000
10000
5000
0
0.0051
0.0267
Baseline
POD 3 sham
POD 3 BDL
POD 7 sham
POD 7 BDL

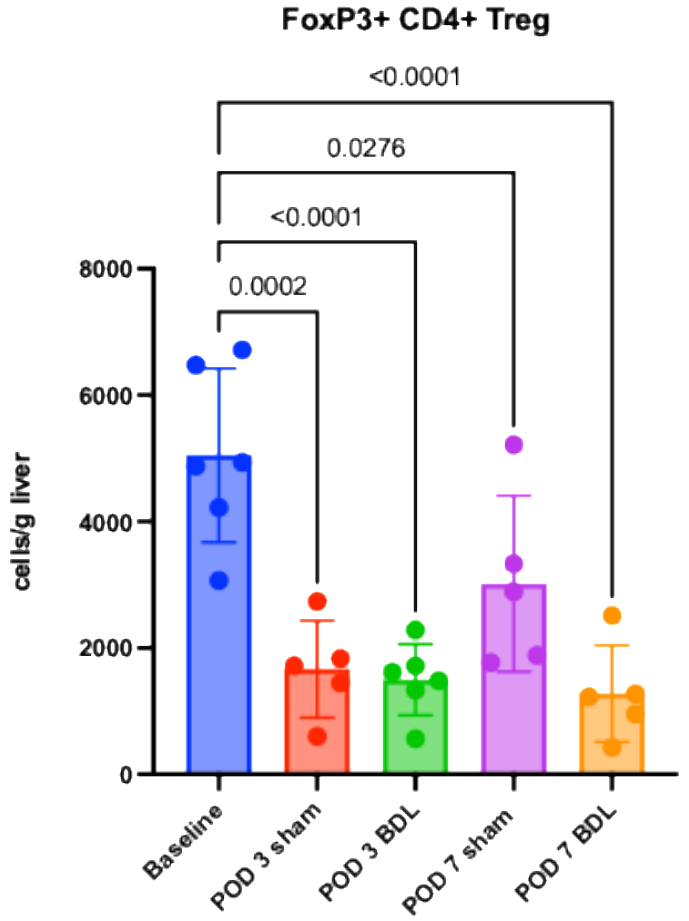
FoxP3+ CD4+ Treg
cells/g liver
8000
6000
4000
2000
0
<0.0001
0.0276
<0.0001
0.0002
Baseline
POD 3 sham
POD 3 BDL
POD 7 sham
POD 7 BDL

T cell ratios

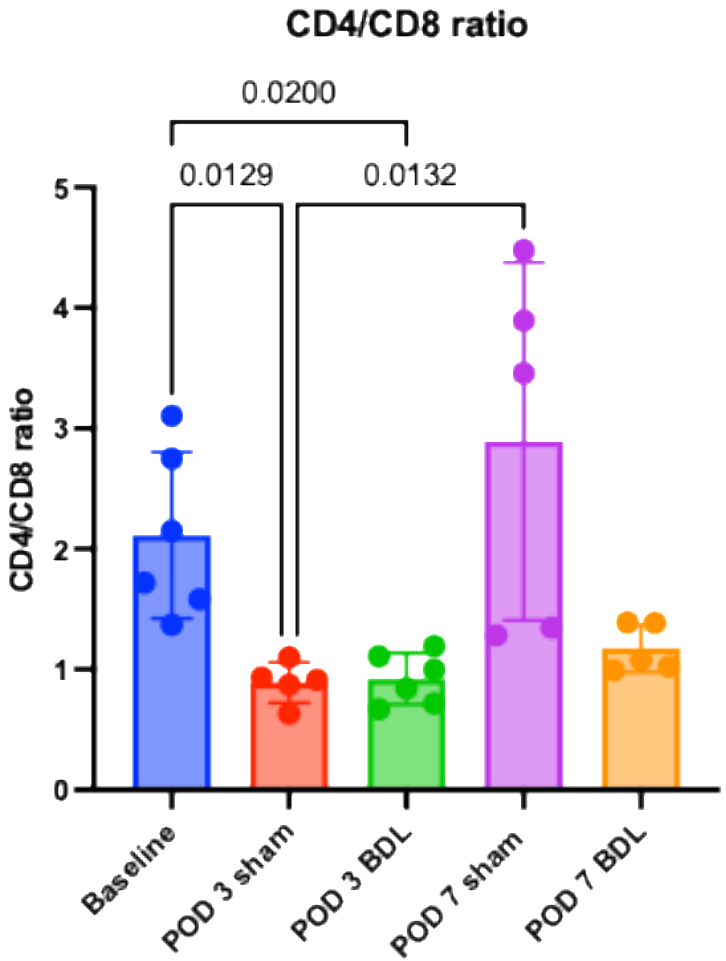

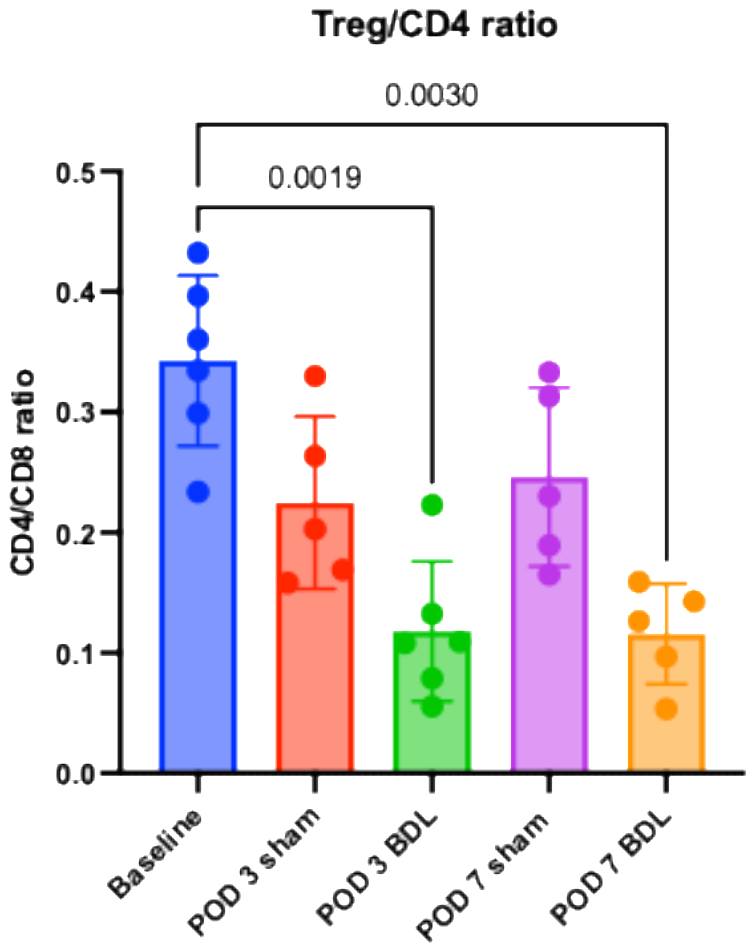

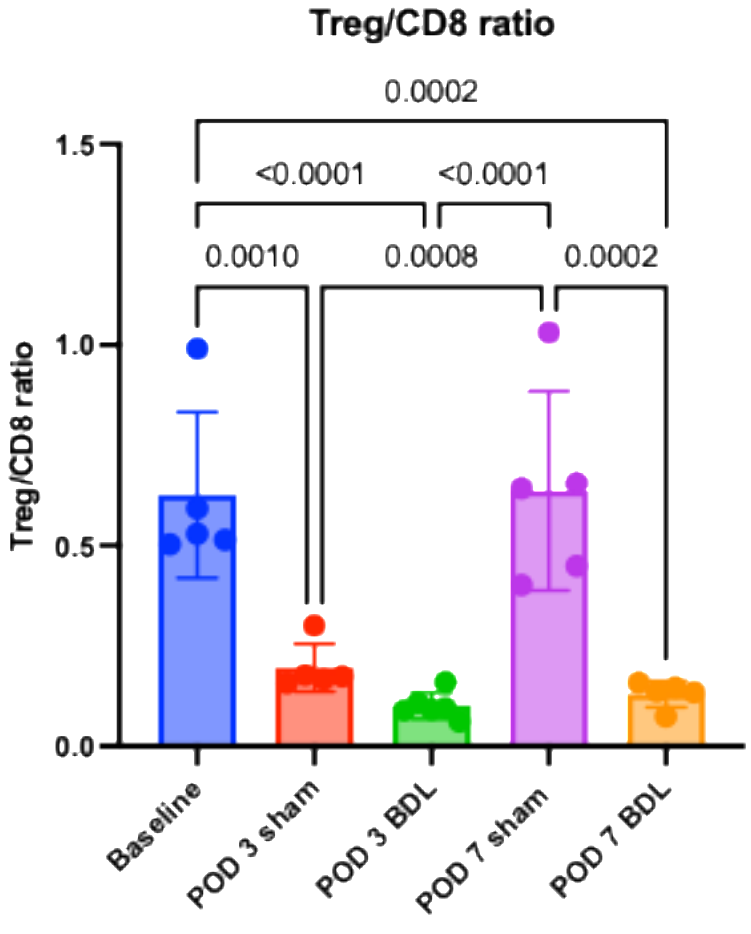

Macrophages

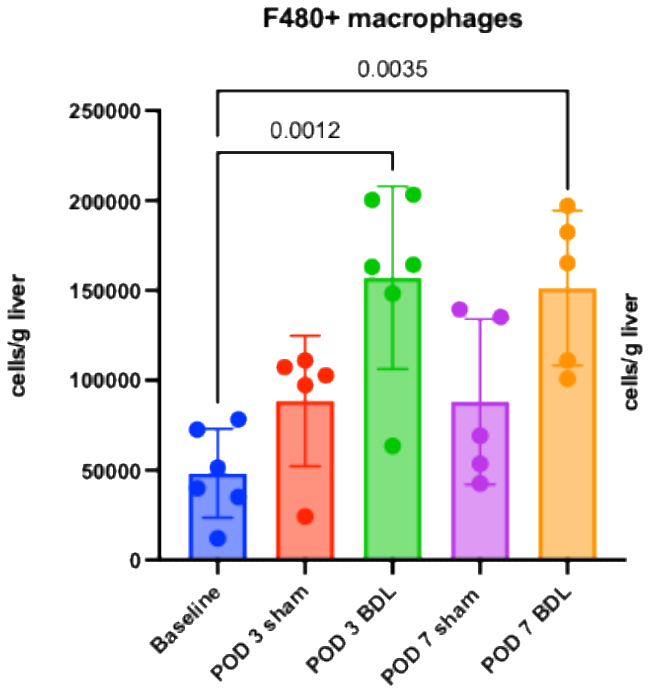

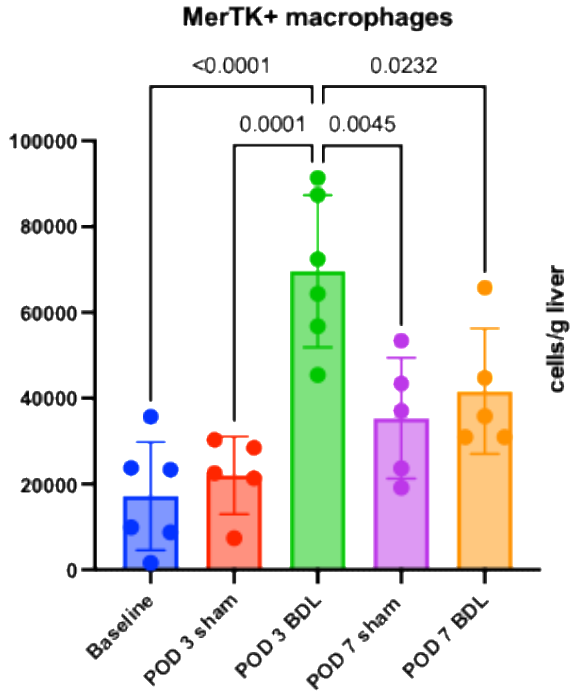

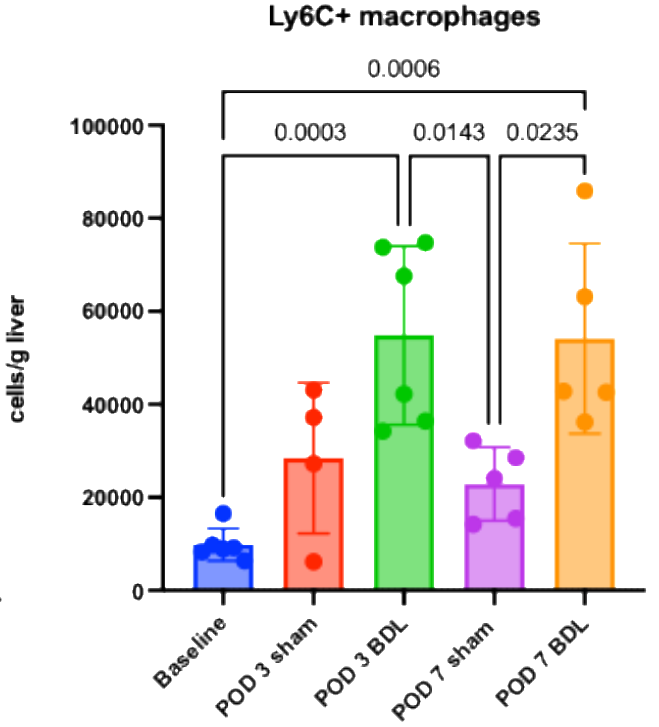

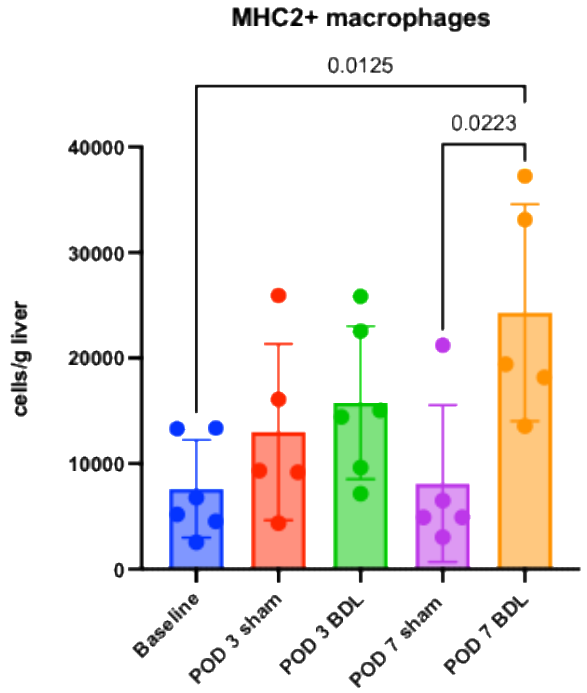

scRNA-seq

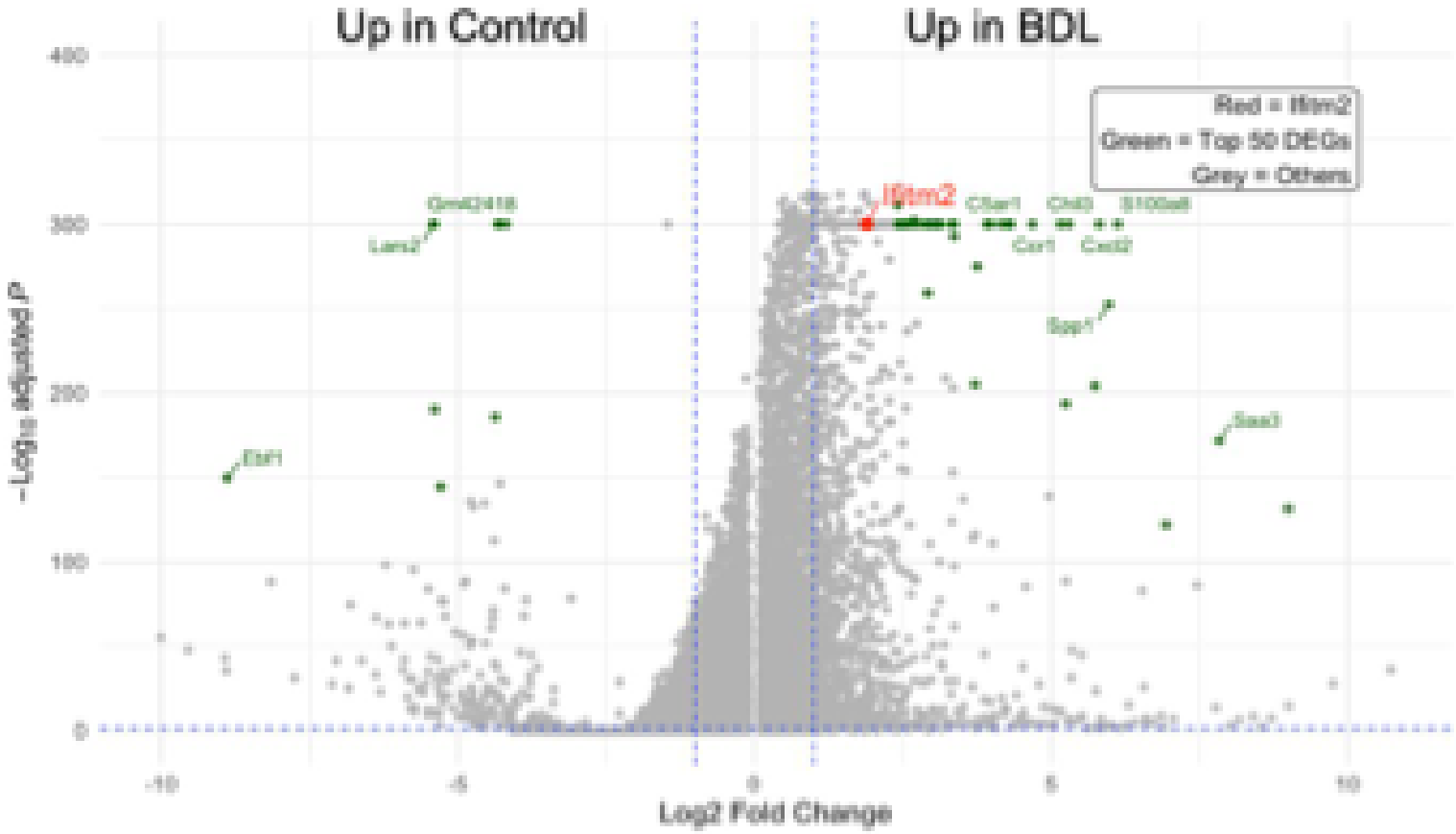
Up in Control
Up in BDL
Red = Ifitm2
Green = Top 50 DEGs
Grey = Others
Ifitm2
Gm42418
Lamc2
Ctsl1
Ctsh
S100a8
Ccr1
Ccl2
Spp1
Saa3
Ctrl1
400
300
200
100
0
-10
-5
0
5
10
Log2 Fold Change
−Log10 adjusted p

scRNA- seq: macrophages by cluster

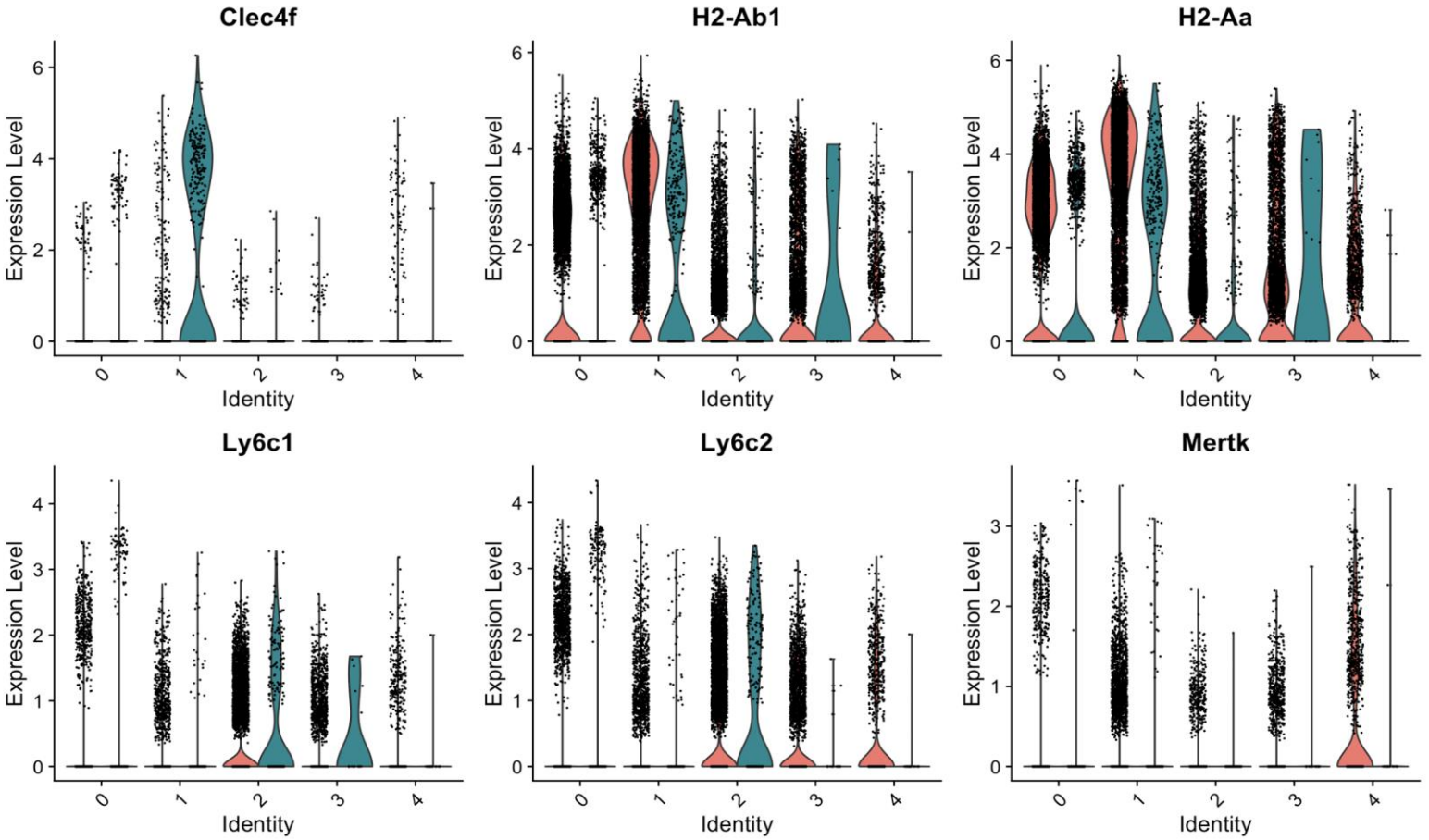

Adult healthy: macrophage clusters

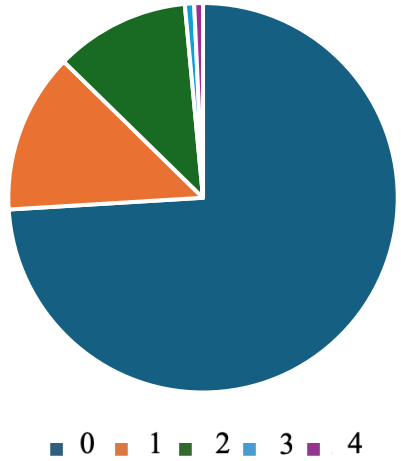

Adult BDL: macrophage clusters

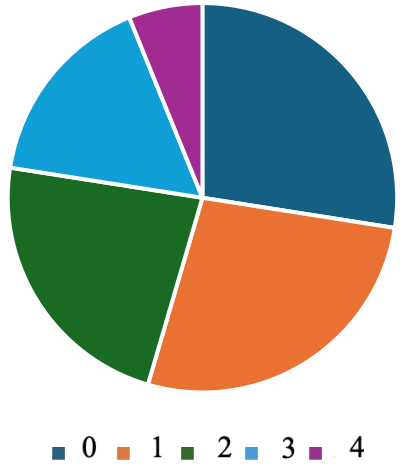

Conclusions and Future Directions

- In a murine BDL model of obstructive cholestasis, at POD 3 the cholestatic group has significantly more CD8 and CD4 T cells, although fewer FoxP3 T regulatory CD4 t cells than baseline or sham surgical condition.

- At POD 7 the sham surgical group demonstrates shift in T cell compartment closer to baseline, while the cholestatic group shows persistent decrease in CD4/CD8 ratio compared to baseline.

- At POD 3 animals who underwent BDL have significantly tissue resident macrophages and those of inflammatory phenotype than sham or baseline groups. At POD 7, cholestatic mice demonstrate persistent inflammatory macrophage phenotype and increased number of MHC2 positive macrophages, indicating an increase in antigen presentation compacities.

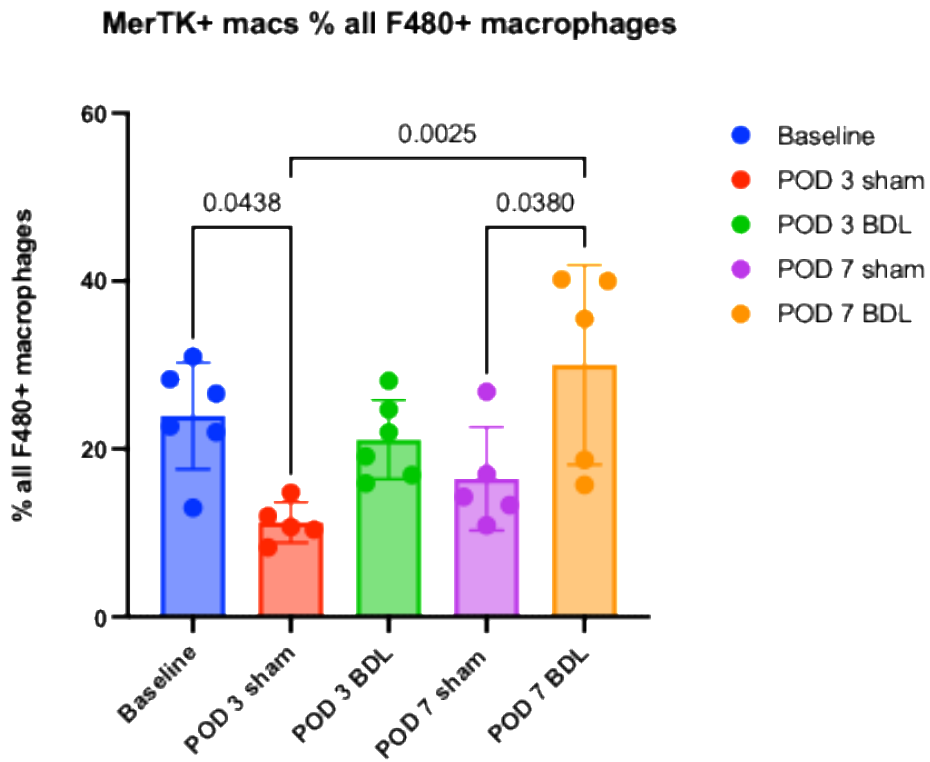
MerTK+ macs % all F480+ macrophages
% all F480+ macrophages
60
40
20
0
0.0025
0.0438
0.0380
Baseline
POD 3 sham
POD 3 BDL
POD 7 sham
POD 7 BDL
Baseline
POD 3 sham
POD 3 BDL
POD 7 sham
POD 7 BDL

Cellular Senescence in Obstructive Cholangiopathies

Ioannis A. Ziogas, MD, MPH
PGY4 General Surgery Resident
PhD Student in Clinical Investigation

Mentor: Sarah A. Taylor, MD
Associate Professor of Pediatrics

StARR Research Meeting

December 11, 2025

Children's Hospital Colorado
Here, it's different.™

Affiliated with
School of Medicine
UNIVERSITY OF COLORADO
ANSCHUTZ MEDICAL CAMPUS

Background

- Biliary atresia (BA) is the most common indication for pediatric liver transplantation (LT)
- Restoration of bile flow with Kasai portoenterostomy is crucial
- Characterized by cholestatic liver injury with cellular apoptosis and immune cell recruitment (i.e., macrophages [MΦs])

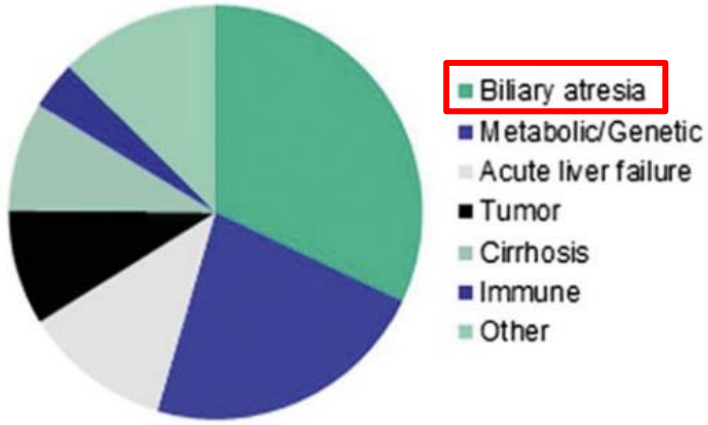

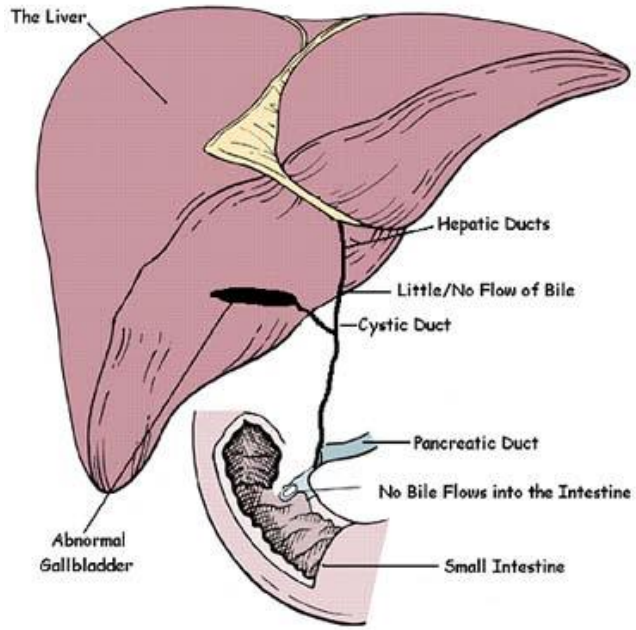

Cellular Senescence

- State of cell cycle arrest but active
- Natural response to DNA damage to prevent proliferation of abnormal cells
- Favorable role in tissue repair and regeneration or promote tissue injury
- Effect of senescent cells on tissue injury is influenced by senescent cell-cell interactions

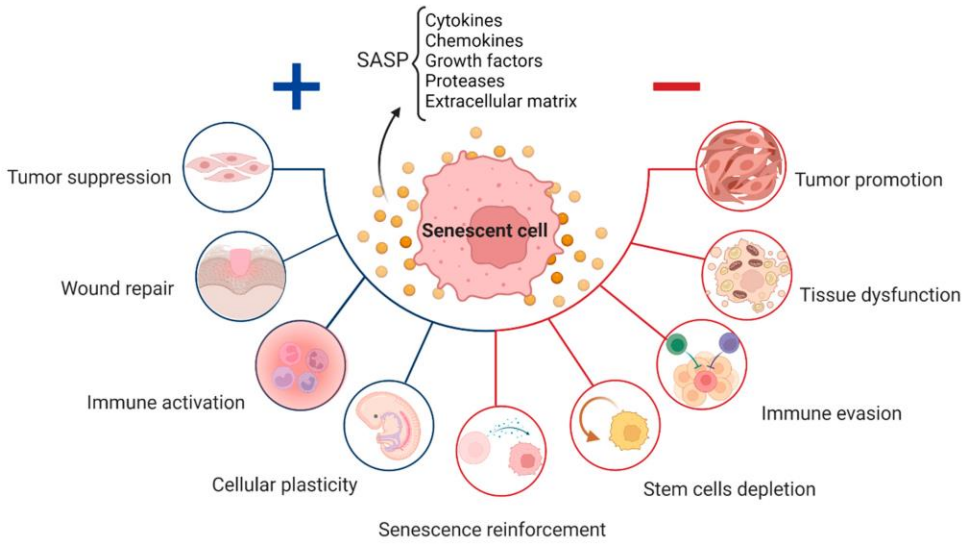

Cellular Senescence in Biliary Atresia

- Increased numbers of senescent cells in murine BA

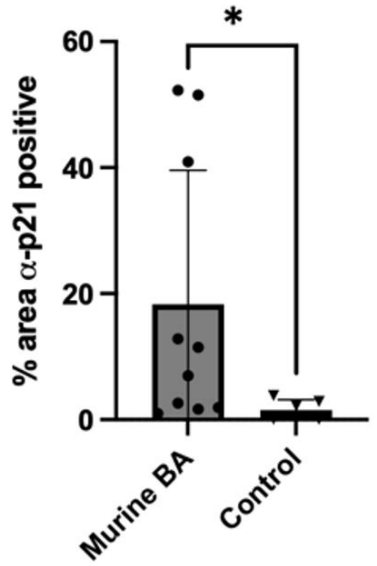

- Increased cellular senescence at diagnosis is associated with improved outcome in children with BA as defined by longer duration of survival with the native liver

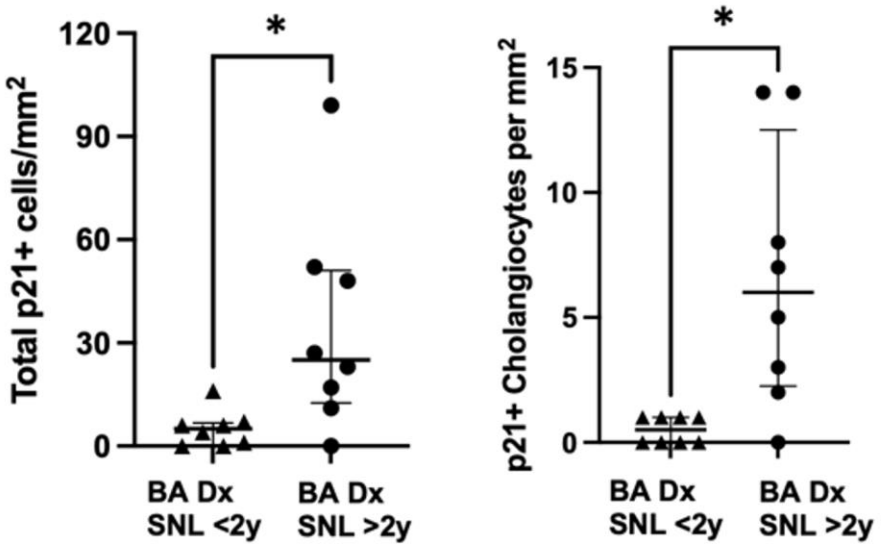

Central Hypothesis

- MΦ efferocytosis of senescent cells promotes tissue regeneration in neonatal obstructive cholestasis whereas senescent cells impair efferocytosis and exacerbate tissue injury in older patients

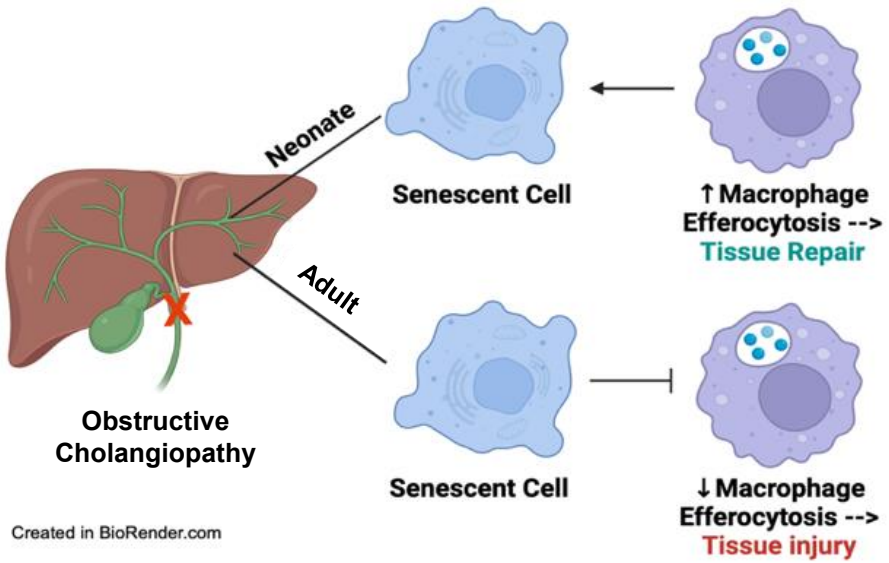

Specific Aim/Research Question

- How does senescent cell depletion impact severity of liver injury in neonatal versus adult mice after bile duct ligation (BDL)?

Experimental Design

- Murine Model of BDL in C57BL/6 (B6) mice
  - Responsible Conduct of Research - IACUC approval
- BDL replicates clinical features of cholestasis
- Outcome analyses:
  - Neonate (BDL on day of life 10 [DOL10]): postoperative day 7 (POD7) or DOL17
  - Adult (BDL on week 8-12): POD7

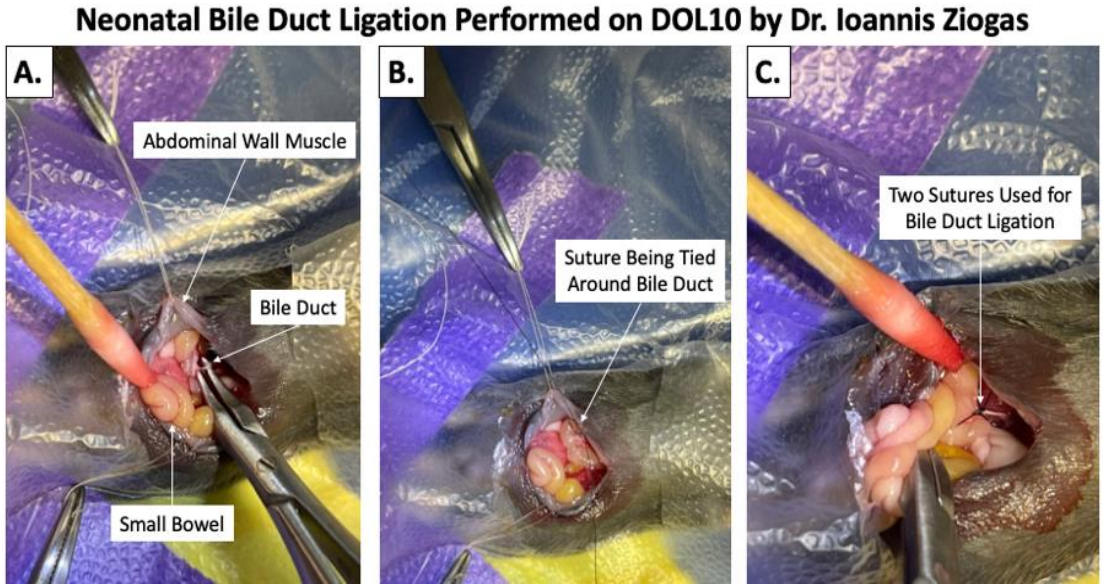

Figure. A. Identification of bile duct in neonatal mouse weighing 8 g. **B-C.** Ligation of murine bile duct with two 8-0 Nylon sutures

- Dasatinib (5 mg/kg)
- Quercetin (50 mg/kg)

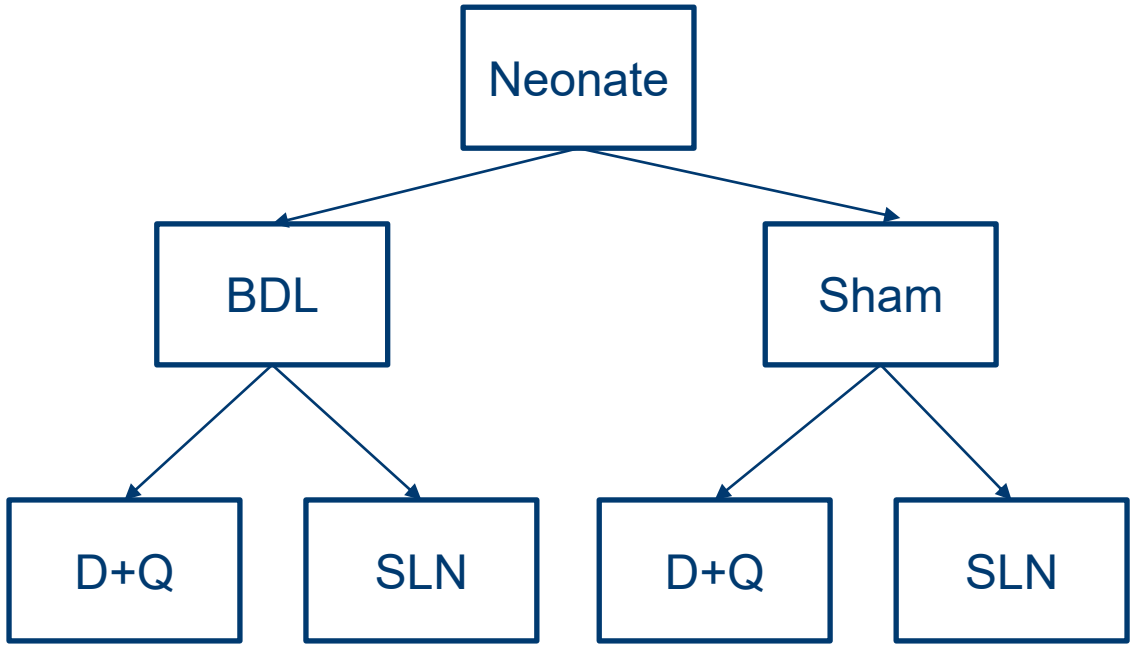

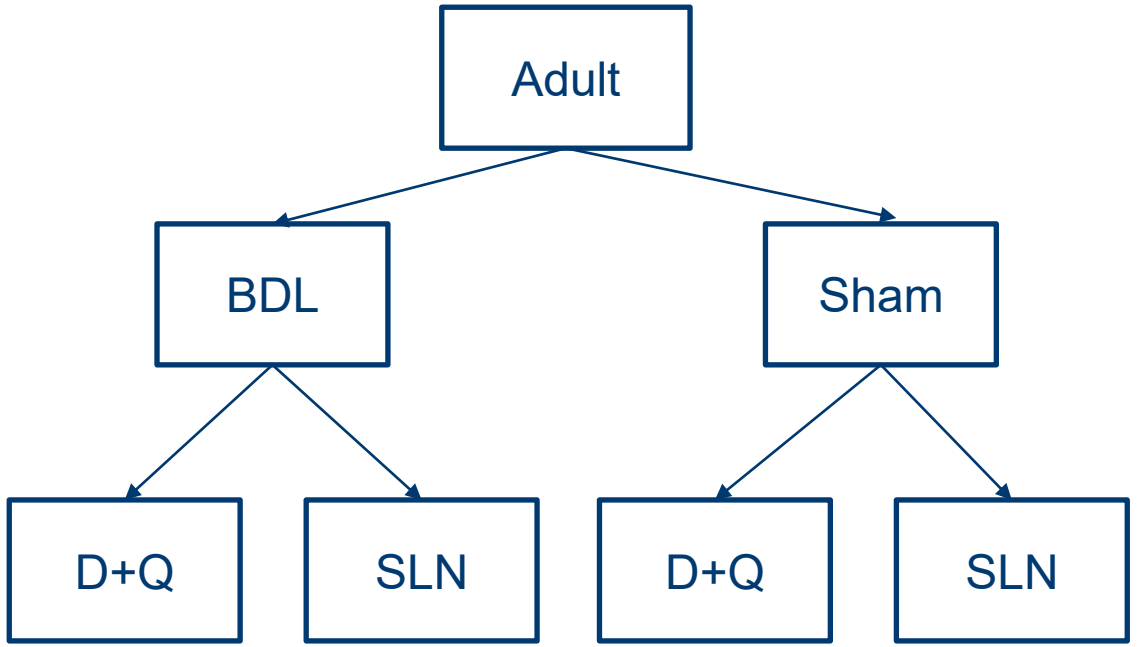

Outcome Measures

- Biochemical markers of cholestatic liver injury
- Histologic liver injury (Ishak score)
- qPCR analysis for expression of markers of senescence
- Flow cytometry for senescent cells (e.g., cholangiocytes)

Preliminary Results

- Still perfecting neonatal BDL model given maternal cannibalism of pups, so started proof of concept experiments with adult mice for the efficacy of D+Q injections and determination of optimal dosing

Adult (8-12-week-old) C57BL/6 mice

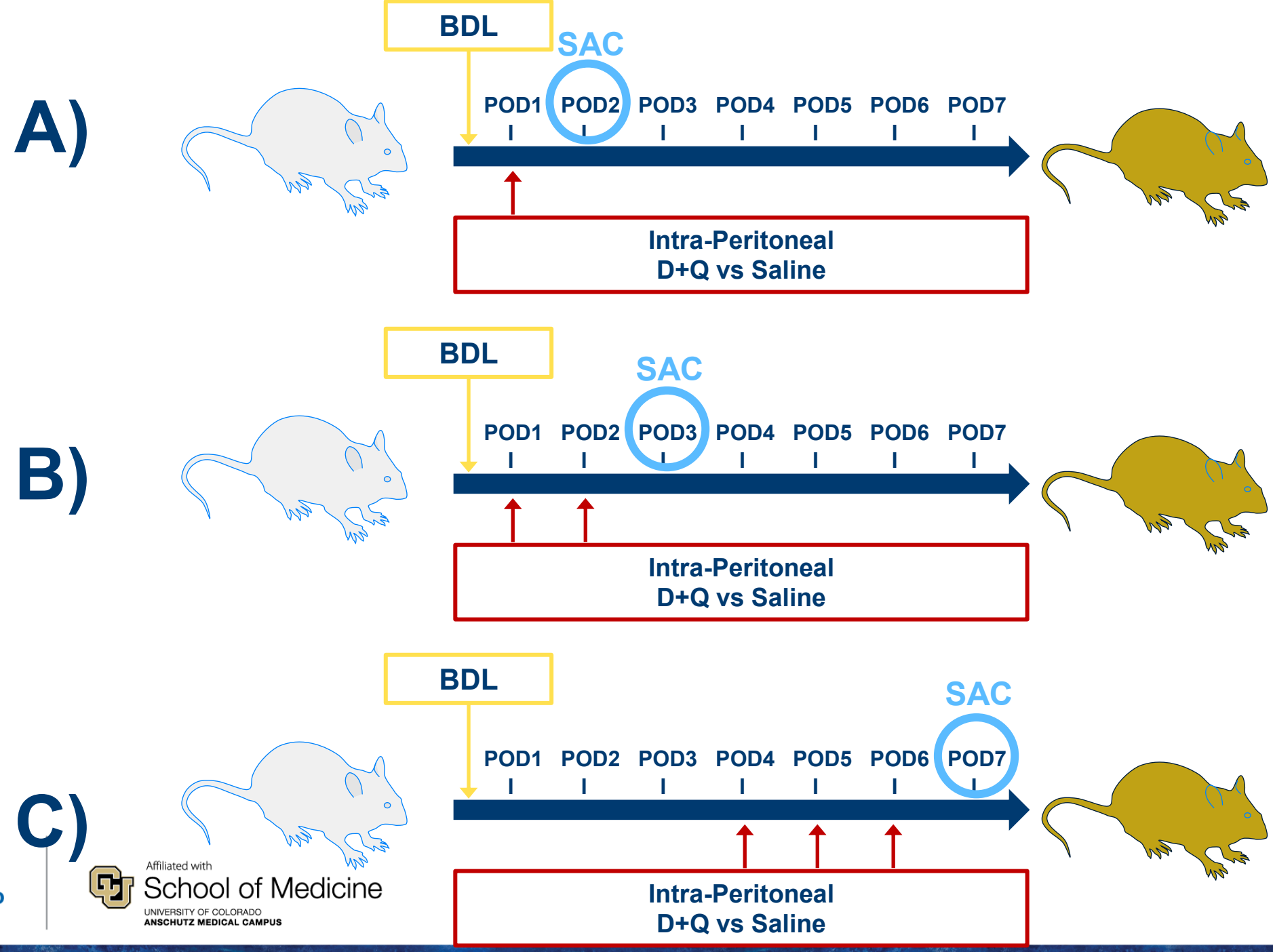

Children's Hospital Colorado
Here, it's different.™

Affiliated with
School of Medicine
UNIVERSITY OF COLORADO
ANSCHUTZ MEDICAL CAMPUS

A) BDL POD1 inj POD2 sac

Blood Chemistry

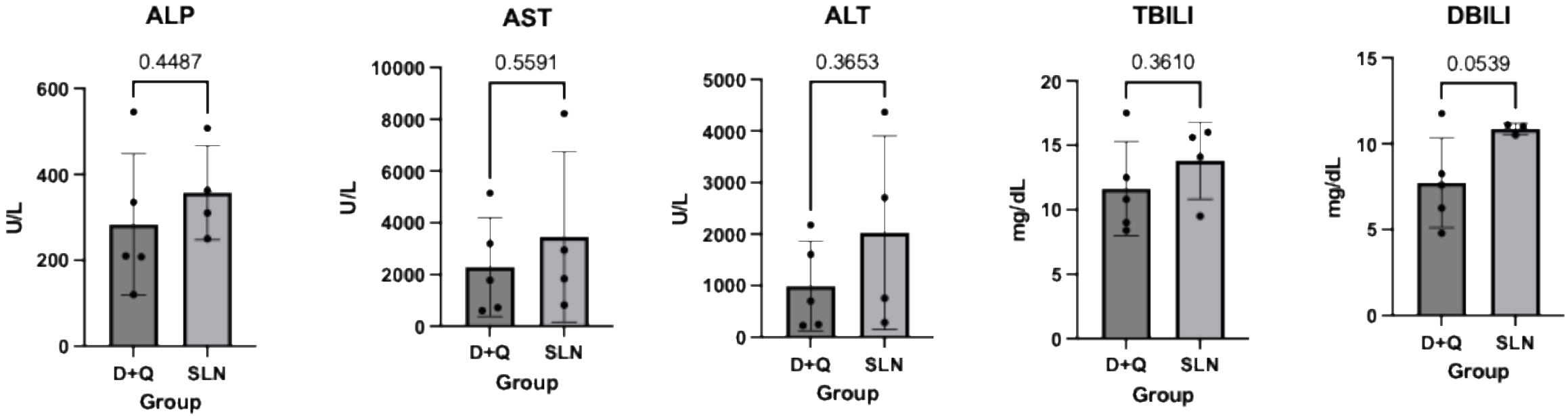

t-test with Welch's correction in 12 mice

Excluding 1 with abnormal ascites and 2 females

Children's Hospital Colorado
Here, it's different.™

Affiliated with
School of Medicine
UNIVERSITY OF COLORADO
ANSCHUTZ MEDICAL CAMPUS

qPCR Analysis

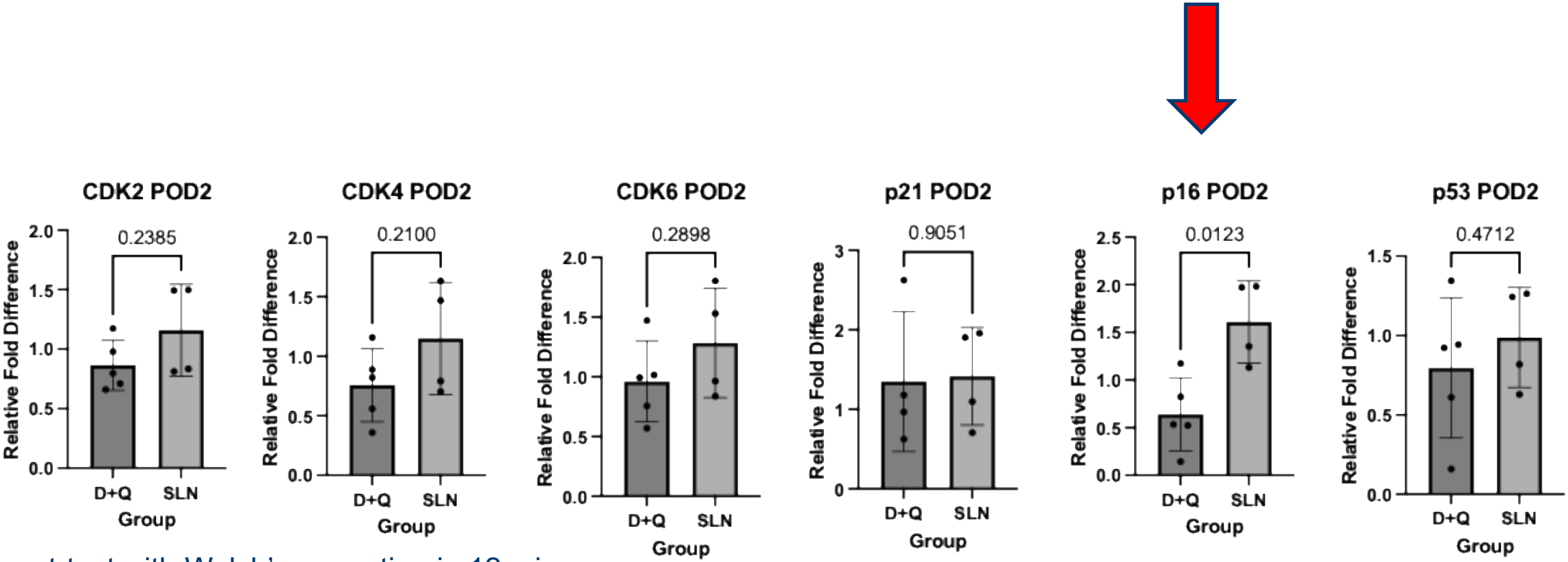

t-test with Welch's correction in 12 mice

Excluding 1 with abnormal ascites and 2 females

Children's Hospital Colorado
Here, it's different.™

Affiliated with
School of Medicine
UNIVERSITY OF COLORADO
ANSCHUTZ MEDICAL CAMPUS

B) BDL POD1+2 inj POD3 sac

Blood Chemistry

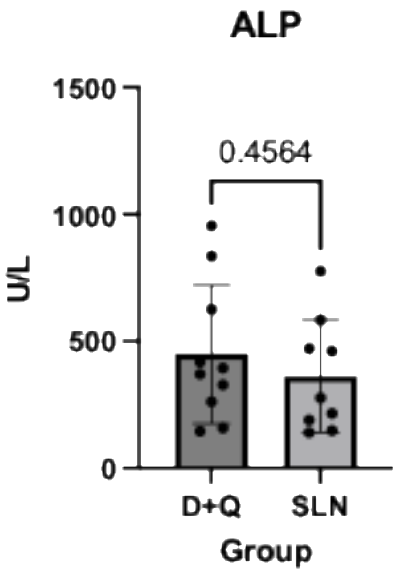

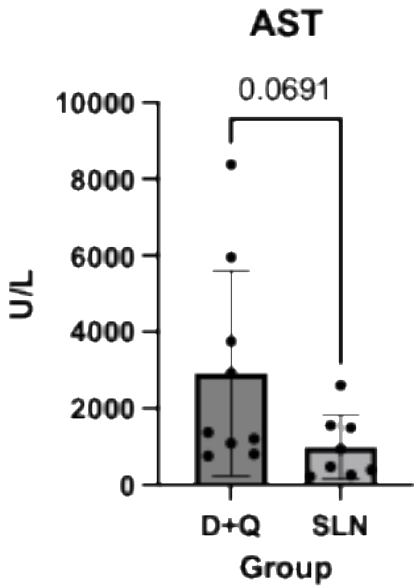

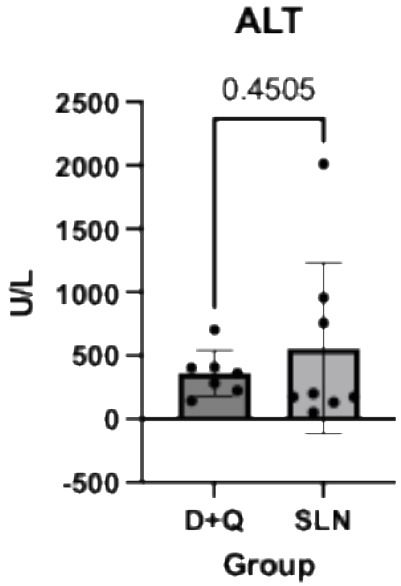

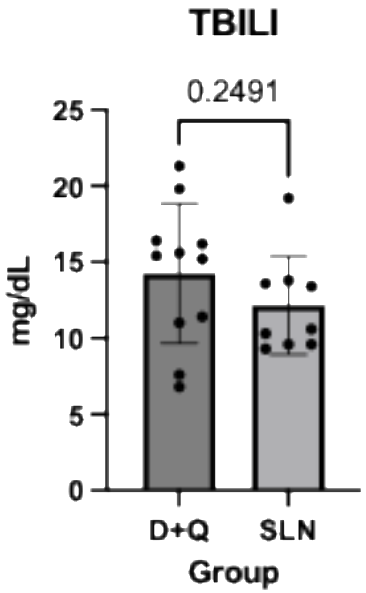

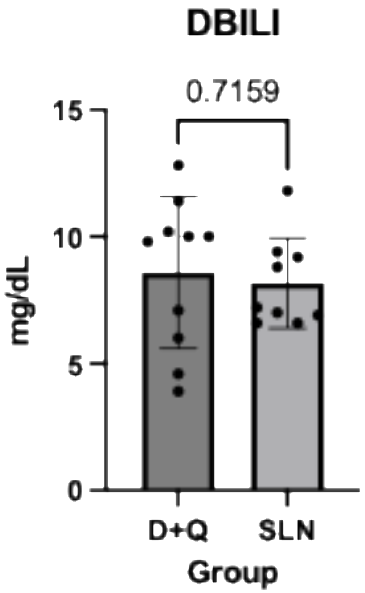

t-test with Welch's correction in 21 mice

Children's Hospital Colorado
Here, it's different.™

Affiliated with
School of Medicine
UNIVERSITY OF COLORADO
ANSCHUTZ MEDICAL CAMPUS

Ishak Score

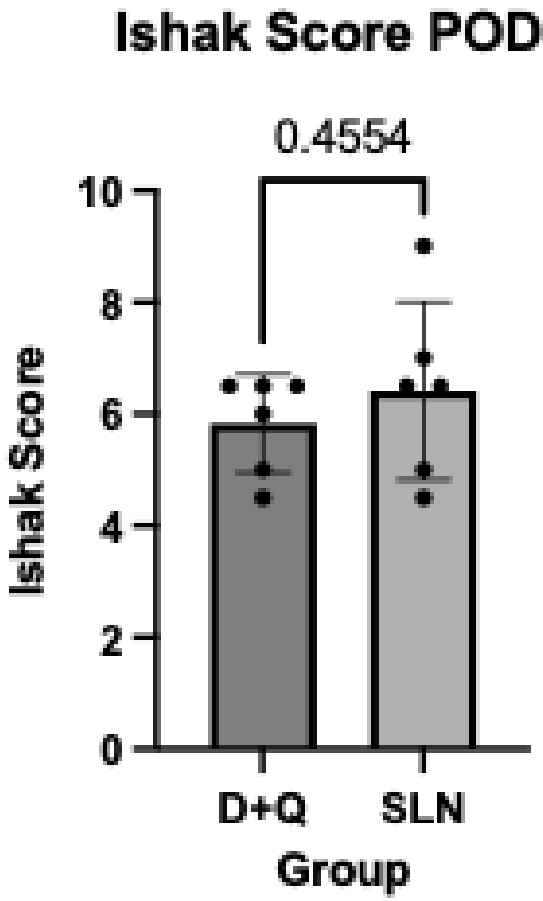

t-test with Welch's correction in 12 mice

qPCR Analysis

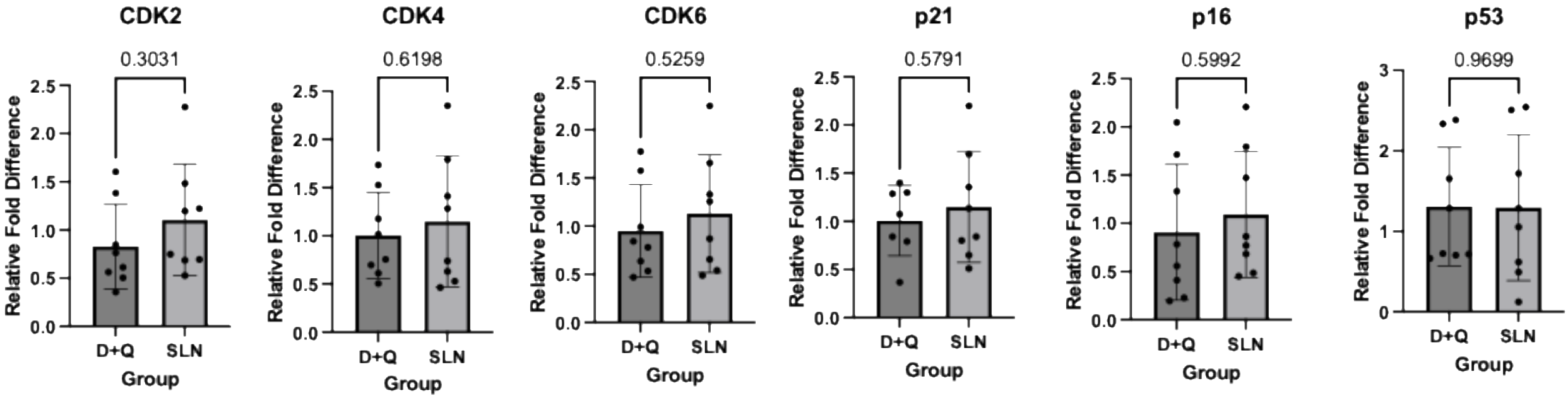

t-test with Welch's correction in 16 mice

Children's Hospital Colorado
Here, it's different.™

Affiliated with
School of Medicine
UNIVERSITY OF COLORADO
ANSCHUTZ MEDICAL CAMPUS

C) BDL POD4-6 inj POD7 sac

Blood Chemistry

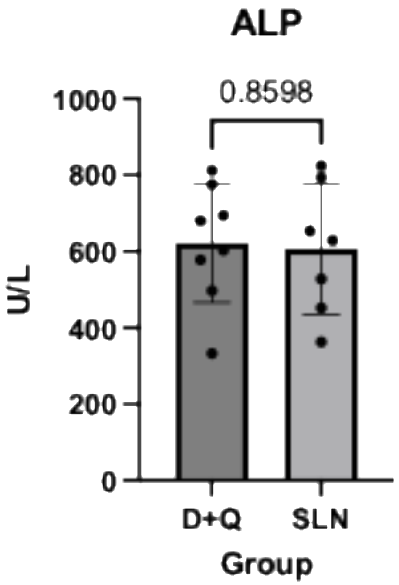

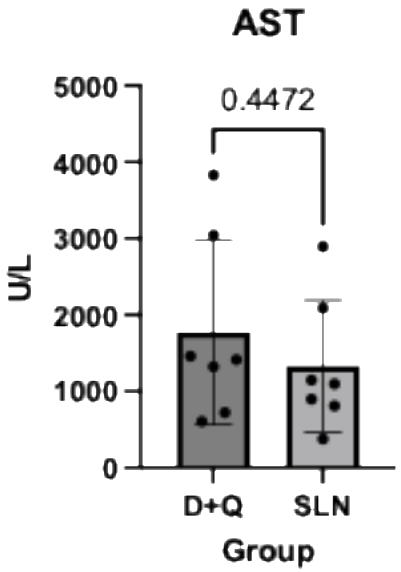

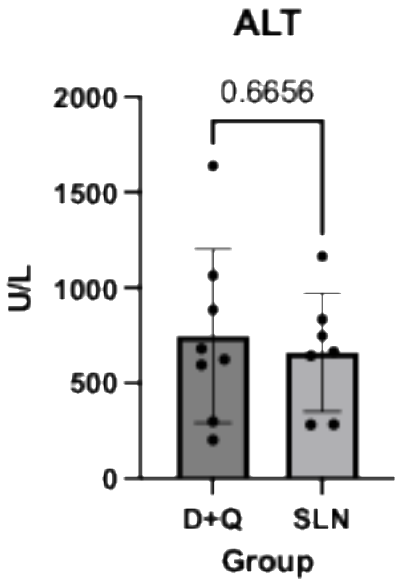

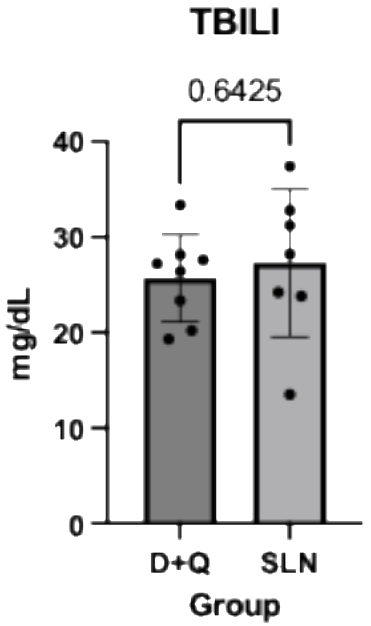

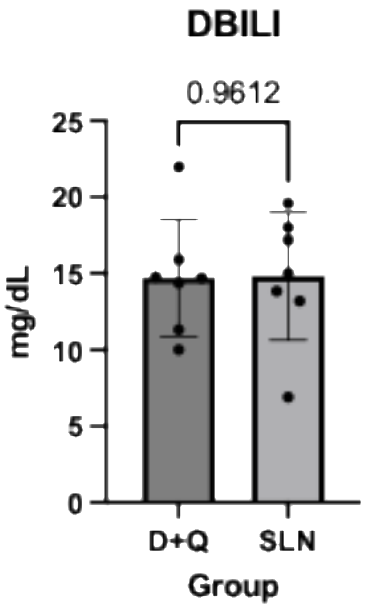

t-test with Welch's correction in 15 mice

Ishak Score

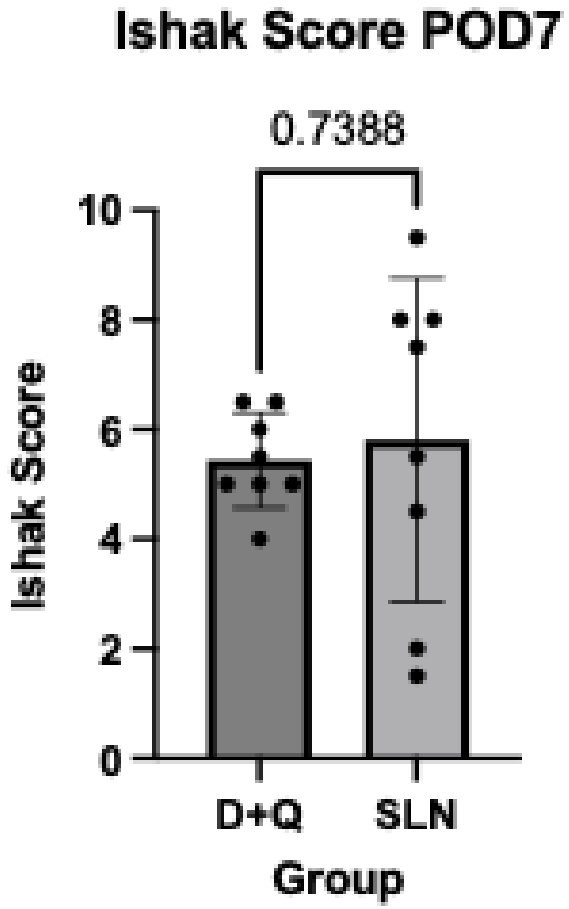

t-test with Welch's correction in 16 mice

qPCR Analysis

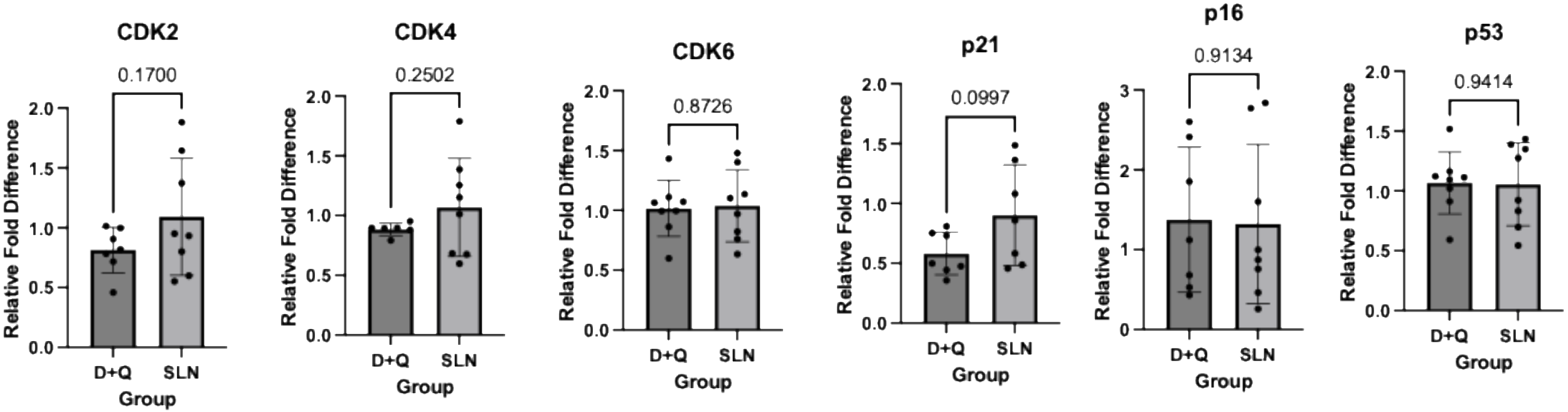

t-test with Welch's correction in 16 mice

Children's Hospital Colorado
Here, it's different.™

Affiliated with
School of Medicine
UNIVERSITY OF COLORADO
ANSCHUTZ MEDICAL CAMPUS

Flow Cytometry

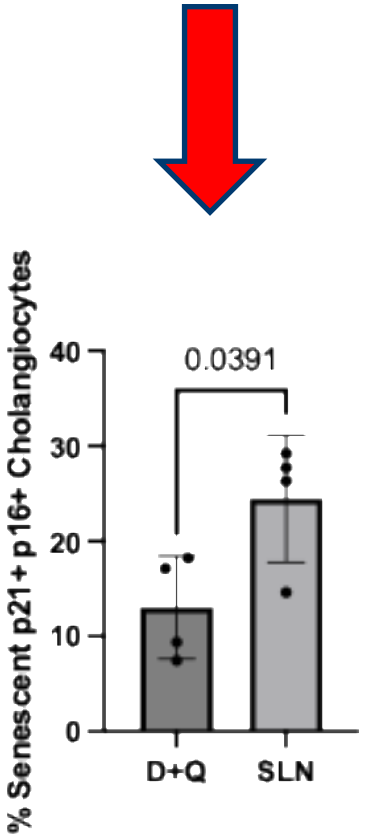

t-test with Welch's correction in 8 mice

Conclusions & Future Directions

- Combination of dasatinib & quercetin can lead to depletion of senescent cells, yet the dosing and impact on disease progression warrants further investigation

- Next steps will include:
  - qPCR analysis of additional fibrosis and senescence-associated secretory phenotype factors
  - Beta-gal, CK19, Ki-67, sirius red staining
  - Neonatal BDL
  - Evaluation of fisetin (flavonoid senolytic agent)

Questions?

Contact info:

- Email: ioannis.ziogas@cuanschutz.edu
- X: @IA_Ziogas

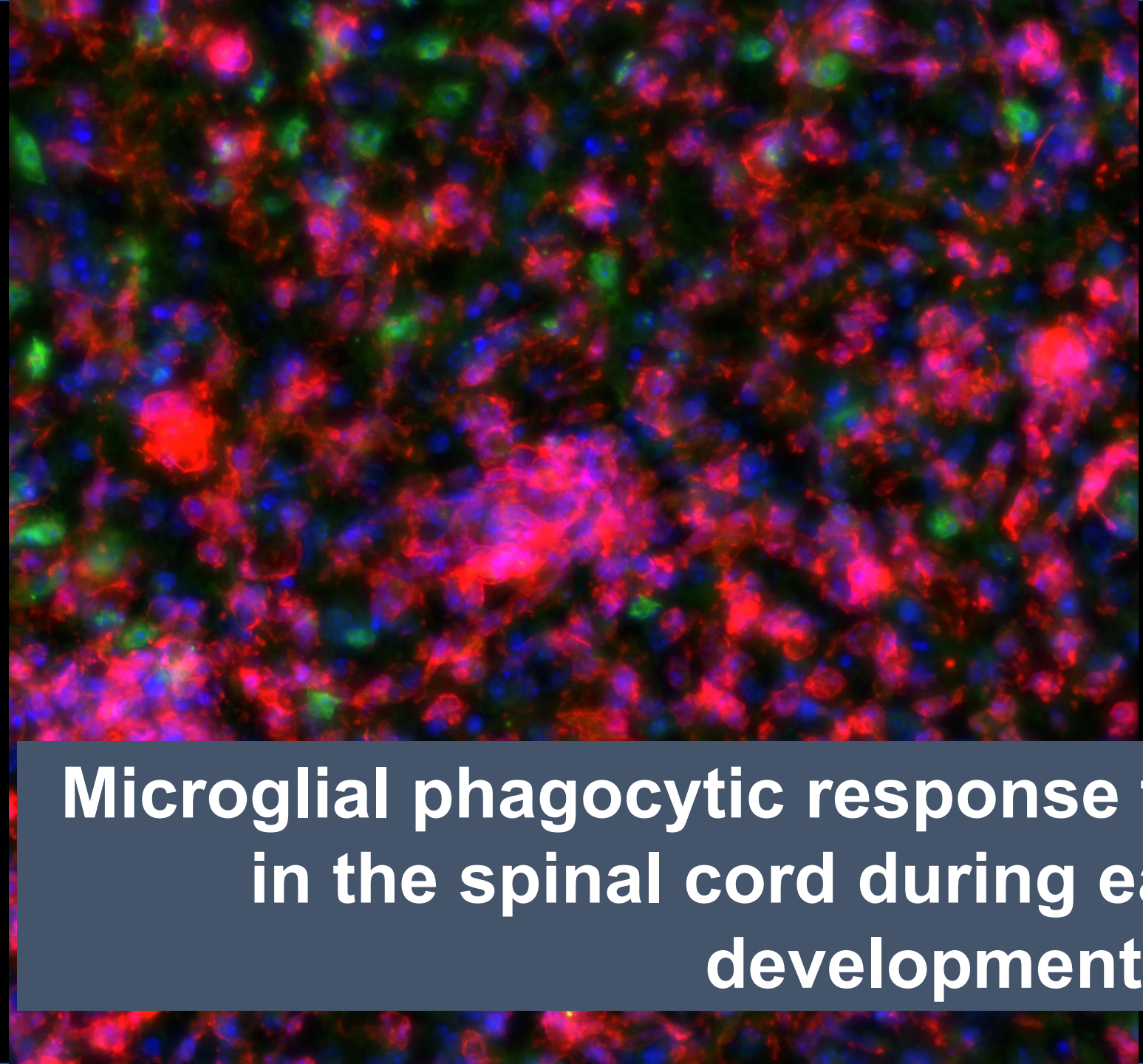

Sadie Meller
MD/PhD
Tyler Laboratory

StARR Research Meeting
December 11th, 2025

Microglial phagocytic response to EV-D68 infection in the spinal cord during early postnatal development

Enterovirus D68 and Age Specific Vulnerability to Acute Flaccid Myelitis

- Enterovirus D68 (EV-D68) is a respiratory pathogen that has emerged as a cause of acute flaccid myelitis (AFM) in children in the past decade

- Over 90% of EV-D68 associated AFM cases occur in patients who are younger than 18 years old, with a median age of 7.1 years in the 2014 outbreak (Sejvar et al., 2016) and 5.3 years during the 2018 outbreak (Kidd et al., 2021).

EV-D68 RNA in the Anterior Horn Neurons of the Spinal Cord of 5 year old boy who died of an AFM-like illness in 2008

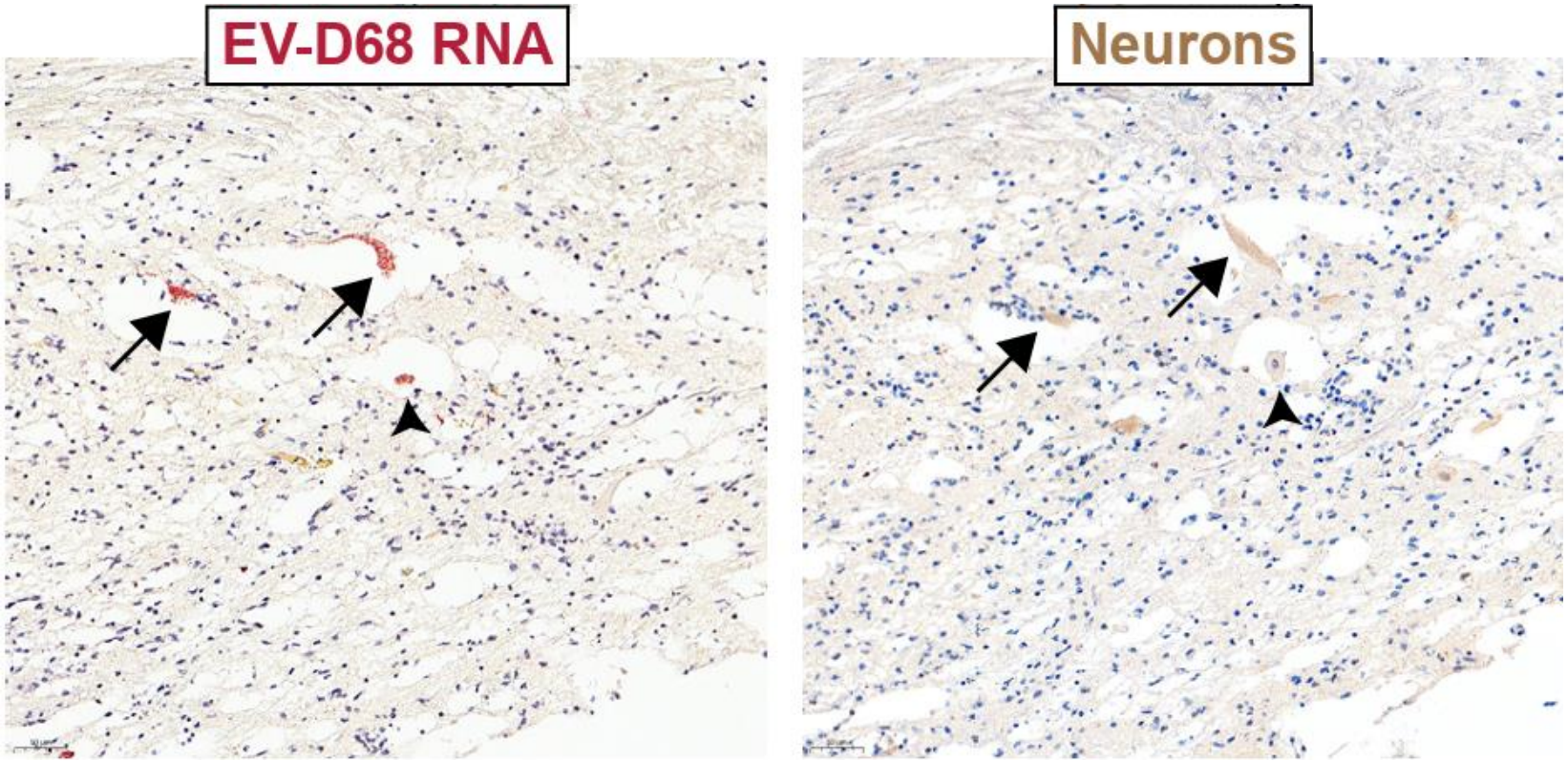

Enterovirus D68 (EV-D68)–specific genomic RNA is demonstrated by in situ hybridization

Vogt et al., N Engl J Med. 2022 386(21):2059-2060.

Mouse Model of EV-D68 and Acute Flaccid Myelitis

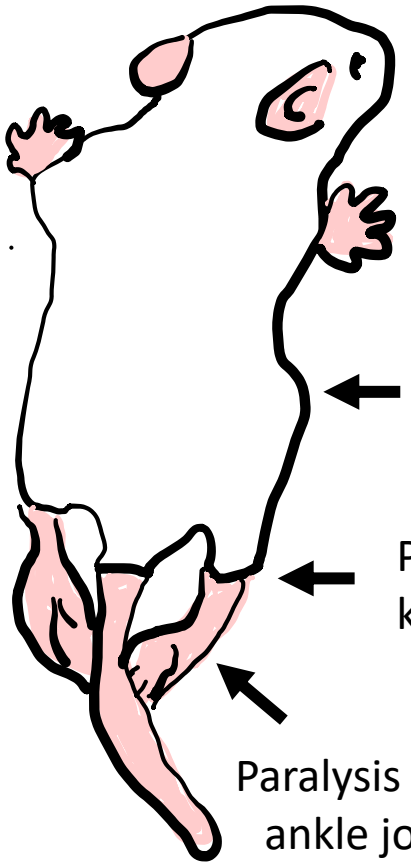

Paralysis at hip joint =3

Paralysis beyond knee joint =2

Paralysis beyond ankle joint =1

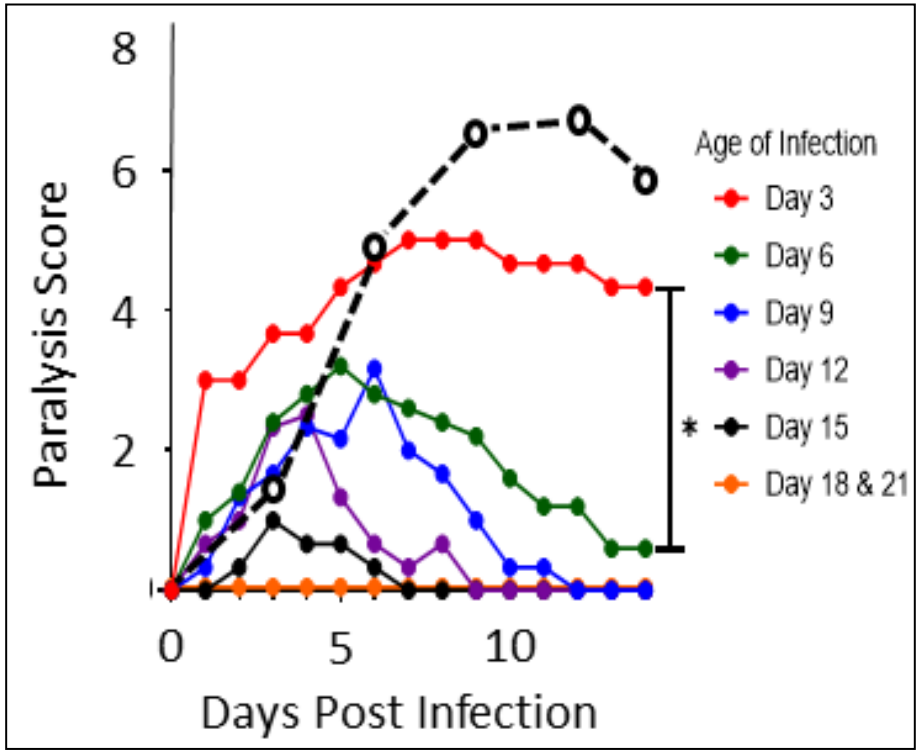

Hixon et al., PLOS Pathogen. 2017; 13(2)

Motor neuron is larger in size than surrounding interneurons

Lumbar Spinal Cord

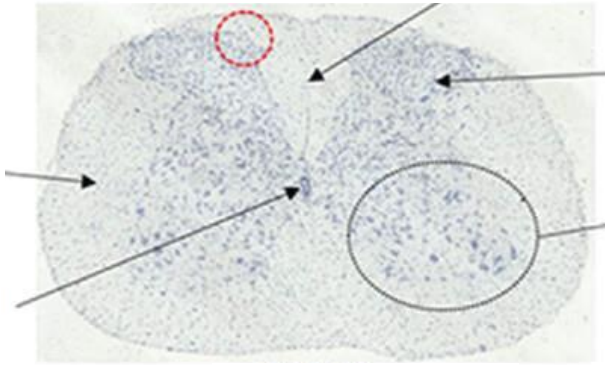

Gray matter (darker staining)

White matter (paler staining)

Ventral horn

Central Canal

Ventral

Gallocyanin

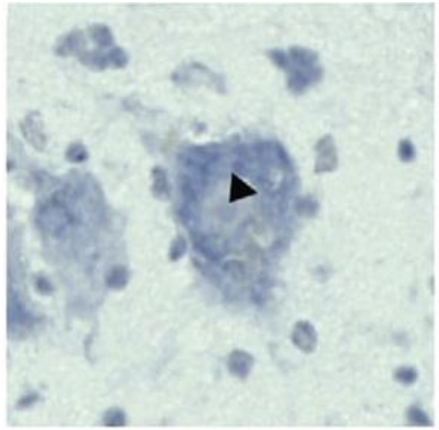

Austen et al., Curr Protoc. 2022 May;2(5):e428.

Microglia: Brain Resident Immune Cells

Do microglia help mediate age-dependent susceptibility to development of acute flaccid myelitis?

Microglia are immune cells responsible for responding to disruptions in homeostasis, including:

- Infection
- Injury

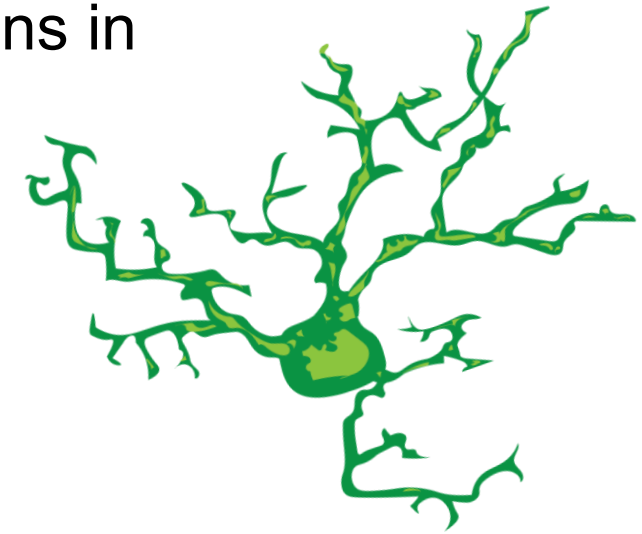

- Microglia are involved in developmental events such as neurogenesis and myelinogenesis and may respond differently to environmental cues during these periods
- Viral infection during critical periods may thus result in a dysregulated microglia response

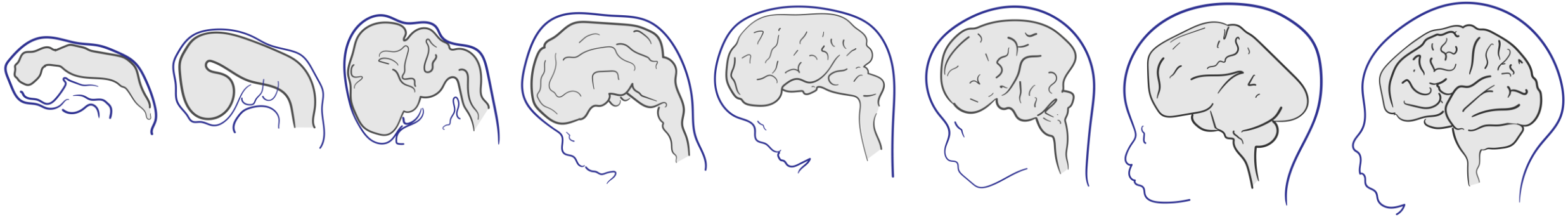

Microglia in the CNS exhibit phagocytic predominance in the first postnatal week

Single cell microglia analysis identified a microglia subset that showed a distinct gene expression profile in the first postnatal week associated with areas of proliferation

- CD11c+ microglia (Wlodarczyk et al., 2017)
- Axon tract associated microglia (Hammond et al., 2019)
- Proliferative region-associated microglia (Li et al., 2019)
- Youth-associated microglia (YAM) (Silvin et al., 2022)
- Aringase-1+ microglia (Stratoulias et al., 2023)

Common Markers
CDllc (Itgax)
Spp1
Gpnmb
Igf1
Clec7a

Proportion of CD11c+ microglia highest at postnatal day 4 in the spinal cord

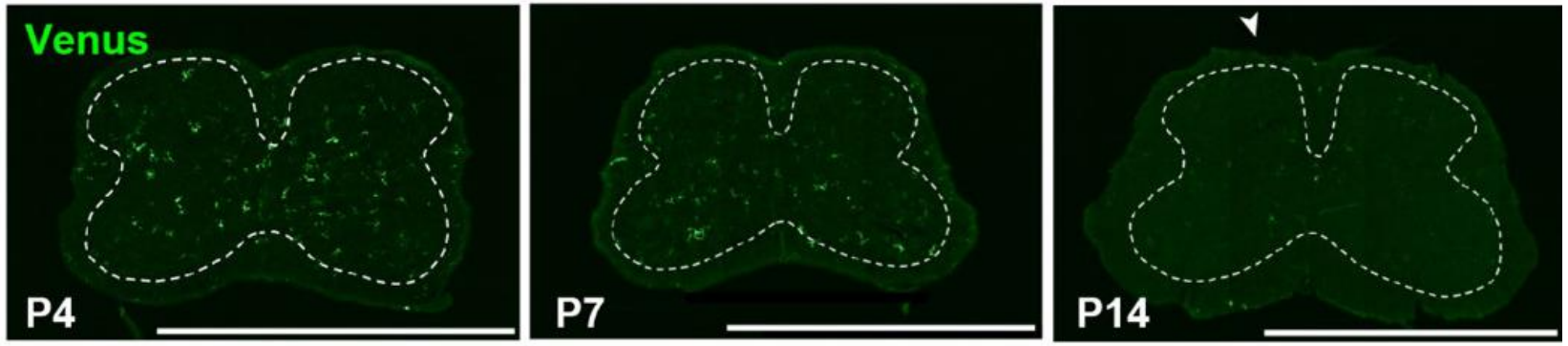

Nomaki et al., 2024, Molecular Brain 17:24

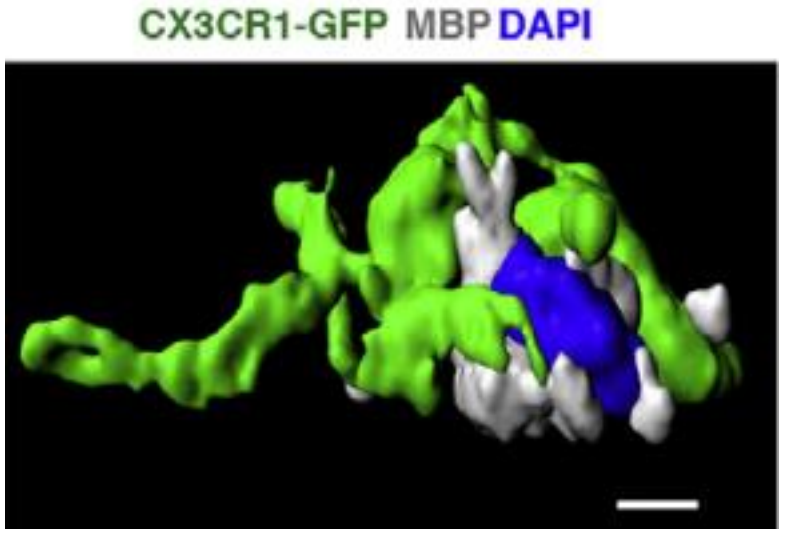

Li et al., 2019, Neuron 101, 207–223

Objective

Do microglia help mediate age-dependent susceptibility to development of acute flaccid myelitis?

Objective: Perform time course to assess for peak microglial response and phagocytic activity following EV-D68 infection.

Experiment: Infect Swiss–Webster mouse pups with EV-D68 at postnatal day 1 (when paralysis is expected) and PBS in the left hindlimb. Obtain samples at 2, 4, 6 and 8 days post-infection to determine time point for peak microglia response.

Immunohistochemistry Markers

Microglia & Phagocytosis	Neuron
Iba1	NeuN
Cd68	ChAT

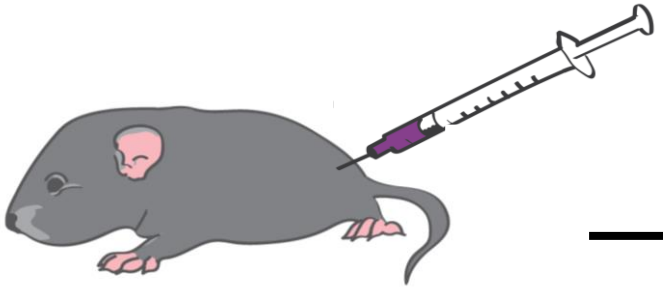

Postnatal Day 1

Days Post Infection

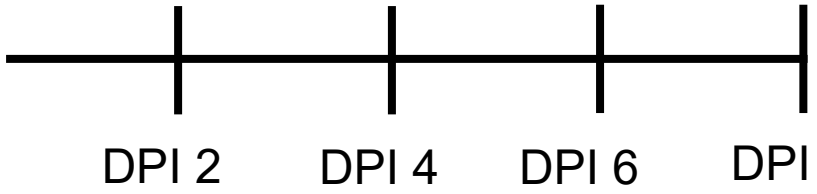

IM injection of EV-D68 at postnatal day 1 induces paralysis

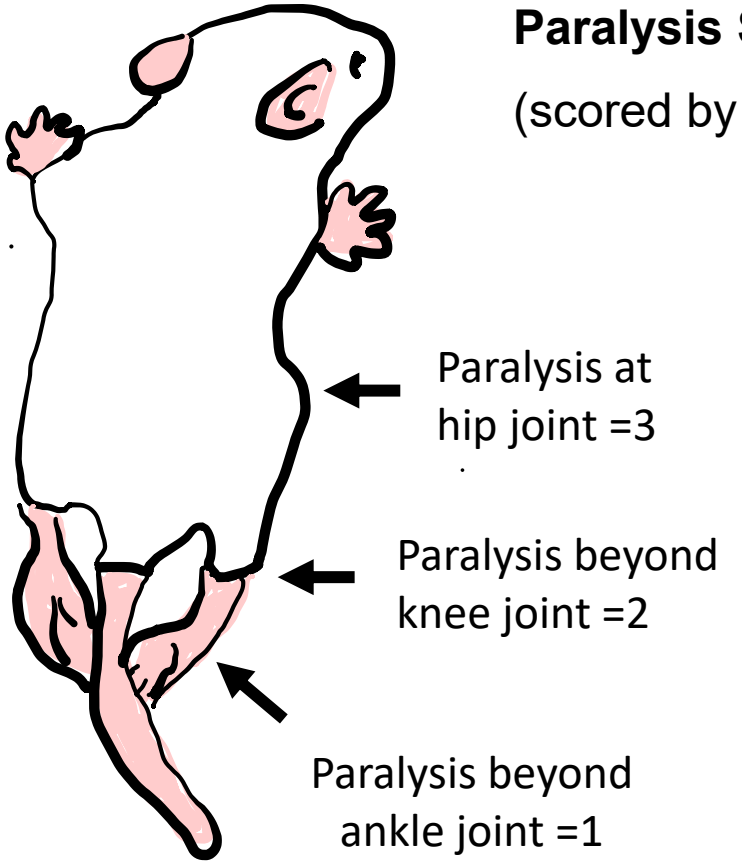

Paralysis Scoring

(scored by a blinded observer):

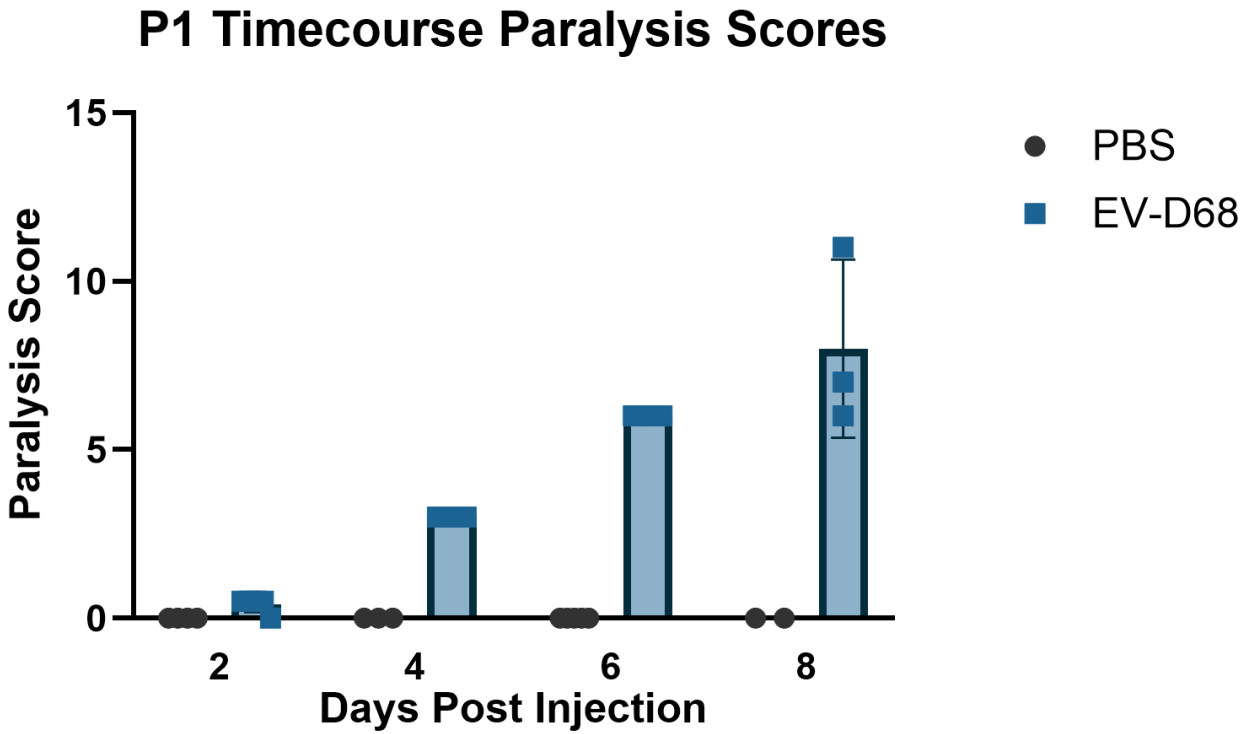

	PBS		EV-D68	
Days Post Injection	N	Paralysis Score [Average]	N	Paralysis Score [Average]
DPI 2	4	0 [0]	5	0.5, 0.5, 0.5, 0.5, 0 [0.4]
DPI 4	3	0 [0]	4	3, 3, 3, 3 [3]
DPI 6	5	0 [0]	4	6, 6, 6, 6 [6]
DPI 8	2	0 [0]	3	11, 6, 7 [8]

Confirm infection with EV-D68 Viral Capsid Protein VP2

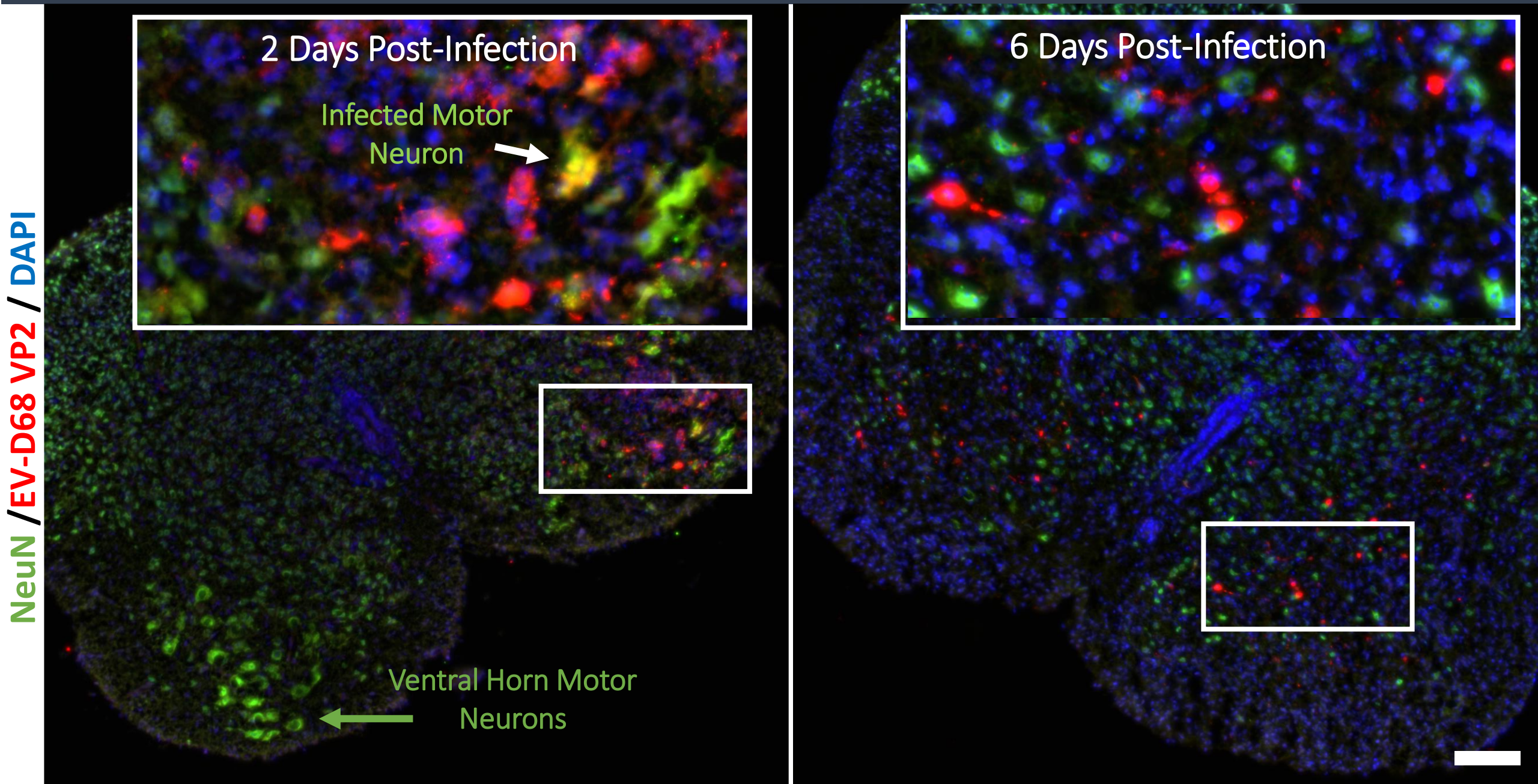

EV-D68 infection associated with microglia accumulation

Four days after injection with PBS or EV-D68 in left hindlimb

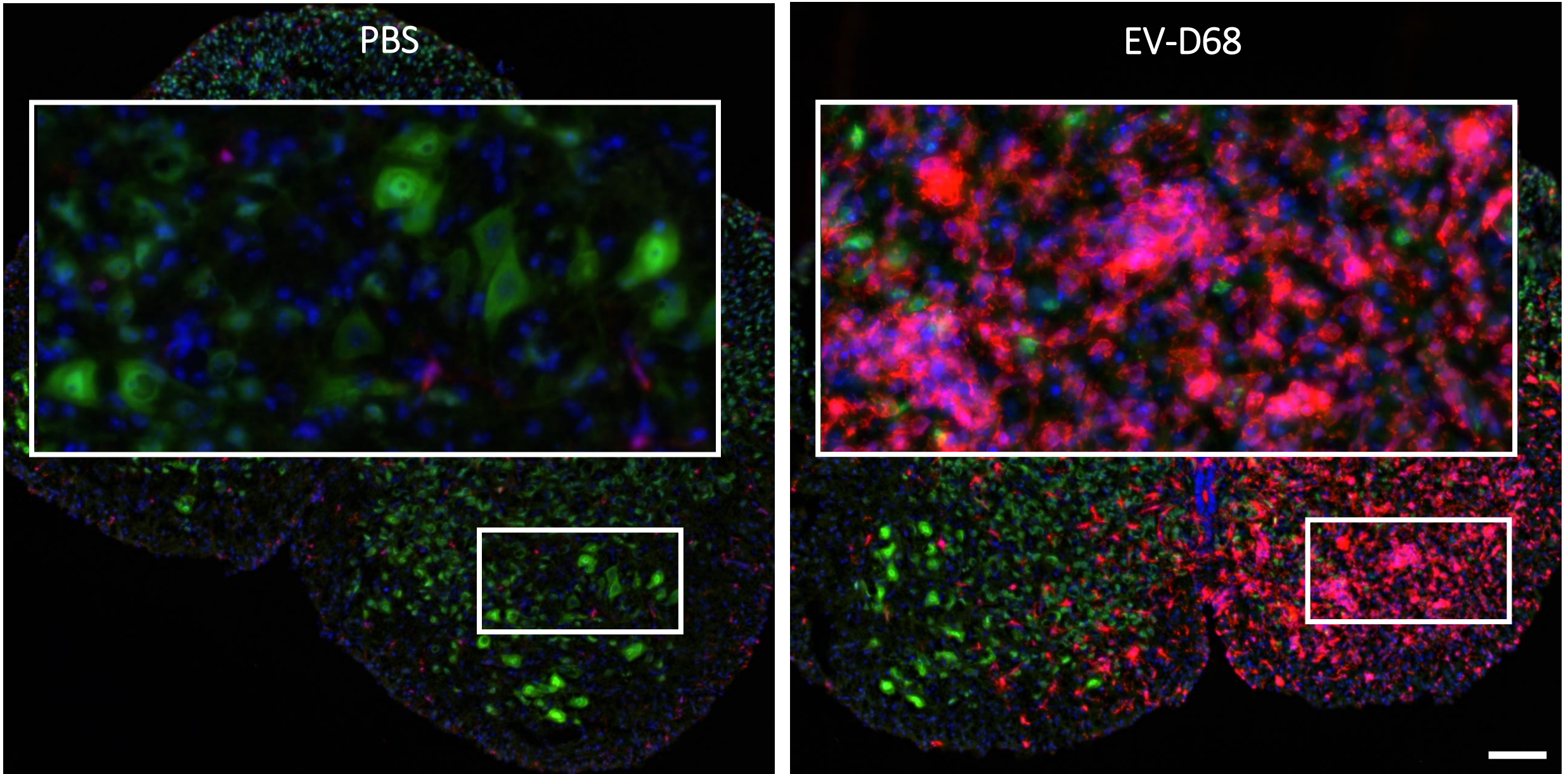

EV-D68 infection associated with motor neuron loss

Six days after injection with PBS or EV-D68 in left hindlimb

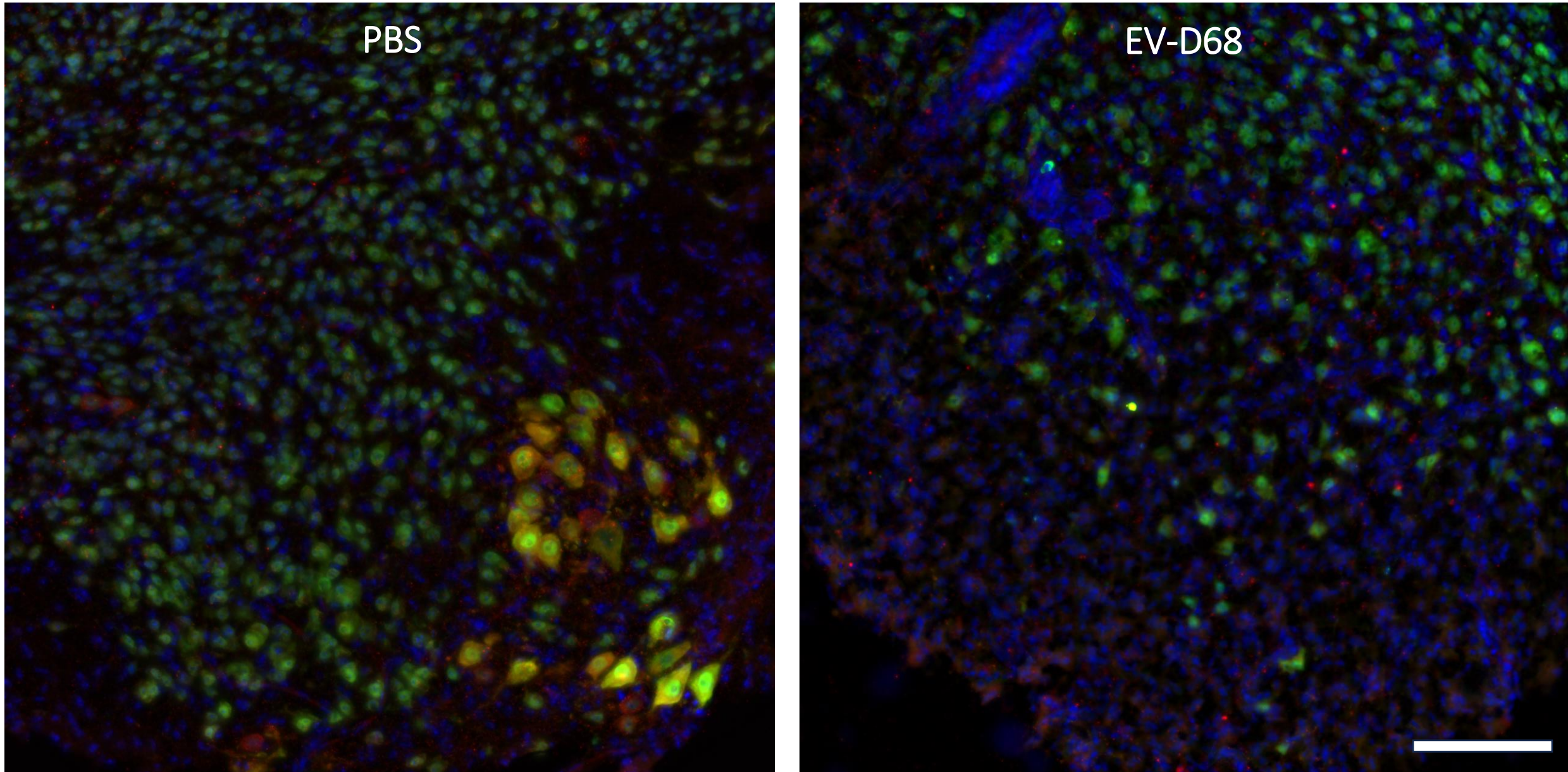

Microglia Density Analysis

DPI 4; EV-D68

NeuN / Iba1 / DAPI

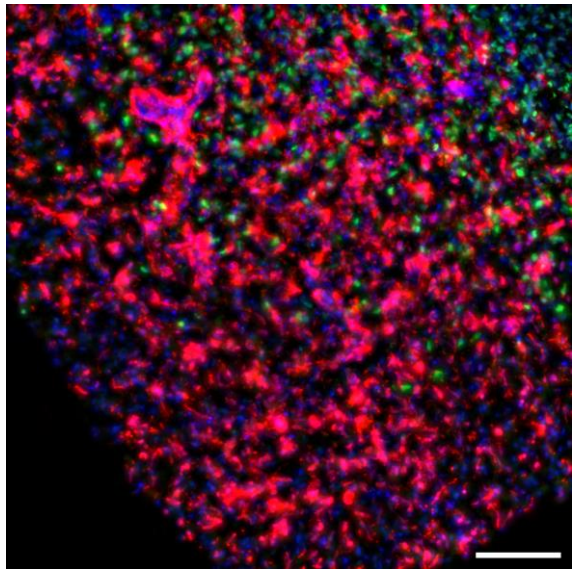

ROI Drawn on DAPI

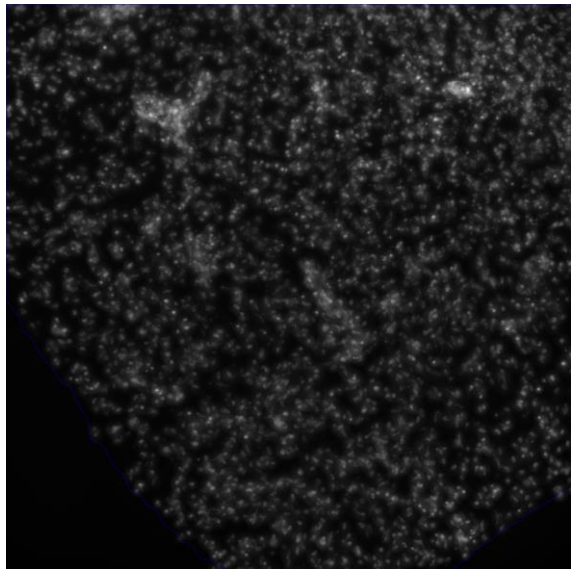

Iba1

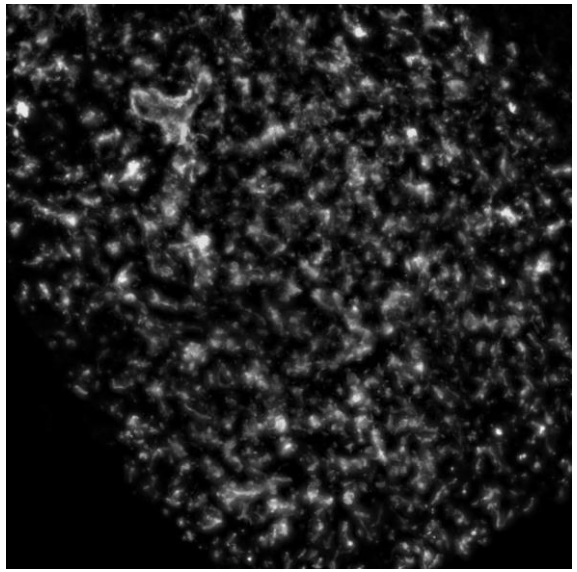

Iba1+ Objects

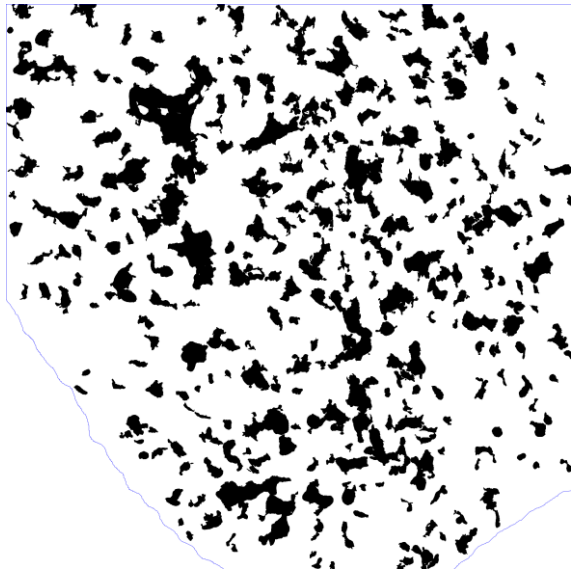

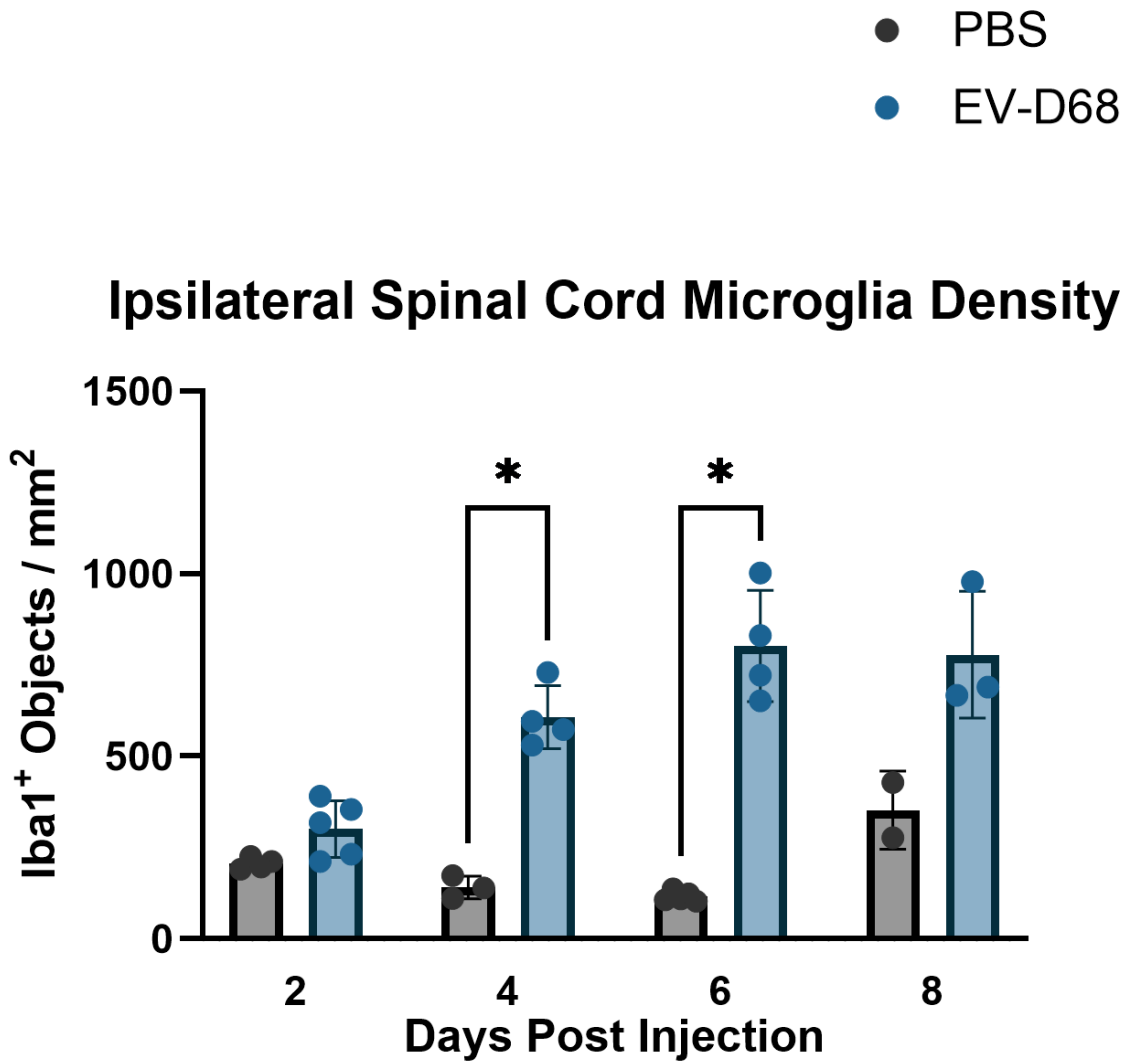

EV-D68 infection associated with increase in microglia CD68

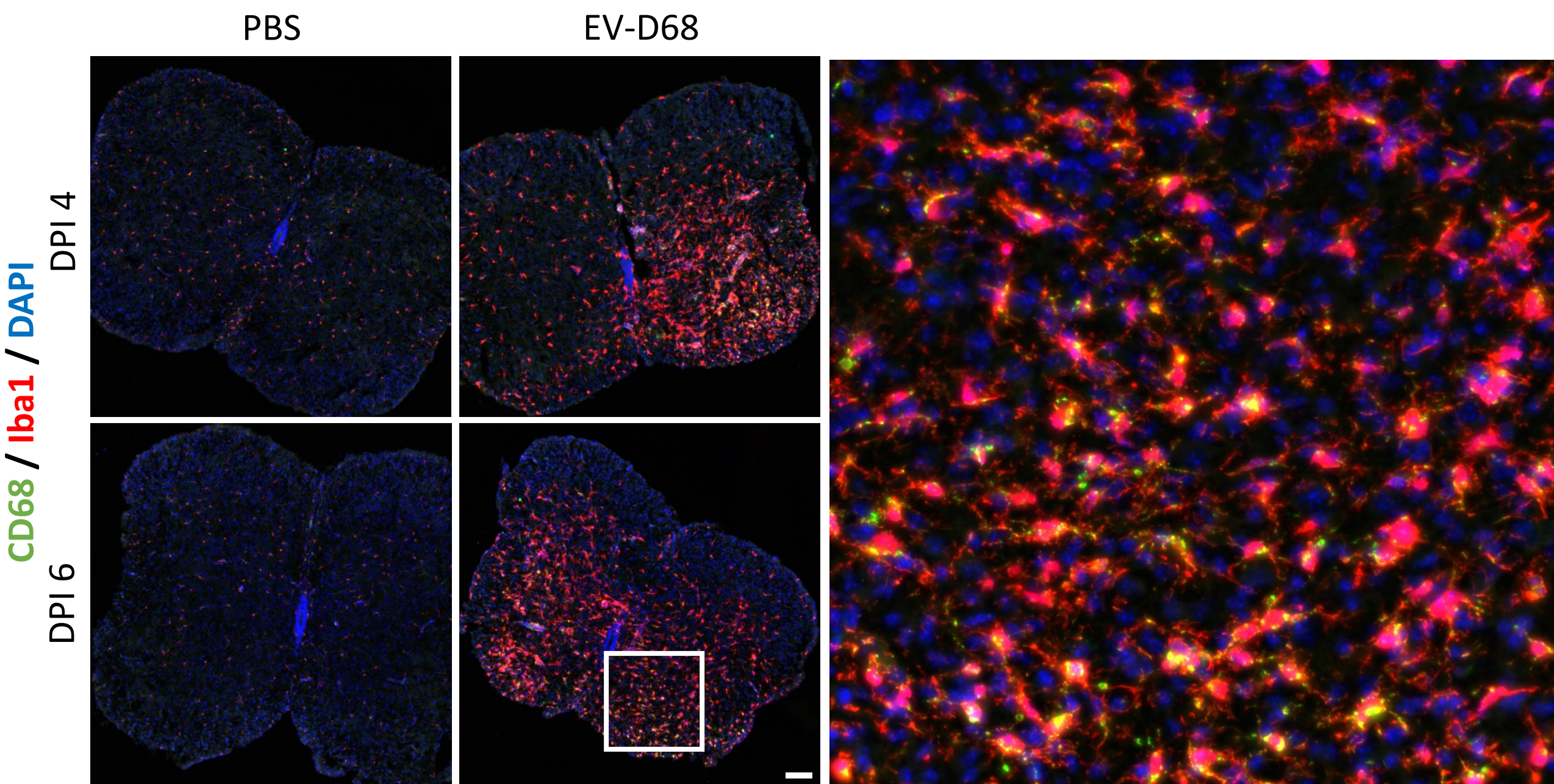

EV-D68 infection associated with increase in microglia CD68

DPI 6; EV-D68

CD68; Iba1 Object Mask Outline

CD68 / Iba1 / DAPI

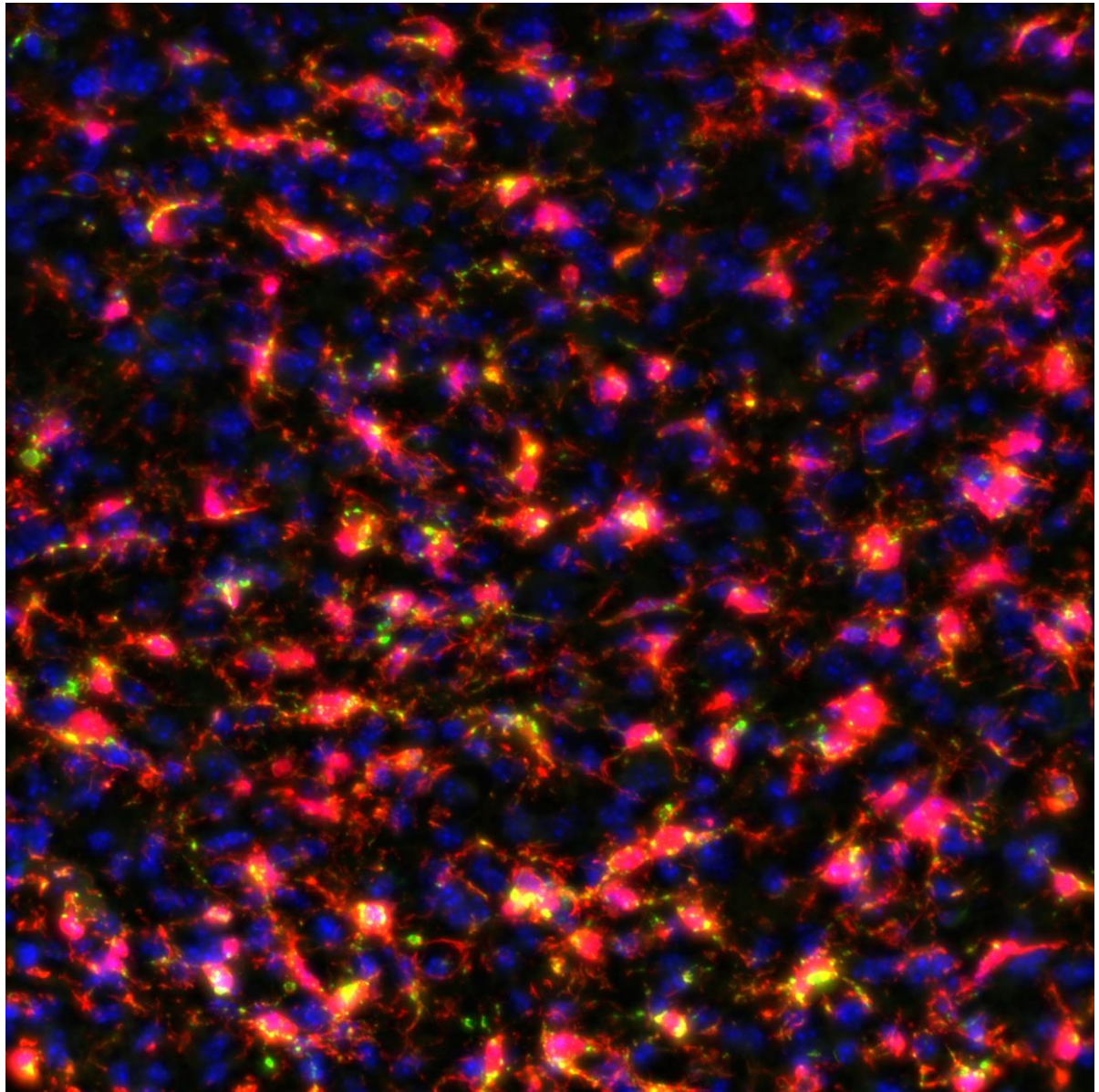

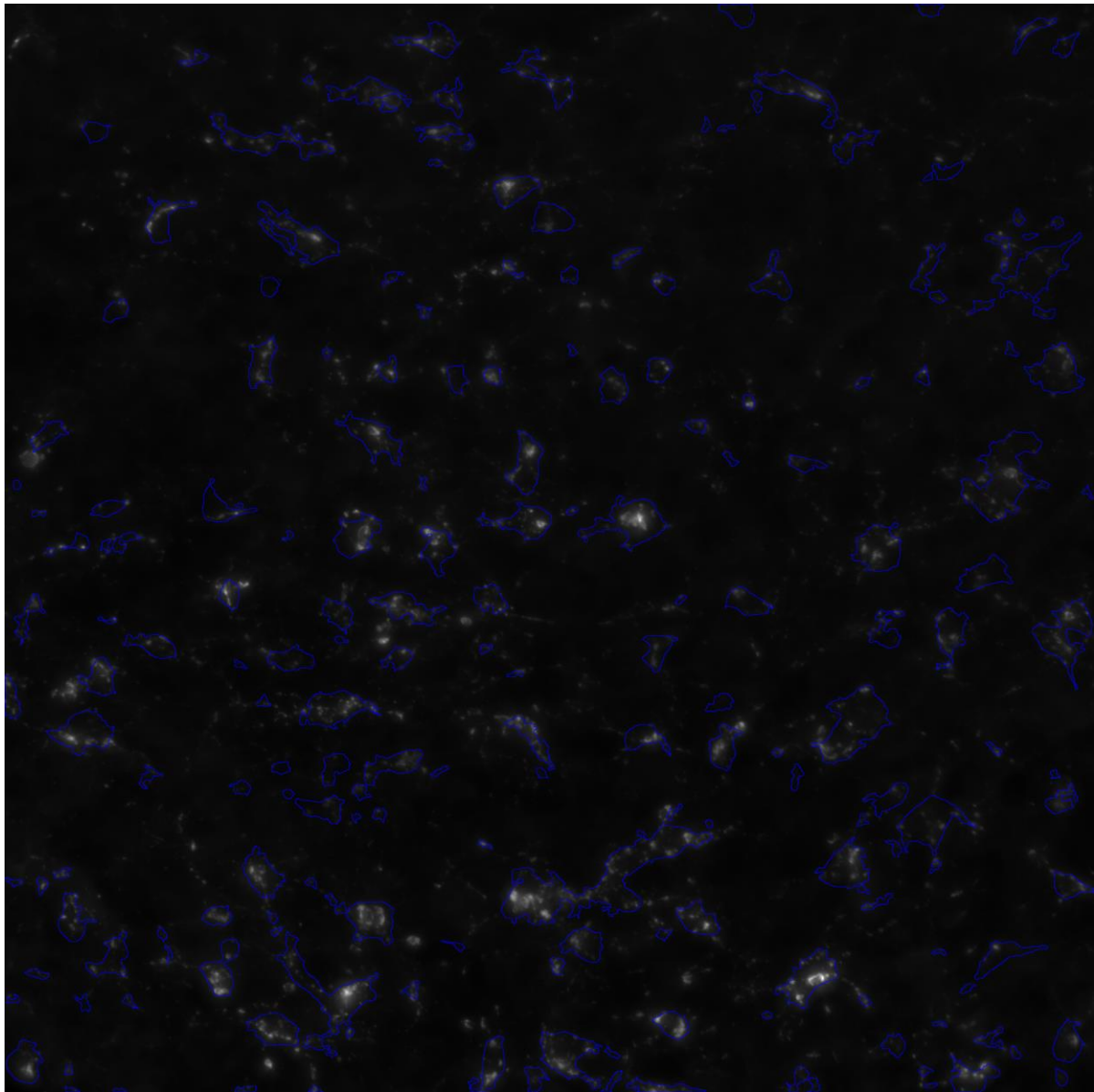

EV-D68 infection associated with increase in microglia density

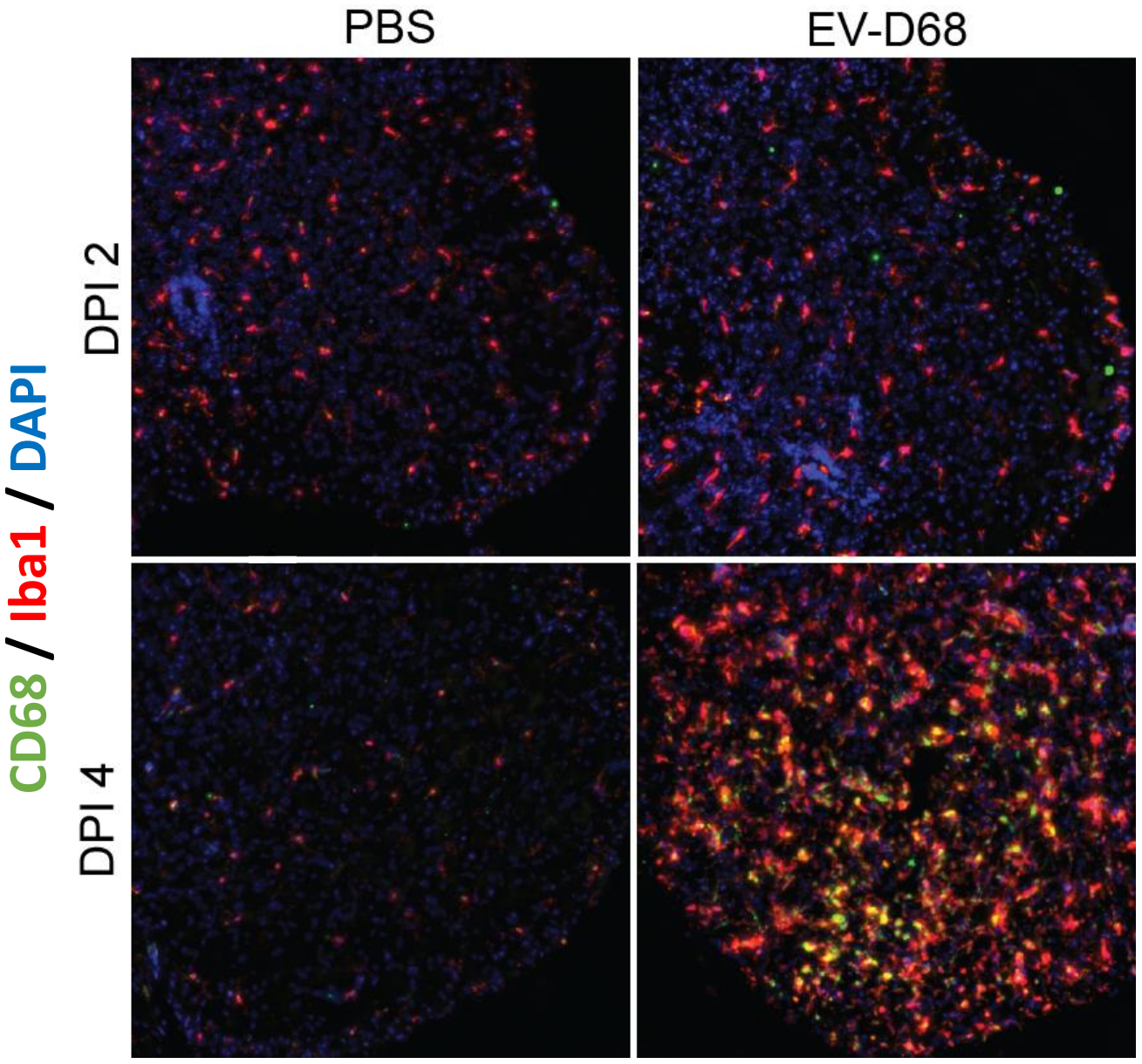

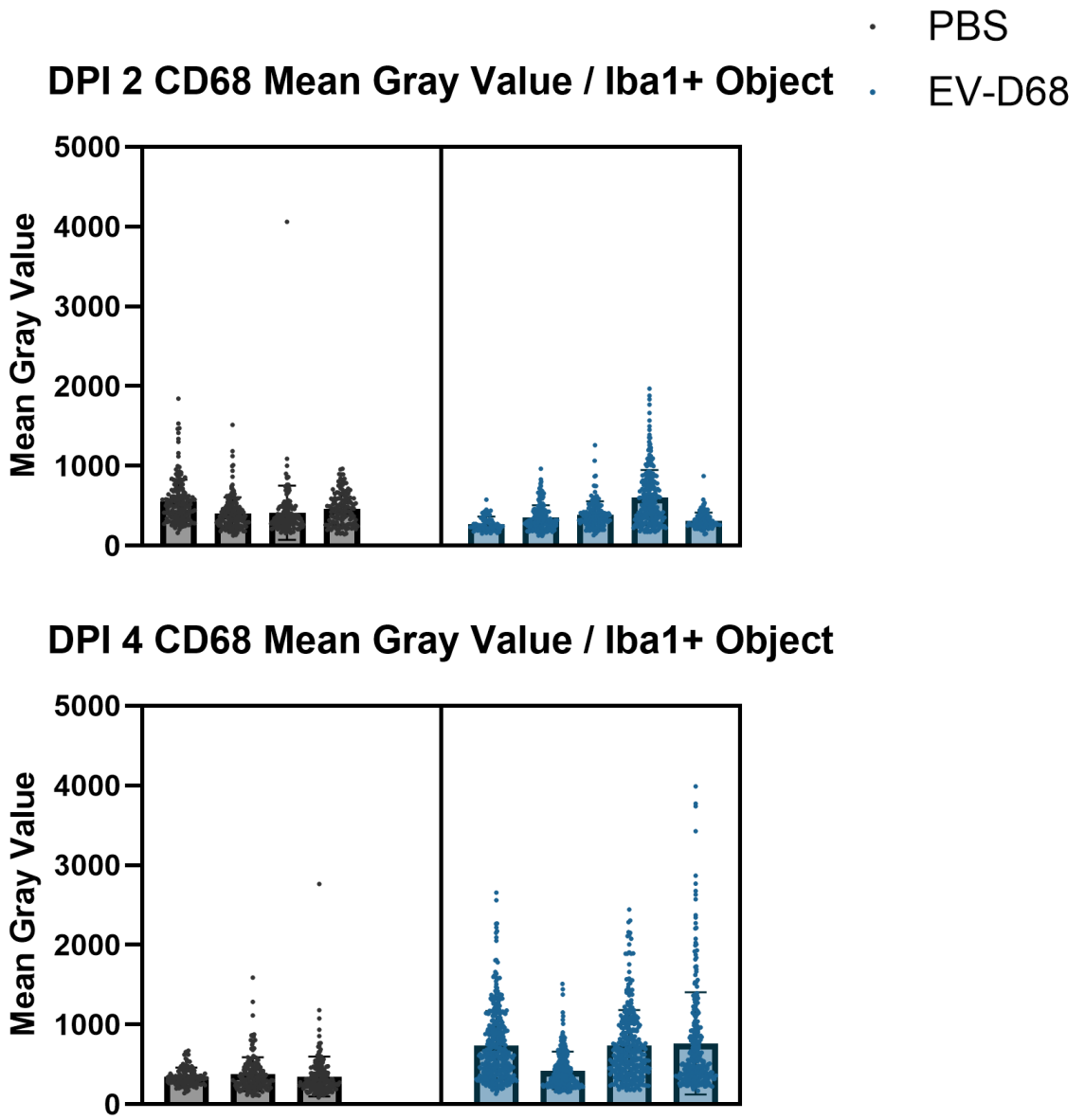

EV-D68 infection associated with increase in microglia density

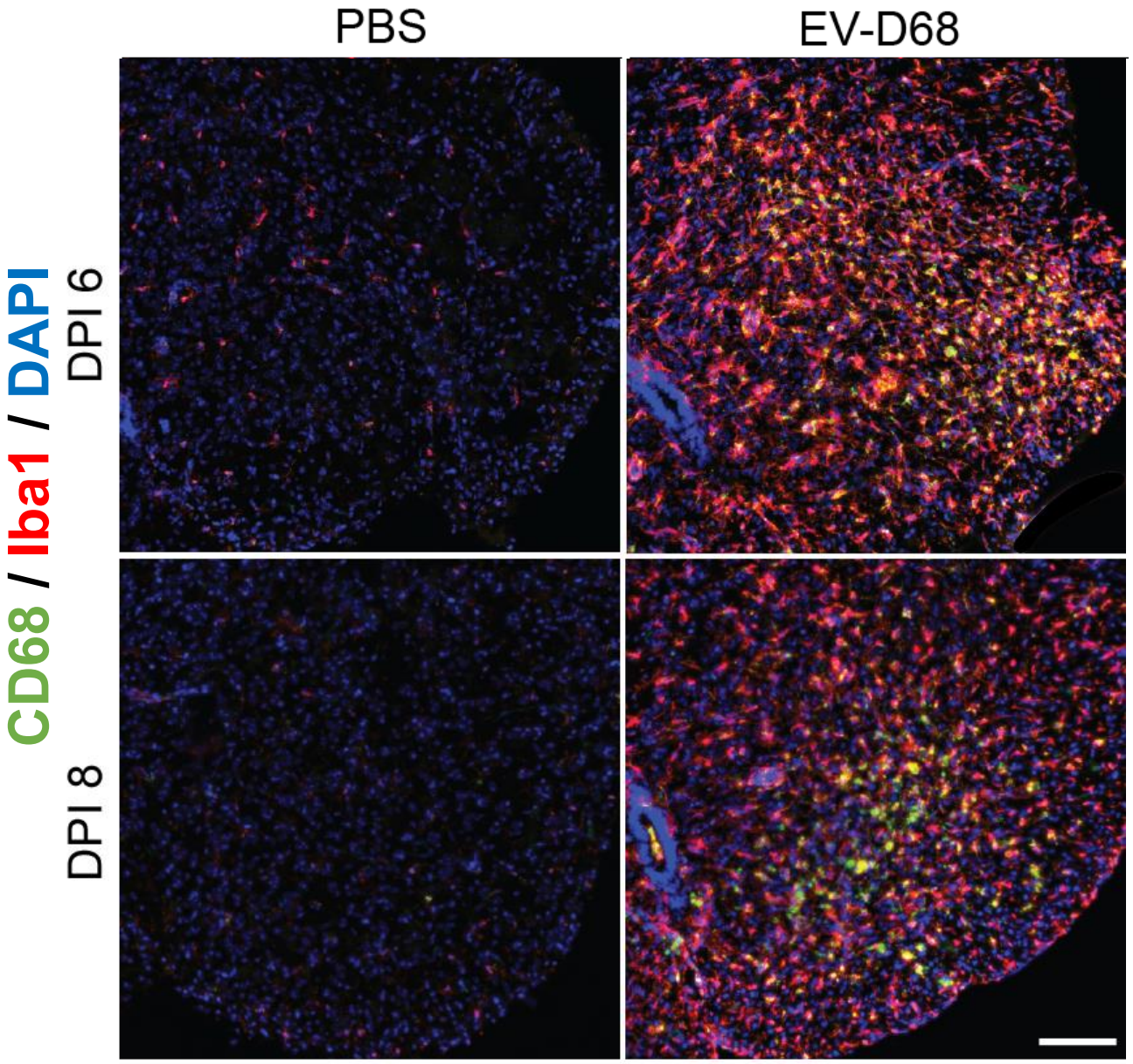

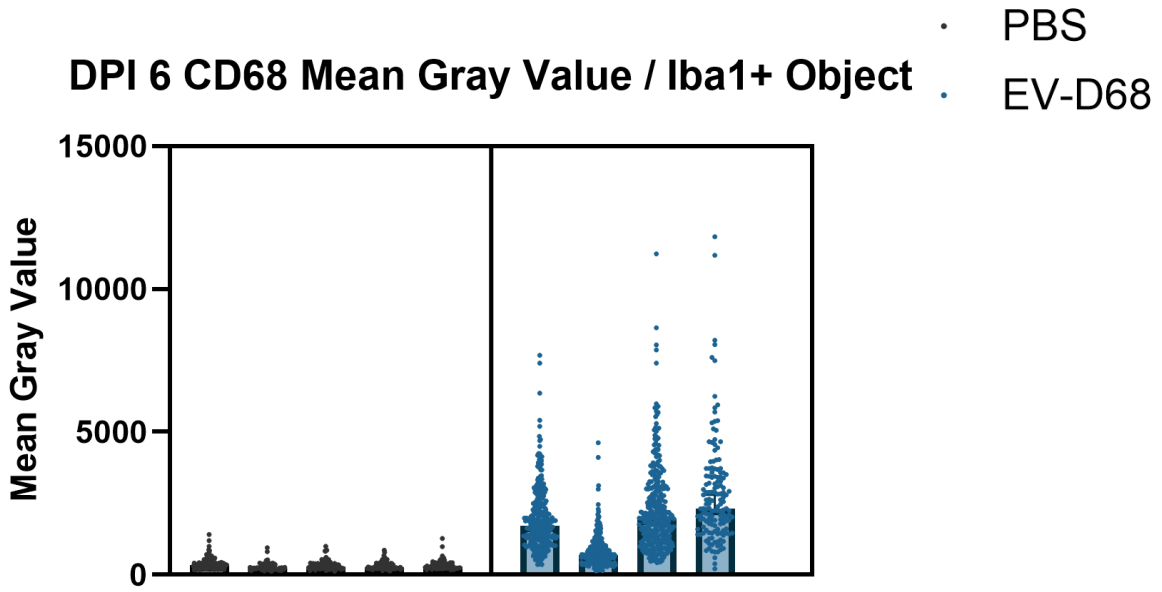

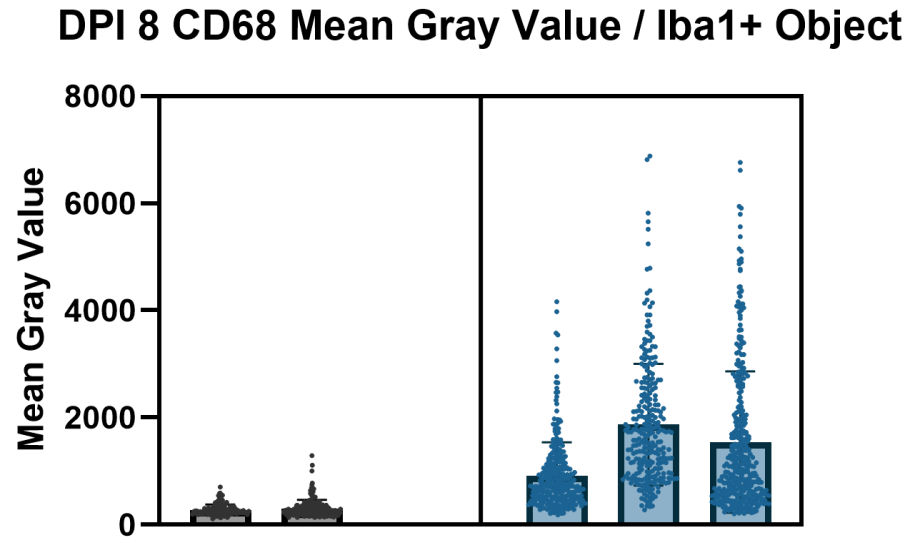

EV-D68 infection associated with increase in microglia CD68

6 Days Post-Injection
CD68 / Iba1 / DAPI

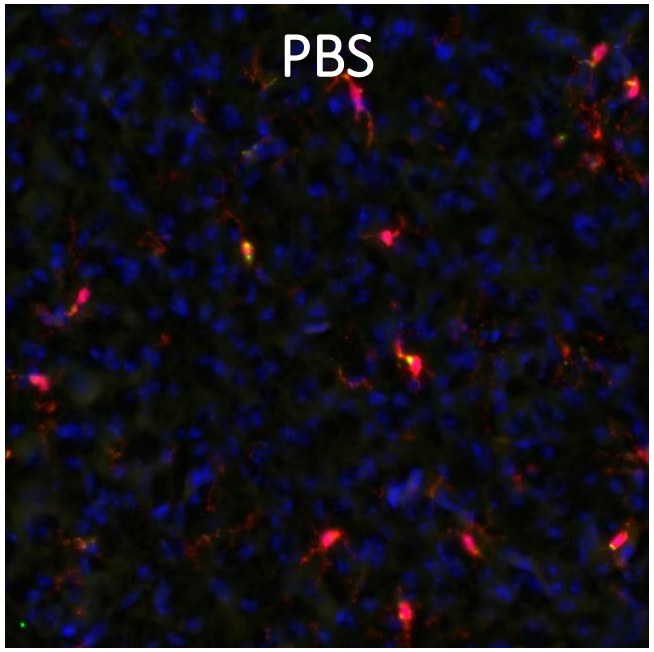

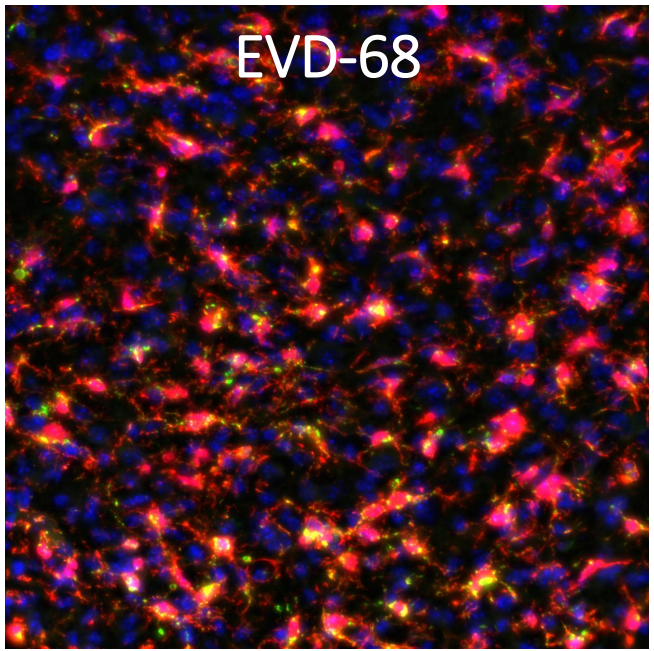

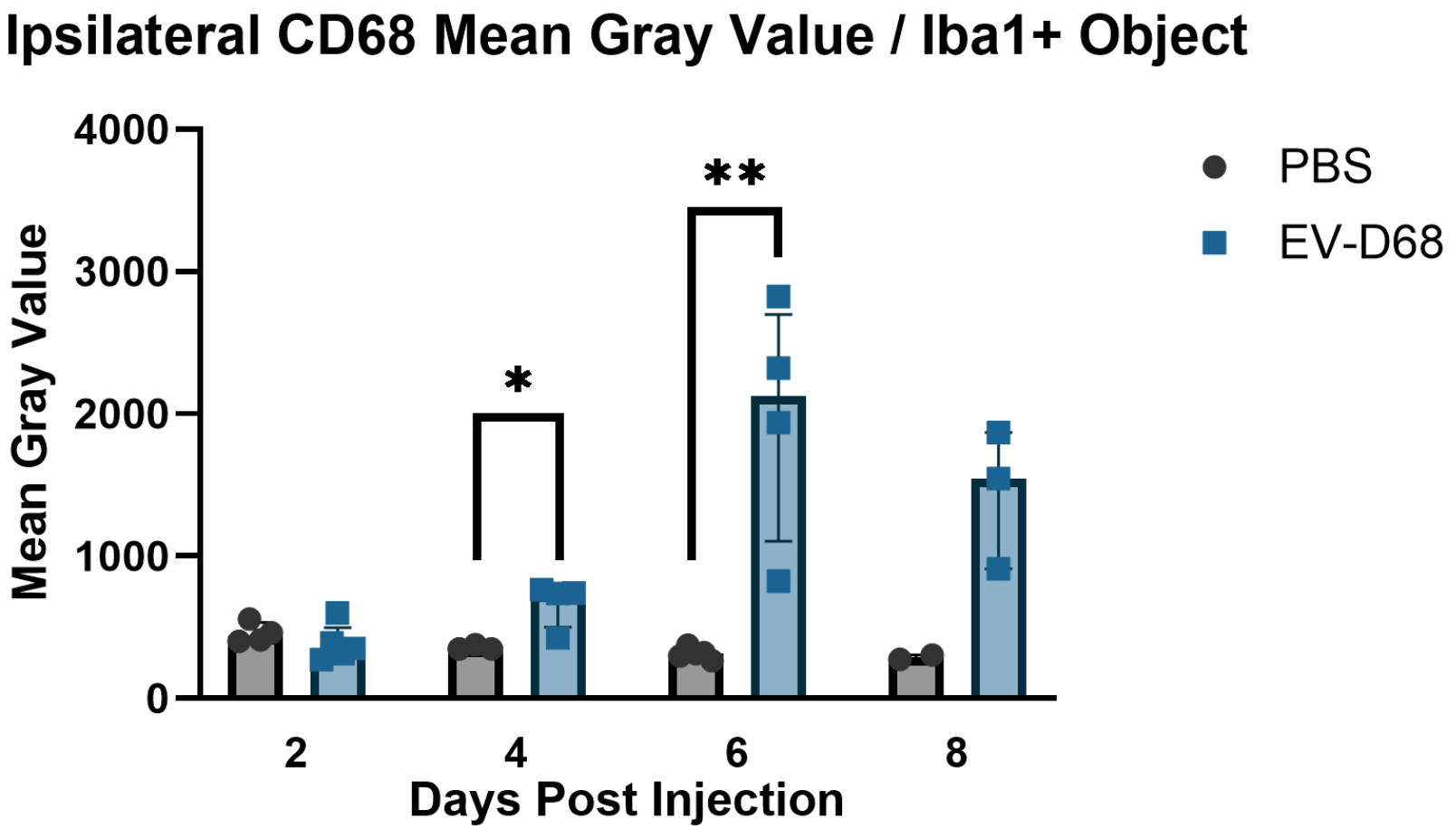

Key Takeaways

- EV-D68 infection in first postnatal week induces paralysis in mouse model of acute flaccid myelitis

- EV-D68 infection is associated with spinal cord ventral horn motor neuron loss

- EV-D68 infection promotes microglia accumulation and increased microglial phagocytic activity

8 Days Post-Infection

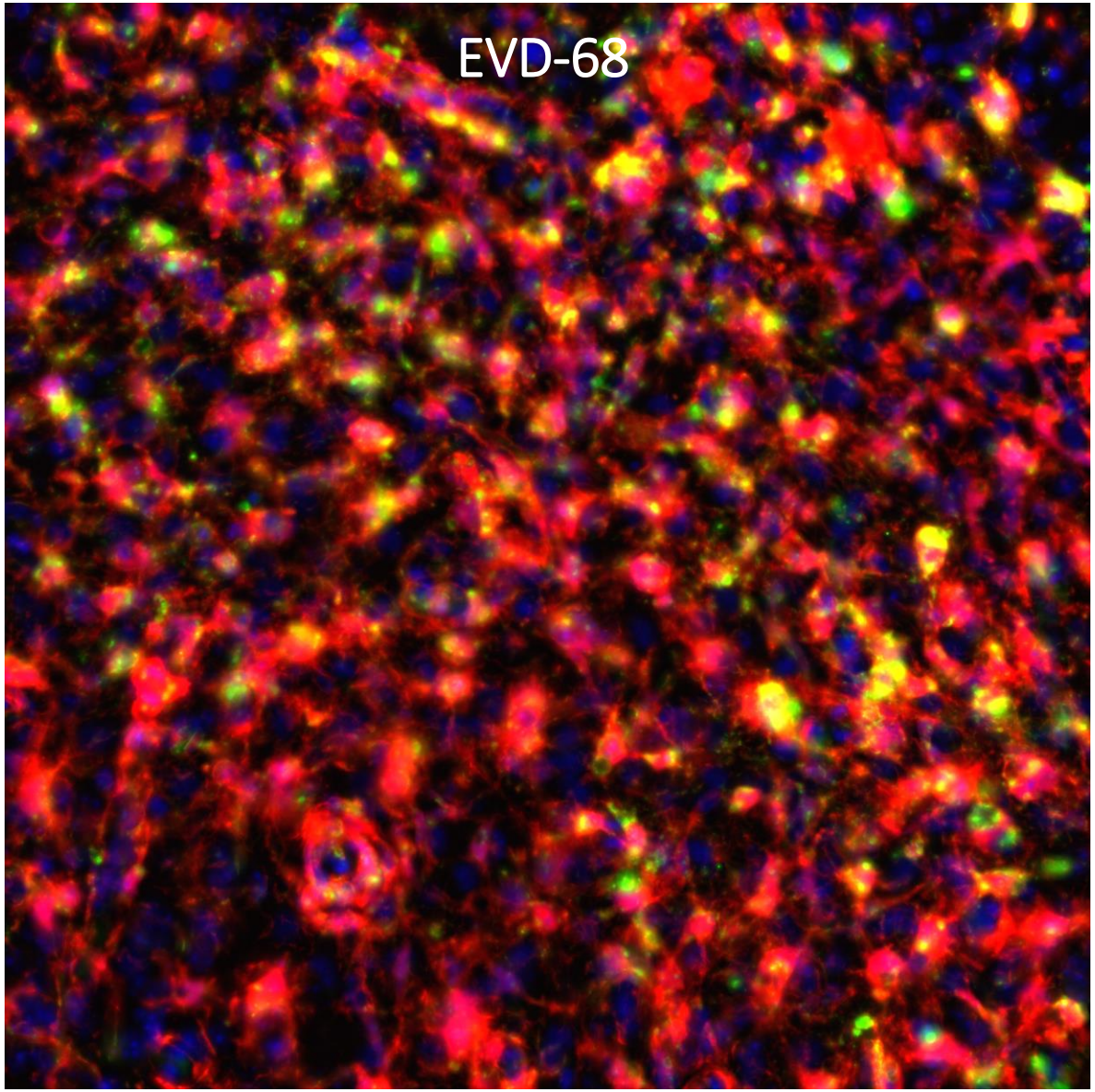

Up Next: Contrast microglia response to EV-D68 infection in the spinal cord during early and late postnatal development

Postnatal Day 1

DPI 6

Postnatal Day 15

DPI 6

Treatment	Paralysis	Virus in Spinal Cord	Accession #	Source
PBS	No	No		
IL/14-18952	Yes	Yes	KM851230	2014, USA, Respiratory
2022-23447	No	Prelim data-yes	OR235127	2022, USA, Respiratory

Immunohistochemistry & Mass Cytometry:

Microglia Subtype	Phagocytosis	Neuron
Cdllc (Itgax)	Clec7a	NeuN
IFITM3	Cd68	ChAT
Clec7a	MERTK	CC3

Paralysis Scores 6 Days Post Infection

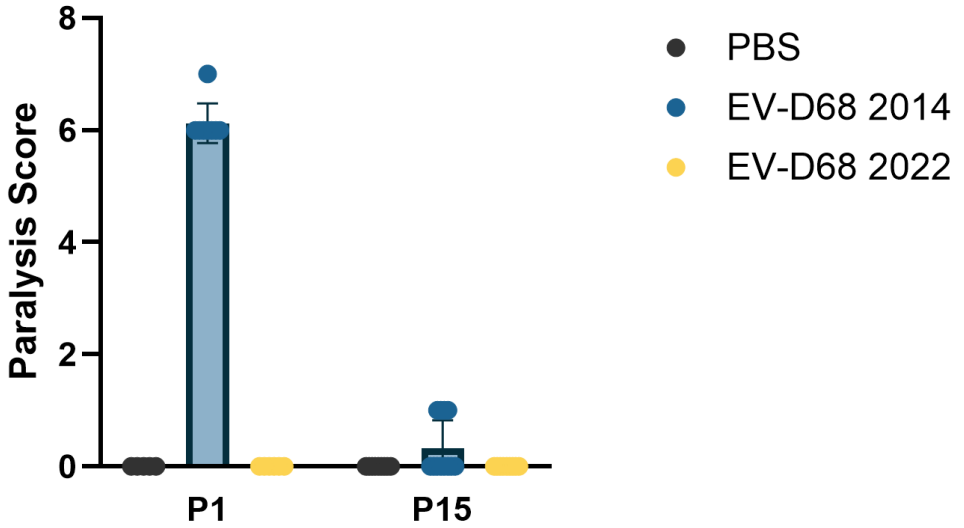

Future Questions:

- Does microglia depletion prior to infection with EV-D68 at postnatal day 1 mitigate the development of paralysis?

- Does disrupting microglia phagocytosis “rescue” otherwise viable motor neurons or prevent microglial antigen presentation to T cells and the resulting inflammatory response following EV-D68 infection?

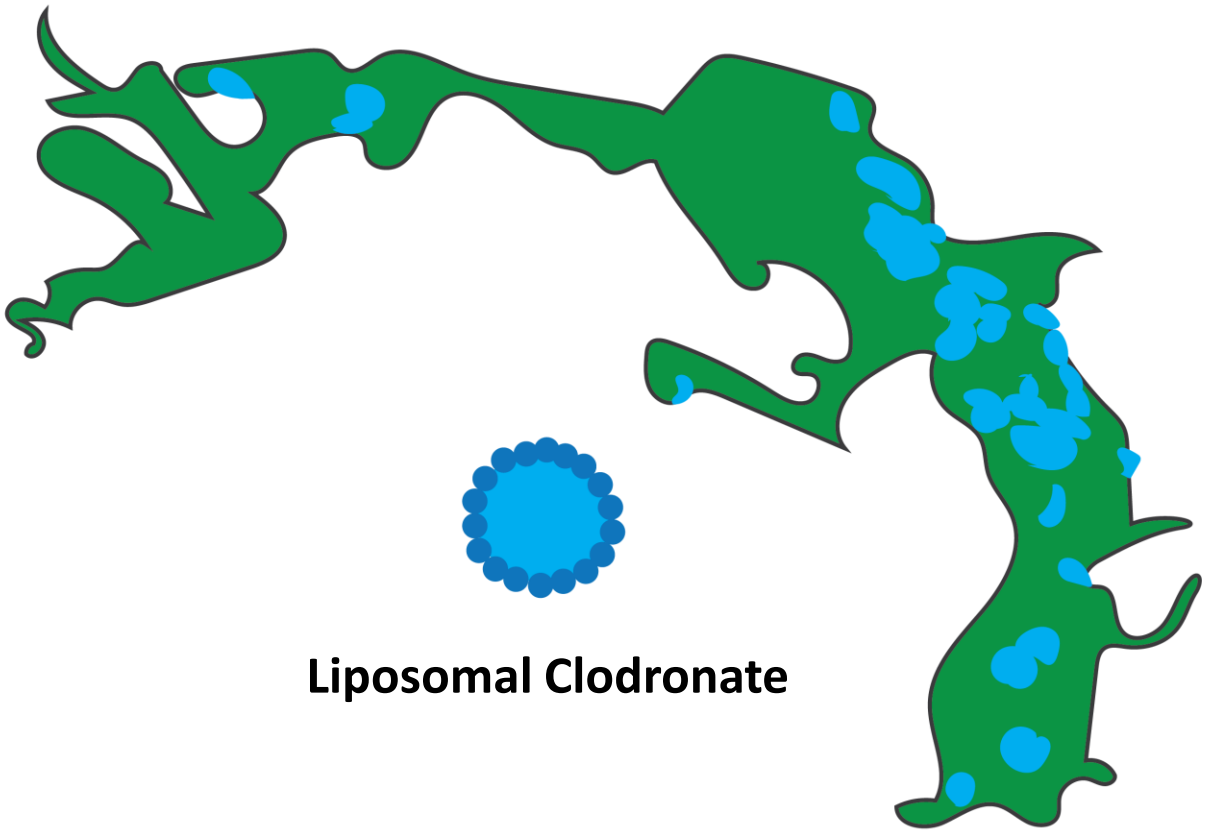

Liposomal Clodronate

Acknowledgements

Tyler Lab

Ken Tyler
Penny Clarke
Mike Rudy
Smith Lesser
Jon Teetsel
Dani Baker
The Mice

StARR Program

David Schwartz
Sarah Miller
Steve Abman
Peter Buttrick

Animal Facilities

Pediatrics Residency Program

Jason Espinoza
The Chief Residents

Child Neurology Residency Program

Teri Schreiner
Elizabeth Troy
Andra Dingman
Laura Konopka
Priscilla Harlan

Exploring Mitochondrial Transplantation as a Novel Therapy for Embolic Stroke

StARR Scholar: Brian Wu, MD

General Surgery Resident PGY-4

Mentors: Dr. Buttrick and Dr. Reece

Outline

- Introduction
- Aim and Hypothesis
- Study Design
- Model Preparation
  - Arm 1: Intranasal mitochondrial delivery
  - Arm 2: Embolic stroke model
- Current Progress

Introduction

- Cardiac and aortic surgery have higher incidence of perioperative stroke compared to non-cardiac surgery
- The incidence of stroke in extensive aortic arch replacement for acute Type A dissection can be up to 20%

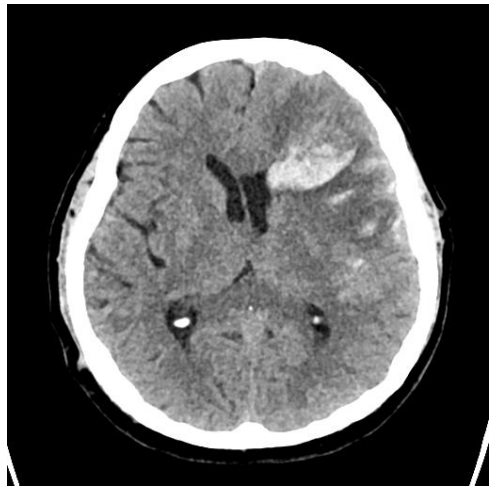

Embolic stroke with hemorrhagic conversion

Fanning, JP, et al., PNat Rev Dis Primers, 2024.
Gaudino, M, et al. Circulation, 2020.
Ghoreishi, M, et al. JTCVS, 2020.

Preventive Strategies Against Stroke

Delay elective cardiac surgery in those with recent stroke

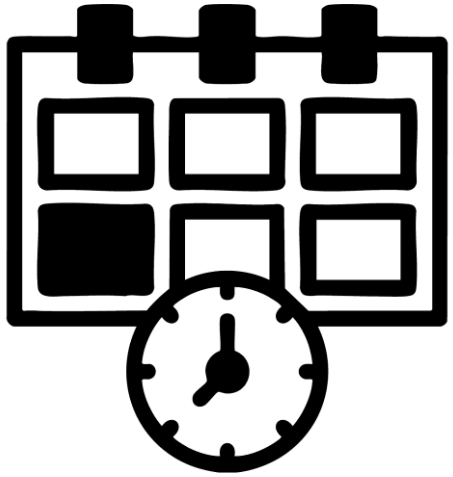

Minimize aortic manipulation and optimize cerebral perfusion

Implement atrial fibrillation prophylaxis and treatment

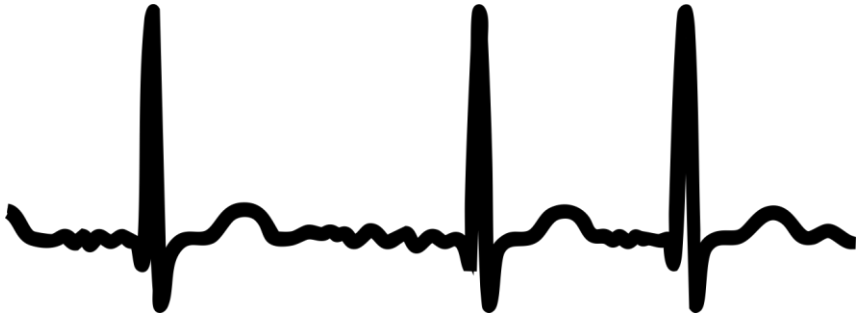

Gaudino, M, et al. Circulation, 2020.

Challenges in Management of Perioperative Stroke

Limited treatment options

- Thrombolysis and thrombectomy are often not feasible in post-cardiotomy patients due to risk of bleeding and need for crossing fresh anastomoses

Ischemia-reperfusion (IR) injury

- Restoration of cerebral blood flow can trigger a secondary IR injury
- The sudden oxygen influx and oxidative stress can lead to mitochondrial dysfunction, DNA damage, inflammatory response, and activation of apoptosis

Hayashida, K, et al. J Transl Med, 2021.
Wu, MY, et al. Cell Physiol Biochem, 2018.

Challenges in Management of Perioperative Stroke

- Mitochondrial transplantation (MTx) has shown promising results in mitigating neuronal injuries in traumatic and ischemic models

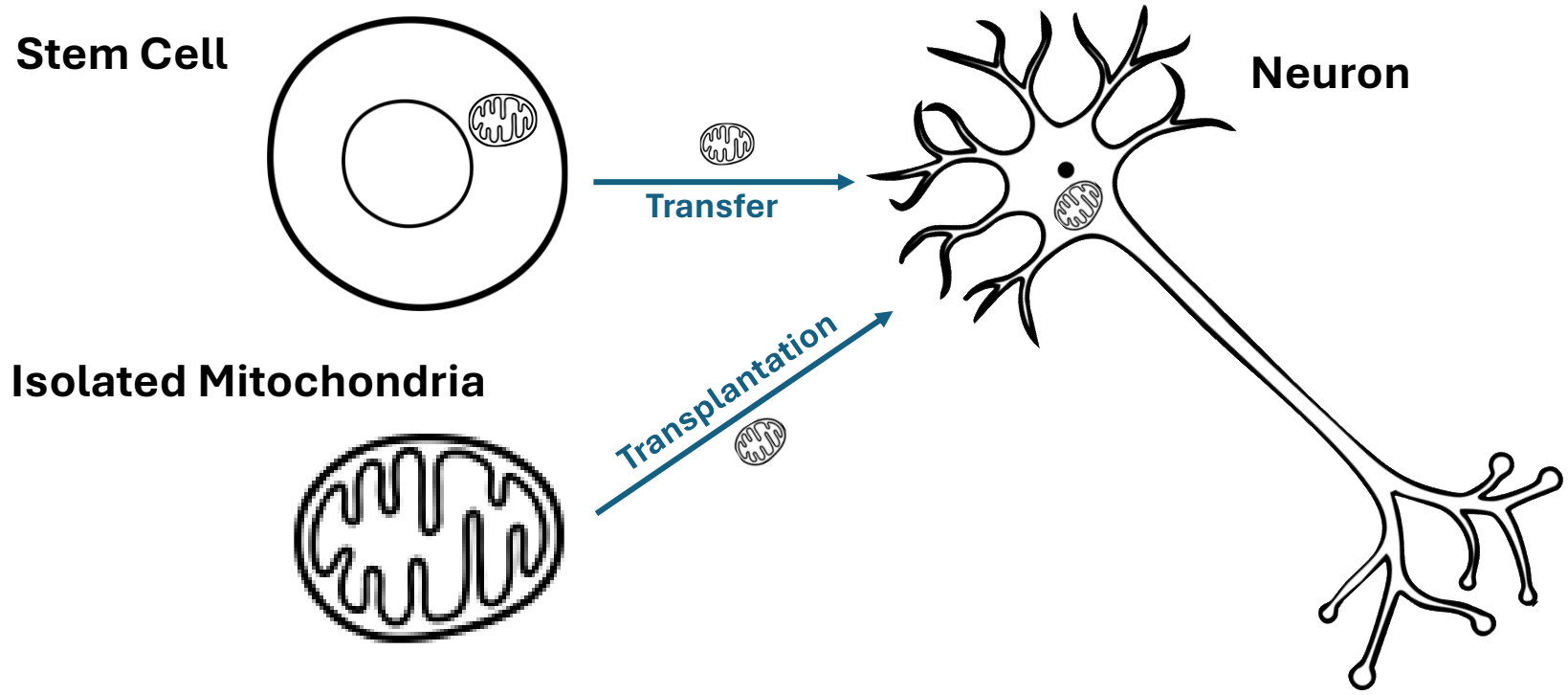

Spees, JL, et al. Proc Natl Acad Sci USA, 2006.
McCully, JD, et al., Am J Physiol Heart Circ Physiol, 2009.
Zhang, B, et al. World Neurosurg, 2020.
Nakamura, Y, et al. Stroke, 2020.

Can we prevent permanent cerebral injury?

- Mitochondrial transplantation (MTx) has shown promising results in mitigating neuronal injuries in traumatic and ischemic models

Our first cell model

Pre-ischemic MTx

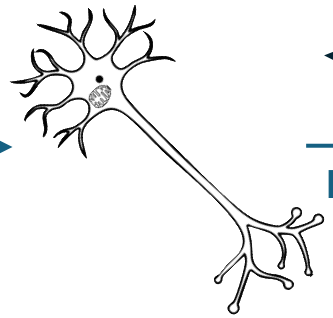

Ischemia

No benefit or worse cell survival

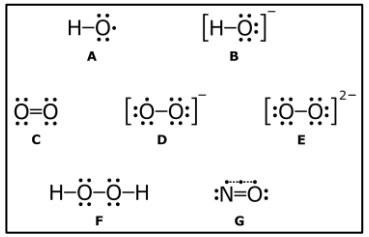

Excessive ROS?

Our refined cell model

Nicorandil

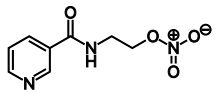

MTx during ischemia

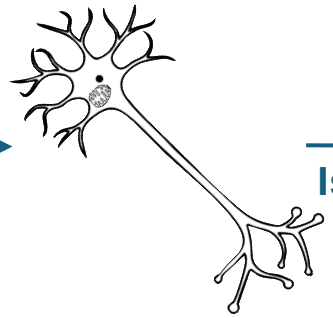

Ischemia continued

Preserved cell viability/proliferation and Mitochondrial respiration
Fewer dysregulated genes

Ikeno, Y, et al. Ann Thora Surg, 2021.
Wu, BCB et al. Circulation (Abstract), 2025.

MTx Improved Cell Viability and Proliferation

- Ischemic (OGD) subgroup: Untreated vs. Mito

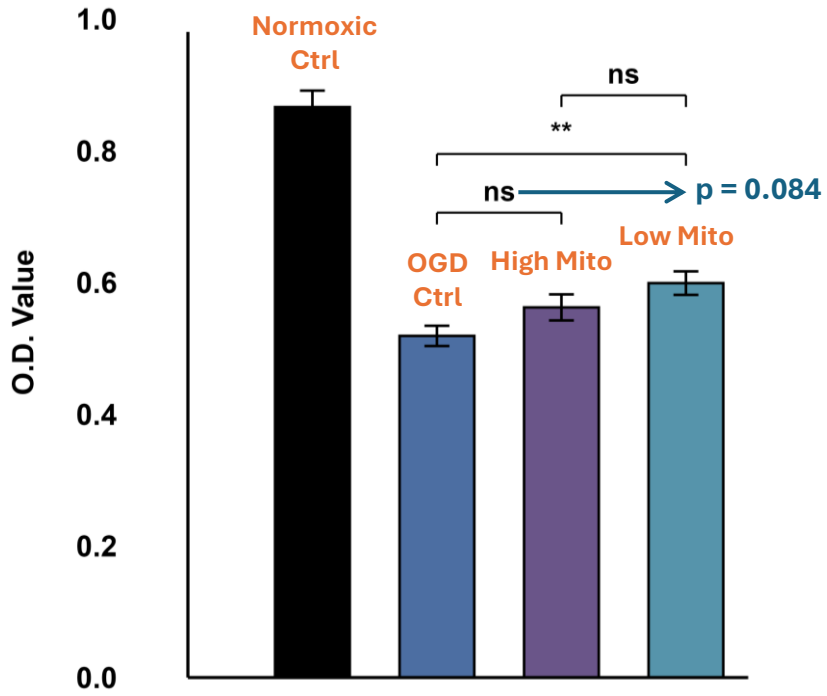

Cell Viability (MTS)

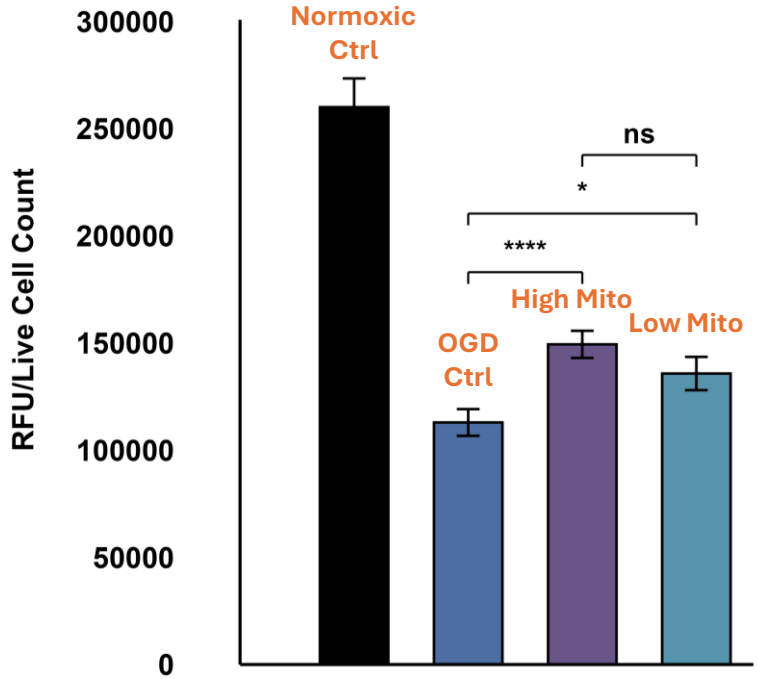

Cell Proliferation (CyQUANT)

Wu, BCB et al. Circulation (Abstract), 2025.

Nicorandil Further Enhanced the Effects

- Ischemic (OGD) subgroup: Untreated vs. Higher dose of Mito ± NIC

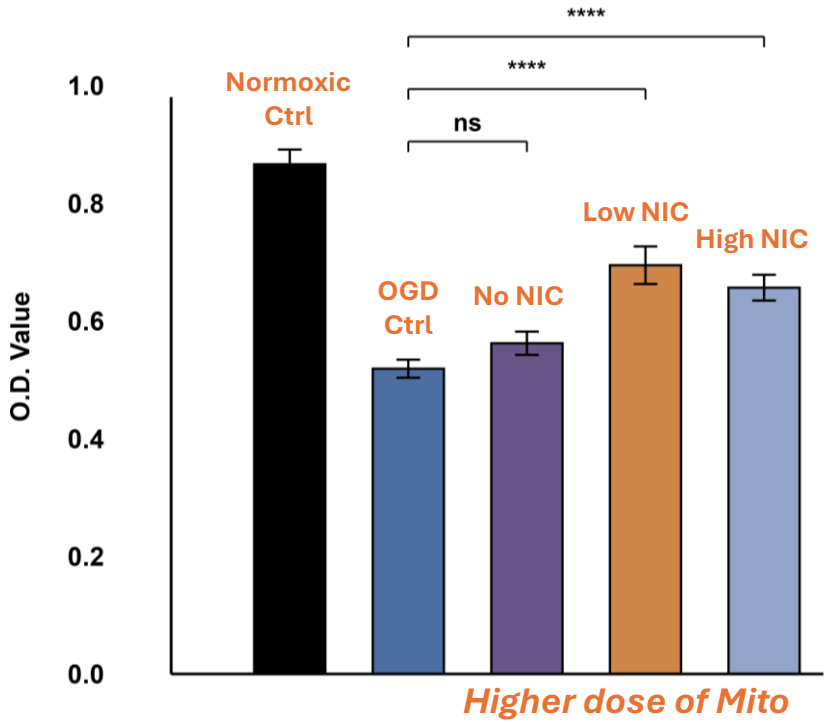

Cell Viability (MTS)

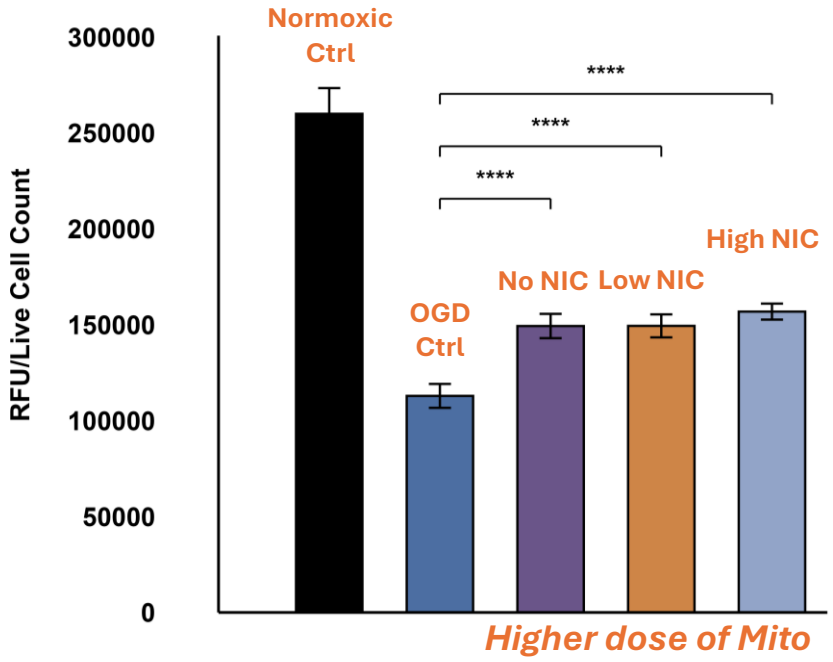

Cell Proliferation (CyQUANT)

Wu, BCB et al. Circulation (Abstract), 2025.

MTx Improved ATP Production

- Ischemic (OGD) subgroup: Untreated vs. Mito

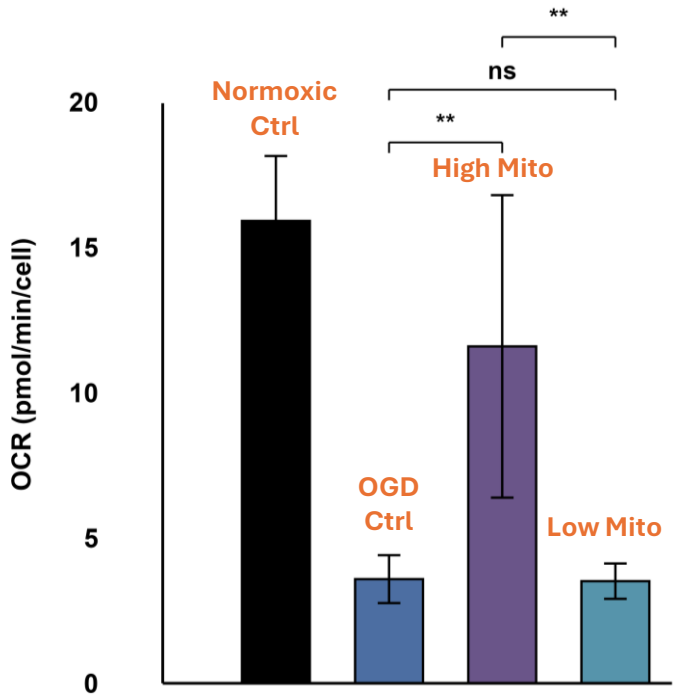

Wu, BCB et al. Circulation (Abstract), 2025.

Nicorandil Further Augmented ATP Production

- Ischemic (OGD) subgroup: Untreated vs. Higher dose of Mito ± NIC

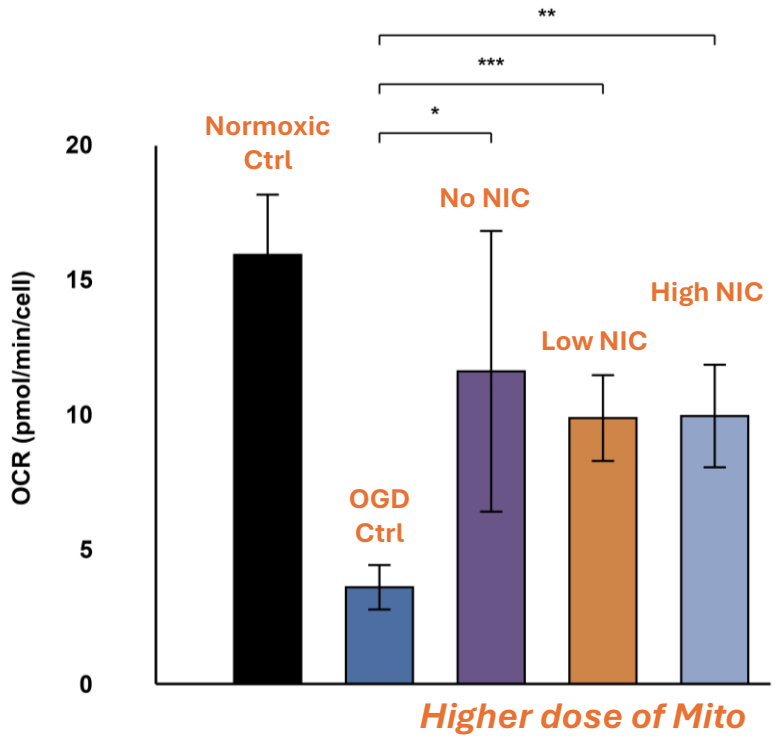

Wu, BCB et al. Circulation (Abstract), 2025.

Aims: From *In Vitro* to *In Vivo*

- We evaluated whether mitochondrial pre-treatment prior to ischemia reduces stroke severity and irreversible cerebral injury *in vivo*
  - **Aim 1:** Demonstrate the neuroprotective effect of pre-ischemia mitochondrial transplantation
  - **Aim 2:** Optimize dosing and timing for mitochondrial transplantation

Hypothesis

- Mitochondrial transplantation prior to ischemic stroke will reduce the severity of neurological deficits and preserve neurons

Study Design

1. Rodent stroke model (embolic)
2. Non-invasive intranasal delivery of exogenous mitochondria
3. Comparison of the neurobehavioral outcomes, brain imaging, and histological outcomes among **Sham, Stroke without Mito Pre-treatment, Stroke with Mito Pre-treatment**, and Sham with Mito-Pretreatment

Refinement of In Vivo Stroke Models

- Started with murine embolic stroke model
  - ➔Murine microfilament middle cerebral artery occlusion model
  - ➔Murine bilateral carotid artery occlusion model
  - ➔**Rat embolic stroke model using microbeads**

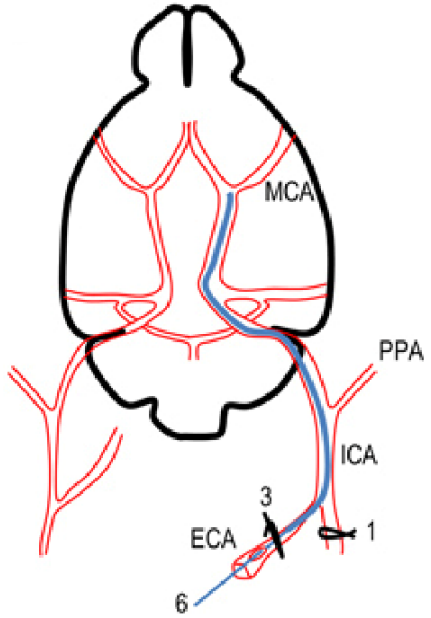

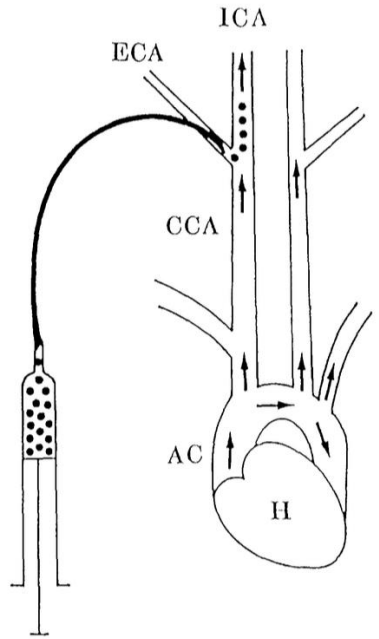

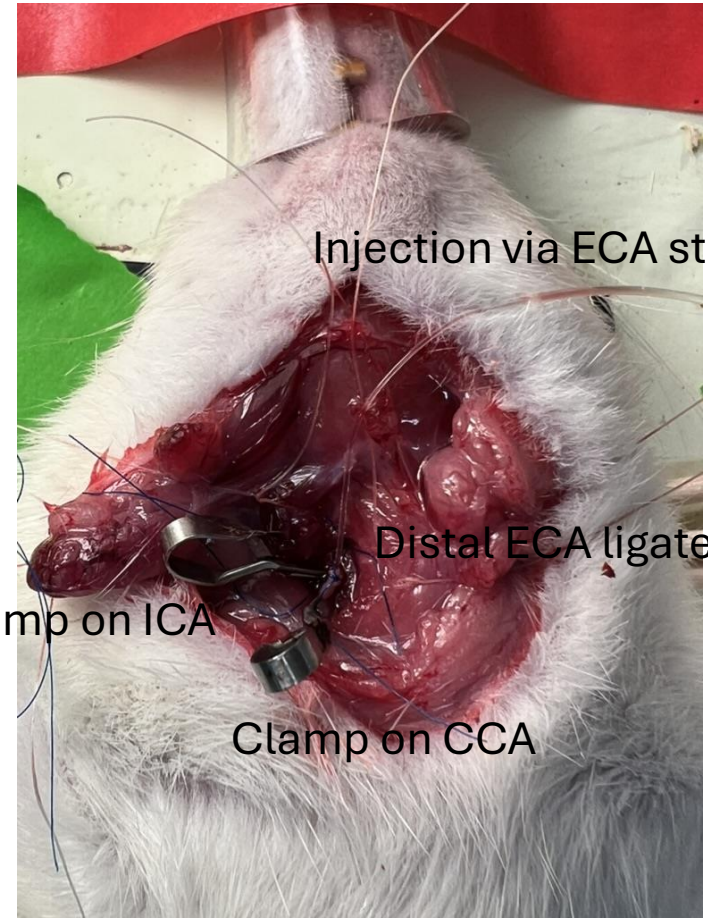

Rat with Embolic MCA Stroke

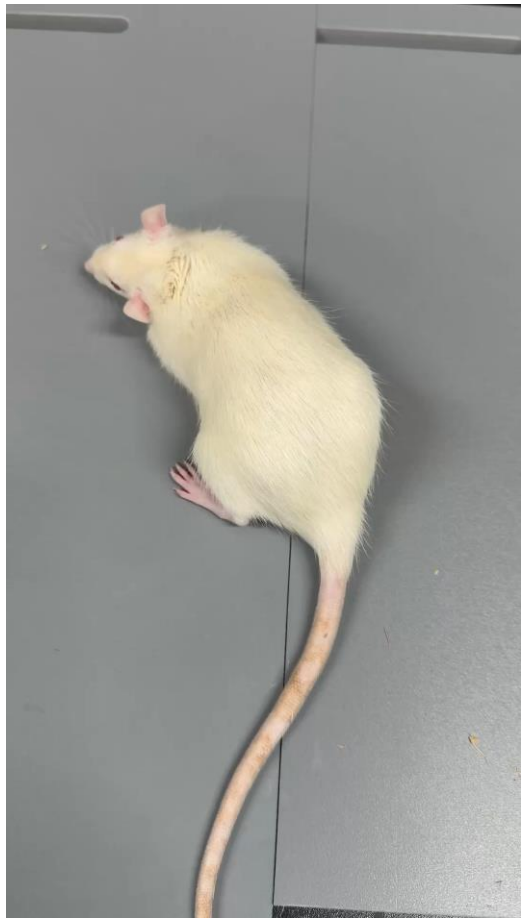

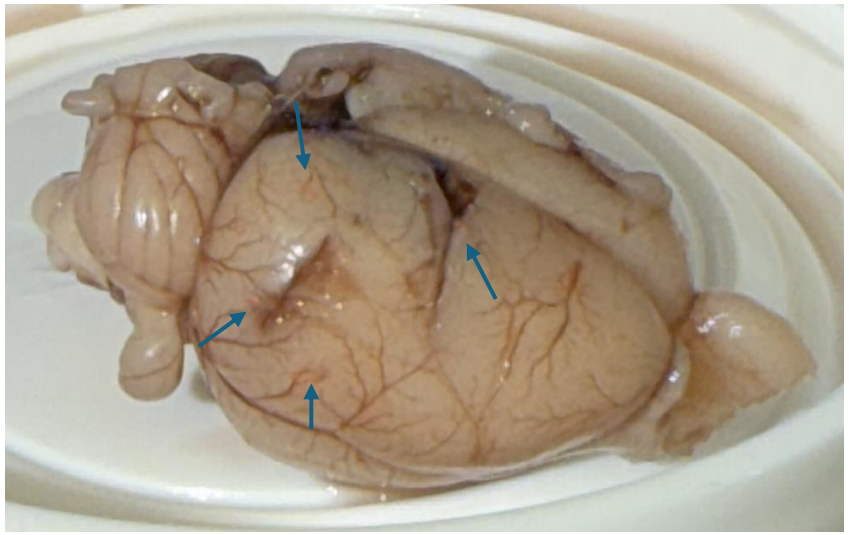

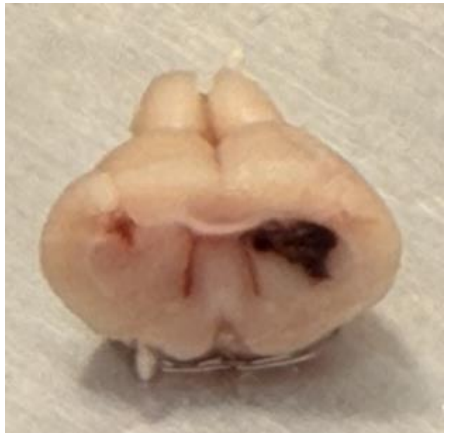

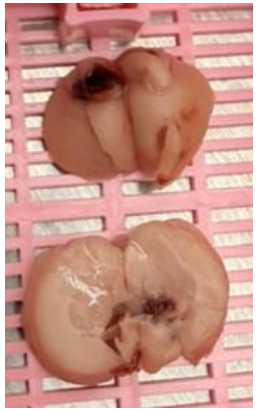

Preparation for Mitochondrial Transplantation

Quadriceps Muscle Harvest from Adult SD Rat

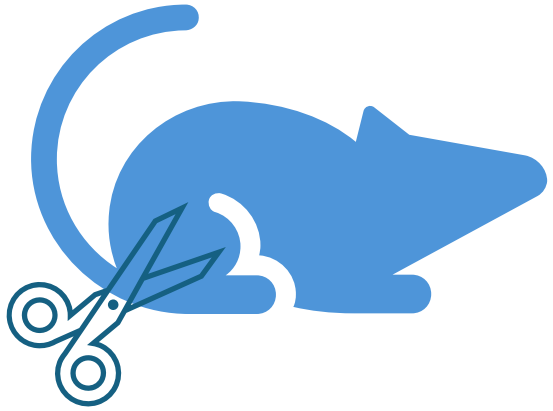

Tissue Homogenization and Serial Centrifugation

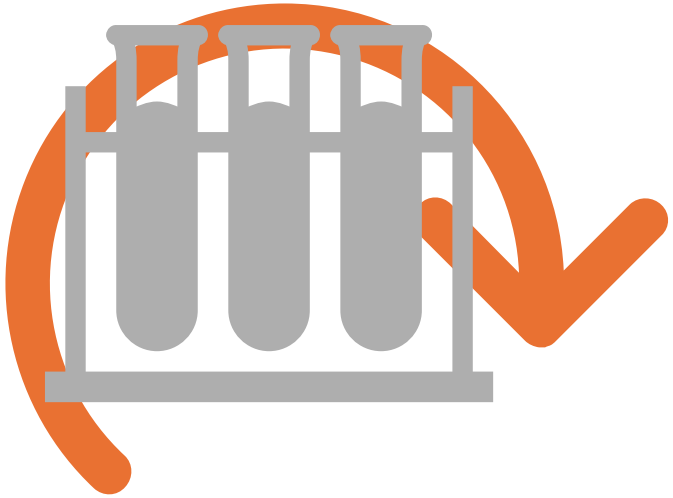

Mitochondrial Staining

Intranasal Mitochondrial Delivery

- *In vitro*, we labeled donor mitochondria with MitoTracker Red to visualize uptake by recipient cells
- *In vivo*, we found unreliable results with the MitoTracker or other membrane labeling, likely due to dye leakage
  - BrdU-labeled mitochondria were subsequently used to track migration from the nasal cavity to the brain

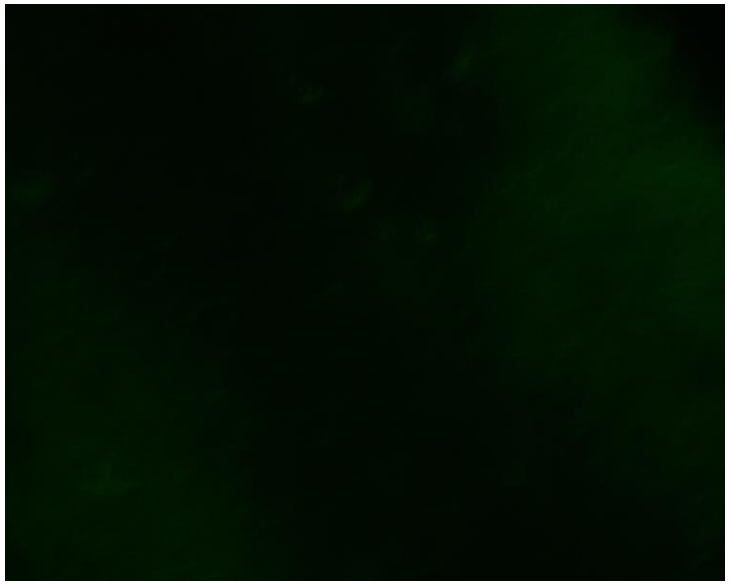

Ctrl Rat: No Mito given

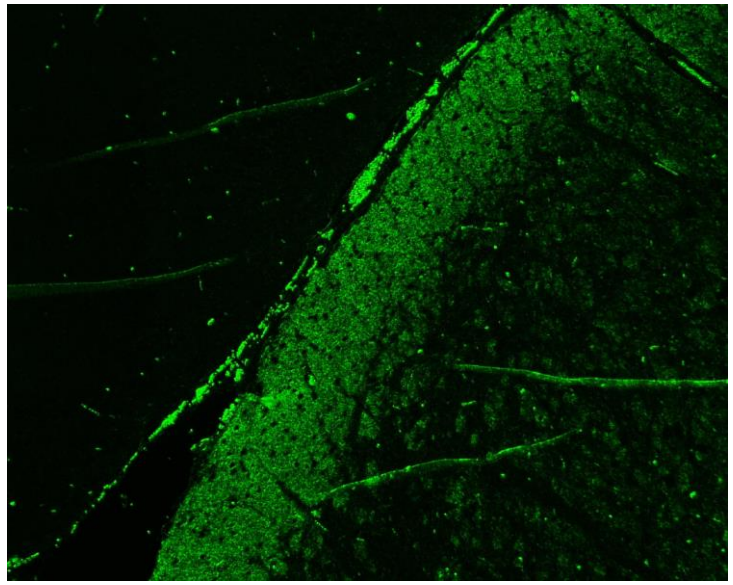

Rat#1: total 200 µg Mito
Anterior/Middle

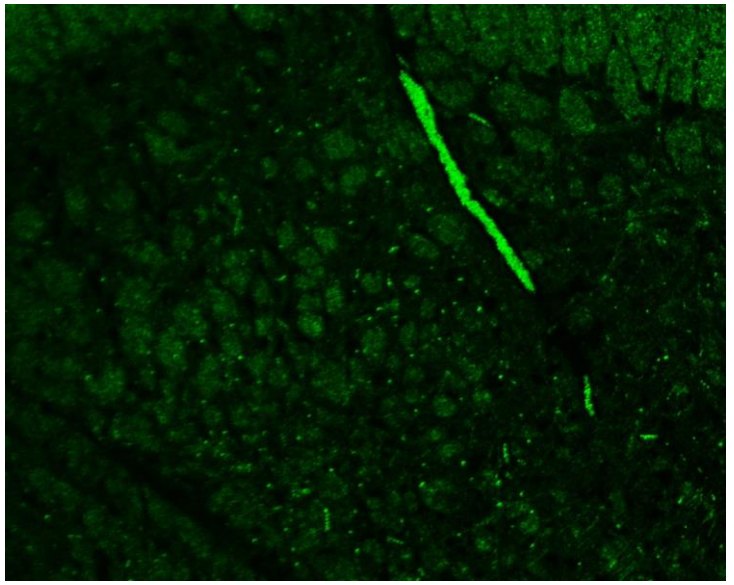

Rat#1: total 200 µg Mito
Posterior

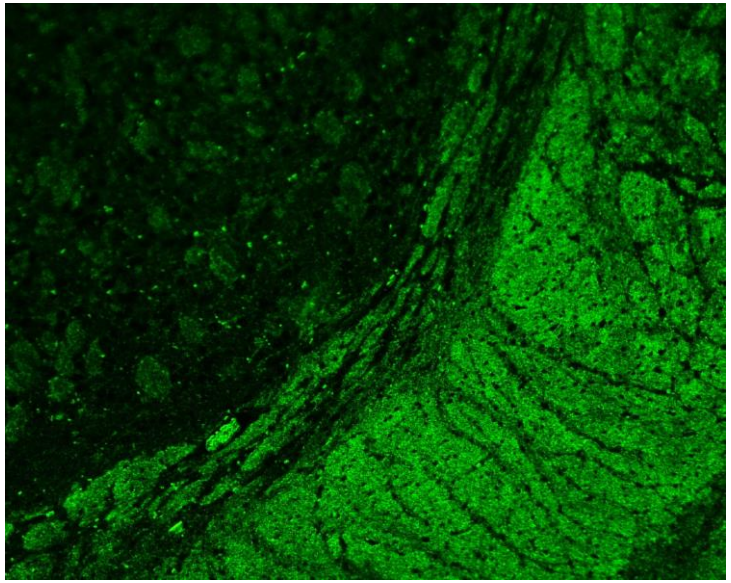

Rat#2: total 200 µg Mito
Anterior/Middle

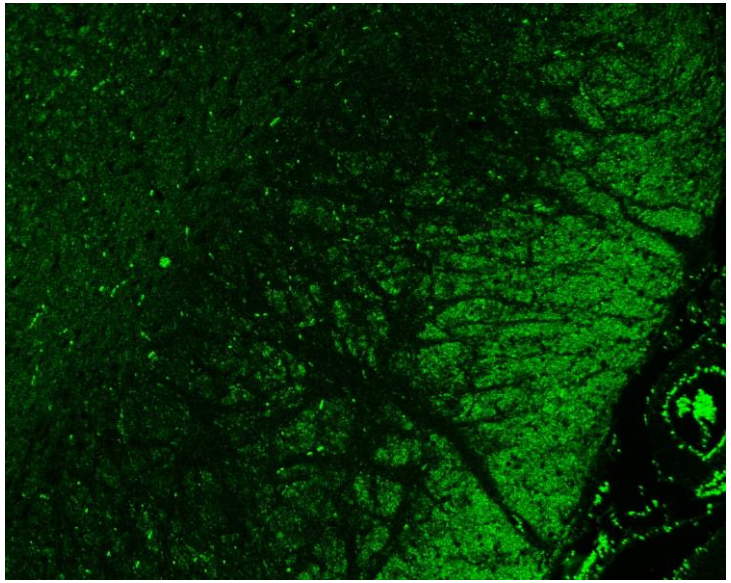

Rat#3: total 720 µg Mito
Anterior/Middle

Brain MRI Imaging Protocol

- AISR Protocol
  - High-resolution T2-turboRARE MRI (sagittal, axial and coronal planes)
  - DWI with 6 b-values (axial plane)
  - SWI (axial plane)
  - Bruker 9.4 Tesla BioSpec Rat Head Array Coil
- Timeline: Baseline, Post-Stroke Day 1, and possible more
- **Currently we have obtained baseline brain images from 5 rats for reference. Additionally, we have performed brain MRI on five stroke rats on day 1**

First Mitochondria Pre-treatment Model

- Group
  - Sham x3 (One died d/t anesthesia)
  - Mito x 2
  - Stroke x4 (One died during recovery from anesthesia on POD0)
- Mitochondria labeled using BrdU
- Sham received intranasal hyaluronidase (50 µL x 2) + saline (50 µL x 2)
- Mito received intranasal hyaluronidase (50 µL x 2) + mitochondria (50 µL x 2 / 16 µg/µL ->1600 µg)
- Stroke received intranasal hyaluronidase (50 µL x 2) + saline (50 µL x 2)

Blinded Behavioral Assessment

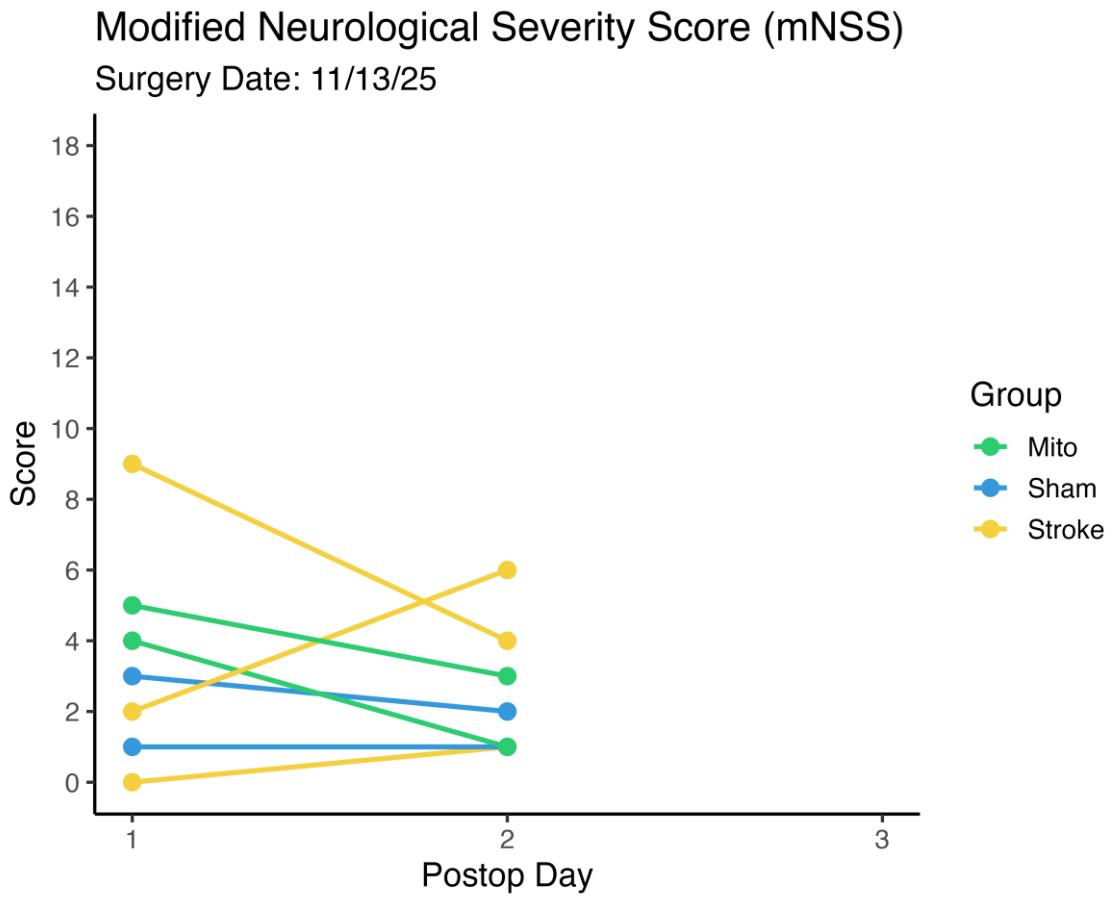

Balance beam test
One component of mNSS

Open Field 11/17/25 (POD4)

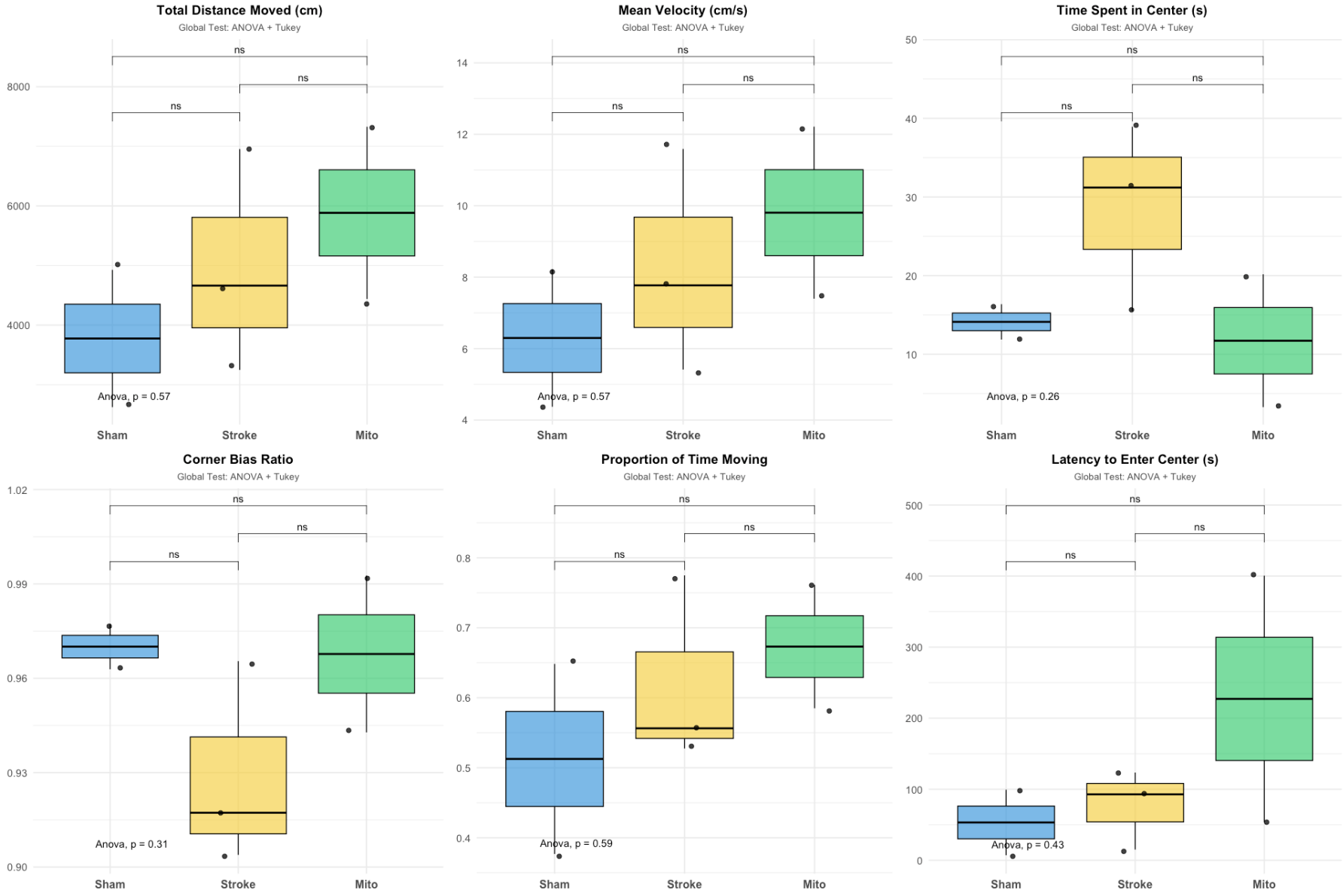

Current Mitochondrial Pre-treatment Model

- Three independent experiments since mid November 2025
  1. 11/18
     - Mito x 2
     - Stroke x2 (One found dead on post-stroke day 1)
  2. 12/03
     - Stroke x 3 (One euthanized on post-stroke day 2 due to respiratory concern)
     - Mito x 2
  3. 12/08
     - Sham x 3
     - Stroke x 3
     - Mito x 3
- Mito received intranasal hyaluronidase (25 µL x 2) + mitochondria (25 µL x 2 / 16 µg/µL -> 800 µg)
- Stroke received intranasal hyaluronidase (25 µL x 2) + saline (25 µL x 2)
- Sham received intranasal hyaluronidase (25 µL x 2) + saline (25 µL x 2)

Blinded Behavioral Assessment

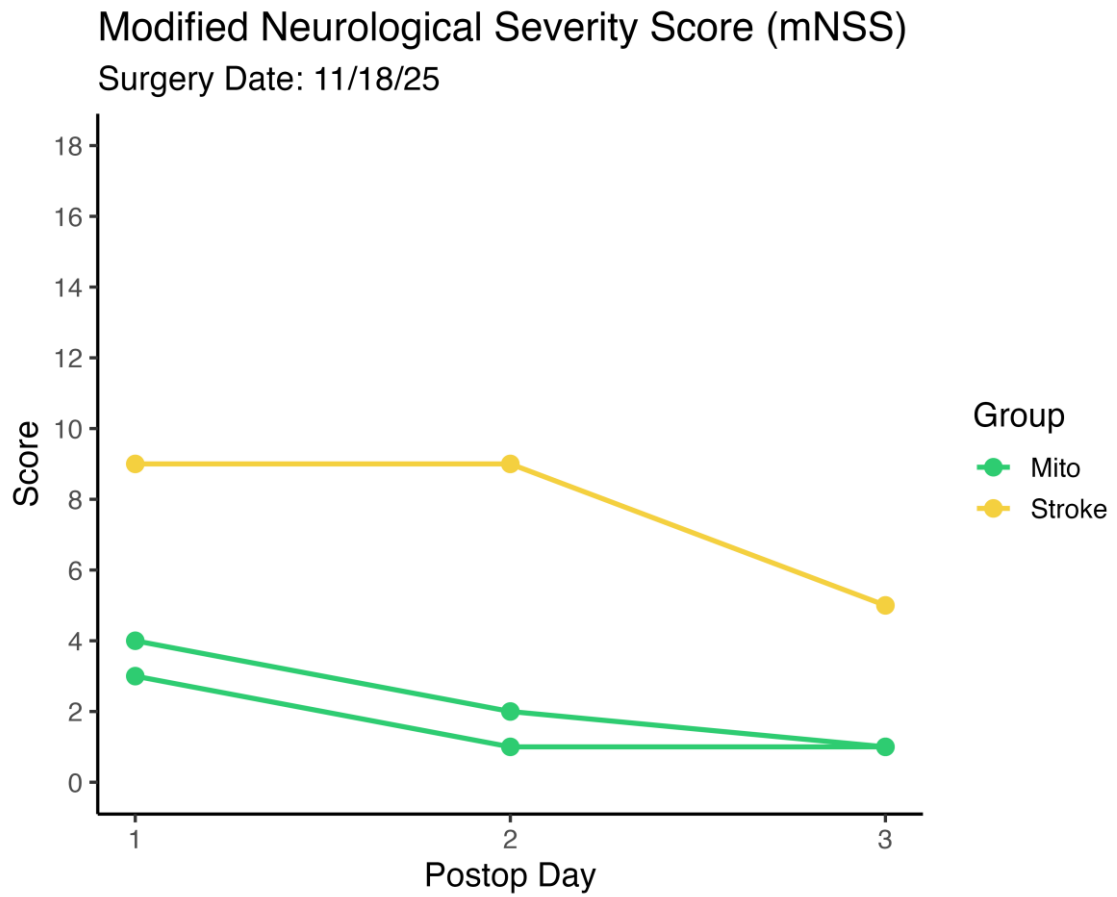

Blinded Behavioral Assessment

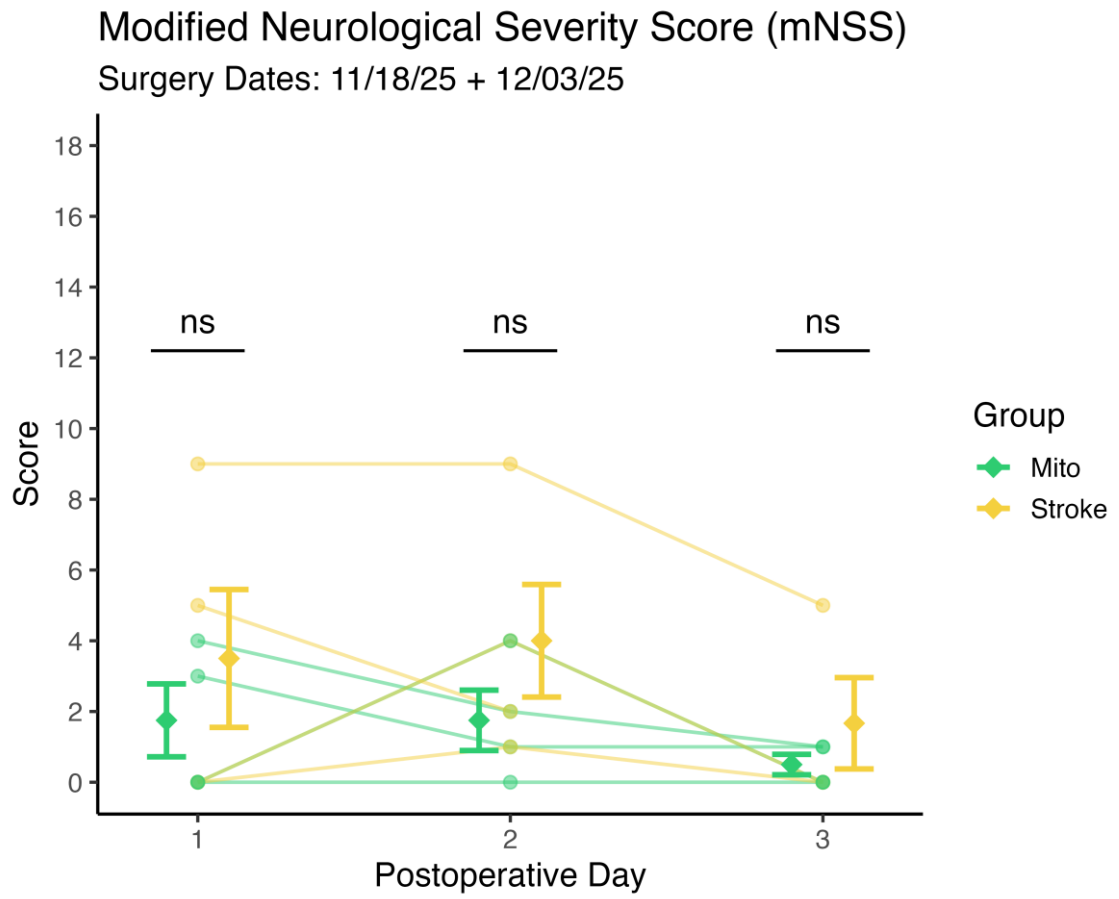

Sample size

- Stroke n = 5 - 1
- Mito n = 4

Survival status

- One untreated rat died on POD1 and one euthanized on POD2
- All treated rats were alive by POD3

Brain MRI Outcome

- Baseline results from two normal rats
- Post-stroke images obtained from 5 stroke rats without treatment

Rat #1 (09/16/25, 289 g)
T2_TurboRARE_sagittal

This is a high-resolution fast-spin echo T2-weighted protocol for structural/ volumetric assessment of brain compartments/ tissue injury/ edema.

T2 RARE sequence
TR/ TE = 2,511/ 33 ms
Slice thickness: 1.2 mm
Slice gap: 0.3 mm
Number of slices: 24 (sag)/ 22 (ax)/ 10 (cor)
FOV: 35x35 mm
Matrix size: 256x256
Number of repetitions: 4

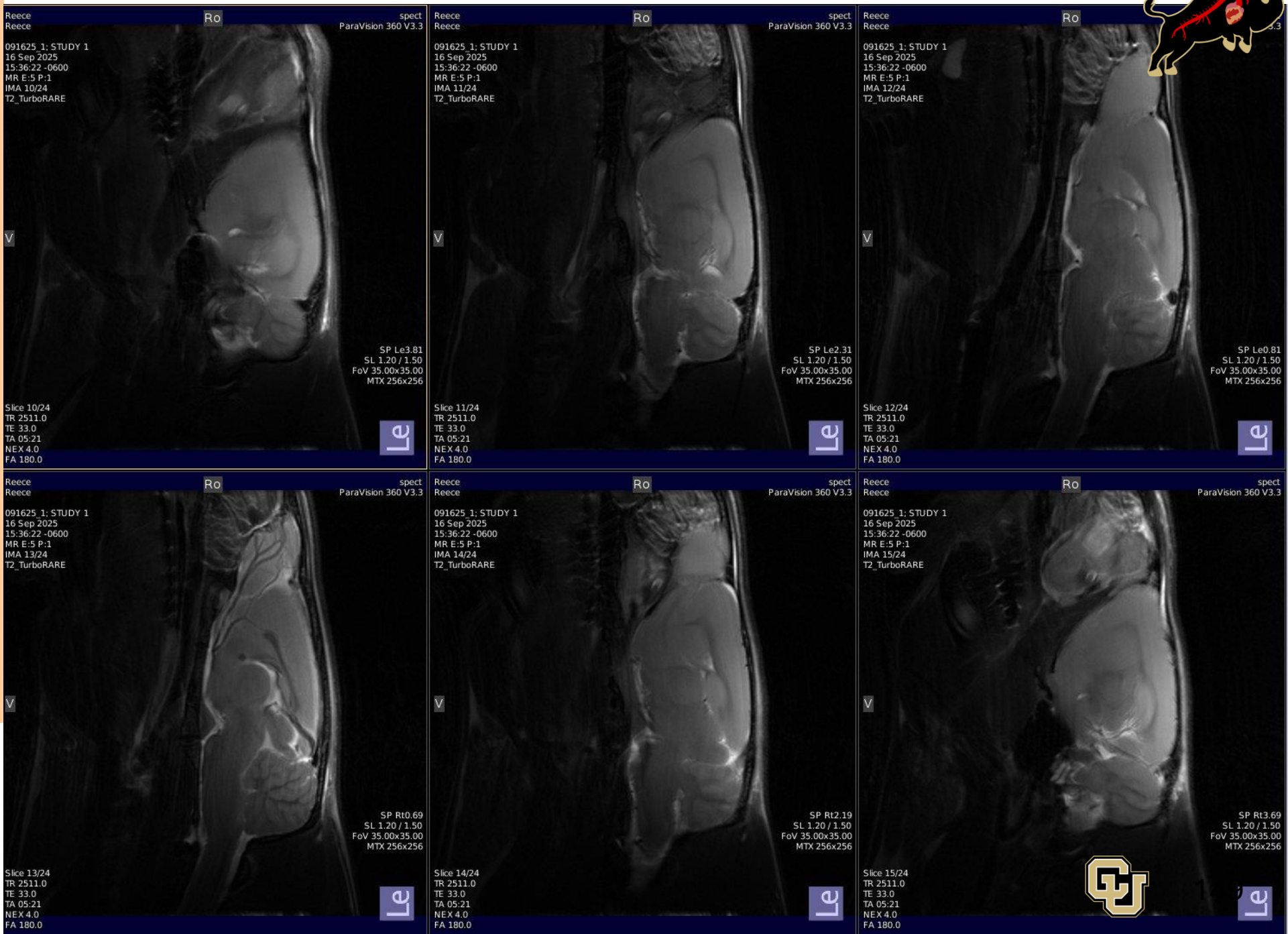

Rat #1 (09/16/25, 289 g)

T2_TurboRARE_Axial

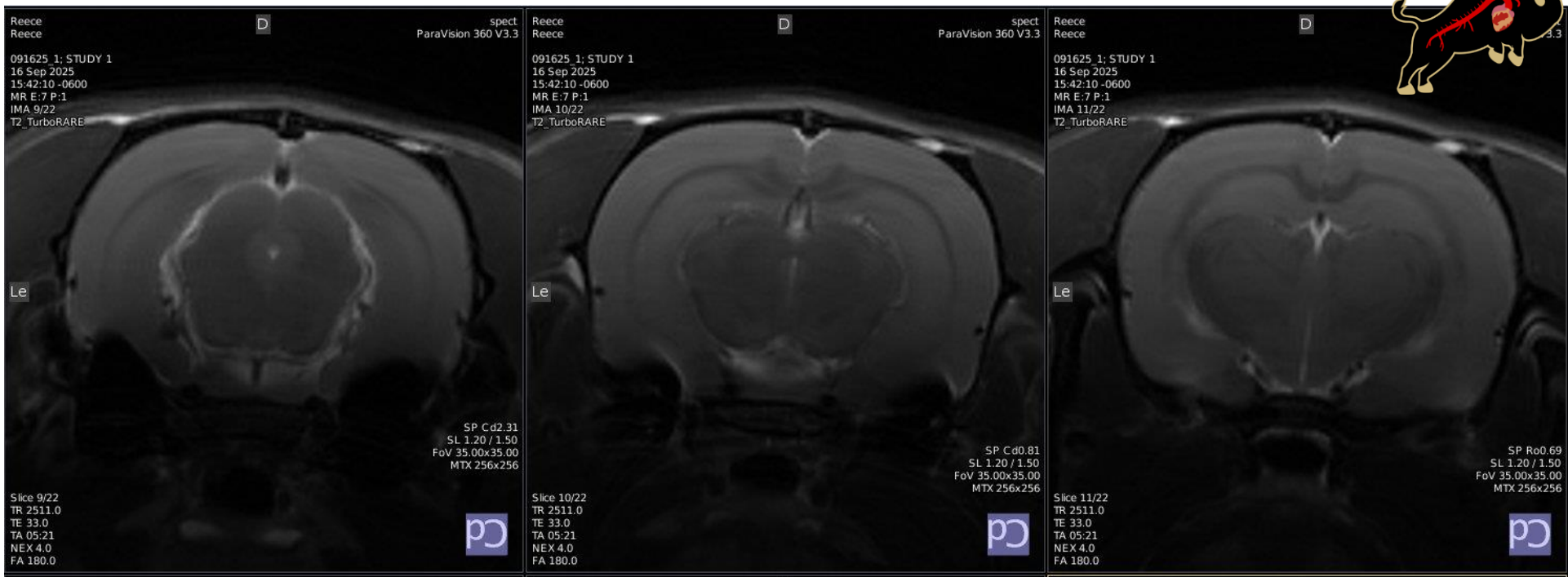

Rat #1 (09/16/25, 289 g)
T2_TurboRARE_Coronal

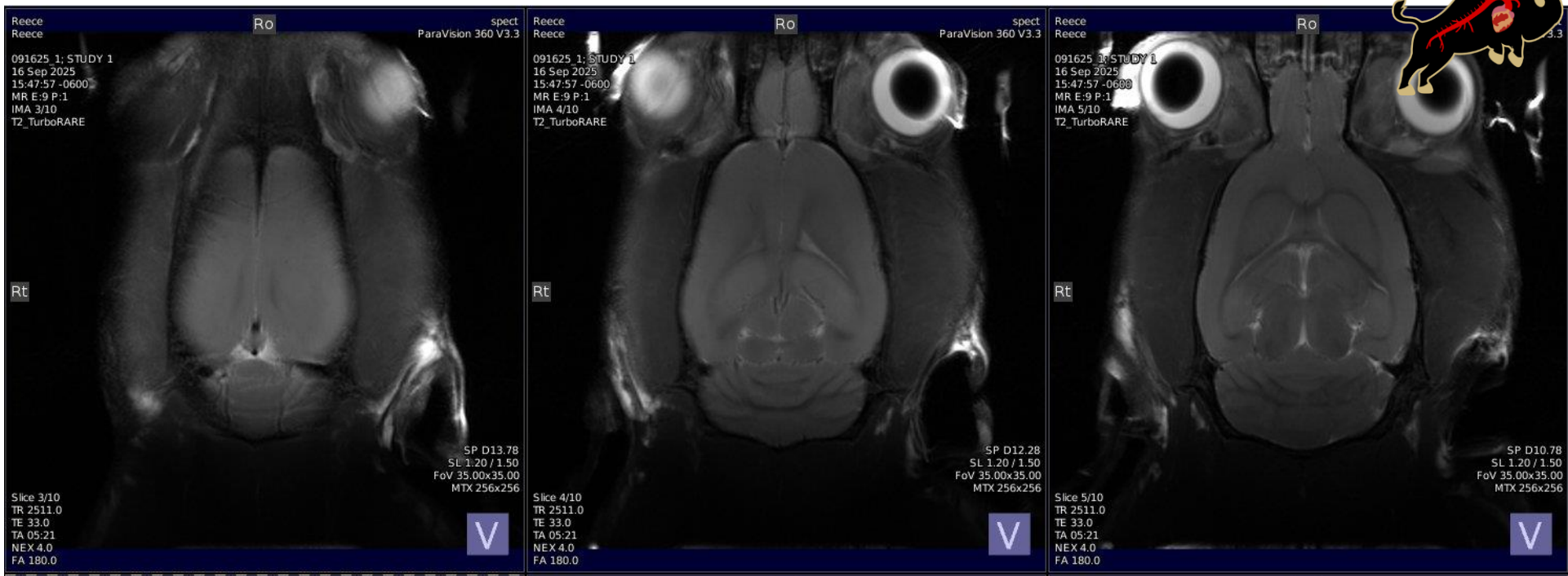

Rat #1 (09/16/25, 289 g)
DWI_Axial

This is a physiological echo-planar diffusion weighted protocol to determine apparent diffusion coefficients (ADC) reflective for brain cytotoxic edema and tissue regeneration.

DTIEPI sequence
TR/ TE = 3200/ 33 ms
Slice thickness: 2.0 mm
Slice gap: 0.5 mm
Number of slices: 7 (ax)
FOV: 25x25 mm
Matrix size: 96x96
Number of repetitions: 2
6 b-values (0, 200, 500, 800, 1000, 1200)

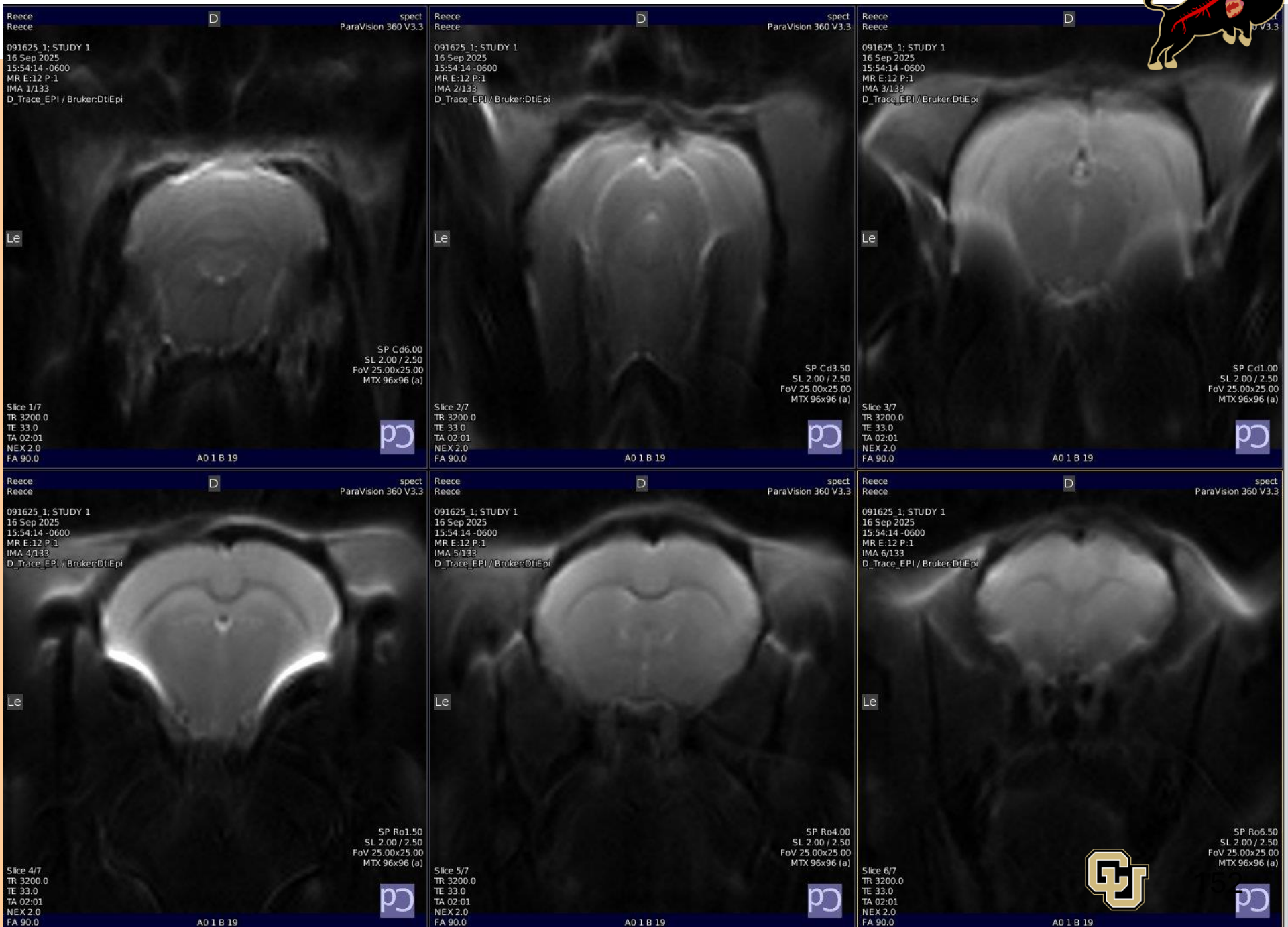

Rat #1 (09/16/25, 289 g)
SWI_Axial

This is a physiological susceptibility weighted protocol to detect hemorrhage, microbleeds and iron accumulation in the brain

SWI FLASH sequence
TR/ TE = 350/ 26 ms
Slice thickness: 0.5 mm
Slice gap: 0.1 mm
Number of slices: 9 (ax)
FOV: 25x25 mm
Matrix size: 96x96
Number of repetitions: 6

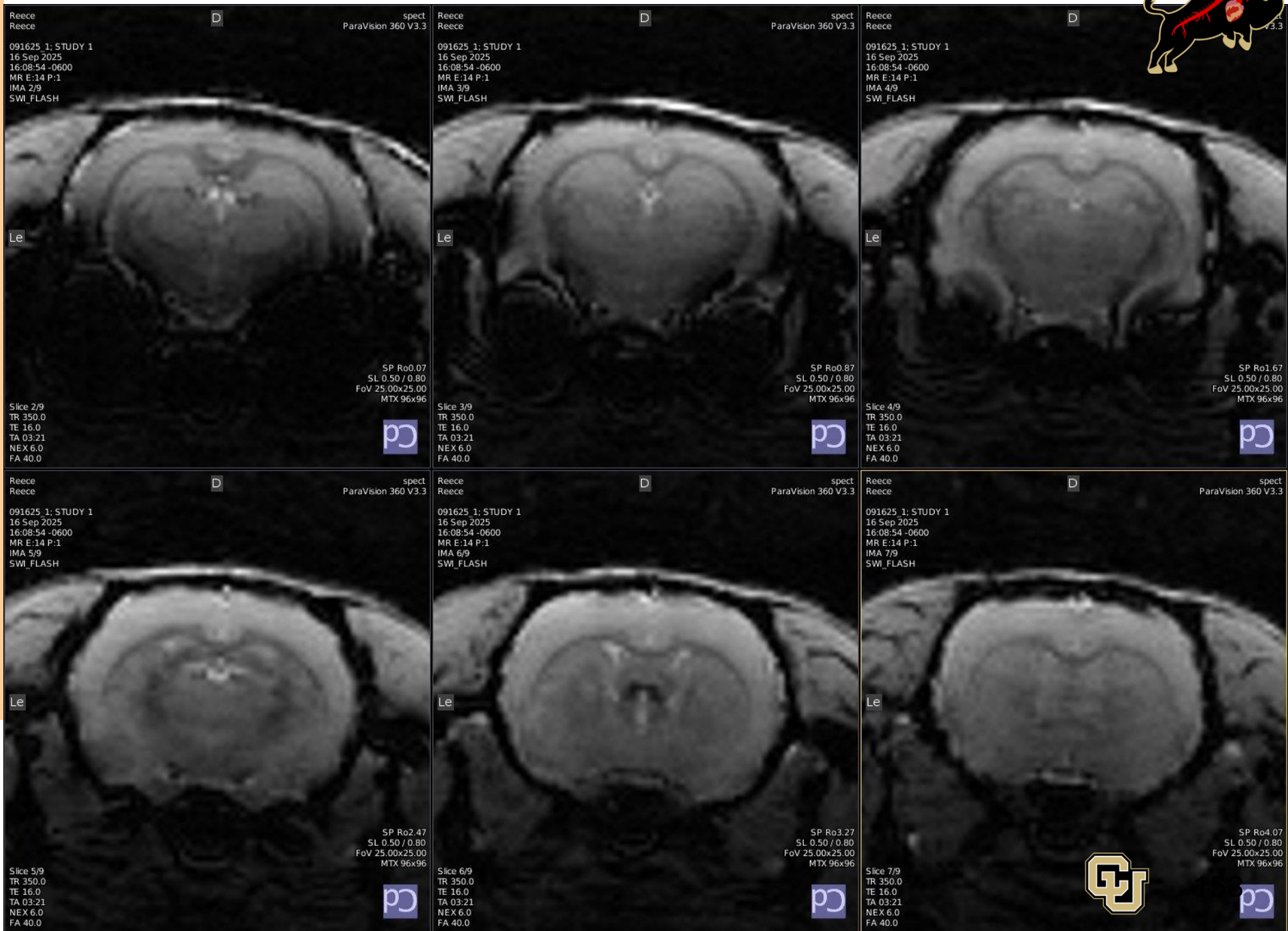

Rat #2 (09/16/25, 300 g)

T2_Turbo_SAG

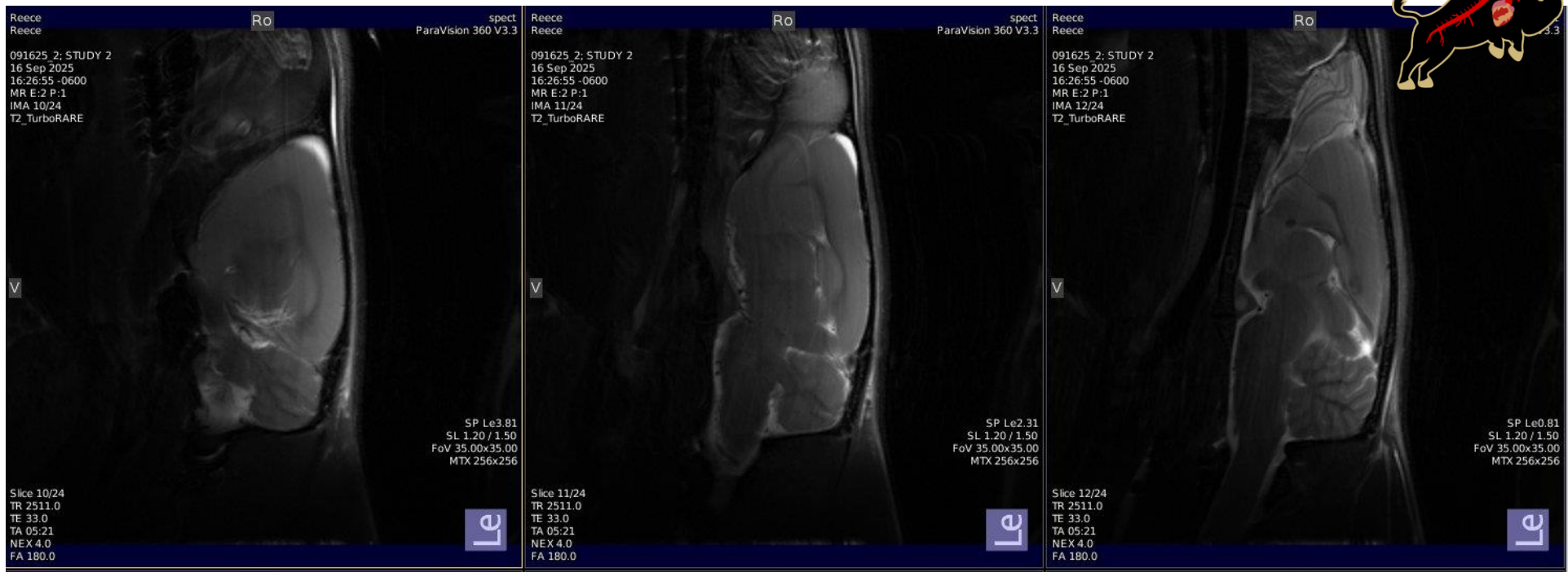

Rat #1 (09/16/25, 300 g)

T2_Turbo_AX

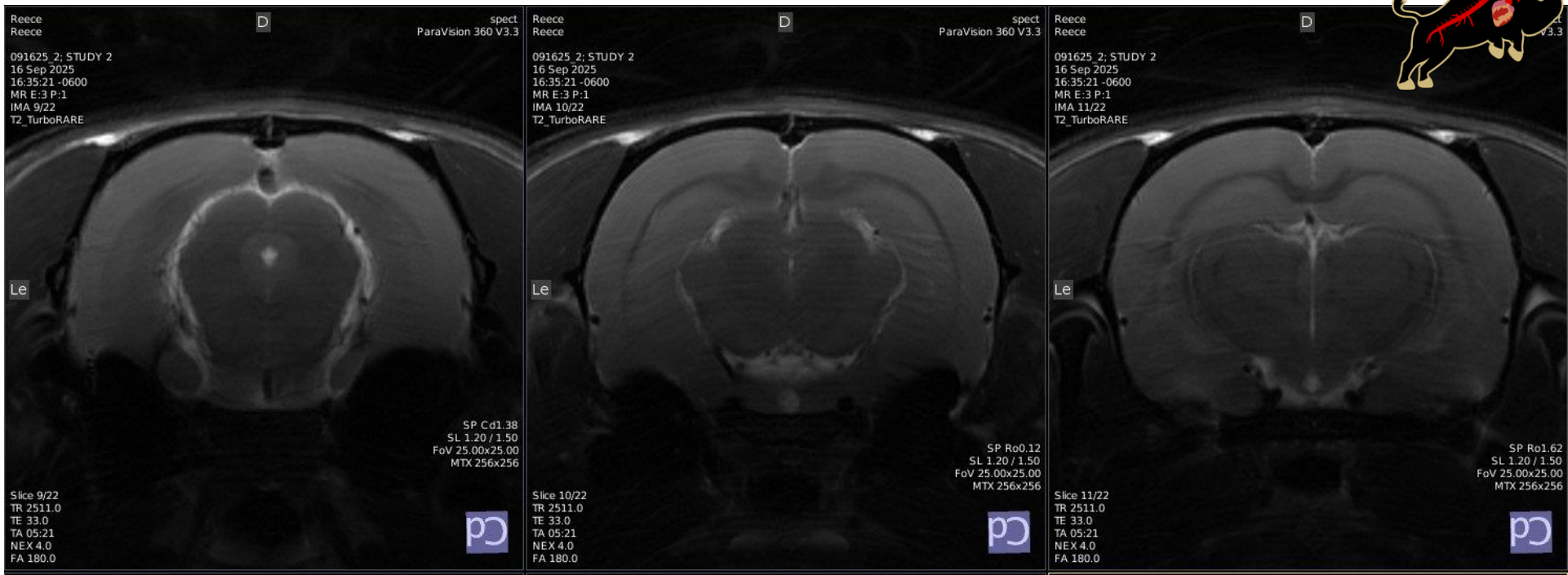

Rat #1 (09/16/25, 300 g)

T2_Turbo_COR

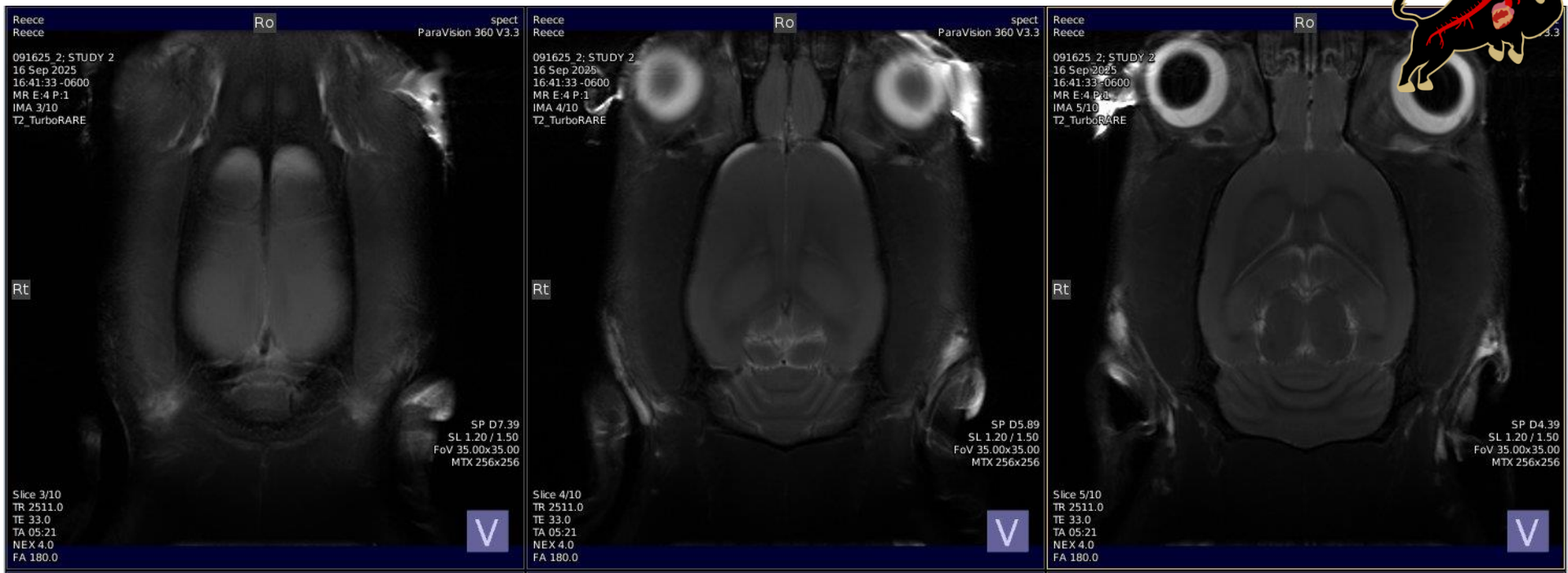

Rat #1 (09/16/25, 300 g)

DWI_AX

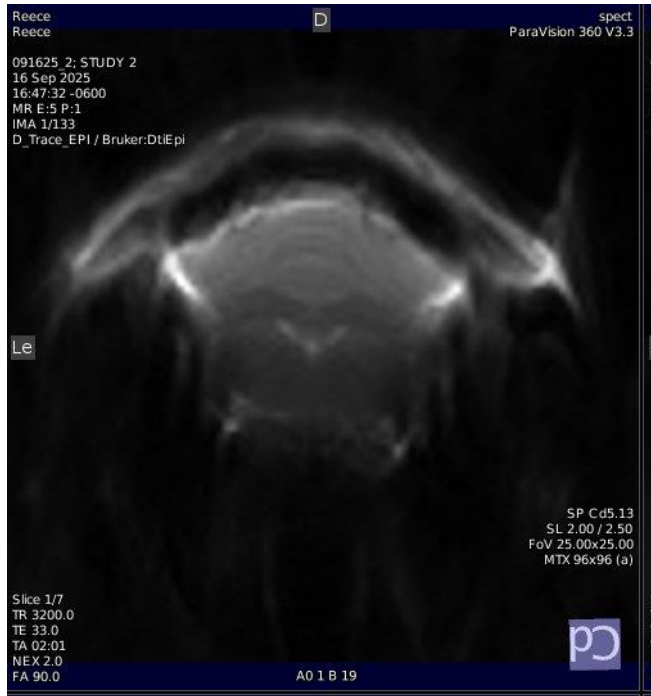

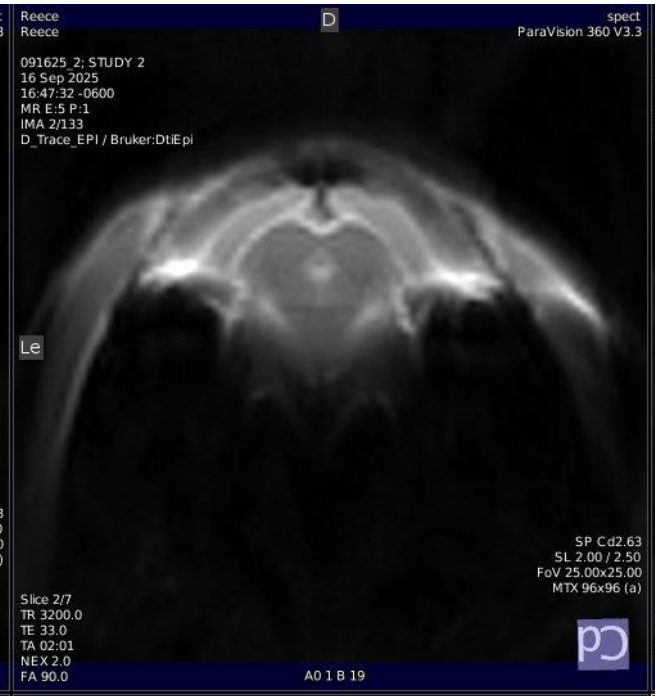

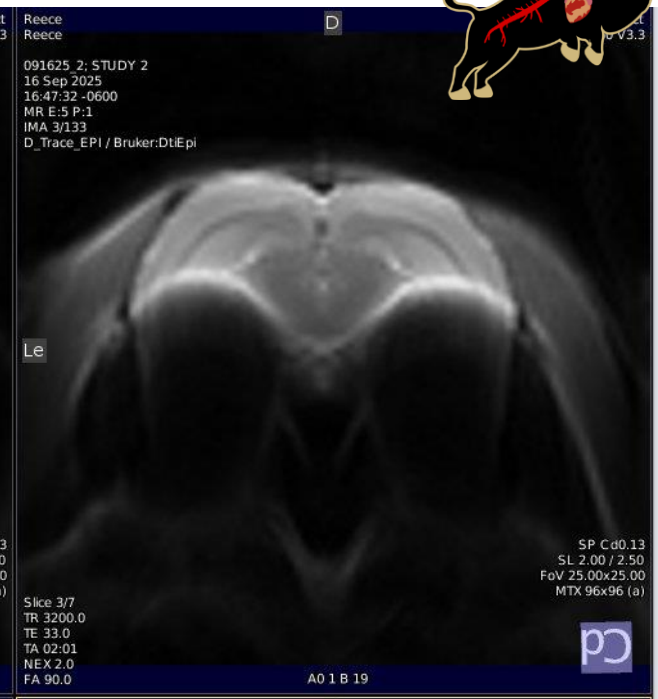

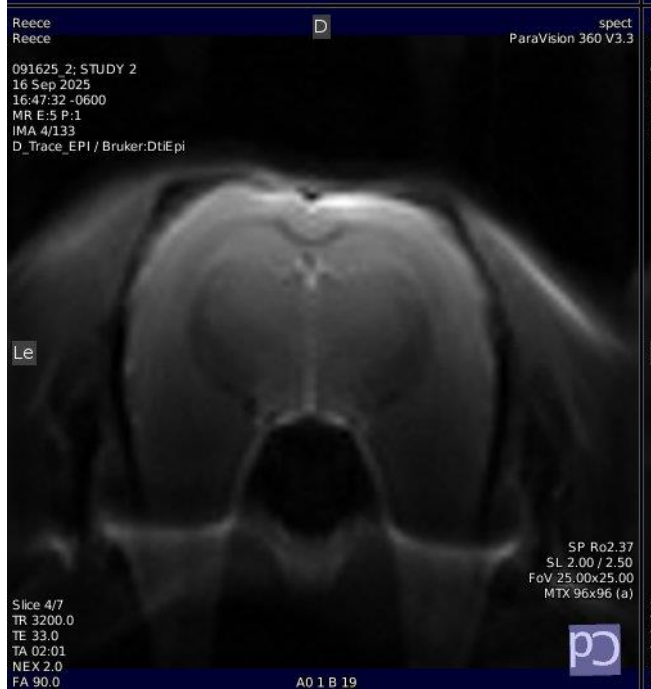

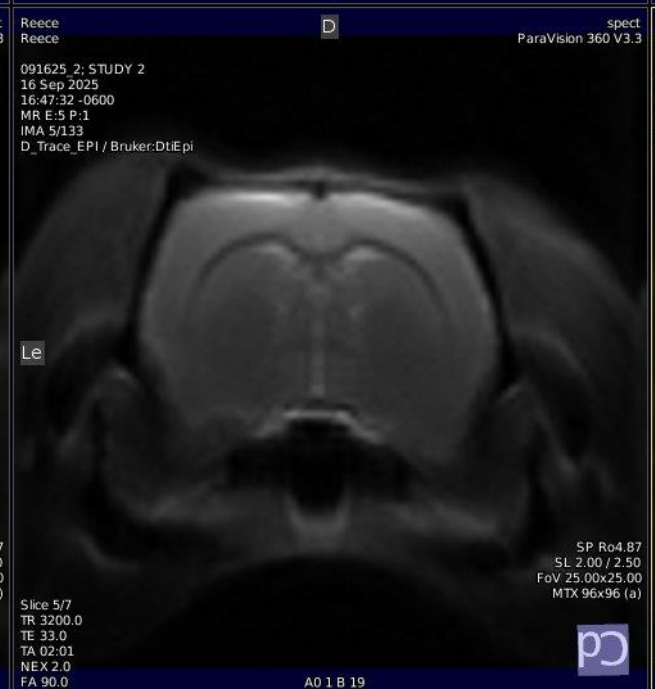

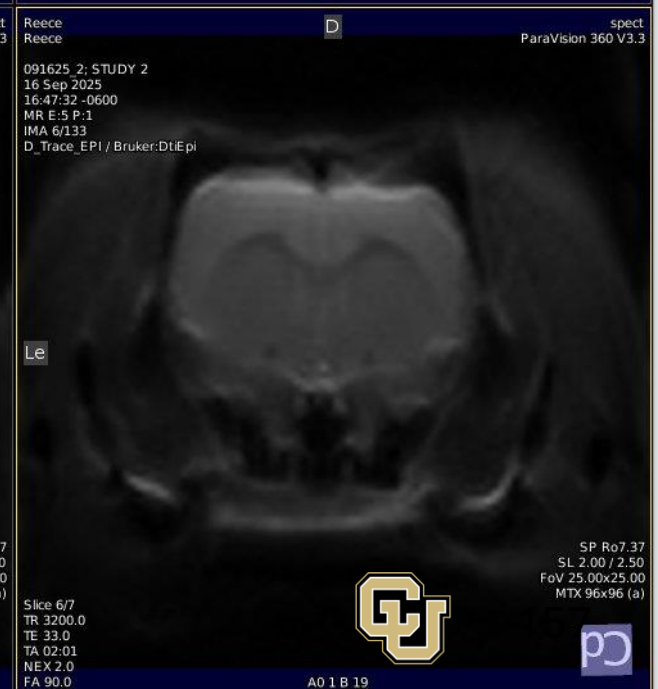

Rat #1 (09/16/25, 300 g)
SWI_AX

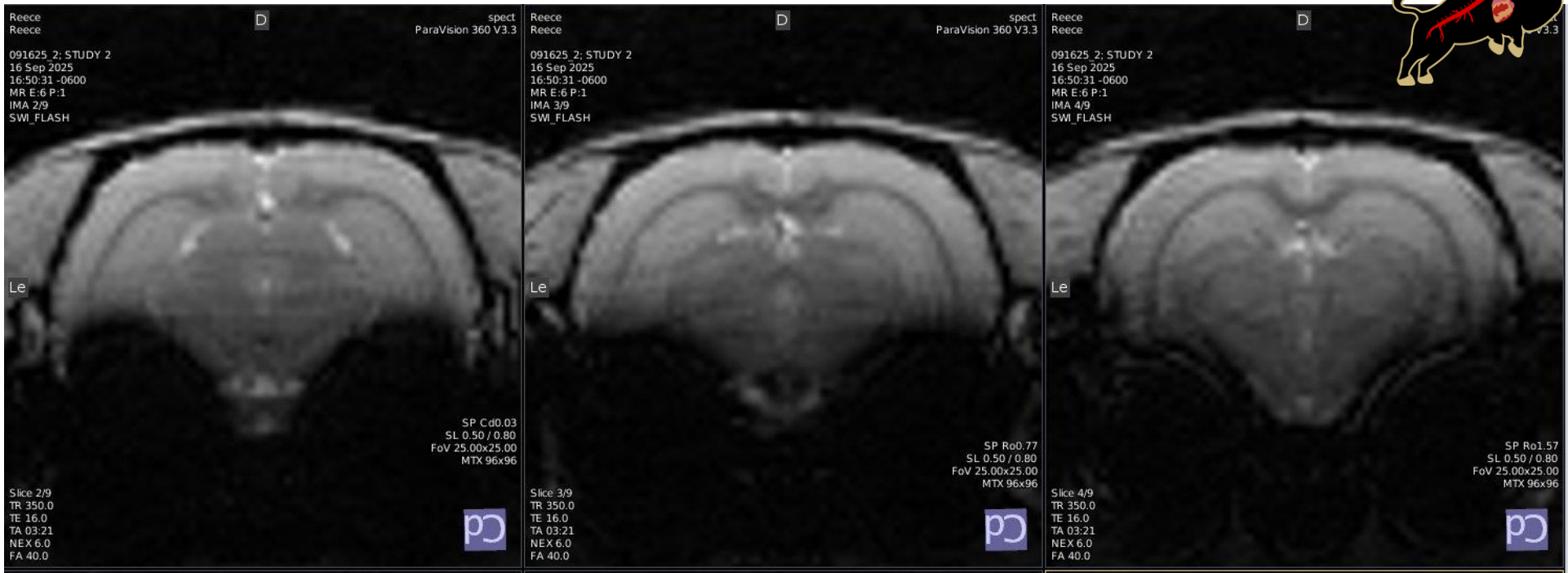

Future Plan

- December 2025 – February 2026: Establish sufficient samples in each group for neurobehavioral assessment (main cohort)
- March – April 2026: Complete tissue analysis – neuron counting, quantify ischemia area, other special staining. Collect additional tissue samples as needed
- April – May 2026: Complete the image cohort (secondary)
- May – June 2026: Finalize statistical analysis and generate results for an abstract and/or manuscript

Thank You